Eur. Phys. J. C (2016) 76:278
DOI 10.1140/epjc/s10052-016-4072-2

THE EUROPEAN PHYSICAL JOURNAL C

CrossMark

Regular Article - Theoretical Physics

COSMOS-e'-GTachyon from string theory

Sayantan Choudhury[1,a], **Sudhakar Panda**[2,3]

[1] Department of Theoretical Physics, Tata Institute of Fundamental Research, Colaba, Mumbai 400005, India
[2] Institute of Physics, Sachivalaya Marg, Bhubaneswar, Odisha 751005, India
[3] Harish-Chandra Research Institute, Allahabad 211019, India

Received: 23 December 2015 / Accepted: 10 April 2016 / Published online: 19 May 2016

Abstract In this article, our prime objective is to study the inflationary paradigm in the context of the generalized tachyon (GTachyon) living on the world volume of a non-BPS string theory. The tachyon action is considered here is modified compared to the original action. One can quantify the amount of the modification via a power q instead of $1/2$ in the effective action. Using this set-up we study inflation by various types of tachyonic potentials, using which we constrain the index q within, $1/2 < q < 2$, and a specific combination ($\propto \alpha' M_s^4/g_s$) of the Regge slope α', the string coupling constant g_s and the mass scale of tachyon M_s, from the recent Planck 2015 and Planck+BICEP2/Keck Array joint data. We explicitly study the inflationary consequences from single field, assisted field and multi-field tachyon set-ups. Specifically for the single field and assisted field cases we derive the results in the quasi-de Sitter background in which we will utilize the details of cosmological perturbations and quantum fluctuations. Also we derive the expressions for all inflationary observables using any arbitrary vacuum and the Bunch–Davies vacuum. For the single field and the assisted field cases we derive the inflationary flow equations, new sets of consistency relations. Also we derive the field excursion formula for the tachyon, which shows that assisted inflation is on the safe side compared to the single field case to validate the effective field theory framework. Further we study the features of the CMB angular power spectrum from TT, TE and EE correlations from scalar fluctuations within the allowed range of q for each of the potentials from the single field set-up. We also put constraints from the temperature anisotropy and polarization spectra, which shows that our analysis is consistent with the Planck 2015 data. Finally, using the δN formalism we derive the expressions for inflationary observables in the context of multi-field tachyons.

Sayantan Choudhury: Presently working as a Visiting (Post-Doctoral) fellow at DTP, TIFR, Mumbai
On lien from Harish-Chandra Research Institute, Allahabad, India.

[a] e-mails: sayantan@theory.tifr.res.in; sayanphysicsisi@gmail.com

Contents

1 Introduction

The primordial inflationary paradigm is a very sublime thought aimed to explain various aspects of the early universe, in which perturbations occur and matter is created. For recent developments see Refs. [1–10]. The success of primordial inflation can be gauged by the current observations arising from the cosmic microwave background (CMB) radiation [11–13]. The observations from Planck have put interestingly tight bounds on a number of cosmological observables related to the perturbations, which also determines any departure from the Gaussian perturbations and the constraint on the tensor-to-scalar ratio, $r_\star$, which can potentially reveal the scale of New Physics within any given effective field theory set-up. But a big issue may crop up in model discrimination and also in the removal of the degeneracy of cosmological parameters obtained from CMB observations. Non-canonical interactions in the effective theory set-up [14–23] are among the possibilities through which one can address this issue.[1] The natural source for such non-canonical interactions is string theory. The most promising example is the Dirac–Bonn–Infeld (DBI) effective action for the tachyon field [48–51]. In this paper, we will only focus on tachyons in weakly coupled Type-IIA/IIB string theory [52,53].

The phenomenon of tachyon condensation was introduced in Refs. [48,49], where Type-IIA/IIB string theory and the tachyon instability on D-branes have been studied elaborately. The rolling tachyon [54–56] in weakly coupled Type-IIA/IIB string theory may be described in terms of an effective field theory for the tachyon condensate in Refs. [57–73]. The cosmological implications of the tachyon were studied in [74–86]. For more details see also Refs. [87–95]. In the context of cosmology, the detailed consequences have been studied in the following topics over many years:

1. Inflationary paradigm [75–86,92],
2. Primordial non-Gaussianity and CMB aspects [96–104],
3. Reheating scenario and particle creation [105,106],
4. Late time cosmic acceleration (dark energy) [107–110].

In this work, we introduce the most generalized version of the tachyon effective action in which we are interested to study the cosmological consequences from the non-canonical higher-dimensional effective field theory operators, originating from string theory. Technically we rename such a non-canonical field a generalized tachyon (GTachyon), which name we will frequently use throughout the rest of the paper. The prime motivation of writing this paper is the following:[2]

- To update the present status of non-canonical interaction for stringy tachyon field appearing within the framework of string theory after releasing the Planck 2015 data.
- To explicitly study the role of tachyon field and its generalized version, GTachyon, to explain the observed temperature anisotropy and polarization in the CMB angular power spectrum.
- To study the specific role of the most generalized version of non-canonical higher-dimensional effective field theory Wilsonian operators.
- To give a broad overview of the present constraints on the inflationary paradigm from the most generalized version of the tachyon string theory.
- To test the explicit dynamical features of various tachyonic potentials obtained from string theory and also to learn about the specific structural form of effective field theory operators for a specific type of potential.

Throughout the paper we have taken the following assumptions:

1. The tachyon field T is minimally coupled to the Einstein gravity sector.
2. The initial condition for inflation is fixed via Bunch–Davies (BD) vacuum [111]. For completeness we also present the results obtained from an arbitrary vacuum (AV). For a classical initial condition the amplitude of

[1] The other possibilities are: non-minimal interactions between the matter and gravity sector [(example: SM Higgs with Einstein gravity [24,25]], addition of higher derivative terms in the gravity sector (example: Starobinsky model [26]), modification of the gravity sector through extra dimensions (example: 5D membrane models [27–47]).

[2] Since the Gtachyon contains non-minimal interactions, it is naturally expected that it will sufficiently modify the consistency relations. Also due to such non-canonical interactions it is expected that the amount of primordial non-Gaussianity is getting enhanced by a sufficient amount, by breaking the non-Gaussian consistency relations known in cosmological literature. For completeness it is important to mention here that we have not investigated the issues related to primordial non-Gaussianity yet in this paper. We will report on these issues in our future work.

the primordial gravitational waves would be very tiny and practically undetectable, therefore this can be treated as the first observable evidence of quantum theory gravity, such as string theory. However, apart from the importance and applicability of the quantum version of a Bunch–Davis vacuum on its theoretical and observational ground, it is still not at all well understood from the previous works in this area whether the quantum Bunch–Davies vacuum is the only possible source generating a large value of the tensor-to-scalar ratio during the inflationary epoch or not. One of the prime possibilities coming from the deviation from the quantum Bunch–Davies vacuum and consideration of the quantum non-Bunch–Davies or an arbitrary vacuum in the present non-canonical picture may also be responsible for the generation of a large tensor-to-scalar ratio and large non-Gaussianity during inflation. Within the framework of effective field theory, such an arbitrary vacuum is commonly identified with the α-vacuum [112–118], which has a string theoretic origin.

3. We would like to point out that the tachyon mode appears in the quantization of the open string struck to the non-BPS brane. The effective action of this tachyon field is constructed on the assumption that the tachyon field couples only to the graviton of the closed string sector with fixed vacuum expectation value for the dilation field. The open string tachyon condensation phenomenon fits in well with this assumption.
4. The sound speed is $c_S < 1$ in general for non-canonical interactions [14–23], which is the most promising ingredient for a tachyonic set-up, to generate simultaneously a detectable value of the tensor-to-scalar ratio and large non-Gaussianity. This fact can be more clearly visualized when we go to an all higher order expansion in slow-roll or more precisely by taking the exact solution of the mode functions for scalar and tensor fluctuations as obtained from cosmological perturbation theory by appropriately choosing the Bunch–Davies case or any arbitrary initial conditions for inflation.
5. UV cut-off of the effective field theory is fixed at $\Lambda_{\rm UV} \sim M_p$, where $M_p = 2.43 \times 10^{18}$ GeV is the reduced Planck mass. But in principle one can fix the scale between GUT scale and the reduced Planck scale, i.e., $\Lambda_{\rm GUT} < \Lambda_{\rm UV} \leq M_p$. But in such a situation $\Lambda_{\rm UV}$ acts as a regulating parameter in the effective field theory [23,119].
6. Within the region of $N_\star(=N_{\rm cmb}) \approx \mathcal{O}(50\text{–}70)$ e-foldings, we will use the following constraints in the background of ΛCDM model for:

Planck (2015)+WMAP-9+high L(TT) data: [120]

$$r(k_\star) \leq 0.11 \ \ (\text{within } 2\sigma\ C.L.), \tag{1.1}$$
$$\ln(10^{10} P_S) = 3.089 \pm 0.036 \ \ (\text{within } 2\sigma\ C.L.), \tag{1.2}$$
$$n_S = 0.9569 \pm 0.0077 \ \ (\text{within } 3\sigma\ C.L.), \tag{1.3}$$
$$\alpha_S = \mathrm{d}n_S/\mathrm{d}\ln k = 0.011^{+0.014}_{-0.013} \ \ (\text{within } 1.5\sigma\ C.L.), \tag{1.4}$$
$$\kappa_S = \mathrm{d}^2 n_S/\mathrm{d}\ln k^2 = 0.029^{+0.015}_{-0.016} \ \ (\text{within } 1.5\sigma\ C.L.). \tag{1.5}$$

Planck (2015)+BICEP2/Keck Array joint data: [121]

$$r(k_\star) \leq 0.12 \ \ (\text{within } 2\sigma\ C.L.), \tag{1.6}$$
$$\ln(10^{10} P_S) = 3.089^{+0.024}_{-0.027} \ \ (\text{within } 2\sigma\ C.L.), \tag{1.7}$$
$$n_S = 0.9600 \pm 0.0071 \ \ (\text{within } 3\sigma\ C.L.), \tag{1.8}$$
$$\alpha_S = \mathrm{d}n_S/\mathrm{d}\ln k = -0.022 \pm 0.010 \ \ (\text{within } 1.5\sigma\ C.L.), \tag{1.9}$$
$$\kappa_S = \mathrm{d}^2 n_S/\mathrm{d}\ln k^2 = 0.020^{+0.016}_{-0.015} \ \ (\text{within } 1.5\sigma\ C.L.). \tag{1.10}$$

The plan of the paper is as follows:

- In Sect. 2, we have discussed the role of tachyon in non-BPS barnes in weakly coupled Type-IIA/IIB string theory and also introduced the GTachyon in the effective action of string theory.
- In Sect. 3, we have introduced and studied the features from variants of the tachyonic potentials inspired by non-BPS branes in string theory.
- In Sect. 4, we have studied the cosmological dynamics from GTachyons, in which we have explicitly discussed the unperturbed evolution and dynamical solution in various phases of the universe.
- In Sect. 5, we have explicitly studied inflationary paradigm from single, assisted and multi-field Gtachyons. Particularly for the single field and assisted field cases in the presence of GTachyon, we have derived the inflationary Hubble flow and potential dependent flow equations, new sets of consistency relations, which are valid in the slow-roll regime and field excursion formula for tachyon in terms of the inflationary observables.
- In Sect. 6, we have mentioned the future prospects of the present work and summarized the context of the present work.

In this paper, we have explored various cosmological consequences from the GTachyonic field. We start with the basic introduction of tachyons in the context of non-BPS string theory, where we also introduce the GTachyon field, in the presence of which the tachyon action is modified and one can quantify the amount of the modification via a superscript q instead of $1/2$. This modification exactly mimics the role of effective field theory operators and studying the various cosmological features from this theory, one of our final objectives is to constrain the index q and a specific combination ($\propto \alpha' M_s^4/g_s$) of the Regge slope parameter α', the string coupling constant g_s and mass scale of tachyon M_s, from the recent Planck 2015 and Planck+BICEP2/Keck Array joint data. To serve this purpose, we introduce various types of tachyonic potentials: the inverse cosh, logarithmic, exponential and inverse polynomials, using which we constrain the index q. To explore this issue in detail, we start with the characteristic features of the each potentials. Next we discuss the dynamics of GTachyon as well as usual tachyon for single, assisted and multi-field scenario. Next we have explicitly studied the inflationary paradigm from a single field, assisted field and multi-field tachyon set-up. Specifically for the single field and assisted field cases we have derived the results in the quasi-de Sitter background in which we have utilized the details of: (1) cosmological perturbations and quantum fluctuations for scalar and tensor modes, (2) the slow-roll prescription. In this context we have derived the expressions for all inflationary observables using any arbitrary vacuum and also for Bunch–Davies vacuum. For single field and assisted field case in the presence of GTachyon we have derived the inflationary Hubble flow and potential dependent flow equations, new sets of consistency relations valid in the slow-roll regime and also derived the expression for the field excursion formula for the tachyon in terms of the inflationary observables from both of the solutions obtained from arbitrary and Bunch–Davies initial conditions for inflation. Particularly the derived formula for the field excursion for GTachyon can be treated as an one of the important probes through which one can distinguish between various tachyon models and also check the validity of effective field theory prescription and compare the results obtained from assisted inflation as well. The results obtained in this context explicitly show that assisted inflation is better compared to single field inflation from the tachyon portal, provided the number of identical tachyon fields is required to be large to validate effective field theory prescription. Next using the explicit form of the tachyonic potentials we have studied the inflationary constraints and quantify the allowed range of the generalized index q for each of the potentials. Hence using each specific form of the tachyonic potentials in the context of the single field scenario, we have studied the features of CMB angular power spectrum from TT, TE and EE correlations from scalar fluctuations within the allowed range of q for each potentials. We also put the constraints from the Planck temperature anisotropy and polarization data, which shows that our analysis is consistent with the data. We have additionally studied the features of the tensor contribution in the CMB angular power spectrum from TT, BB, TE and EE correlations, which will give more interesting information in near future while the signature of primordial B-modes can be detected. Further, using the δN formalism, we have derived the expressions for inflationary observables in the context of multi-field tachyons and demonstrated the results for inverse cosh potential for completeness.

2 GTachyon in string theory

In this section we explicitly study the world volume actions for non-BPS branes which finally govern their cosmological dynamics. For the sake of simplicity in this discussion we neglect the contribution from the fermions and concentrate only on the massless bosonic fields for the non-BPS branes. The world volume action for non-BPS branes is described by the sum of the Dirac–Born–Infeld (DBI) and the Wess–Zumino (WZ) terms in Type-IIA/IIB string theory. The effective action for DBI in a non-BPS p-brane is given by [122–124]

$$S^{(p)}_{\rm DBI} = -\mathcal{T}_p \int d^{p+1}\sigma\, e^{-\phi} \sqrt{-\det\left(\mathcal{Z}_{\mu\nu} + \mathcal{F}_{\mu\nu}\right)}, \tag{2.1}$$

where the metric has signature $(-,+,+,+)$ and $\mathcal{Z}_{\mu\nu}$ is defined as

$$\mathcal{Z}_{\mu\nu} = G_{\mu\nu} + \alpha' \partial_\mu T \partial_\nu T. \tag{2.2}$$

Here T is the dimensionless tachyon field whose properties have been discussed later in detail. Also in Eq. (2.1) $\mathcal{T}_p$ represents the brane tension defined as [122–124]

$$\mathcal{T}_p = \sqrt{2}(2\pi)^{-p} g_s^{-1} \tag{2.3}$$

and α' represents the Regge slope parameter in string theory. Here Type-IIA/IIB string theory contains the non-BPS Dp-branes [125], which have precisely those dimensions which BPS D-branes do not have explicitly. This implies that Type-IIA string theory has non-BPS Dp-branes for only odd p and Type-IIB string theory has non-BPS Dp-branes only for even p in the present context. Additionally, it is important to note that g_s characterizes the string coupling constant. Also in Eq. (2.1), $G_{\mu\nu}$ is defined via the following transformation equation:

$$G_{\mu\nu} = G_{MN} \partial_\mu X^M \partial_\nu X^N. \tag{2.4}$$

In Eq. (2.4) M, N characterize the ten-dimensional ($D = 10$) indices, which run from $0, 1, \ldots, 9$; $\sigma^\mu (0 \le \mu \le p)$ denotes the world volume coordinates of the Dp brane. Also it is important to note that, in this discussion, G_{MN} represents the ten-dimensional ($D = 10$) background metric for Type-IIA/IIB string theory.

It is important to mention here that, in the context of non-BPS D-brane, the stringy tachyon comes from only one specific sector of string theory and consequently it is a real scalar field using which we will explain the cosmological dynamics in this article for $p = 3$. Additionally it is also important to note that Type-IIA/IIB string theories contain unstable non-BPS D-branes in their spectra. The most easiest way to define these types of D-branes in the context of IIA/IIB string theory is to start the computation with a coincident BPS Dp-$\bar{\text{D}}p$-brane pair in Type-IIB/IIA string theory, and then take a specific orbifold of the string theory by $(-1)^{F_L}$, where F_L signifies the specific contribution to the space-time fermion number from the left-moving sector of the world-sheet string theory. Now in this context the Ramond–Ramond (RR) fields are odd under $(-1)^{F_L}$ transformation and consequently all the Ramond–Ramond (RR) fields of Type-IIB/IIA string theory are projected out by the same amount via $(-1)^{F_L}$ projection. As a result the twisted sector stringy states then give us back the RR fields of Type-IIA/IIB string theory in the present context. Most importantly, here the $(-1)^{F_L}$ projection reverses the signature of the RR charge and consequently it transforms a BPS Dp-brane to a $\bar{\text{D}}p$-brane and vice versa. This further implies that due to its operation on the open string states on a Dp–$\bar{\text{D}}p$-brane stringy system will do the job of conjugate operation on the Chan–Paton factor by the action of exchange operator σ_1 in this context. Thus technically the modding out operation on the Dp–$\bar{\text{D}}p$-brane by exactly the amount of $(-1)^{F_L}$ eliminates all the open string states which carry a Chan–Paton factor σ_2 and σ_3, as both of them anti-commute with the exchange operator σ_1. Additionally it is important to note that this operation finally keeps the open string states which are characterized via the Chan–Paton factors I and σ_1. Finally all such operations give us a non-BPS Dp-brane in the present context. Although in this discussion we are only interested in the non-BPS D-branes, the most important characteristic feature that distinguishes the physics of non-BPS D-branes from BPS D-branes is that the mass spectrum of open strings on a non-BPS D-brane contains a single mode of negative mass squared besides an infinite number of other modes of positive definite mass squared. This negative mass squired mode is identified with the tachyonic mode which is exactly equivalent to a particular linear combination of the two tachyonic modes living on the original brane–antibrane pair stringy system that survives the previously mentioned $(-1)^{F_L}$ projection and contains exactly the same mass squared contribution.

In our analysis for the sake of simplicity we have neglected the contribution from the antisymmetric Kalb–Ramond two form field from the effective action but the gauge invariance of the action requires the presence of all such antisymmetric tensor contributions in the original version of the string effective action. In the present context, it is important to note that $G_{\mu\nu}$ can be physically interpreted as the induced metric on the membrane. Additionally it is important to note that the background metric G_{MN} is not at all arbitrary for the present set-up but the structural form of the metric is restricted in the specific sense that it has to satisfy the sets of background field equations in this context. Also in our discussion the transverse component of the fluctuations of the D-membrane is described by $(9-p)$ scalar fields X^i, where the index i runs from $p+1 \le i \le 9$, and the gauge field A_μ describes the fluctuations along the longitudinal direction of the membrane.

Before writing down the total effective action for non-BPS D-brane in string theory it is important to mention that the non-BPS p-brane has an extra tachyon field appearing in both of the Dirac–Born–Infeld (DBI) and the Wess–Zumino (WZ) stringy effective actions. The corresponding effective actions can be written in the non-BPS string theory set-up as [122–124]

$$S^{(p)}_{\text{DBI}} = -\int \mathrm{d}^{p+1}\sigma\, e^{-\phi}\sqrt{-\det\left(\mathcal{Z}_{\mu\nu}+\mathcal{F}_{\mu\nu}\right)} \times\Theta(T,\partial_\mu T, D_\mu\partial_\nu T), \tag{2.5}$$

$$S^{(p)}_{\text{WZ}} = \int \mathrm{d}^{p+1}\sigma\, C\wedge \mathrm{d}T\wedge e^{\mathcal{F}}, \tag{2.6}$$

where the field C contains Ramond–Ramond (RR) fields and the leading term has a $(p+1)$-differential form. This also mimics the role of a source term for the membrane and its presence is explicitly required for consistency of the specific version of the field theory like anomaly cancellation within the set-up of string theory. It is important to mention here that we have the world volume action for a Dp-brane in the $(p+1)$-dimensional case, where p characterizes the spatial dimension and 1 stands for time. The WZ term plays an important role since the BPS Dp-brane is charged under a $(p+1)$ rank RR gauge field. Consequently the total action is therefore the DBI action together with the WZ action. For the non-BPS Dp-brane, the brane is charged under a rank p RR gauge field. As a result the WZ action consists of a wedge product of this p form and additionally a one form $\mathrm{d}T$, where T is the tachyon field. Also it is important to note that for the non-BPS case $\mathcal{F}_{\mu\nu}$ is explicitly defined as [122–124]

$$\begin{aligned}\mathcal{F}_{\mu\nu} &= B_{\mu\nu}+2\pi\alpha' F_{\mu\nu}+\partial_\mu Y^I\partial_\nu Y^I \\ &\quad +(G_{IJ}+B_{IJ})\,\partial_\mu Y^I\partial_\nu Y^J+\left(G_{\mu I}+B_{\mu I}\right)\partial_\nu Y^I \\ &\quad +\ (G_{I\nu}+B_{I\nu})\,\partial_\mu Y^I,\end{aligned} \tag{2.7}$$

and T represents the dimensionless tachyon field and Θ characterizes the generalized functional in non-BPS p-membrane. In Eq. (2.7), the rank-2 field strength tensor $F_{\mu\nu}$ is defined as

$$F_{\mu\nu} = \partial_{[\mu}A_{\nu]} \tag{2.8}$$

and $B_{\mu\nu}$ represents a rank-2 Kalb–Ramond field and sometimes this can be interpreted as the pullback of B_{MN} onto the D-brane world volume. Using this specific action, mentioned in Eq. (2.7), we can compute the source contributions and terms for various closed string fields produced by the membrane. Additionally, it is important to note that, on a non-BPS Dp-membrane world volume we have an infinite tower of massive fields, a U(1) gauge field A_μ with the restriction on gauge indices, $0 \leq \mu \leq p$, and a set of scalar fields Y^I, one for each direction y^I transverse besides the tachyonic field to the D-brane. Here it is important to note that $(p+1) \leq I \leq D$, where D is 9 for superstring theory and 25 for bosonic string theory. Within the present set-up the tachyon field is defined in such a way that for

$$T = 0, \quad F = \mathcal{T}_p, \tag{2.9}$$

the a constraint condition is explicitly satisfied. For a non-BPS p membrane the field content C as appearing in the Wess–Zumino (WZ) action contains the Ramond–Ramond (RR) fields but careful observation clearly indicates that the leading order contribution in C is characterized by the p form in the effective action. Also it is important to mention here that, for constant tachyon background T, the Wess–Zumino (WZ) effective action automatically vanishes in the present context as

$$\mathrm{d}T = 0, \tag{2.10}$$

and for such a specific background the generalized functional Θ can be recast in the following form:

$$\Theta(T, \partial_\mu T, D_\mu \partial_\nu T) = V(T), \tag{2.11}$$

where $V(T)$ represents the effective tachyon potential within which the contribution from the membrane tension is already taken. Consequently Eq. (2.5) can be recast in the following simplified form:

$$S^{(p)}_{\mathrm{DBI}} = -\int \mathrm{d}^{p+1}\sigma\; e^{-\phi}\; V(T)\, \sqrt{-\det\left(\mathcal{Z}_{\mu\nu} + \mathcal{F}_{\mu\nu}\right)}. \tag{2.12}$$

For non-BPS string theory in the constant dilaton background the purely tachyonic part of the action, after inclusion of the massless fields on the Dp-membrane world volume around the tachyon vacuum, is given by

$$S^{(p)}_{\mathrm{D}} = -\int \mathrm{d}^{p+1}\sigma\; V(T)\, \sqrt{-\det\left(\mathcal{Z}_{\mu\nu} + F_{\mu\nu} + \partial_\mu Y^I \partial_\nu Y^I\right)}. \tag{2.13}$$

After neglecting the contribution from the massless fields for non-BPS string theory the tachyonic part of the effective action describing the Dp-brane world volume is given by [122–124] the following simplified form:

$$\begin{aligned} S^{(p)}_{\mathrm{D}} &= -\int \mathrm{d}^{p+1}\sigma\; V(T)\, \sqrt{-\det\left(\mathcal{Z}_{\mu\nu}\right)} \\ &= -\int \mathrm{d}^{p+1}\sigma\; V(T)\, \sqrt{-\det\left(G_{\mu\nu} + \alpha' \partial_\mu T \partial_\nu T\right)} \\ &= -\int \mathrm{d}^{p+1}\sigma\; \sqrt{-g}\; V(T)\, \sqrt{1 + \alpha' g^{\mu\nu} \partial_\mu T \partial_\nu T}. \end{aligned} \tag{2.14}$$

In a more generalized prescription Eq. (2.14) can be modified into the following effective action:

$$S^{(pq)}_{\mathrm{D}} = -\int \mathrm{d}^{p+1}\sigma\; \sqrt{-g}\; V(T)\; \left(1 + \alpha' g^{\mu\nu} \partial_\mu T \partial_\nu T\right)^q, \tag{2.15}$$

which we identified with the most generalized Gtachyon action in string theory. Here for $p = 3$, i.e., for the D3 brane, Eq. (2.14) refers to the following crucial issues:

- Here $p = 3, q = 1/2$ corresponds to the exact tachyonic behavior of the effective action and it is commonly used to describe the cosmological dynamics,
- Here $p = 3, q = 1$ corresponds to the single field behavior in cosmological dynamics where the kinetic term of the tachyon field is non-canonical. In this case the non-canonical contribution in the effective action is given by $\alpha' V(T)$, where $V(T)$ is the tachyon effective potential. This situation is different from the usual single field models of inflation where the kinetic term is canonical within the framework of string theory.
- For $p = 3, 1/2 < q < 1$ or $p = 3, q < 1/2$ or $p = 3, q > 1$ it contains various non-trivial features in cosmological dynamics. In this case the effective action is significantly different from the usual tachyon action as appearing in the context of string theory. In this case the effective action describes a huge class of effective field theories of inflationary models which can be embedded within the framework of tachyon in string theory. In the present context, the generalized factor $V(T)\; \left(1 + \alpha' g^{\mu\nu} \partial_\mu T \partial_\nu T\right)^q$ with exponent q can be treated as Wilsonian operators as appearing in the context of effective field theory. For an example let us consider a situation where we treat the Regge slope parameter α' to be small. In this case the generalized factor $V(T)\; \left(1 + \alpha' g^{\mu\nu} \partial_\mu T \partial_\nu T\right)^q$ takes the following structure:

$$\begin{aligned} &V(T)\; \left(1 + \alpha' g^{\mu\nu} \partial_\mu T \partial_\nu T\right)^q \\ &\quad = V(T) \sum_{k=0}^{q} {}^qC_k \left(\alpha' g^{\mu\nu} \partial_\mu T \partial_\nu T\right)^k \\ &\quad = V(T) \Bigg[1 + q\left(\alpha' g^{\mu\nu} \partial_\mu T \partial_\nu T\right) \\ &\qquad + \frac{q(q-1)}{2} \left(\alpha' g^{\mu\nu} \partial_\mu T \partial_\nu T\right)^2 + \cdots\Bigg], \end{aligned} \tag{2.16}$$

where $\cdots$ contains higher order terms which are suppressed by the powers of the Regge slope parameter α'. Here for each value of $k(= 0, 1, 2, \ldots, q)$ the expansion factor ${}^qC_k\,(\alpha')^k$ mimics the role of Wilson coefficients.

Here we would like to point out that the tachyon mode appears in the quantization of the open string struck to the non-BPS brane. The effective action of this tachyon field is constructed on the assumption that the tachyon field couples only to the graviton of the closed string sector with fixed vacuum expectation value for dilation field. The open string tachyon condensation phenomenon fits in well with this assumption.

For a multi-tachyonic field scenario one can generalize the tachyonic part of the non-BPS action as stated in Eqs. (2.14) and (2.15):

$$S_{\rm D}^{(p)} = -\sum_{i=1}^{N}\int {\rm d}^{p+1}\sigma\,\sqrt{-g}\,V(T_i)\,\sqrt{1+\alpha' g^{\mu\nu}\partial_\mu T_i \partial_\nu T_i}, \tag{2.17}$$

$$S_{\rm D}^{(pq)} = -\sum_{i=1}^{N}\int {\rm d}^{p+1}\sigma\,\sqrt{-g}\,V(T_i)\,\left(1+\alpha' g^{\mu\nu}\partial_\mu T_i \partial_\nu T_i\right)^q . \tag{2.18}$$

In this case one can introduce a total effective potential of tachyonic fields $V_E(T)$, which can be expressed in terms of N component tachyonic fields as

$$V_E(T) = \sum_{i=1}^{N} V(T_i), \tag{2.19}$$

which is very useful to study the cosmological dynamics for the $p = 3$ case, i.e., for the D3 brane.

Also for the assisted case one can assume all N multi-tachyonic fields are identical to each other, i.e.,

$$T_i = T \quad \forall\, i = 1, 2, 3, \ldots, N. \tag{2.20}$$

Consequently in such a prescription Eqs. (2.17) and (2.18) can be rewritten as

$$\begin{aligned} S_{\rm D}^{(p)} &= -\sum_{i=1}^{N}\int {\rm d}^{p+1}\sigma\,\sqrt{-g}\,V(T)\,\sqrt{1+\alpha' g^{\mu\nu}\partial_\mu T \partial_\nu T} \\ &= -\int {\rm d}^{p+1}\sigma\,\sqrt{-g}\,NV(T)\,\sqrt{1+\alpha' g^{\mu\nu}\partial_\mu T \partial_\nu T}, \end{aligned} \tag{2.21}$$

$$\begin{aligned} S_{\rm D}^{(pq)} &= -\sum_{i=1}^{N}\int {\rm d}^{p+1}\sigma\,\sqrt{-g}\,V(T)\,\left(1+\alpha' g^{\mu\nu}\partial_\mu T \partial_\nu T_i\right)^q \\ &= -\int {\rm d}^{p+1}\sigma\,\sqrt{-g}\,NV(T)\,\left(1+\alpha' g^{\mu\nu}\partial_\mu T \partial_\nu T\right)^q . \end{aligned} \tag{2.22}$$

In this case the total effective potential of the tachyonic fields $V_E(T)$ can be recast as

$$V_E(T) = \sum_{i=1}^{N} V(T_i) = \sum_{i=1}^{N} V(T) = NV(T). \tag{2.23}$$

In the next section we will discuss the various aspects of tachyonic potential $V(T)$ and also mention the various models of tachyonic potential that can be derived from a string theory background.

3 Variants of tachyonic models in string theory

On general string theoretic grounds, one can argued that at the specified minimum T_0 of the effective potential $V(T)$ vanishes [122–124], i.e.,

$$V(T_0) = 0. \tag{3.1}$$

Consequently the world volume action vanishes identically and in this situation the gauge field mimics the role of Lagrange multiplier field. Finally this imposes a constraint on the non-BPS set-up such that the gauge current also vanishes identically. This implies that all the states which are charged under this gauge field are to disappear from the spectrum. Also it is important to mention another important feature of the tachyonic potential in which it admits kink profile for the stringy tachyonic field. Also on an unstable non-BPS p-brane tachyon condensation occurs to form a kink profile and finally it forms a stable BPS $(p-1)$ brane configuration. This kink profile for the tachyon is expected to give a δ-function from ${\rm d}T$ - contribution and thus to reproduce the standard WZ term in the resulting $D(p-1)$-brane. Most importantly, the kink solution effectively reduces the dimension of the world volume by one. Although finding an explicit form of the tachyonic potential is a very difficult, string theory predicts the approximated form of the tachyonic potential. Additionally, we also assume that the tachyonic potential $V(T)$ satisfies the following properties to describe the cosmological dynamics for the non-BPS D3 brane set-up:

1. The tachyonic potential at $T = 0$ satisfies

$$V(T = 0) = \lambda = \frac{M_s^4}{(2\pi)^3 g_s}, \tag{3.2}$$

where g_s is the string coupling constant and M_s signifies the mass scale of the tachyonic string theory. For multi-tachyonic field and assisted case Eq. (3.2) is modified as

$$\begin{aligned} V_E(T = 0) &= \sum_{i=1}^{N} V(T_i = 0) = \sum_{i=1}^{N} \lambda_i \\ &= \sum_{i=1}^{N} \frac{M_s^4}{(2\pi)^3 g_s^{(i)}}, \end{aligned} \tag{3.3}$$

$$V_E(T=0)=\sum_{i=1}^{N}V(T_i=T=0)=\sum_{i=1}^{N}\lambda_i=N\lambda$$
$$=\frac{M_s^4 N}{(2\pi)^3 g_s}. \quad (3.4)$$

Here $g_s^{(i)}$ represents the string coupling constant for the ith field content, which are not same for all N tachyonic degrees of freedom. For the sake of simplicity, here we also assume that the mass scale associated with N tachyons for multi-tachyonic case and assisted case is identical for all degrees of freedom. On the other hand, for the assisted case we assume all couplings are exactly identical and consequently we get an overall factor of N multiplied with the result obtained for the single tachyonic field case.

2. Inflation generally takes place at an energy scale:

$$V_{\rm inf}^{1/4}=V^{1/4}(\tilde{T}_0)\propto\lambda^{1/4} \quad (3.5)$$

with the single tachyon field fixed at $T\sim\tilde{T}_0$, and within the set-up of string theory $\tilde{T}_0$ is identified to be the mass scale of the tachyon by in the following fashion:

$$\tilde{T}_0\sim M_s. \quad (3.6)$$

For the multi-tachyonic field case Eqs. (3.5) and (3.6) are modified as

$$V_{\rm inf}^{1/4}=V_E^{1/4}=\left\{\sum_{i=1}^{N}V(\tilde{T}_{0i})\right\}^{1/4}\propto\left\{\sum_{i=1}^{N}\lambda_i\right\}^{1/4}$$
$$=\left\{\sum_{i=1}^{N}\frac{M_s^4}{(2\pi)^3 g_s^{(i)}}\right\}^{1/4}, \quad (3.7)$$

$$\tilde{T}_0\sim\sum_{i=1}^{N}\tilde{T}_{0i}=M_s. \quad (3.8)$$

Similarly, for the assisted case Eqs. (3.5) and (3.6) are modified as

$$V_{\rm inf}^{1/4}=V_E^{1/4}=\left\{\sum_{i=1}^{N}V(\tilde{T}_{0i})\right\}^{1/4}\propto\left\{\sum_{i=1}^{N}\lambda_i\right\}^{1/4}$$
$$=(N\lambda)^{1/4}=\left\{\frac{M_s^4 N}{(2\pi)^3 g_s}\right\}^{1/4}, \quad (3.9)$$

$$\tilde{T}_0\sim\sum_{i=1}^{N}\tilde{T}_{0i}=\sum_{i=1}^{N}\tilde{T}_0=N\tilde{T}_0=NM_s. \quad (3.10)$$

3. For $T>0$ the first derivative of the single tachyonic potential is always positive, i.e.,

$$V'(T>0)>0 \quad (3.11)$$

where $'$ represents differentiation with respect to the tachyon field T. For the multi-tachyonic and assisted cases Eq. (3.11) can be recast as

$$V_E'(T>0)=\sum_{i=1}^{N}\frac{\mathrm{d}V(T_i>0)}{\mathrm{d}T_i}>0, \quad (3.12)$$

$$V_E'(T>0)=\sum_{i=1}^{N}\frac{\mathrm{d}V(T_i>0)}{\mathrm{d}T_i}=\sum_{i=1}^{N}\frac{\mathrm{d}V(T>0)}{\mathrm{d}T}$$
$$=NV'(T>0)>0. \quad (3.13)$$

4. At the asymptotic case of the single tachyonic field $|T|\to\infty$ the potential should satisfy

$$V(|T|\to\infty)\to 0. \quad (3.14)$$

For the multi-tachyonic and assisted cases Eq. (3.13) can be recast thus:

$$V_E(|T|\to\infty)=\sum_{i=1}^{N}V(|T_i|\to\infty)\to 0, \quad (3.15)$$

$$V_E(|T|\to\infty)=\sum_{i=1}^{N}V(|T_i|\to\infty)$$
$$=NV(|T|\to\infty)\to 0. \quad (3.16)$$

5. Also one can consider that the tachyonic potential contains a global maximum at $T=0$, i.e.,

$$V''(T=0)<0 \quad (3.17)$$

for which the value of the potential is given by Eq. (3.2). Similarly for the multi-tachyonic and assisted cases Eq. (3.18) can be recast thus:

$$V_E''(T=0)=\sum_{i=1}^{N}\frac{\mathrm{d}^2V(T_i>0)}{\mathrm{d}T_i^2}<0, \quad (3.18)$$

$$V_E''(T=0)=\sum_{i=1}^{N}\frac{\mathrm{d}^2V(T_i>0)}{\mathrm{d}T_i^2}=\sum_{i=1}^{N}\frac{\mathrm{d}^2V(T>0)}{\mathrm{d}T^2}$$
$$=NV''(T=0)<0. \quad (3.19)$$

In the next subsections we mention variants of the tachyonic potentials which satisfy the various above mentioned characteristics.

3.1 Model I: inverse cosh potential

For single field case the first model of the tachyonic potential is given by [55,56,84,126]

$$V(T)=\frac{\lambda}{\cosh\left(\frac{T}{T_0}\right)}, \tag{3.20}$$

and for the multi-tachyonic and assisted cases the total effective potential is given by

$$V_E(T)=\begin{cases}\displaystyle\sum_{i=1}^{N}\frac{\lambda_i}{\cosh\left(\frac{T_i}{T_{0i}}\right)}, & \text{for Multi tachyonic,}\\ \displaystyle\sum_{i=1}^{N}\frac{\lambda}{\cosh\left(\frac{T}{T_0}\right)} & \\ \quad =\frac{N\lambda}{\cosh\left(\frac{T}{T_0}\right)}, & \text{for Assisted tachyonic.}\end{cases} \tag{3.21}$$

Here the potential satisfies the following criteria:

- At $T=0$ for the single field tachyonic potential:

  $$V(T=0)=\lambda \tag{3.22}$$

  and for the multi-tachyonic and assisted cases we have

  $$V_E(T=0)=\sum_{i=1}^{N}\lambda_i, \tag{3.23}$$

  $$V_E(T=0)=\sum_{i=1}^{N}\lambda_i=N\lambda. \tag{3.24}$$

- At $T=T_0$ for the single field tachyonic potential:

  $$V(T=T_0)=\frac{\lambda}{\cosh(1)}\neq 0 \tag{3.25}$$

  and for the multi-tachyonic and assisted cases we have

  $$V_E(T=0)=\sum_{i=1}^{N}\frac{\lambda_i}{\cosh(1)}\neq 0, \tag{3.26}$$

  $$V_E(T=0)=\sum_{i=1}^{N}\frac{\lambda_i}{\cosh(1)}=\frac{N\lambda}{\cosh(1)}\neq 0. \tag{3.27}$$

- For the single field tachyonic potential:

  $$V'(T)=-\frac{\lambda}{T_0}\text{sech}\left(\frac{T}{T_0}\right)\tanh\left(\frac{T}{T_0}\right), \tag{3.28}$$

  $$V''(T)=-\frac{\lambda}{T_0^2}\left[\text{sech}^3\left(\frac{T}{T_0}\right)-\text{sech}\left(\frac{T}{T_0}\right)\tanh^2\left(\frac{T}{T_0}\right)\right]. \tag{3.29}$$

Now to find the extrema of the potential we substitute

$$V'(T)=0 \tag{3.30}$$

which give rise to the following solutions for the tachyonic field:

$$|T|=2m\ T_0\pi,\quad (2m+1)\ T_0\pi \tag{3.31}$$

where $m\in\mathbb{Z}$. Further substituting the solutions for tachyonic field in Eq. (3.29) we get

$$V''(|T|=2m\ T_0\pi)=-\frac{\lambda}{T_0^2}, \tag{3.32}$$

$$V''(|T|=(2m+1)\ T_0\pi)=-\frac{\lambda}{T_0^2}, \tag{3.33}$$

and at these points the value of the potential is computed as

$$V(|T|=2m\ T_0\pi)=\frac{\lambda}{\cosh(2m\ \pi)}=\lambda\ \text{sech}\,(2m\ \pi), \tag{3.34}$$

$$V(|T|=(2m+1)\ T_0\pi)=\frac{\lambda}{\cosh((2m+1)\ \pi)}=\lambda\ \text{sech}\,((2m+1)\ \pi). \tag{3.35}$$

It is important to note for the single tachyonic case that for $\lambda>0$, $V''(|T|=2m\ T_0\pi,\ (2m+1)\ T_0\pi)>0$, i.e., we get maxima on the potential and for the assisted case the results are the same, provided the following replacement occurs:

$$\lambda\rightarrow N\lambda, \tag{3.36}$$

and finally for the multi-tachyonic case we have

$$V'(T_i)=-\frac{\lambda_i}{T_{0i}}\text{sech}\left(\frac{T_i}{T_{0i}}\right)\tanh\left(\frac{T_i}{T_{0i}}\right), \tag{3.37}$$

$$V''(T_i)=-\frac{\lambda_i}{T_{0i}^2}\left[\text{sech}^3\left(\frac{T_i}{T_{0i}}\right)-\text{sech}\left(\frac{T_i}{T_{0i}}\right)\tanh^2\left(\frac{T_i}{T_{0i}}\right)\right]. \tag{3.38}$$

Now to find the extrema of the potential we substitute

$$V'(T_j)=0\quad\forall\ j=1,2,\ldots,N \tag{3.39}$$

which gives rise to the following solutions for the jth tachyonic field:

$$|T_j| = 2m\ T_{0j}\pi, \quad (2m+1)\ T_{0j}\pi \quad \forall\ j = 1, 2, \ldots, N \tag{3.40}$$

where $m \in \mathbb{Z}$. Further substituting the solutions for tachyonic field in Eq. (3.38) we get

$$V''(|T_j| = 2m\ T_{0j}\pi) = -\frac{\lambda_j}{T_{0j}^2}, \tag{3.41}$$

$$V''(|T_j| = (2m+1)\ T_{0j}\pi) = -\frac{\lambda_j}{T_{0j}^2}, \tag{3.42}$$

and at these points the value of the total effective potential is computed as

$$V_E^{(1)} = \sum_{j=1}^{N} V(|T_j| = 2m\ T_{0j}\pi) = \sum_{j=1}^{N} \frac{\lambda_j}{\cosh(2m\ \pi)} = \operatorname{sech}(2m\ \pi) \sum_{j=1}^{N} \lambda_j, \tag{3.43}$$

$$V_E^{(2)} = \sum_{j=1}^{N} V(|T_j| = (2m+1)\ T_{0j}\pi) = \sum_{j=1}^{N} \frac{\lambda_j}{\cosh((2m+1)\ \pi)} = \operatorname{sech}((2m+1)\ \pi) \sum_{j=1}^{N} \lambda_j. \tag{3.44}$$

It is important to note for the multi-tachyonic case that for $\lambda_j > 0$, $V''(|T_j| = 2m\ T_{0j}\pi,\ \ (2m+1)\ T_{0j}\pi) > 0$, i.e., we get maxima on the potential $V(T_j)$ as well as in $V_E(T)$.

3.2 Model II: logarithmic potential

For single field case the second model of the tachyonic potential is given by [79]

$$V(T) = \lambda \left\{ \left(\frac{T}{T_0}\right)^2 \left[\ln\left(\frac{T}{T_0}\right)\right]^2 + 1 \right\}, \tag{3.45}$$

and for the multi-tachyonic and assisted cases the total effective potential is given by

$$V_E(T) = \begin{cases} \sum_{i=1}^{N} \lambda_i \left\{ \left(\frac{T_i}{T_{0i}}\right)^2 \left[\ln\left(\frac{T_i}{T_{0i}}\right)\right]^2 + 1 \right\}, & \text{for Multi tachyonic,} \\ \sum_{i=1}^{N} \lambda \left\{ \left(\frac{T}{T_0}\right)^2 \left[\ln\left(\frac{T}{T_0}\right)\right]^2 + 1 \right\} \\ = N\lambda \left\{ \left(\frac{T}{T_0}\right)^2 \left[\ln\left(\frac{T}{T_0}\right)\right]^2 + 1 \right\}, & \text{for Assisted tachyonic.} \end{cases} \tag{3.46}$$

Here the potential satisfies the following criteria:

- At $T = 0$ for the single field tachyonic potential:

$$V(T = 0) = \lambda \tag{3.47}$$

and for the multi-tachyonic and assisted cases we have

$$V_E(T = 0) = \sum_{i=1}^{N} \lambda_i, \tag{3.48}$$

$$V_E(T = 0) = \sum_{i=1}^{N} \lambda_i = N\lambda. \tag{3.49}$$

- At $T = T_0$ for the single field tachyonic potential:

$$V(T = T_0) = \lambda, \tag{3.50}$$

and for the multi-tachyonic and assisted cases we have

$$V_E(T = T_0) = \sum_{i=1}^{N} \lambda_i, \tag{3.51}$$

$$V_E(T = T_0) = \sum_{i=1}^{N} \lambda_i = N\lambda. \tag{3.52}$$

- For the single field tachyonic potential:

$$V'(T) = \frac{2T\lambda}{T_0^2} \ln\left(\frac{T}{T_0}\right) \left[1 + \ln\left(\frac{T}{T_0}\right)\right], \tag{3.53}$$

$$V''(T) = \frac{2\lambda}{T_0^2} \left[1 + 3\ln\left(\frac{T}{T_0}\right) + \ln^2\left(\frac{T}{T_0}\right)\right]. \tag{3.54}$$

Now to find the extrema of the potential we substitute

$$V'(T) = 0 \tag{3.55}$$

which give rise to the following solutions for the tachyonic field:

$$T = 0, \quad T_0, \quad \frac{T_0}{e}. \tag{3.56}$$

Further substituting the solutions for the tachyonic field in Eq. (3.54) we get

$$V''(T=0) \to \infty, \tag{3.57}$$
$$V''(T=T_0) = \frac{2\lambda}{T_0^2}, \tag{3.58}$$
$$V''\left(T=\frac{T_0}{e}\right) = -\frac{2\lambda}{T_0^2}, \tag{3.59}$$

and at these points the value of the potential is computed as

$$V(T=0) = \lambda, \tag{3.60}$$
$$V(T=T_0) = \lambda, \tag{3.61}$$
$$V\left(T=\frac{T_0}{e}\right) = \lambda\left(1+\frac{1}{e^2}\right). \tag{3.62}$$

It is important to note for the single tachyonic case that for $\lambda > 0$, $V''(T=T_0) > 0$ and $V''(T=\frac{T_0}{e}) < 0$ i.e., we get both maxima and minima on the potential. For the assisted case the results are the same, provided the following replacement occurs:

$$\lambda \to N\lambda, \tag{3.63}$$

and finally for the multi-tachyonic case we have

$$V'(T_i) = \frac{2\lambda_i T_i}{T_{0i}^2}\ln\left(\frac{T_i}{T_{0i}}\right)\left[1+\ln\left(\frac{T_i}{T_{0i}}\right)\right], \tag{3.64}$$
$$V''(T_i) = \frac{2\lambda_i}{T_{0i}^2}\left[1+3\ln\left(\frac{T_i}{T_{0i}}\right)+\ln^2\left(\frac{T_i}{T_{0i}}\right)\right]. \tag{3.65}$$

Now to find the extrema of the potential we substitute

$$V'(T_j) = 0 \quad \forall j = 1,2,\ldots,N \tag{3.66}$$

which give rise to the following solutions for the jth tachyonic field:

$$T_j = 0, \quad T_{0j}, \quad \frac{T_{0j}}{e} \quad \forall\, j = 1,2,\ldots,N. \tag{3.67}$$

Further substituting the solutions for the tachyonic field in Eq. (3.65) we get

$$V''(T_j=0) \to \infty, \tag{3.68}$$
$$V''(T_j=T_{0j}) = \frac{2\lambda_j}{T_{0j}^2}, \tag{3.69}$$
$$V''\left(T_j=\frac{T_{0j}}{e}\right) = -\frac{2\lambda_j}{T_{0j}^2}, \tag{3.70}$$

and at these points the value of the total effective potential is computed as

$$V_E^{(1)} = \sum_{j=1}^{N} V(T_j=0) = \sum_{j=1}^{N}\lambda_j, \tag{3.71}$$
$$V_E^{(2)} = \sum_{j=1}^{N} V(T_j=T_{0j}) = \sum_{j=1}^{N}\lambda_j, \tag{3.72}$$
$$V_E^{(3)} = \sum_{j=1}^{N} V\left(T_j=\frac{T_{0j}}{e}\right) = \left(1+\frac{1}{e^2}\right)\sum_{j=1}^{N}\lambda_j. \tag{3.73}$$

It is important to note for the multi-tachyonic case that for $\lambda_j > 0$, $V''(T=T_{0j}) > 0$ and $V''(T=\frac{T_{0j}}{e}) < 0$, i.e., we get both maxima and minima on the potential $V(T_j)$ as well as in $V_E(T)$.

3.3 Model III: exponential potential Type-I

For single field case the third model of the tachyonic potential is given by [83]

$$V(T) = \lambda\exp\left(-\frac{T}{T_0}\right), \tag{3.74}$$

and for the multi-tachyonic and assisted cases the total effective potential is given by

$$V_E(T) = \begin{cases} \sum_{i=1}^{N}\lambda_i\exp\left(-\frac{T_i}{T_{0i}}\right), & \text{for Multi tachyonic,} \\ \sum_{i=1}^{N}\lambda\exp\left(-\frac{T}{T_0}\right) & \\ \quad = N\lambda\exp\left(-\frac{T}{T_0}\right), & \text{for Assisted tachyonic.} \end{cases} \tag{3.75}$$

Here the potential satisfies the following criteria:

- At $T=0$ for the single field tachyonic potential:

$$V(T=0) = \lambda \tag{3.76}$$

and for the multi-tachyonic and assisted cases we have

$$V_E(T=0) = \sum_{i=1}^{N}\lambda_i, \tag{3.77}$$
$$V_E(T=0) = \sum_{i=1}^{N}\lambda_i = N\lambda. \tag{3.78}$$

- At $T = T_0$ for the single field tachyonic potential:

$$V(T = T_0) = \frac{\lambda}{e} \tag{3.79}$$

and for the multi-tachyonic and assisted cases we have

$$V_E(T = T_0) = \frac{1}{e}\sum_{i=1}^{N}\lambda_i, \tag{3.80}$$

$$V_E(T = T_0) = \frac{1}{e}\sum_{i=1}^{N}\lambda_i = \frac{N\lambda}{e}. \tag{3.81}$$

- For the single field tachyonic potential:

$$V'(T) = -\frac{\lambda}{T_0}\exp\left(-\frac{T}{T_0}\right), \tag{3.82}$$

$$V''(T) = \frac{\lambda}{T_0^2}\exp\left(-\frac{T}{T_0}\right). \tag{3.83}$$

Now to find the extrema of the potential we substitute

$$V'(T) = 0, \tag{3.84}$$

which gives rise to the following solution for the tachyonic field:

$$T \to \infty. \tag{3.85}$$

Further substituting the solutions for the tachyonic field in Eq. (3.83) we get

$$V''(T \to \infty) \to 0, \tag{3.86}$$

and also at the points $T = 0,\ T_0$ we have

$$V''(T = 0) = \frac{\lambda}{T_0^2}, \tag{3.87}$$

$$V''(T = T_0) = \frac{\lambda}{eT_0^2}, \tag{3.88}$$

and at these points the value of the potential is computed as

$$V(T \to \infty) \to 0, \tag{3.89}$$

$$V(T = 0) = \lambda, \tag{3.90}$$

$$V(T = T_0) = \frac{\lambda}{e}. \tag{3.91}$$

It is important to note for the single tachyonic case that for $\lambda > 0$, $V''(T = 0,\ \ T_0) > 0$, i.e., we get an asymptotic behavior of the potential. For the assisted case the results are the same, provided the following replacement occurs:

$$\lambda \to N\lambda, \tag{3.92}$$

and finally for the multi-tachyonic case we have

$$V'(T_i) = -\frac{\lambda_i}{T_0}\exp\left(-\frac{T_i}{T_{0i}}\right), \tag{3.93}$$

$$V''(T_i) = \frac{\lambda_i}{T_{0i}^2}\exp\left(-\frac{T_i}{T_{0i}}\right). \tag{3.94}$$

Now to find the extrema of the potential we substitute

$$V'(T_j) = 0 \quad \forall\ j = 1, 2, \ldots, N \tag{3.95}$$

which gives rise to the following solutions for the jth tachyonic field:

$$T_j \to \infty. \tag{3.96}$$

Further substituting the solutions for the tachyonic field in Eq. (3.94) we get

$$V''(T_j \to \infty) \to 0, \tag{3.97}$$

and also at the points $T_j = 0,\ T_{0j}$ we have

$$V''(T_j = 0) = \frac{\lambda_j}{T_{0j}^2}, \tag{3.98}$$

$$V''(T_j = T_{0j}) = \frac{\lambda_j}{eT_{0j}^2}, \tag{3.99}$$

and at these points the value of the total effective potential is computed as

$$V_E^{(1)} = \sum_{j=1}^{N} V(T_j \to \infty) \to 0, \tag{3.100}$$

$$V_E^{(2)} = \sum_{j=1}^{N} V(T_j = 0) = \sum_{j=1}^{N}\lambda_j, \tag{3.101}$$

$$V_E^{(3)} = \sum_{j=1}^{N} V(T_j = T_{0j}) = \frac{1}{e}\sum_{j=1}^{N}\lambda_j. \tag{3.102}$$

It is important to note for the multi-tachyonic case that for $\lambda_j > 0$, $V''(T = 0,\ \ T_{0j}) > 0$, i.e., we get an asymptotic behavior of the potential $V(T_j)$ as well as in $V_E(T)$.

3.4 Model IV: exponential potential Type-II (Gaussian)

For single field case the first model of the tachyonic potential is given by [127]

$$V(T) = \lambda \exp\left[-\left(\frac{T}{T_0}\right)^2\right], \tag{3.103}$$

and for the multi-tachyonic and assisted cases the total effective potential is given by

$$V_E(T) = \begin{cases} \sum_{i=1}^{N} \lambda \exp\left[-\left(\frac{T}{T_0}\right)^2\right], & \text{for Multi tachyonic} \\ \sum_{i=1}^{N} \lambda \exp\left[-\left(\frac{T}{T_0}\right)^2\right] \\ \quad = N\lambda \exp\left[-\left(\frac{T}{T_0}\right)^2\right], & \text{for Assisted tachyonic.} \end{cases} \tag{3.104}$$

Here the potential satisfies the following criteria:

- At $T = 0$ for single field tachyonic potential:

$$V(T = 0) = \lambda \tag{3.105}$$

and for the multi-tachyonic and assisted cases we have

$$V_E(T = 0) = \sum_{i=1}^{N} \lambda_i, \tag{3.106}$$

$$V_E(T = 0) = \sum_{i=1}^{N} \lambda_i = N\lambda. \tag{3.107}$$

- At $T = T_0$ for the single field tachyonic potential:

$$V(T = T_0) = \frac{\lambda}{e} \tag{3.108}$$

and for the multi-tachyonic and assisted cases we have

$$V_E(T = T_0) = \frac{1}{e}\sum_{i=1}^{N} \lambda_i, \tag{3.109}$$

$$V_E(T = T_0) = \frac{1}{e}\sum_{i=1}^{N} \lambda_i = \frac{N\lambda}{e}. \tag{3.110}$$

- For the single field tachyonic potential:

$$V'(T) = -\frac{2\lambda T}{T_0^2} \exp\left[-\left(\frac{T}{T_0}\right)^2\right], \tag{3.111}$$

$$V''(T) = -\frac{2\lambda}{T_0^2} \exp\left[-\left(\frac{T}{T_0}\right)^2\right]\left\{1 - \frac{2T^2}{T_0^2}\right\}. \tag{3.112}$$

Now to find the extrema of the potential we substitute

$$V'(T) = 0, \tag{3.113}$$

which gives rise to the following solution for the tachyonic field:

$$T = 0,\ \infty. \tag{3.114}$$

Further substituting the solutions for the tachyonic field in Eq. (3.112) we get

$$V''(T = 0) = -\frac{2\lambda}{T_0^2}, \tag{3.115}$$

$$V''(T \to \infty) \to 0 \tag{3.116}$$

and also additionally for $T = T_0$ we have

$$V''(T = T_0) = \frac{2\lambda}{eT_0^2}, \tag{3.117}$$

and at these points the value of the potential is computed as

$$V(T \to \infty) \to 0, \tag{3.118}$$

$$V(T = 0) = \lambda, \tag{3.119}$$

$$V(T = T_0) = \frac{\lambda}{e}. \tag{3.120}$$

It is important to note for the single tachyonic case that for $\lambda > 0$, $V''(T = 0,\ \ T_0) > 0$, i.e., we get maxima on the potential. For the assisted case the results are the same, provided the following replacement occurs:

$$\lambda \to N\lambda, \tag{3.121}$$

and finally for the multi-tachyonic case we have

$$V'(T_i) = -\frac{2\lambda_i T_i}{T_{0i}^2} \exp\left[-\left(\frac{T_i}{T_{0i}}\right)^2\right], \tag{3.122}$$

$$V''(T_i) = -\frac{2\lambda_i}{T_{0i}^2} \exp\left[-\left(\frac{T_i}{T_{0i}}\right)^2\right]\left\{1 - \frac{2T_i^2}{T_{0i}^2}\right\}. \tag{3.123}$$

Now to find the extrema of the potential we substitute

$$V'(T_j) = 0 \quad \forall\ j = 1, 2, \ldots, N \tag{3.124}$$

which give rise to the following solutions for the jth tachyonic field:

$$T_j = 0,\ \infty. \tag{3.125}$$

Further substituting the solutions for the tachyonic field in Eq. (3.123) we get

$$V''(T_j = 0) = -\frac{2\lambda}{T_0^2}, \tag{3.126}$$

$$V''(T_j \to \infty) \to 0, \tag{3.127}$$

Additionally for the point $T_j = T_{0j}$ we have

$$V''(T_j = T_{0j}) = \frac{2\lambda_j}{eT_{0j}^2}, \tag{3.128}$$

and at these points the value of the total effective potential is computed as

$$V_E^{(1)} = \sum_{j=1}^{N} V(T_j \to \infty) \to 0, \tag{3.129}$$

$$V_E^{(2)} = \sum_{j=1}^{N} V(T_j = 0) = \sum_{j=1}^{N} \lambda_j, \tag{3.130}$$

$$V_E^{(3)} = \sum_{j=1}^{N} V(T_j = T_{0j}) = \frac{1}{e}\sum_{j=1}^{N} \lambda_j. \tag{3.131}$$

It is important to note for the multi-tachyonic case that for $\lambda_j > 0$, $V''(T = 0,\ \ T_{0j}) > 0$, i.e., we get maxima on the potential $V(T_j)$ as well as in $V_E(T)$.

3.5 Model V: inverse power-law potential

For the single field case the first model of the tachyonic potential is given by [86,128]

$$V(T) = \frac{\lambda}{\left[1 + \left(\frac{T}{T_0}\right)^4\right]}, \tag{3.132}$$

and for the multi-tachyonic and assisted cases the total effective potential is given by

$$V_E(T) = \begin{cases} \displaystyle\sum_{i=1}^{N} \frac{\lambda_i}{\left[1 + \left(\frac{T_i}{T_{0i}}\right)^4\right]}, & \text{for Multi tachyonic} \\ \displaystyle\sum_{i=1}^{N} \frac{\lambda}{\left[1 + \left(\frac{T}{T_0}\right)^4\right]} \\ \displaystyle = \frac{N\lambda}{\left[1 + \left(\frac{T}{T_0}\right)^4\right]}, & \text{for Assisted tachyonic.} \end{cases} \tag{3.133}$$

Here the potential satisfies the following criteria:

- At $T = 0$ for the single field tachyonic potential:

$$V(T = 0) = \lambda, \tag{3.134}$$

and for the multi-tachyonic and assisted cases we have

$$V_E(T = 0) = \sum_{i=1}^{N} \lambda_i, \tag{3.135}$$

$$V_E(T = 0) = \sum_{i=1}^{N} \lambda_i = N\lambda. \tag{3.136}$$

- At $T = T_0$ for the single field tachyonic potential:

$$V(T = T_0) = \frac{\lambda}{2} \tag{3.137}$$

and for the multi-tachyonic and assisted cases we have

$$V_E(T = T_0) = \frac{1}{2}\sum_{i=1}^{N} \lambda_i, \tag{3.138}$$

$$V_E(T = T_0) = \frac{1}{2}\sum_{i=1}^{N} \lambda_i = \frac{N\lambda}{2}. \tag{3.139}$$

- For single field tachyonic potential:

$$V'(T) = -\frac{4\lambda T^3}{T_0^4\left[1 + \left(\frac{T}{T_0}\right)^4\right]^2}, \tag{3.140}$$

$$V''(T) = \frac{32\lambda T^6}{T_0^8\left[1 + \left(\frac{T}{T_0}\right)^4\right]^3} - \frac{12\lambda T^2}{T_0^4\left[1 + \left(\frac{T}{T_0}\right)^4\right]^2}. \tag{3.141}$$

Now to find the extrema of the potential we substitute

$$V'(T) = 0, \tag{3.142}$$

which give rise to the following solution for the tachyonic field:

$$T = 0,\ \infty. \tag{3.143}$$

Further substituting the solutions for the tachyonic field in Eq. (3.141) we get

$$V''(T = 0) = 0, \tag{3.144}$$

$$V''(T \to \infty) \to 0 \tag{3.145}$$

and also additionally for $T = T_0$ we have

$$V''(T = T_0) = \frac{\lambda}{T_0^2}, \tag{3.146}$$

and at these points the value of the potential is computed as

$$V(T \to \infty) \to 0, \tag{3.147}$$

$$V(T = 0) = \lambda, \tag{3.148}$$

$$V(T = T_0) = \frac{\lambda}{2}. \tag{3.149}$$

It is important to note for the single tachyonic case that for $\lambda > 0$, $V''(T = 0, \ T_0) > 0$, i.e., we get maxima on the potential. For the assisted case the results are the same, provided the following replacement occurs:

$$\lambda \to N\lambda, \tag{3.150}$$

and finally for the multi-tachyonic case we have

$$V'(T_i) = -\frac{4\lambda_i T_i^3}{T_{0i}^4\left[1+\left(\frac{T_i}{T_{0i}}\right)^4\right]^2}, \tag{3.151}$$

$$V''(T_i) = \frac{32\lambda_i T_i^6}{T_{0i}^8\left[1+\left(\frac{T_i}{T_{0i}}\right)^4\right]^3} - \frac{12\lambda_i T_i^2}{T_{0i}^4\left[1+\left(\frac{T_i}{T_{0i}}\right)^4\right]^2}. \tag{3.152}$$

Now to find the extrema of the potential we substitute:

$$V'(T_j) = 0 \ \ \forall\ j = 1, 2, \ldots, N \tag{3.153}$$

which give rise to the following solutions for the jth tachyonic field:

$$T_j = 0, \ \infty. \tag{3.154}$$

Further substituting the solutions for the tachyonic field in Eq. (3.152) we get

$$V''(T_j = 0) = 0, \tag{3.155}$$

$$V''(T_j \to \infty) \to 0, \tag{3.156}$$

Additionally for the point $T_j = T_{0j}$ we have

$$V''(T_j = T_{0j}) = \frac{\lambda_j}{T_{0j}^2}, \tag{3.157}$$

and at these points the value of the total effective potential is computed as

$$V_E^{(1)} = \sum_{j=1}^{N} V(T_j \to \infty) \to 0, \tag{3.158}$$

$$V_E^{(2)} = \sum_{j=1}^{N} V(T_j = 0) = \sum_{j=1}^{N} \lambda_j, \tag{3.159}$$

$$V_E^{(3)} = \sum_{j=1}^{N} V(T_j = T_{0j}) = \frac{1}{2}\sum_{j=1}^{N} \lambda_j. \tag{3.160}$$

It is important to note for the multi-tachyonic case that for $\lambda_j > 0$, $V''(T = 0, \ T_{0j}) > 0$, i.e., we get maxima on the potential $V(T_j)$ as well as in $V_E(T)$.

4 Cosmological dynamics from GTachyon

4.1 Unperturbed evolution

For $p = 3$ non-BPS branes the total tachyonic model action can be written as

$$S_T = \begin{cases} \displaystyle\int d^4\sigma\,\sqrt{-g}\left[\frac{M_p^2}{2}R - V(T)\sqrt{1+\alpha' g^{\mu\nu}\partial_\mu T\partial_\nu T}\right], & \text{for Single,} \\ \displaystyle\int d^4\sigma\,\sqrt{-g}\left[\frac{M_p^2}{2}R - \sum_{i=1}^{N} V(T_i)\sqrt{1+\alpha' g^{\mu\nu}\partial_\mu T_i\partial_\nu T_i}\right], & \text{for Multi,} \\ \displaystyle\int d^4\sigma\,\sqrt{-g}\left[\frac{M_p^2}{2}R - NV(T)\sqrt{1+\alpha' g^{\mu\nu}\partial_\mu T\partial_\nu T}\right], & \text{for Assisted,} \end{cases} \tag{4.1}$$

and in a more generalized situation Eq. (4.1) is modified as

$$S_T^{(q)} = \begin{cases} \int d^4\sigma \sqrt{-g}\left[\frac{M_p^2}{2}R - V(T)\left(1+\alpha' g^{\mu\nu}\partial_\mu T\partial_\nu T\right)^q\right], & \text{for Single,} \\ \int d^4\sigma \sqrt{-g}\left[\frac{M_p^2}{2}R - \sum_{i=1}^{N} V(T_i)\left(1+\alpha' g^{\mu\nu}\partial_\mu T_i\partial_\nu T_i\right)^q\right], & \text{for Multi,} \\ \int d^4\sigma \sqrt{-g}\left[\frac{M_p^2}{2}R - NV(T)\left(1+\alpha' g^{\mu\nu}\partial_\mu T\partial_\nu T\right)^q\right], & \text{for Assisted,} \end{cases} \tag{4.2}$$

where M_p is the reduced Planck mass, $M_p = 2.43 \times 10^{18}$GeV. By varying the action as stated in Eqs. (4.1) and (4.2), with respect to the metric $g_{\mu\nu}$ we get the following equation of motion:

$$G_{\mu\nu} = \frac{T_{\mu\nu}}{M_p^2} \tag{4.3}$$

where $G_{\mu\nu}$ is defined as

$$G_{\nu\nu} = R_{\mu\nu} - \frac{1}{2}g_{\mu\nu}R \tag{4.4}$$

and the energy-momentum stress tensor $T_{\mu\nu}$ is defined as

$$T_{\mu\nu} = -\frac{2}{\sqrt{-g}}\frac{\delta(\sqrt{-g}\mathcal{L}_{\text{Tachyon}})}{\delta g^{\mu\nu}} \tag{4.5}$$

where $\mathcal{L}_{\text{Tachyon}}$ is the tachyonic part of the Lagrangian for non-BPS set-up. Explicitly using Eq. (4.1) the energy-momentum stress tensor can be computed as

$$T_{\mu\nu} = \begin{cases} V(T)\left[\frac{\alpha'\partial_\mu T\partial_\nu T}{\sqrt{1+\alpha' g^{\mu\nu}\partial_\mu T\partial_\nu T}} - g_{\mu\nu}\sqrt{1+\alpha' g^{\mu\nu}\partial_\mu T\partial_\nu T}\right], & \text{for Single,} \\ \sum_{i=1}^{N} V(T_i)\left[\frac{\alpha'\partial_\mu T_i\partial_\nu T_i}{\sqrt{1+\alpha' g^{\mu\nu}\partial_\mu T_i\partial_\nu T_i}} - g_{\mu\nu}\sqrt{1+\alpha' g^{\mu\nu}\partial_\mu T_i\partial_\nu T_i}\right], & \text{for Multi,} \\ NV(T)\left[\frac{\alpha'\partial_\mu T\partial_\nu T}{\sqrt{1+\alpha' g^{\mu\nu}\partial_\mu T\partial_\nu T}} - g_{\mu\nu}\sqrt{1+\alpha' g^{\mu\nu}\partial_\mu T\partial_\nu T}\right], & \text{for Assisted,} \end{cases} \tag{4.6}$$

and similarly in a more generalized situation using Eq. (4.2) the energy-momentum stress tensor can be computed as

$$T_{\mu\nu}^{(q)} = \begin{cases} V(T)\left[\frac{2q\alpha'\partial_\mu T\partial_\nu T}{\left(1+\alpha' g^{\mu\nu}\partial_\mu T\partial_\nu T\right)^{1-q}} - g_{\mu\nu}\left(1+\alpha' g^{\mu\nu}\partial_\mu T\partial_\nu T\right)^q\right], & \text{for Single,} \\ \sum_{i=1}^{N} V(T_i)\left[\frac{2q\alpha'\partial_\mu T_i\partial_\nu T_i}{\left(1+\alpha' g^{\mu\nu}\partial_\mu T_i\partial_\nu T_i\right)^{1-q}} - g_{\mu\nu}\left(1+\alpha' g^{\mu\nu}\partial_\mu T_i\partial_\nu T_i\right)^q\right], & \text{for Multi,} \\ NV(T)\left[\frac{2q\alpha'\partial_\mu T\partial_\nu T}{\left(1+\alpha' g^{\mu\nu}\partial_\mu T\partial_\nu T\right)^{1-q}} - g_{\mu\nu}\left(1+\alpha' g^{\mu\nu}\partial_\mu T\partial_\nu T\right)^q\right], & \text{for Assisted.} \end{cases} \tag{4.7}$$

It clearly appears that, for $q = 1/2$, the result is perfectly consistent with Eq. (4.6). Further using the perfect fluid assumption the energy-momentum stress tensor can be written as

$$T_{\mu\nu} = \begin{cases} (\rho+p)u_\mu u_\nu + g_{\mu\nu}p, & \text{for Single,} \\ \sum_{i=1}^{N}(\rho_i+p_i)u_\mu^{(i)}u_\nu^{(i)} + g_{\mu\nu}p_i, & \text{for Multi,} \\ N\left[(\rho+p)u_\mu u_\nu + g_{\mu\nu}p\right], & \text{for Assisted,} \end{cases} \tag{4.8}$$

where for the assisted case we assume that the density and pressure of all identical tachyonic modes are the same. Here u_μ signifies the four velocity of the fluid, which is defined as

$$u_\mu = \begin{cases} \dfrac{\partial_\mu T}{\sqrt{-g^{\alpha\beta}\partial_\alpha T \partial_\beta T}}, & \text{for Single,} \\ \displaystyle\sum_{i=1}^{N} \dfrac{\partial_\mu T_i}{\sqrt{-g^{\alpha\beta}\partial_\alpha T_i \partial_\beta T_i}}, & \text{for Multi,} \\ \dfrac{N\partial_\mu T}{\sqrt{-g^{\alpha\beta}\partial_\alpha T \partial_\beta T}}, & \text{for Assisted.} \end{cases} \tag{4.9}$$

Further comparing Eqs. (4.6) and (4.8) the density ρ and the pressure p for the tachyonic field can be computed as

$$\rho = \begin{cases} \dfrac{V(T)}{\sqrt{1-\alpha'\dot{T}^2}}, & \text{for Single,} \\ \displaystyle\sum_{i=1}^{N} \dfrac{V(T)}{\sqrt{1-\alpha'\dot{T}^2}}, & \text{for Multi,} \\ \dfrac{NV(T)}{\sqrt{1-\alpha'\dot{T}^2}}, & \text{for Assisted,} \end{cases} \tag{4.10}$$

and

$$p = \begin{cases} -V(T)\sqrt{1-\alpha'\dot{T}^2}, & \text{for Single,} \\ -\displaystyle\sum_{i=1}^{N} V(T)\sqrt{1-\alpha'\dot{T}^2}, & \text{for Multi,} \\ -NV(T)\sqrt{1-\alpha'\dot{T}^2}, & \text{for Assisted.} \end{cases} \tag{4.11}$$

Similarly for the generalized situation comparing Eqs. (4.7) and (4.8) the density ρ and pressure p for tachyonic field can be computed as

$$\rho = \begin{cases} \dfrac{V(T)}{\left(1-\alpha'\dot{T}^2\right)^{1-q}}\left[1-\alpha'(1-2q)\dot{T}^2\right], & \text{for Single,} \\ \displaystyle\sum_{i=1}^{N} \dfrac{V(T_i)}{\left(1-\alpha'\dot{T}_i^2\right)^{1-q}}\left[1-\alpha'(1-2q)\dot{T}_i^2\right], & \text{for Multi,} \\ \dfrac{NV(T)}{\left(1-\alpha'\dot{T}^2\right)^{1-q}}\left[1-\alpha'(1-2q)\dot{T}^2\right], & \text{for Assisted,} \end{cases} \tag{4.12}$$

and

$$p = \begin{cases} -V(T)\left(1-\alpha'\dot{T}^2\right)^q, & \text{for Single,} \\ -\displaystyle\sum_{i=1}^{N} V(T_i)\left(1-\alpha'\dot{T}_i^2\right)^q, & \text{for Multi,} \\ -NV(T)\left(1-\alpha'\dot{T}^2\right)^q, & \text{for Assisted.} \end{cases} \tag{4.13}$$

Next using Eqs. (4.10) and (4.11) one can write down the expression for the equation of state parameter:

$$w = \begin{cases} \dfrac{p}{\rho} = \left(\alpha'\dot{T}^2 - 1\right), & \text{for Single,} \\ \displaystyle\sum_{i=1}^{N} \dfrac{p_i}{\rho_i} = \sum_{i=1}^{N}\left(\alpha'\dot{T}_i^2 - 1\right), & \text{for Multi,} \\ \dfrac{Np}{\rho} = N\left(\alpha'\dot{T}^2 - 1\right), & \text{for Assisted,} \end{cases} \tag{4.14}$$

and for the generalized case using Eqs. (4.12) and (4.13) one can write down the expression for the equation of state parameter:

$$w = \begin{cases} \dfrac{p}{\rho} = \dfrac{\left(\alpha'\dot{T}^2 - 1\right)}{\left[1-\alpha'(1-2q)\dot{T}^2\right]}, & \text{for Single,} \\ \displaystyle\sum_{i=1}^{N} \dfrac{p_i}{\rho_i} = \sum_{i=1}^{N}\dfrac{\left(\alpha'\dot{T}_i^2 - 1\right)}{\left[1-\alpha'(1-2q)\dot{T}_i^2\right]}, & \text{for Multi,} \\ \dfrac{Np}{\rho} = \dfrac{N\left(\alpha'\dot{T}^2 - 1\right)}{\left[1-\alpha'(1-2q)\dot{T}^2\right]}, & \text{for Assisted.} \end{cases} \tag{4.15}$$

Further using the spatially flat $k = 0$ FLRW metric defined through the following line element:

$$ds^2 = -dt^2 + a^2(t)d\mathbf{x}^2, \tag{4.16}$$

the Friedmann equations can be written as

$$H^2 = \left(\frac{\dot{a}}{a}\right)^2 = \frac{\rho}{3M_p^2}, \tag{4.17}$$

$$\dot{H} + H^2 = \frac{\ddot{a}}{a} = -\frac{(\rho + 3p)}{6M_p^2}, \tag{4.18}$$

where the density ρ and pressure p is computed in Eqs. (4.10)–(4.11). Also H is the Hubble parameter, defined as

$$H = \frac{1}{a(t)}\frac{da(t)}{dt} = \frac{\dot{a}}{a}. \tag{4.19}$$

On the other hand, varying the action as stated in Eq. (4.1) with respect to the tachyon field the equation of motion can be written as

$$0=\begin{cases}\frac{1}{\sqrt{-g}}\partial_\mu\left(\sqrt{-g}V(T)\sqrt{1+g^{\alpha\beta}\partial_\alpha T\partial_\beta T}\right)=\frac{\alpha'\ddot{T}}{(1-\alpha'\dot{T}^2)}+3H\alpha'\dot{T}+\frac{\mathrm{d}V(T)}{V(T)\mathrm{d}T}, & \text{for Single},\\ \frac{1}{\sqrt{-g}}\partial_\mu\left(\sqrt{-g}V(T_i)\sqrt{1+g^{\alpha\beta}\partial_\alpha T_i\partial_\beta T_i}\right)=\frac{\alpha'\ddot{T}_i}{(1-\alpha'\dot{T}_i^2)}+3H\alpha'\dot{T}_i+\frac{\mathrm{d}V(T_i)}{V(T_i)\mathrm{d}T_i}, & \text{for Multi},\\ \frac{1}{\sqrt{-g}}\partial_\mu\left(\sqrt{-g}V(T)\sqrt{1+g^{\alpha\beta}\partial_\alpha T\partial_\beta T}\right)=\frac{\alpha'\ddot{T}}{(1-\alpha'\dot{T}^2)}+3H\alpha'\dot{T}+\frac{\mathrm{d}V(T)}{V(T)\mathrm{d}T}, & \text{for Assisted}.\end{cases} \tag{4.20}$$

Similarly, in the most generalized case, varying the action as stated in Eq. (4.2) with respect to the tachyon field the equation of motion can be written as

$$0=\begin{cases}\frac{1}{\sqrt{-g}}\partial_\mu\left(\sqrt{-g}V(T)\left(1+g^{\alpha\beta}\partial_\alpha T\partial_\beta T\right)^q\right)=\frac{2q\alpha'\ddot{T}}{(1-\alpha'\dot{T}^2)}+6q\alpha' H\frac{\dot{T}}{1-\alpha'(1-2q)\dot{T}^2}+\frac{\mathrm{d}V(T)}{V(T)\mathrm{d}T}, & \text{for Single},\\ \frac{1}{\sqrt{-g}}\partial_\mu\left(\sqrt{-g}V(T_i)\left(1+g^{\alpha\beta}\partial_\alpha T_i\partial_\beta T_i\right)^q\right)=\frac{2q\alpha'\ddot{T}_i}{(1-\alpha'\dot{T}_i^2)}+6q\alpha' H\frac{\dot{T}_i}{1-\alpha'(1-2q)\dot{T}_i^2}+\frac{\mathrm{d}V(T_i)}{V(T_i)\mathrm{d}T_i}, & \text{for Multi},\\ \frac{1}{\sqrt{-g}}\partial_\mu\left(\sqrt{-g}V(T)\left(1+g^{\alpha\beta}\partial_\alpha T\partial_\beta T\right)^q\right)=\frac{2q\alpha'\ddot{T}}{(1-\alpha'\dot{T}^2)}+6q\alpha' H\frac{\dot{T}}{1-\alpha'(1-2q)\dot{T}^2}+\frac{\mathrm{d}V(T)}{V(T)\mathrm{d}T}, & \text{for Assisted}.\end{cases} \tag{4.21}$$

Further using Eqs. (4.10), (4.11) and (5.328) the expression for the adiabatic sound speed c_A turns out to be

$$c_A=\begin{cases}\sqrt{\frac{\dot{p}}{\dot{\rho}}}=\sqrt{-w\left[1+\frac{2}{3H\alpha'\dot{T}}\frac{\mathrm{d}V(T)}{V(T)\mathrm{d}T}\right]}, & \text{for Single},\\ \sqrt{\sum_{i=1}^{N}\frac{\dot{p}_i}{\dot{\rho}_i}}=\sqrt{\sum_{i=1}^{N}\left\{-w_i\left[1+\frac{2}{3H\alpha'\dot{T}_i}\frac{\mathrm{d}V(T_i)}{V(T_i)\mathrm{d}T_i}\right]\right\}}, & \text{for Multi},\\ \sqrt{\frac{N\dot{p}}{\dot{\rho}}}=\sqrt{-wN\left[1+\frac{2}{3H\alpha'\dot{T}}\frac{\mathrm{d}V(T)}{V(T)\mathrm{d}T}\right]}, & \text{for Assisted},\end{cases} \tag{4.22}$$

and for the generalized case using Eqs. (4.10), (4.11) and (4.21) the expression for the adiabatic sound speed turns out to be:

$$c_A=\begin{cases}\sqrt{\frac{-w\left[1+\frac{(1-\alpha'(1-2q)\dot{T}^2)}{3qH\alpha'\dot{T}}\frac{\mathrm{d}V(T)}{V(T)\mathrm{d}T}\right]}{\left[\left(\frac{1}{q}-1\right)\left\{1-\frac{(1-2q)}{(1-q)}w\right\}\left\{1+\frac{(1-\alpha'(1-2q)\dot{T}^2)}{6qH\alpha'\dot{T}}\frac{\mathrm{d}V(T)}{V(T)\mathrm{d}T}\right\}-\frac{(1-\alpha'(1-2q)\dot{T}^2)}{6qH\alpha'\dot{T}}\frac{\mathrm{d}V(T)}{V(T)\mathrm{d}T}\right]}}, & \text{for Single},\\ \sqrt{\sum_{i=1}^{N}\left\{\frac{-w_i\left[1+\frac{(1-\alpha'(1-2q)\dot{T}_i^2)}{3qH\alpha'\dot{T}_i}\frac{\mathrm{d}V(T_i)}{V(T_i)\mathrm{d}T_i}\right]}{\left[\left(\frac{1}{q}-1\right)\left\{1-\frac{(1-2q)}{(1-q)}w_i\right\}\left\{1+\frac{(1-\alpha'(1-2q)\dot{T}_i^2)}{6qH\alpha'\dot{T}_i}\frac{\mathrm{d}V(T_i)}{V(T_i)\mathrm{d}T_i}\right\}-\frac{(1-\alpha'(1-2q)\dot{T}_i^2)}{6qH\alpha'\dot{T}_i}\frac{\mathrm{d}V(T_i)}{V(T_i)\mathrm{d}T_i}\right]}\right\}}, & \text{for Multi},\\ \sqrt{\frac{-wN\left[1+\frac{(1-\alpha'(1-2q)\dot{T}^2)}{3qH\alpha'\dot{T}}\frac{\mathrm{d}V(T)}{V(T)\mathrm{d}T}\right]}{\left[\left(\frac{1}{q}-1\right)\left\{1-\frac{(1-2q)}{(1-q)}w\right\}\left\{1+\frac{(1-\alpha'(1-2q)\dot{T}^2)}{6qH\alpha'\dot{T}}\frac{\mathrm{d}V(T)}{V(T)\mathrm{d}T}\right\}-\frac{(1-\alpha'(1-2q)\dot{T}^2)}{6qH\alpha'\dot{T}}\frac{\mathrm{d}V(T)}{V(T)\mathrm{d}T}\right]}}, & \text{for Assisted}.\end{cases} \tag{4.23}$$

It is important to mention here that, substituting $q=1/2$ in Eq. (4.23) one can get back the result obtained in Eq. (4.22). Similarly in the present context the effective sound speed c_S is defined as

$$c_S = \begin{cases} \sqrt{\dfrac{\frac{\partial p}{\partial \dot{T}^2}}{\frac{\partial \rho}{\partial \dot{T}^2}}} = \sqrt{-w}, & \text{for Single,} \\ \sqrt{\displaystyle\sum_{i=1}^{N} \dfrac{\frac{\partial p_i}{\partial \dot{T}_i^2}}{\frac{\partial \rho_i}{\partial \dot{T}_i^2}}} = \sqrt{-\displaystyle\sum_{i=1}^{N} w_i}, & \text{for Multi,} \\ \sqrt{N \dfrac{\frac{\partial p}{\partial \dot{T}^2}}{\frac{\partial \rho}{\partial \dot{T}^2}}} = \sqrt{-wN}, & \text{for Assisted,} \end{cases} \tag{4.24}$$

and for the generalized case the effective sound speed c_S is defined as

$$c_S = \begin{cases} \sqrt{\dfrac{\frac{\partial p}{\partial \dot{T}^2}}{\frac{\partial \rho}{\partial \dot{T}^2}}} = \sqrt{\left[1 + \dfrac{2(q-1)(1+w)}{1+(1-2q)(2w+1)}\right]}, & \text{for Single,} \\ \sqrt{\displaystyle\sum_{i=1}^{N} \dfrac{\frac{\partial p_i}{\partial \dot{T}_i^2}}{\frac{\partial \rho_i}{\partial \dot{T}_i^2}}} = \sqrt{\displaystyle\sum_{i=1}^{N} \left[1 + \dfrac{2(q-1)(1+w_i)}{1+(1-2q)(2w_i+1)}\right]}, & \text{for Multi,} \\ \sqrt{N \dfrac{\frac{\partial p}{\partial \dot{T}^2}}{\frac{\partial \rho}{\partial \dot{T}^2}}} = \sqrt{N \left[1 + \dfrac{2(q-1)(1+w)}{1+(1-2q)(2w+1)}\right]}, & \text{for Assisted.} \end{cases} \tag{4.25}$$

Finally comparing Eqs. (4.22), (4.23), (4.24) and (4.25) we get the following relationship between adiabatic and effective sound speed in tachyonic field theory:

$$c_A = \begin{cases} \sqrt{\dfrac{\dot{p}}{\dot{\rho}}} = c_S \sqrt{\left[1 + \dfrac{2}{3H\alpha'\dot{T}} \dfrac{\mathrm{d}V(T)}{V(T)\mathrm{d}T}\right]}, & \text{for Single,} \\ \sqrt{\displaystyle\sum_{i=1}^{N} \dfrac{\dot{p}_i}{\dot{\rho}_i}} = \sqrt{\displaystyle\sum_{i=1}^{N} \left\{c_{S,i}^2 \left[1 + \dfrac{2}{3H\alpha'\dot{T}_i} \dfrac{\mathrm{d}V(T_i)}{V(T_i)\mathrm{d}T_i}\right]\right\}}, & \text{for Multi,} \\ \sqrt{\dfrac{N\dot{p}}{\dot{\rho}}} = c_S \sqrt{\left[1 + \dfrac{2}{3H\alpha'\dot{T}} \dfrac{\mathrm{d}V(T)}{V(T)\mathrm{d}T}\right]}, & \text{for Assisted,} \end{cases} \tag{4.26}$$

and for the generalized case we get

$$c_A = \begin{cases} \sqrt{\dfrac{\dfrac{c_S^2}{\left[1+\frac{(1-2q)}{(1-q)}\left(c_S^2-1\right)\right]}\left[1+\frac{(1-\alpha'(1-2q)\dot{T}^2)}{3qH\alpha'\dot{T}}\frac{\mathrm{d}V(T)}{V(T)\mathrm{d}T}\right]}{\left[\left(\frac{1}{q}-1\right)\left\{1+\dfrac{\frac{(1-2q)}{(1-q)}c_S^2}{\left[1+\frac{(1-2q)}{(1-q)}\left(c_S^2-1\right)\right]}\right\}\left\{1+\frac{(1-\alpha'(1-2q)\dot{T}^2)}{6qH\alpha'\dot{T}}\frac{\mathrm{d}V(T)}{V(T)\mathrm{d}T}\right\}-\frac{(1-\alpha'(1-2q)\dot{T}^2)}{6qH\alpha'\dot{T}}\frac{\mathrm{d}V(T)}{V(T)\mathrm{d}T}\right]}}, & \text{for Single,} \\ \sqrt{\displaystyle\sum_{i=1}^{N}\left\{\dfrac{\dfrac{c_{S,i}^2}{\left[1+\frac{(1-2q)}{(1-q)}\left(c_{S,i}^2-1\right)\right]}\left[1+\frac{\left(1-\alpha'(1-2q)\dot{T}_i^2\right)}{3qH\alpha'\dot{T}_i}\frac{\mathrm{d}V(T_i)}{V(T_i)\mathrm{d}T_i}\right]}{\left[\left(\frac{1}{q}-1\right)\left\{1+\dfrac{\frac{(1-2q)}{(1-q)}c_{S,i}^2}{\left[1+\frac{(1-2q)}{(1-q)}\left(c_{S,i}^2-1\right)\right]}\right\}\left\{1+\frac{\left(1-\alpha'(1-2q)\dot{T}_i^2\right)}{6qH\alpha'\dot{T}_i}\frac{\mathrm{d}V(T_i)}{V(T_i)\mathrm{d}T_i}\right\}-\frac{\left(1-\alpha'(1-2q)\dot{T}_i^2\right)}{6qH\alpha'\dot{T}_i}\frac{\mathrm{d}V(T_i)}{V(T_i)\mathrm{d}T_i}\right]}\right\}}, & \text{for Multi,} \\ \sqrt{\dfrac{\dfrac{c_S^2}{\left[1+\frac{(1-2q)}{(1-q)}\left(\frac{c_S^2}{N}-1\right)\right]}\left[1+\frac{(1-\alpha'(1-2q)\dot{T}^2)}{3qH\alpha'\dot{T}}\frac{\mathrm{d}V(T)}{V(T)\mathrm{d}T}\right]}{\left[\left(\frac{1}{q}-1\right)\left\{1+\dfrac{\frac{(1-2q)}{(1-q)}c_S^2}{N\left[1+\frac{(1-2q)}{(1-q)}\left(\frac{c_S^2}{N}-1\right)\right]}\right\}\left\{1+\frac{(1-\alpha'(1-2q)\dot{T}^2)}{6qH\alpha'\dot{T}}\frac{\mathrm{d}V(T)}{V(T)\mathrm{d}T}\right\}-\frac{(1-\alpha'(1-2q)\dot{T}^2)}{6qH\alpha'\dot{T}}\frac{\mathrm{d}V(T)}{V(T)\mathrm{d}T}\right]}}, & \text{for Assisted.} \end{cases} \tag{4.27}$$

Let us mention other crucial issues which we use throughout the analysis performed in this paper:

1. *At early times* the tachyonic field satisfies the following small field criteria to validate the effective field theory prescription within the framework of tachyonic string theory:

$$\frac{|T|}{M_p} << 1, \tag{4.28}$$

$$|\dot{T}| << \frac{1}{\sqrt{\alpha'}} \tag{4.29}$$

and for the generalized $q \neq 1/2$ case additionally we have to satisfy another constraint:

$$\sqrt{(1-2q)}|\dot{T}| << \frac{1}{\sqrt{\alpha'}}. \tag{4.30}$$

2. *At early times* using Eqs. (4.28), (4.29) and (4.30) in Eqs. (4.14) and (4.15), the equation of state parameter w can be approximated by

$$w \approx -1. \tag{4.31}$$

3. *At late times* the tachyonic field satisfies the following small field criteria within the framework of tachyonic string theory:

$$\frac{|T|}{M_p} \sim 1, \tag{4.32}$$

$$\frac{|\dot{T}|}{M_p^2} \sim \frac{1}{\sqrt{\alpha'}} \tag{4.33}$$

and for the generalized $q \neq 1/2$ case additionally we have to satisfy another constraint:

$$\sqrt{(1-2q)}|\dot{T}| \sim \frac{1}{\sqrt{\alpha'}}. \tag{4.34}$$

4. *At late times* using Eqs. (4.32), (4.33) and (4.34) in Eqs. (4.14) and (4.15), the equation of state parameter w can be approximated by

$$w \approx 0. \tag{4.35}$$

5. There might be another interesting possibility appear in the present context, where the tachyonic modes satisfy the large field criteria, represented by the following constraint:

$$\frac{|T|}{M_p} >> 1, \tag{4.36}$$

$$|\dot{T}| >> \frac{1}{\sqrt{\alpha'}} \tag{4.37}$$

and for the generalized $q \neq 1/2$ case additionally we have to satisfy another constraint:

$$\sqrt{(1-2q)}|\dot{T}| >> \frac{1}{\sqrt{\alpha'}}. \tag{4.38}$$

6. Further using Eqs. (4.36), (4.37) and (4.38) in Eqs. (4.14) and (4.15), the equation of state parameter w can be approximated by

$$w = \begin{cases} \frac{p}{\rho} = \alpha'\dot{T}^2, & \text{for Single,} \\ \sum_{i=1}^{N}\frac{p_i}{\rho_i} = \sum_{i=1}^{N}\alpha'\dot{T}_i^2, & \text{for Multi,} \\ \frac{Np}{\rho} = N\alpha'\dot{T}^2, & \text{for Assisted,} \end{cases} \tag{4.39}$$

and for the generalized $q \neq 1/2$ case we have

$$w = \begin{cases} \frac{p}{\rho} = \frac{1}{(2q-1)}, & \text{for Single,} \\ \sum_{i=1}^{N}\frac{p_i}{\rho_i} = \sum_{i=1}^{N}\frac{1}{(2q-1)}, & \text{for Multi,} \\ \frac{Np}{\rho} = \frac{N}{(2q-1)}, & \text{for Assisted.} \end{cases} \tag{4.40}$$

Here one can control the parameter q and N to get the desired value of equation of state parameter w, which is necessarily required to explain the cosmological dynamics.

7. Additionally, it is important to note that, within the setup of string theory, the tachyonic modes can form cluster on small cosmological scales. Consequently tachyonic string theory can be treated as a unified prescription to explain the inflationary paradigm and dark matter.
8. Reheating and creation of matter particles in a class of specific models where the minimum of the tachyon potential $V(T)$ is at $T \to \infty$, which is a pathological issue in the present context because the tachyon field in such a type of string theories does not participate in oscillations.[3] To solve this crucial pathological problem in the present context, one can think about a particular physical situation where the universe is initially dominated by a inflationary epoch and this can be explained via the energy density of the tachyon condensate as mentioned

[3] Here it is important to note that the oscillations are necessarily required to explain the reheating phenomenon.

in the introduction of this article and according to this proposal the set-up will always remain dominated by the tachyons. To resolve this pathological issue it may happen that the tachyon condensation phenomenon is potentially responsible for a short period of an inflationary epoch prior, which occurs at a Planckian mass scale, $M_p \sim 2.43 \times 10^{18}$ GeV and also one needs to require a second stage of inflationary epoch just followed by the previous one which occurs at the vicinity of the GUT scale (10^{16} GeV). This directly implies that the tachyon serves no crucial purpose in the post inflationary epoch till at the very later stages of its cosmological evolution on time scales. All these crucial pathological problems do not appear in the context of the well-known hybrid inflationary set-up where the complex tachyon field has a specific minimum value at the sub-Planckian ($<M_p$) regime given by the list of constraint equations as stated in Eqs. (4.28), (4.29), and Eq. (4.30). In this paper, we have studied the cosmological consequences from different classes of tachyonic potentials appearing in the context of string theory which have no connection to the hybrid inflationary model, but to explain CMB constraints the tachyon condensation phenomenon plays an important role. Instead of studying the tachyon condensation phenomenon, in this paper we study the cosmological perturbation theory and its physical consequences in detail in later sections.

9. The energy density of tachyons after inflation should be fine tuned to be sub-dominant until the very later stages of the cosmological evolution of the universe.

4.2 Dynamical solution for various phases

In this section our prime objective is to study the dynamical behavior of the tachyonic field in the background of spatially flat FLRW metric and in the presence of the Einstein–Hilbert term in the gravity sector. Below we explicitly show that the solution for the tachyonic field can explain various phases of the universe starting from inflation to the dust formation. To study the cosmological dynamics from the tachyonic string field theoretic set-up let us start with the following solution ansatz of the tachyon field:

$$\dot{T} = \begin{cases} \frac{1}{\sqrt{\alpha'}}\left(\frac{\exp\left(\frac{2t}{bT_0}\right)-1}{\exp\left(\frac{2t}{bT_0}\right)+1}\right) = \frac{1}{\sqrt{\alpha'}}\tanh\left(\frac{t}{bT_0}\right), & \text{for Single,} \\ \sum_{i=1}^{N}\dot{T}_i = \sum_{i=1}^{N}\frac{1}{\sqrt{\alpha'}}\left(\frac{\exp\left(\frac{2t}{bT_{0i}}\right)-1}{\exp\left(\frac{2t}{bT_{0i}}\right)+1}\right) = \sum_{i=1}^{N}\frac{1}{\sqrt{\alpha'}}\tanh\left(\frac{t}{bT_{0i}}\right), & \text{for Multi,} \\ \frac{N}{\sqrt{\alpha'}}\left(\frac{\exp\left(\frac{2t}{bT_0}\right)-1}{\exp\left(\frac{2t}{bT_0}\right)+1}\right) = \frac{N}{\sqrt{\alpha'}}\tanh\left(\frac{t}{bT_0}\right), & \text{for Assisted,} \end{cases} \tag{4.41}$$

which will satisfy the equation of motion of the tachyon field as stated in Eqs. (5.328) and (4.21) respectively. Here b is a new parameter of the theory which has inverse square mass dimension, i.e., $[M]^{-1}$. Consequently the argument of the hyperbolic functions, i.e., $(\frac{t}{bT_0})$ is dimensionless. From various cosmological observations it is possible to put stringent constraint on the newly introduced parameter b. Further integrating Eq. (4.41) we get the following solutions for the tachyonic field:

$$T(t) = \begin{cases} \frac{bT_0}{\sqrt{\alpha'}}\ln\left[\cosh\left(\frac{t}{bT_0}\right)\right], & \text{for Single,} \\ \sum_{i=1}^{N}T_i(t) = \sum_{i=1}^{N}\frac{bT_{0i}}{\sqrt{\alpha'}}\ln\left[\cosh\left(\frac{t}{bT_{0i}}\right)\right], & \text{for Multi,} \\ \frac{NbT_0}{\sqrt{\alpha'}}\ln\left[\cosh\left(\frac{t}{bT_0}\right)\right], & \text{for Assisted.} \end{cases} \tag{4.42}$$

For both of the cases we fix the boundary condition in such a way that the tachyonic field T satisfy the constraint: $T(t=0) = T(0) = 0$. Further using Eqs. (4.17) and (5.328) we get the following constraint condition for the cosmological time dependent potential $V(t)$:

$$0=\begin{cases}\left[\frac{1}{bT_0}+\frac{\dot{V}}{V}\coth\left(\frac{t}{bT_0}\right)+\sqrt{\frac{3V}{\cosh\left(\frac{t}{bT_0}\right)}}\frac{\sinh\left(\frac{t}{bT_0}\right)}{M_p}\right], & \text{for Single},\\ \sum_{i=1}^{N}\left[\frac{1}{bT_{0i}}+\frac{\dot{V}}{V}\coth\left(\frac{t}{bT_{0i}}\right)+\sqrt{\frac{3V}{\cosh\left(\frac{t}{bT_{0i}}\right)}}\frac{\sinh\left(\frac{t}{bT_{0i}}\right)}{M_p}\right], & \text{for Multi},\\ N\left[\frac{1}{bT_0}+\frac{\dot{V}}{V}\coth\left(\frac{t}{bT_0}\right)+\sqrt{\frac{3V}{\cosh\left(\frac{t}{bT_0}\right)}}\frac{\sinh\left(\frac{t}{bT_0}\right)}{M_p}\right], & \text{for Assisted},\end{cases} \tag{4.43}$$

and for the generalized case we get

$$0=\begin{cases}\left[\frac{1}{bT_0}+\frac{1}{2q}\frac{\dot{V}}{V}\coth\left(\frac{t}{bT_0}\right)+\frac{\sqrt{\frac{3V}{\cosh\left(\frac{t}{bT_0}\right)}}\sinh\left(\frac{t}{bT_0}\right)}{M_p\left[1-(1-2q)\tanh^2\left(\frac{t}{bT_0}\right)\right]}\right], & \text{for Single},\\ \sum_{i=1}^{N}\left[\frac{1}{bT_{0i}}+\frac{1}{2q}\frac{\dot{V}}{V}\coth\left(\frac{t}{bT_{0i}}\right)+\frac{\sqrt{\frac{3V}{\cosh\left(\frac{t}{bT_{0i}}\right)}}\sinh\left(\frac{t}{bT_{0i}}\right)}{M_p\left[1-(1-2q)\tanh^2\left(\frac{t}{bT_{0i}}\right)\right]}\right], & \text{for Multi},\\ N\left[\frac{1}{bT_0}+\frac{1}{2q}\frac{\dot{V}}{V}\coth\left(\frac{t}{bT_0}\right)+\frac{\sqrt{\frac{3V}{\cosh\left(\frac{t}{bT_0}\right)}}\sinh\left(\frac{t}{bT_0}\right)}{M_p\left[1-(1-2q)\tanh^2\left(\frac{t}{bT_0}\right)\right]}\right], & \text{for Assisted}.\end{cases} \tag{4.44}$$

The solutions of Eqs. (4.43) and (4.44) are given by

$$V(t)=\begin{cases}\frac{\lambda}{\cosh\left(\frac{t}{bT_0}\right)}\left[\frac{1}{1+\frac{\sqrt{3\lambda}bT_0}{2M_p}\left\{\frac{t}{bT_0}-\tanh\left(\frac{t}{bT_0}\right)\right\}}\right]^2, & \text{for Single},\\ \sum_{i=1}^{N}V_i(t)=\sum_{i=1}^{N}\frac{\lambda_i}{\cosh\left(\frac{t}{bT_{0i}}\right)}\left[\frac{1}{1+\frac{\sqrt{3\lambda}bT_{0i}}{2M_p}\left\{\frac{t}{bT_{0i}}-\tanh\left(\frac{t}{bT_{0i}}\right)\right\}}\right]^2, & \text{for Multi},\\ \frac{N\lambda}{\cosh\left(\frac{t}{bT_0}\right)}\left[\frac{1}{1+\frac{\sqrt{3\lambda}bT_0}{2M_p}\left\{\frac{t}{bT_0}-\tanh\left(\frac{t}{bT_0}\right)\right\}}\right]^2, & \text{for Assisted},\end{cases} \tag{4.45}$$

and for the generalized case we get

$$V(t)=\begin{cases}\frac{\lambda}{\left[\cosh\left(\frac{t}{bT_0}\right)\right]^{2q}}\left[\frac{1}{1+\frac{\sqrt{3\lambda}bT_0}{2M_p}\left\{\frac{t}{bT_0}-\tanh\left(\frac{t}{bT_0}\right)\right\}}\right]^2, & \text{for Single},\\ \sum_{i=1}^{N}V_i(t)=\sum_{i=1}^{N}\frac{\lambda_i}{\left[\cosh\left(\frac{t}{bT_{0i}}\right)\right]^{2q}}\left[\frac{1}{1+\frac{\sqrt{3\lambda}bT_{0i}}{2M_p}\left\{\frac{t}{bT_{0i}}-\tanh\left(\frac{t}{bT_{0i}}\right)\right\}}\right]^2, & \text{for Multi},\\ \frac{N\lambda}{\left[\cosh\left(\frac{t}{bT_0}\right)\right]^{2q}}\left[\frac{1}{1+\frac{\sqrt{3\lambda}bT_0}{2M_p}\left\{\frac{t}{bT_0}-\tanh\left(\frac{t}{bT_0}\right)\right\}}\right]^2, & \text{for Assisted},\end{cases} \tag{4.46}$$

where to get the analytical solution from the generalized case we assume that the time scale of our consideration satisfies the following constraint:

$$t << bT_0 \tanh^{-1}\left[\sqrt{\frac{1}{2q-1}}\right] \tag{4.47}$$

which is valid for all values of q except $q \neq 1/2$. For the usual tachyonic case and for the generalized situation we use the following normalization condition:

$$V(t=0) = V(0) = \lambda \tag{4.48}$$

to fix the value of arbitrary integration constant. Further using the explicit solution for the tachyonic field as appearing in Eq. (4.42), we can write the time as a function of tachyonic field as

$$t = \begin{cases} bT_0\left[\cosh^{-1}\left\{\exp\left(\frac{\sqrt{\alpha'}T}{bT_0}\right)\right\}\right], & \text{for Single} \\ \sum_{i=1}^{N} bT_{0i}\left[\cosh^{-1}\left\{\exp\left(\frac{\sqrt{\alpha'}T}{bT_{0i}}\right)\right\}\right], & \text{for Multi,} \\ NbT_0\left[\cosh^{-1}\left\{\exp\left(\frac{\sqrt{\alpha'}T}{bT_0}\right)\right\}\right], & \text{for Assisted,} \end{cases} \tag{4.49}$$

and further substituting Eq. (4.49) in Eqs. (4.45) and (4.46) we get the following expression for the potential as a function of tachyonic field:

$$V(T) = \begin{cases} \lambda \exp\left(-\frac{\sqrt{\alpha'}T}{bT_0}\right)\left[\frac{1}{1+\frac{\sqrt{3\lambda}bT_0}{2M_p}\left\{\cosh^{-1}\left\{\exp\left(\frac{\sqrt{\alpha'}T}{bT_0}\right)\right\} - \tanh\left(\cosh^{-1}\left\{\exp\left(\frac{\sqrt{\alpha'}T}{bT_0}\right)\right\}\right)\right\}}\right]^2, & \text{for Single,} \\ \sum_{i=1}^{N}\lambda_i \exp\left(-\frac{\sqrt{\alpha'}T_i}{bT_{0i}}\right)\left[\frac{1}{1+\frac{\sqrt{3\lambda}bT_{0i}}{2M_p}\left\{\cosh^{-1}\left\{\exp\left(\frac{\sqrt{\alpha'}T_i}{bT_{0i}}\right)\right\} - \tanh\left(\cosh^{-1}\left\{\exp\left(\frac{\sqrt{\alpha'}T_i}{bT_{0i}}\right)\right\}\right)\right\}}\right]^2, & \text{for Multi,} \\ N\lambda \exp\left(-\frac{\sqrt{\alpha'}T}{bT_0}\right)\left[\frac{1}{1+\frac{\sqrt{3\lambda}bT_0}{2M_p}\left\{\cosh^{-1}\left\{\exp\left(\frac{\sqrt{\alpha'}T}{bT_0}\right)\right\} - \tanh\left(\cosh^{-1}\left\{\exp\left(\frac{\sqrt{\alpha'}T}{bT_0}\right)\right\}\right)\right\}}\right]^2, & \text{for Assisted,} \end{cases} \tag{4.50}$$

and for the generalized case we get

$$V(T) = \begin{cases} \lambda \exp\left(-\frac{2q\sqrt{\alpha'}T}{bT_0}\right)\left[\frac{1}{1+\frac{\sqrt{3\lambda}bT_0}{2M_p}\left\{\cosh^{-1}\left\{\exp\left(\frac{2q\sqrt{\alpha'}T}{bT_0}\right)\right\} - \tanh\left(\cosh^{-1}\left\{\exp\left(\frac{2q\sqrt{\alpha'}T}{bT_0}\right)\right\}\right)\right\}}\right]^2, & \text{for Single,} \\ \sum_{i=1}^{N}\lambda_i \exp\left(-\frac{2q\sqrt{\alpha'}T_i}{bT_{0i}}\right)\left[\frac{1}{1+\frac{\sqrt{3\lambda}bT_{0i}}{2M_p}\left\{\cosh^{-1}\left\{\exp\left(\frac{2q\sqrt{\alpha'}T_i}{bT_{0i}}\right)\right\} - \tanh\left(\cosh^{-1}\left\{\exp\left(\frac{2q\sqrt{\alpha'}T_i}{bT_{0i}}\right)\right\}\right)\right\}}\right]^2, & \text{for Multi,} \\ N\lambda \exp\left(-\frac{2q\sqrt{\alpha'}T}{bT_0}\right)\left[\frac{1}{1+\frac{\sqrt{3\lambda}bT_0}{2M_p}\left\{\cosh^{-1}\left\{\exp\left(\frac{2q\sqrt{\alpha'}T}{bT_0}\right)\right\} - \tanh\left(\cosh^{-1}\left\{\exp\left(\frac{2q\sqrt{\alpha'}T}{bT_0}\right)\right\}\right)\right\}}\right]^2, & \text{for Assisted.} \end{cases} \tag{4.51}$$

Next we use the following redefinition in the tachyonic field:

$$\frac{\sqrt{\alpha'}T}{bT_0} \rightarrow \frac{T}{T_0}, \tag{4.52}$$

$$\frac{\sqrt{\alpha'}T}{bT_{0i}} \rightarrow \frac{T}{T_{0i}}. \tag{4.53}$$

Hence using the redefinition, the potential as stated in Eqs. (4.50) and (4.51) can be re-expressed as

$$V(T) = \begin{cases} \lambda \exp\left(-\frac{T}{T_0}\right)\left[\frac{1}{1+\frac{\sqrt{3\lambda}bT_0}{2M_p}\left\{\cosh^{-1}\left\{\exp\left(\frac{\sqrt{\alpha'}T}{bT_0}\right)\right\} - \tanh\left(\cosh^{-1}\left\{\exp\left(\frac{\sqrt{\alpha'}T}{bT_0}\right)\right\}\right)\right\}}\right]^2, & \text{for Single,} \\ \sum_{i=1}^{N}\lambda_i \exp\left(-\frac{T_i}{T_{0i}}\right)\left[\frac{1}{1+\frac{\sqrt{3\lambda}bT_{0i}}{2M_p}\left\{\cosh^{-1}\left\{\exp\left(\frac{\sqrt{\alpha'}T_i}{bT_{0i}}\right)\right\} - \tanh\left(\cosh^{-1}\left\{\exp\left(\frac{\sqrt{\alpha'}T_i}{bT_{0i}}\right)\right\}\right)\right\}}\right]^2, & \text{for Multi,} \\ N\lambda \exp\left(-\frac{T}{T_0}\right)\left[\frac{1}{1+\frac{\sqrt{3\lambda}bT_0}{2M_p}\left\{\cosh^{-1}\left\{\exp\left(\frac{\sqrt{\alpha'}T}{bT_0}\right)\right\} - \tanh\left(\cosh^{-1}\left\{\exp\left(\frac{\sqrt{\alpha'}T}{bT_0}\right)\right\}\right)\right\}}\right]^2, & \text{for Assisted,} \end{cases} \tag{4.54}$$

and for the generalized case we get

$$V(T) = \begin{cases} \lambda \exp\left(-\frac{2qT}{T_0}\right)\left[\frac{1}{1+\frac{\sqrt{3\lambda}bT_0}{2M_p}\left\{\cosh^{-1}\left\{\exp\left(\frac{2q\sqrt{\alpha'}T}{bT_0}\right)\right\} - \tanh\left(\cosh^{-1}\left\{\exp\left(\frac{2q\sqrt{\alpha'}T}{bT_0}\right)\right\}\right)\right\}}\right]^2, & \text{for Single,} \\ \sum_{i=1}^{N}\lambda_i \exp\left(-\frac{2qT_i}{T_{0i}}\right)\left[\frac{1}{1+\frac{\sqrt{3\lambda}bT_{0i}}{2M_p}\left\{\cosh^{-1}\left\{\exp\left(\frac{2q\sqrt{\alpha'}T_i}{bT_{0i}}\right)\right\} - \tanh\left(\cosh^{-1}\left\{\exp\left(\frac{2q\sqrt{\alpha'}T_i}{bT_{0i}}\right)\right\}\right)\right\}}\right]^2, & \text{for Multi,} \\ N\lambda \exp\left(-\frac{2qT}{T_0}\right)\left[\frac{1}{1+\frac{\sqrt{3\lambda}bT_0}{2M_p}\left\{\cosh^{-1}\left\{\exp\left(\frac{2q\sqrt{\alpha'}T}{bT_0}\right)\right\} - \tanh\left(\cosh^{-1}\left\{\exp\left(\frac{2q\sqrt{\alpha'}T}{bT_0}\right)\right\}\right)\right\}}\right]^2, & \text{for Assisted.} \end{cases} \tag{4.55}$$

Now let us explicitly study the limiting behavior of the potential $V(T)$ in detail, which is appended below:

- At $T << T_0$ and $T_i << T_{0i}$ limiting case one can use the following approximation for the usual tachyonic case:

$$\ln\left[\cosh\left(\frac{t}{bT_0}\right)\right] << 1, \tag{4.56}$$

$$\ln\left[\cosh\left(\frac{t}{bT_{0i}}\right)\right] << 1. \tag{4.57}$$

  Using this approximation one can use the following expansion:

$$\ln\left[\cosh\left(\frac{t}{bT_0}\right)\right] \approx \frac{1}{2}\left(\frac{t}{bT_0}\right)^2, \tag{4.58}$$

$$\ln\left[\cosh\left(\frac{t}{bT_{0i}}\right)\right] \approx \frac{1}{2}\left(\frac{t}{bT_{0i}}\right)^2. \tag{4.59}$$

- Hence using the solution obtained for the tachyonic field as stated in Eq. (4.42) we get

$$T(t) = \begin{cases} \frac{T_0}{2}\left(\frac{t}{bT_0}\right)^2, & \text{for Single,} \\ \sum_{i=1}^{N} T_i(t) = \sum_{i=1}^{N} \frac{T_{0i}}{2}\left(\frac{t}{bT_{0i}}\right)^2, & \text{for Multi,} \\ \frac{NT_0}{2}\left(\frac{t}{bT_0}\right)^2, & \text{for Assisted,} \end{cases} \tag{4.60}$$

and by inverting Eq. (4.78) the associated time scale can be computed as

$$t = \begin{cases} bT_0\sqrt{\frac{2T}{T_0}}, & \text{for Single,} \\ \sum_{i=1}^{N} bT_{0i}\sqrt{\frac{2T}{T_{0i}}}, & \text{for Multi,} \\ NbT_0\sqrt{\frac{2T}{T_0}}, & \text{for Assisted.} \end{cases} \tag{4.61}$$

Consequently we have

$$\text{Single}: \quad \tanh\left(\frac{t}{bT_0}\right) \approx \tanh\left(\sqrt{\frac{2T}{T_0}}\right) \approx \sqrt{\frac{2T}{T_0}}, \tag{4.62}$$

$$\text{Multi}: \quad \tanh\left(\frac{t}{bT_{0i}}\right) \approx \tanh\left(\sqrt{\frac{2T}{T_{0i}}}\right) \approx \sqrt{\frac{2T}{T_{0i}}}, \tag{4.63}$$

$$\text{Assisted}: \quad \tanh\left(\frac{t}{bT_0}\right) \approx \tanh\left(\sqrt{\frac{2T}{T_0}}\right) \approx \sqrt{\frac{2T}{T_0}}. \tag{4.64}$$

and finally for the usual tachyonic case the potential $V(T)$ can be approximated by

$$V(T) = \begin{cases} \lambda \exp\left(-\frac{T}{T_0}\right), & \text{for Single,} \\ \sum_{i=1}^{N} V(T_i) = \sum_{i=1}^{N} \lambda_i \exp\left(-\frac{T_i}{T_{0i}}\right), & \text{for Multi,} \\ N\lambda \exp\left(-\frac{T}{T_0}\right), & \text{for Assisted,} \end{cases} \tag{4.65}$$

and for the generalized case we have

$$V(T) = \begin{cases} \lambda \exp\left(-\frac{2qT}{T_0}\right), & \text{for Single,} \\ \sum_{i=1}^{N} V(T_i) = \sum_{i=1}^{N} \lambda_i \exp\left(-\frac{2qT_i}{T_{0i}}\right), & \text{for Multi,} \\ N\lambda \exp\left(-\frac{2qT}{T_0}\right), & \text{for Assisted,} \end{cases} \tag{4.66}$$

where the behavior of these types of potentials has been elaborated in the earlier section.

- At $T >> T_0$ and $T_i >> T_{0i}$ limiting case one can use the following approximation for the usual tachyonic case:

$$\ln\left[\cosh\left(\frac{t}{bT_0}\right)\right] >> 1, \tag{4.67}$$

$$\ln\left[\cosh\left(\frac{t}{bT_{0i}}\right)\right] >> 1. \tag{4.68}$$

Using this approximation one can use the following expansion:

$$\ln\left[\cosh\left(\frac{t}{bT_0}\right)\right] \approx \ln\left[\frac{1}{2}\exp\left(\frac{t}{bT_0}\right)\right] \approx \frac{t}{bT_0}, \tag{4.69}$$

$$\ln\left[\cosh\left(\frac{t}{bT_{0i}}\right)\right] \approx \ln\left[\frac{1}{2}\exp\left(\frac{t}{bT_{0i}}\right)\right] \approx \frac{t}{bT_{0i}}. \tag{4.70}$$

Hence using the solution obtained for the tachyonic field as stated in Eq. (4.42) we get

$$T(t) = \begin{cases} \frac{t}{b}, & \text{for Single} \\ \sum_{i=1}^{N} T_i(t) = \sum_{i=1}^{N} \frac{t}{2b} = \frac{Nt}{b}, & \text{for Multi,} \\ \frac{Nt}{b}, & \text{for Assisted,} \end{cases} \tag{4.71}$$

and by inverting Eq. (4.71) the associated time scale can be computed as

$$t = \begin{cases} bT, & \text{for Single,} \\ \sum_{i=1}^{N} bT_i, & \text{for Multi,} \\ NbT, & \text{for Assisted.} \end{cases} \tag{4.72}$$

Consequently we have

$$\text{Single}:\quad \tanh\left(\frac{t}{bT_0}\right)\approx 1, \tag{4.73}$$

$$\text{Multi}:\quad \tanh\left(\frac{t}{bT_{0i}}\right)\approx 1, \tag{4.74}$$

$$\text{Assisted}:\quad \tanh\left(\frac{t}{bT_0}\right)\approx 1. \tag{4.75}$$

and finally for the usual tachyonic case the potential $V(T)$ can be approximated by

$$V(T)=\begin{cases}\frac{4M_p^2}{3b^2T_0^2}\left(\frac{T_0}{T}\right)^2\exp\left(-\frac{T}{T_0}\right), & \text{for Single,}\\ \sum_{i=1}^{N}V(T_i)=\sum_{i=1}^{N}\frac{4M_p^2}{3b^2T_{0i}^2}\left(\frac{T_{0i}}{T_i}\right)^2\exp\left(-\frac{T_i}{T_{0i}}\right), & \text{for Multi,}\\ \frac{4M_p^2N}{3b^2T_0^2}\left(\frac{T_0}{T}\right)^2\exp\left(-\frac{T}{T_0}\right), & \text{for Assisted,}\end{cases} \tag{4.76}$$

and for the generalized case we have

$$V(T)=\begin{cases}\frac{4M_p^2}{3b^2T_0^2}\left(\frac{T_0}{T}\right)^2\exp\left(-\frac{2qT}{T_0}\right), & \text{for Single,}\\ \sum_{i=1}^{N}V(T_i)=\sum_{i=1}^{N}\frac{4M_p^2}{3b^2T_{0i}^2}\left(\frac{T_{0i}}{T_i}\right)^2\exp\left(-\frac{2qT_i}{T_{0i}}\right), & \text{for Multi,}\\ \frac{4M_p^2N}{3b^2T_0^2}\left(\frac{T_0}{T}\right)^2\exp\left(-\frac{2qT}{T_0}\right), & \text{for Assisted,}\end{cases} \tag{4.77}$$

where the scale of inflation for the usual tachyonic case is fixed by:

$$V_{\rm inf}^{1/4}\propto\begin{cases}\lambda^{1/4}, & \text{for Single}\\ \left\{\sum_{i=1}^{N}\lambda_i\right\}^{1/4}, & \text{for Multi,}\\ (N\lambda)^{1/4}, & \text{for Assisted,}\end{cases} \tag{4.78}$$

and for the generalized case it is fixed by

$$V_{\rm inf}^{1/4}\propto\begin{cases}\left(\frac{4M_p^2}{3b^2T_0^2}\right)^{1/4}, & \text{for Single,}\\ \left\{\sum_{i=1}^{N}\frac{4M_p^2}{3b^2T_{0i}^2}\right\}^{1/4}, & \text{for Multi,}\\ \left(\frac{4M_p^2N}{3b^2T_0^2}\right)^{1/4}, & \text{for Assisted.}\end{cases} \tag{4.79}$$

Here the potential should satisfy the following criteria:

- At $T=0$ for the single field tachyonic potential:

$$V(T=0)\to\infty, \tag{4.80}$$

and for the multi-tachyonic and assisted cases we have

$$V_E(T=0)\to\infty. \tag{4.81}$$

- At $T=T_0$ for the single field tachyonic potential:

$$V(T=T_0)=\frac{4M_p^2}{3eb^2T_0^2} \tag{4.82}$$

and also for the multi-tachyonic and assisted cases we have

$$V_E(T=T_0)=\sum_{i=1}^{N}\frac{4M_p^2}{3eb^2T_{0i}^2}, \tag{4.83}$$

$$V_E(T=T_0)=\frac{4M_p^2N}{3eb^2T_0^2}. \tag{4.84}$$

For the generalized case one can repeat the same computation with the following redefinition of the b parameter of tachyonic field theory:

$$b^{-2}\exp(-2q)\to b^{-2}. \tag{4.85}$$

- For single field tachyonic potential:

$$V'(T)=-\frac{4M_p^2}{3b^2T^3}\exp\left(-\frac{T}{T_0}\right)\left(2+\frac{T}{T_0}\right), \tag{4.86}$$

$$V''(T)=\frac{4M_p^2}{3b^2T^4}\exp\left(-\frac{T}{T_0}\right)\times\left\{6+4\left(\frac{T}{T_0}\right)+\left(\frac{T}{T_0}\right)^2\right\}. \tag{4.87}$$

Now to find the extrema of the potential we substitute

$$V'(T)=0 \tag{4.88}$$

which give rise to the following solution for the tachyonic field:

$$T=-2T_0,\ \infty. \tag{4.89}$$

Further substituting the solutions for the tachyonic field in Eq. (4.87) we get

$$V''(T=-2T_0)=\frac{e^2M_p^2}{6b^2T_0^4}, \tag{4.90}$$

$$V''(T\to\infty)\to 0 \tag{4.91}$$

and also additionally for $T=T_0$ we have

$$V''(T=T_0)=\frac{44M_p^2}{3eb^2T_0^4}, \tag{4.92}$$

and at these points the value of the potential is computed as

$$V(T \to \infty) \to 0, \tag{4.93}$$

$$V(T = -2T_0) = \frac{e^2 M_p^2}{3b^2 T_0^2}, \tag{4.94}$$

$$V(T = T_0) = \frac{4M_p^2}{3b^2 T_0^2}. \tag{4.95}$$

It is important to note for the single tachyonic case that:

- for $b^2 > 0$, $V''(T = -2T_0,\ \ T_0) > 0$, i.e., we get maxima on the potential.
- for $b^2 < 0$, $V''(T = -2T_0,\ \ T_0) < 0$, i.e., we get minima on the potential.

and for the assisted case the results are the same, provided the following replacement occurs:

$$\lambda \to N\lambda, \tag{4.96}$$

and finally for the multi-tachyonic case we have

$$V'(T_i) = -\frac{4M_p^2}{3b^2 T_i^3} \exp\left(-\frac{T_i}{T_{0i}}\right)\left(2 + \frac{T_i}{T_{0i}}\right), \tag{4.97}$$

$$V''(T_i) = \frac{4M_p^2}{3b^2 T_i^4} \exp\left(-\frac{T_i}{T_{0i}}\right) \times \left\{6 + 4\left(\frac{T_i}{T_{0i}}\right) + \left(\frac{T_i}{T_{0i}}\right)^2\right\}. \tag{4.98}$$

Now to find the extrema of the potential we substitute:

$$V'(T_j) = 0 \quad \forall\ j = 1, 2, \ldots, N \tag{4.99}$$

which give rise to the following solutions for the jth tachyonic field:

$$T_j = -2T_{0j},\ \infty. \tag{4.100}$$

Further substituting the solutions for the tachyonic field in Eq. (4.98) we get

$$V''\left(T_j = -2T_{0j}\right) = \frac{e^2 M_p^2}{6b^2 T_{0j}^4}, \tag{4.101}$$

$$V''(T_j \to \infty) \to 0. \tag{4.102}$$

Additionally for the point $T_j = T_{0j}$ we have

$$V''(T_j = T_{0j}) = \frac{44M_p^2}{3eb^2 T_{0j}^4}, \tag{4.103}$$

and at these points the value of the total effective potential is computed as

$$V_E^{(1)} = \sum_{j=1}^{N} V(T_j \to \infty) \to 0, \tag{4.104}$$

$$V_E^{(2)} = \sum_{j=1}^{N} V(T_j = -2T_{0j}) = \sum_{j=1}^{N} \frac{e^2 M_p^2}{3b^2 T_{0j}^2}, \tag{4.105}$$

$$V_E^{(3)} = \sum_{j=1}^{N} V(T_j = T_{0j}) = \frac{4NM_p^2}{3b^2 T_0^2}. \tag{4.106}$$

It is important to note for the multi-tachyonic case that:

- for $b^2 > 0$, $V''(T = -2T_{0j},\ \ T_{0j}) > 0$, i.e., we get maxima on the potential $V_j(T)$ as well in $V_E(T)$.
- for $b^2 < 0$, $V''(T = -2T_{0j},\ \ T_{0j}) < 0$, i.e., we get minima on the potential $V_j(T)$ as well in $V_E(T)$.

Next using Eq. (4.17) the Hubble parameter can be expressed in terms of the usual tachyonic potential $V(T)$ as

$$H^2(t) = \begin{cases} \dfrac{\lambda}{3M_p^2}\left[\dfrac{1}{1 + \frac{\sqrt{3\lambda} bT_0}{2M_p}\left\{\frac{t}{bT_0} - \tanh\left(\frac{t}{bT_0}\right)\right\}}\right]^2, & \text{for Single}, \\ \displaystyle\sum_{i=1}^{N} H_i(t) = \sum_{i=1}^{N} \frac{\lambda_i}{3M_p^2}\left[\frac{1}{1 + \frac{\sqrt{3\lambda} bT_{0i}}{2M_p}\left\{\frac{t}{bT_{0i}} - \tanh\left(\frac{t}{bT_{0i}}\right)\right\}}\right]^2, & \text{for Multi}, \\ \dfrac{N\lambda}{3M_p^2}\left[\dfrac{1}{1 + \frac{\sqrt{3\lambda} bT_0}{2M_p}\left\{\frac{t}{bT_0} - \tanh\left(\frac{t}{bT_0}\right)\right\}}\right]^2, & \text{for Assisted}, \end{cases} \tag{4.107}$$

and for the generalized case we have

$$H^2(t) = \begin{cases} \dfrac{\lambda}{3M_p^2\left[\cosh\left(\frac{t}{bT_0}\right)\right]^{2(2q-1)}}\left[\dfrac{1}{1+\frac{\sqrt{3\lambda}bT_0}{2M_p}\left\{\frac{t}{bT_0}-\tanh\left(\frac{t}{bT_0}\right)\right\}}\right]^2, & \text{for Single} \\ \displaystyle\sum_{i=1}^{N}\dfrac{\lambda_i}{3M_p^2\left[\cosh\left(\frac{t}{bT_{0i}}\right)\right]^{2(2q-1)}}\left[\dfrac{1}{1+\frac{\sqrt{3\lambda}bT_{0i}}{2M_p}\left\{\frac{t}{bT_{0i}}-\tanh\left(\frac{t}{bT_{0i}}\right)\right\}}\right]^2, & \text{for Multi,} \\ \dfrac{N\lambda}{3M_p^2\left[\cosh\left(\frac{t}{bT_0}\right)\right]^{2(2q-1)}}\left[\dfrac{1}{1+\frac{\sqrt{3\lambda}bT_0}{2M_p}\left\{\frac{t}{bT_0}-\tanh\left(\frac{t}{bT_0}\right)\right\}}\right]^2, & \text{for Assisted.} \end{cases} \tag{4.108}$$

Let us study the limiting situation from the expression obtained for the Hubble parameter explicitly:

- In the $T << T_0$ and $T_j << T_{0j}$ limiting situation the Hubble parameter can be approximated for the usual tachyonic case as:

$$H^2(t) = \begin{cases} \dfrac{\lambda}{3M_p^2}, & \text{for Single,} \\ \displaystyle\sum_{i=1}^{N}\dfrac{\lambda_i}{3M_p^2}, & \text{for Multi,} \\ \dfrac{N\lambda}{3M_p^2}, & \text{for Assisted,} \end{cases} \tag{4.109}$$

and for the generalized case we have

$$H^2(t) = \begin{cases} \dfrac{\lambda}{3M_p^2\left[\cosh\left(\frac{t}{bT_0}\right)\right]^{2(2q-1)}}, & \text{for Single,} \\ \displaystyle\sum_{i=1}^{N}\dfrac{\lambda_i}{3M_p^2\left[\cosh\left(\frac{t}{bT_{0i}}\right)\right]^{2(2q-1)}}, & \text{for Multi,} \\ \dfrac{N\lambda}{3M_p^2\left[\cosh\left(\frac{t}{bT_0}\right)\right]^{2(2q-1)}}, & \text{for Assisted.} \end{cases} \tag{4.110}$$

In this limiting situation the solution for the scale factor $a(t)$ from Eq. (4.109) can be expressed as

$$a(t) = \begin{cases} a_{\inf}\exp\left[\dfrac{\sqrt{\lambda}}{\sqrt{3}M_p}(t-t_{\inf})\right], & \text{for Single,} \\ \displaystyle\sum_{i=1}^{N}a_{\inf}\exp\left[\sqrt{\dfrac{\lambda_i}{3M_p^2}}(t-t_{\inf})\right], & \text{for Multi,} \\ a_{\inf}\exp\left[\dfrac{\sqrt{N\lambda}}{\sqrt{3}M_p}(t-t_{\inf})\right], & \text{for Assisted,} \end{cases} \tag{4.111}$$

which is exactly the de Sitter solution required for inflation. Here at the inflationary time scale $t = t_{\inf}$ the scale factor is given by

$$a_{\inf} = a(t = t_{\inf}). \tag{4.112}$$

On the other hand for the generalized case we have the following solution for the scale factor $a(t)$:

$$a(t)=\begin{cases} a_{\rm inf}\exp\left[\frac{\sqrt{\lambda}bT_0}{\sqrt{3}M_p}\left\{\sinh\left(\frac{t}{bT_0}\right)\,{}_2F_1\left[\frac{1}{2},q;\frac{3}{2};-\sinh^2\left(\frac{t}{bT_0}\right)\right]\right\}_{t_{\rm inf}}^{t}\right], & \text{for Single},\\ \sum_{i=1}^{N}a_{\rm inf}\exp\left[\frac{\sqrt{\lambda_i}bT_{0i}}{\sqrt{3}M_p}\left\{\sinh\left(\frac{t}{bT_{0i}}\right)\,{}_2F_1\left[\frac{1}{2},q;\frac{3}{2};-\sinh^2\left(\frac{t}{bT_{0i}}\right)\right]\right\}_{t_{\rm inf}}^{t}\right], & \text{for Multi},\\ a_{\rm inf}\exp\left[\frac{\sqrt{N\lambda}bT_0}{\sqrt{3}M_p}\left\{\sinh\left(\frac{t}{bT_0}\right)\,{}_2F_1\left[\frac{1}{2},q;\frac{3}{2};-\sinh^2\left(\frac{t}{bT_0}\right)\right]\right\}_{t_{\rm inf}}^{t}\right], & \text{for Assisted},\end{cases} \tag{4.113}$$

which replicates the behavior of quasi-de Sitter solution during inflation. For the $q = 1/2$ case it exactly follows the de Sitter behavior.

- In the $T >> T_0$ and $T_j >> T_{0j}$ limiting situation the Hubble parameter can be approximated for the usual tachyonic case as:

$$H^2(t)=\begin{cases}\frac{4}{9t^2}, & \text{for Single}\\ \sum_{i=1}^{N}\frac{4}{9t^2}, & \text{for Multi},\\ \frac{4N}{9t^2}, & \text{for Assisted},\end{cases} \tag{4.114}$$

and for the generalized case we have

$$H^2(t)=\begin{cases}\frac{4}{9t^2\left[\frac{1}{2}\exp\left(\frac{t}{bT_0}\right)\right]^{2(2q-1)}}, & \text{for Single}\\ \sum_{i=1}^{N}\frac{4}{9t^2\left[\frac{1}{2}\exp\left(\frac{t}{bT_{0i}}\right)\right]^{2(2q-1)}}, & \text{for Multi},\\ \frac{4N}{9t^2\left[\frac{1}{2}\exp\left(\frac{t}{bT_0}\right)\right]^{2(2q-1)}}, & \text{for Assisted}.\end{cases} \tag{4.115}$$

In this limiting situation the solution for the scale factor $a(t)$ from Eq. (4.114) can be expressed as

$$a(t)=\begin{cases}a_{\rm dust}\left(\frac{t}{t_{\rm dust}}\right)^{2/3}, & \text{for Single},\\ \sum_{i=1}^{N}a_{\rm dust}\left(\frac{t}{t_{\rm dust}}\right)^{2/3}, & \text{for Multi},\\ a_{\rm dust}\left(\frac{t}{t_{\rm dust}}\right)^{2/3}, & \text{for Assisted},\end{cases} \tag{4.116}$$

which is exactly the dust like solution required for the formation of dark matter. Here at the inflationary time scale $t = t_{\rm dust}$ the scale factor is given by

$$a_{\rm dust} = a(t = t_{\rm dust}). \tag{4.117}$$

On the other hand for the generalized case we have the following solution for the scale factor $a(t)$:

$$a(t)=\begin{cases}a_{\rm dust}\exp\left[\frac{4^q}{3}\left\{{\rm Ei}\left[\left(\frac{t}{bT_0}\right)-2q\right]\right.\right.\\ \quad\left.\left.-{\rm Ei}\left[\left(\frac{t_{\rm dust}}{bT_0}\right)-2q\right]\right\}\right], & \text{for Single},\\ \sum_{i=1}^{N}a_{\rm dust}\exp\left[\frac{4^q}{3}\left\{{\rm Ei}\left[\left(\frac{t}{bT_{0i}}\right)-2q\right]\right.\right.\\ \quad\left.\left.-{\rm Ei}\left[\left(\frac{t_{\rm dust}}{bT_{0i}}\right)-2q\right]\right\}\right], & \text{for Multi},\\ a_{\rm dust}\exp\left[\frac{N4^q}{3}\left\{{\rm Ei}\left[\left(\frac{t}{bT_0}\right)-2q\right]\right.\right.\\ \quad\left.\left.-{\rm Ei}\left[\left(\frac{t_{\rm dust}}{bT_0}\right)-2q\right]\right\}\right], & \text{for Assisted},\end{cases} \tag{4.118}$$

which replicates the behavior of quasi-dust like solution. For the $q = 1/2$ case it exactly follows the dust like behavior.

5 Inflationary paradigm from GTachyon

It is a very well known fact that during cosmological inflation, quantum fluctuations are stretched on the scales larger than the size of the horizon. Consequently, they are frozen until they re-enter the horizon at the end of inflationary phase. In the present context a single tachyonic field drives the inflationary paradigm, which finally gives rise to the large-scale perturbations with a quasi-scale invariant primordial power spectrum corresponding to the scalar and tensor modes. Deviations from the scale invariance in the primordial power spectrum can be measured in terms of the slow-roll parameters which we will explicitly discuss in the next subsections. By detailed computation we explicitly show that at lowest order of the primordial spectrum the scalar perturbations is exactly the same as that obtained for the usual single field inflationary set-up. For completeness the next to leading order corrections to the cosmological perturbations are also derived, which finally give rise to the sufficient change in the cosmological consistency relations with respect to the results obtained for the usual single field inflationary set-up. Hence we apply all the derived results for the tachyonic inflationary models as explicitly mentioned in the previous section and study the CMB constraints by applying the recent Planck 2015 data.

5.1 Computation for single field inflation

5.1.1 Condition for inflation

For single field tachyonic inflation, the prime condition for inflation is given by

$$\dot{H} + H^2 = \left(\frac{\ddot{a}}{a}\right) = -\frac{(\rho + 3p)}{6M_p^2} > 0, \tag{5.1}$$

which can be re-expressed in terms of the following constraint condition in the context of single field tachyonic inflation:

$$\frac{V(T)}{3M_p^2\sqrt{1-\alpha'\dot{T}^2}}\left(1 - \frac{3}{2}\alpha'\dot{T}^2\right) > 0. \tag{5.2}$$

Here Eq. (5.6) implies that, to satisfy inflationary constraints in the slow-roll regime, the following constraint always holds good:

$$\dot{T} < \sqrt{\frac{2}{3\alpha'}}, \tag{5.3}$$

$$\ddot{T} < 3H\dot{T} < \sqrt{\frac{6}{\alpha'}}H. \tag{5.4}$$

Consequently the field equations are approximated by

$$3H\alpha'\dot{T} + \frac{\mathrm{d}V(T)}{V(T)\mathrm{d}T} \approx 0. \tag{5.5}$$

Similarly, in the most generalized case,

$$\frac{V(T)}{3M_p^2\left(1-\alpha'\dot{T}^2\right)^{1-q}}\left(1 - (1+q)\alpha'\dot{T}^2\right) > 0. \tag{5.6}$$

Here Eq. (5.6) implies that to satisfy inflationary constraints in the slow-roll regime the following constraint always holds good:

$$\dot{T} < \sqrt{\frac{1}{\alpha'(1+q)}}, \tag{5.7}$$

$$\ddot{T} < 3H\dot{T} < \sqrt{\frac{9}{\alpha'(1+q)}}H. \tag{5.8}$$

Consequently the field equations are approximated by

$$6q\alpha' H\dot{T} + \frac{\mathrm{d}V(T)}{V(T)\mathrm{d}T} \approx 0. \tag{5.9}$$

Also for both cases in the slow-roll regime the Friedmann equation is modified as

$$H^2 \approx \frac{V(T)}{3M_p^2}. \tag{5.10}$$

Further substituting Eq. (5.10) in Eqs. (5.5) and (5.9) we get

$$\frac{\sqrt{3V(T)}}{M_p}\alpha'\dot{T} + \frac{\mathrm{d}V(T)}{V(T)\mathrm{d}T} \approx 0, \tag{5.11}$$

$$6q\frac{\sqrt{V(T)}}{\sqrt{3}M_p}\alpha'\dot{T} + \frac{\mathrm{d}V(T)}{V(T)\mathrm{d}T} \approx 0. \tag{5.12}$$

Finally the general solution for both cases can be expressed in terms of the single field tachyonic potential $V(T)$ as

$$t - t_i \approx -\frac{\sqrt{3}\alpha'}{M_p}\int_{T_i}^{T}\mathrm{d}T\,\frac{V^{3/2}(T)}{V'(T)}, \tag{5.13}$$

$$t - t_i \approx -\frac{6q\alpha'}{\sqrt{3}M_p}\int_{T_i}^{T}\mathrm{d}T\,\frac{V^{3/2}(T)}{V'(T)}. \tag{5.14}$$

Let us now re-write Eqs. (5.332) and (5.333), in terms of the string theoretic tachyonic potentials as already mentioned in the last section. For the $q = 1/2$ situation we get

$$t - t_i \approx \begin{cases} \dfrac{\alpha' T_0^2}{2M_p}\sqrt{3\lambda}\left\{\ln\left[\dfrac{\left(\sqrt{\operatorname{sech}\left(\frac{T_i}{T_0}\right)}+1\right)\left(1-\sqrt{\operatorname{sech}\left(\frac{T}{T_0}\right)}\right)}{\left(\sqrt{\operatorname{sech}\left(\frac{T}{T_0}\right)}+1\right)\left(1-\sqrt{\operatorname{sech}\left(\frac{T_i}{T_0}\right)}\right)}\right]\right. \\ \left. +2\tan^{-1}\left[\dfrac{\sqrt{\operatorname{sech}\left(\frac{T_i}{T_0}\right)}-\sqrt{\operatorname{sech}\left(\frac{T}{T_0}\right)}}{1+\sqrt{\operatorname{sech}\left(\frac{T_i}{T_0}\right)\operatorname{sech}\left(\frac{T}{T_0}\right)}}\right]\right\}, & \text{for Model 1,} \\ -\dfrac{\alpha' T_0^2}{2M_p}\sqrt{3\lambda}\,\ln\left(\dfrac{\ln\left(\frac{T}{T_0}\right)\left(\ln\left(\frac{T_i}{T_0}\right)+1\right)}{\ln\left(\frac{T_i}{T_0}\right)\left(\ln\left(\frac{T}{T_0}\right)+1\right)}\right), & \text{for Model 2,} \\ -\dfrac{2\alpha' T_0^2}{M_p}\sqrt{3\lambda}\left\{\exp\left[-\dfrac{T}{2T_0}\right]-\exp\left[-\dfrac{T_i}{2T_0}\right]\right\}, & \text{for Model 3,} \\ -\dfrac{\alpha' T_0^2}{4M_p}\sqrt{3\lambda}\left\{\mathrm{Ei}\left(-\dfrac{T_i^2}{2T_0^2}\right)-\mathrm{Ei}\left(-\dfrac{T^2}{2T_0^2}\right)\right\}, & \text{for Model 4,} \\ \dfrac{\alpha' T_0^2}{8M_p}\sqrt{3\lambda}\left\{\ln\left(\dfrac{\sqrt{T_0^4+T^4}+T^2}{\sqrt{T_0^4+T_i^4}+T_i^2}\right)+\sqrt{1+\left(\dfrac{T_0}{T_i}\right)^4}-\sqrt{1+\left(\dfrac{T_0}{T}\right)^4}\right\}, & \text{for Model 5,} \end{cases} \tag{5.15}$$

and for any arbitrary q we get the following generalized result:

$$t - t_i \approx \begin{cases} \dfrac{3q\alpha' T_0^2}{M_p}\sqrt{\dfrac{\lambda}{3}}\left\{\ln\left[\dfrac{\left(\sqrt{\operatorname{sech}\left(\frac{T_i}{T_0}\right)}+1\right)\left(1-\sqrt{\operatorname{sech}\left(\frac{T}{T_0}\right)}\right)}{\left(\sqrt{\operatorname{sech}\left(\frac{T}{T_0}\right)}+1\right)\left(1-\sqrt{\operatorname{sech}\left(\frac{T_i}{T_0}\right)}\right)}\right]\right. \\ \left. +2\tan^{-1}\left[\dfrac{\sqrt{\operatorname{sech}\left(\frac{T_i}{T_0}\right)}-\sqrt{\operatorname{sech}\left(\frac{T}{T_0}\right)}}{1+\sqrt{\operatorname{sech}\left(\frac{T_i}{T_0}\right)\operatorname{sech}\left(\frac{T}{T_0}\right)}}\right]\right\}, & \text{for Model 1,} \\ -\dfrac{3q\alpha' T_0^2}{M_p}\sqrt{\dfrac{\lambda}{3}}\,\ln\left(\dfrac{\ln\left(\frac{T}{T_0}\right)\left(\ln\left(\frac{T_i}{T_0}\right)+1\right)}{\ln\left(\frac{T_i}{T_0}\right)\left(\ln\left(\frac{T}{T_0}\right)+1\right)}\right), & \text{for Model 2,} \\ -\dfrac{12q\alpha' T_0^2}{M_p}\sqrt{\dfrac{\lambda}{3}}\left\{\exp\left[-\dfrac{T}{2T_0}\right]-\exp\left[-\dfrac{T_i}{2T_0}\right]\right\}, & \text{for Model 3,} \\ -\dfrac{3q\alpha' T_0^2}{2M_p}\sqrt{\dfrac{\lambda}{3}}\left\{\mathrm{Ei}\left(-\dfrac{T_i^2}{2T_0^2}\right)-\mathrm{Ei}\left(-\dfrac{T^2}{2T_0^2}\right)\right\}, & \text{for Model 4,} \\ \dfrac{3q\alpha' T_0^2}{4M_p}\sqrt{\dfrac{\lambda}{3}}\left\{\ln\left(\dfrac{\sqrt{T_0^4+T^4}+T^2}{\sqrt{T_0^4+T_i^4}+T_i^2}\right)+\sqrt{1+\left(\dfrac{T_0}{T_i}\right)^4}-\sqrt{1+\left(\dfrac{T_0}{T}\right)^4}\right\}. & \text{for Model 5.} \end{cases} \tag{5.16}$$

Further using Eqs. (5.15), (5.16) and (5.10) we get the following solution for the scale factor in terms of the tachyonic field for the usual $q = 1/2$ and for a generalized value of q as:

$$a = a_i \times \begin{cases} \exp\left[-\frac{\alpha'}{M_p^2}\int_{T_i}^{T} dT\,\frac{V^2(T)}{V'(T)}\right], & \text{for } q = 1/2, \\ \exp\left[-\frac{2q\alpha'}{M_p^2}\int_{T_i}^{T} dT\,\frac{V^2(T)}{V'(T)}\right], & \text{for any arbitrary } q. \end{cases} \tag{5.17}$$

Finally re-writing Eq. (5.334), in terms of the string theoretic tachyonic potentials as already mentioned in the last section for $q = 1/2$, we get

$$a \approx a_i \times \begin{cases} \exp\left[\frac{\alpha' T_0^2\lambda}{M_p^2}\ln\left(\frac{\tanh\left(\frac{T}{2T_0}\right)}{\tanh\left(\frac{T_i}{2T_0}\right)}\right)\right], & \text{for Model 1}, \\ \exp\left[-\frac{\alpha' T_0^2\lambda}{2M_p^2}\ln\left(\frac{\ln\left(\frac{T}{T_0}\right)\left(\ln\left(\frac{T_i}{T_0}\right)+1\right)}{\ln\left(\frac{T_i}{T_0}\right)\left(\ln\left(\frac{T}{T_0}\right)+1\right)}\right)\right], & \text{for Model 2}, \\ \exp\left[\frac{\alpha' T_0^2\lambda}{M_p^2}\left(\exp\left[-\frac{T_i}{T_0}\right]-\exp\left[-\frac{T}{T_0}\right]\right)\right], & \text{for Model 3}, \\ \exp\left[-\frac{\alpha' T_0^2\lambda}{4M_p^2}\left\{\mathrm{Ei}\left(-\frac{T_i^2}{T_0^2}\right)-\mathrm{Ei}\left(-\frac{T^2}{T_0^2}\right)\right\}\right], & \text{for Model 4}, \\ \exp\left[-\frac{\alpha' T_0^4\lambda}{8M_p^2}\left(\frac{1}{T^2}-\frac{1}{T_i^2}\right)\right], & \text{for Model 5}, \end{cases} \tag{5.18}$$

and for any arbitrary q we get

$$a \approx a_i \times \begin{cases} \exp\left[\frac{2q\alpha' T_0^2\lambda}{3M_p^2}\ln\left(\frac{\tanh\left(\frac{T}{2T_0}\right)}{\tanh\left(\frac{T_i}{2T_0}\right)}\right)\right], & \text{for Model 1}, \\ \exp\left[-\frac{q\alpha' T_0^2\lambda}{M_p^2}\ln\left(\frac{\ln\left(\frac{T}{T_0}\right)\left(\ln\left(\frac{T_i}{T_0}\right)+1\right)}{\ln\left(\frac{T_i}{T_0}\right)\left(\ln\left(\frac{T}{T_0}\right)+1\right)}\right)\right], & \text{for Model 2}, \\ \exp\left[\frac{2q\alpha' T_0^2\lambda}{M_p^2}\left(\exp\left[-\frac{T_i}{T_0}\right]-\exp\left[-\frac{T}{T_0}\right]\right)\right], & \text{for Model 3}, \\ \exp\left[-\frac{q\alpha' T_0^2\lambda}{2M_p^2}\left\{\mathrm{Ei}\left(-\frac{T_i^2}{T_0^2}\right)-\mathrm{Ei}\left(-\frac{T^2}{T_0^2}\right)\right\}\right], & \text{for Model 4}, \\ \exp\left[-\frac{q\alpha' T_0^4\lambda}{4M_p^2}\left(\frac{1}{T^2}-\frac{1}{T_i^2}\right)\right]. & \text{for Model 5}. \end{cases} \tag{5.19}$$

Hence using Eqs. (5.15), (5.16), (5.18) and (5.19) one can study the parametric behavior of the scale factor $a(t)$ with respect to time t and expected to be as like exact de Sitter or quasi-de Sitter solution during the inflationary slow-roll phase, as explicitly derived in the previous section.

5.1.2 Analysis using slow-roll formalism

Here our prime objective is to define slow-roll parameters for tachyon inflation in terms of the Hubble parameter and the single field tachyonic inflationary potential. Using the slow-roll approximation one can expand various cosmological observables in terms of small dynamical quantities derived from the appropriate derivatives of the Hubble parameter and of the inflationary potential. To start with here we use the horizon-flow parameters based on derivatives of Hubble parameter with respect to the number of e-foldings N, defined as

$$N(t) = \int_t^{t_{\text{end}}} H(t)\,dt, \tag{5.20}$$

where t_{end} signifies the end of inflation. Further using Eqs. (5.5), (5.9), (5.10) and (5.335) we get

$$\frac{dT}{dN} = \frac{\dot{T}}{H} = \begin{cases} -\frac{2H'}{3\alpha' H^3}, & \text{for } q = 1/2, \\ -\frac{2H'}{3\alpha' H^3}\left(\frac{1-\alpha'(1-2q)\dot{T}^2}{2q}\right), & \text{for any arbitrary } q, \end{cases} \tag{5.21}$$

where $H' > 0$ which makes always $\dot{T} > 0$ during the inflationary phase. Further using Eq. (5.21) we get the following differential operator identity for tachyonic inflation:

$$\frac{1}{H}\frac{d}{dt} = \frac{d}{dN} = \frac{d}{d\ln k} = \begin{cases} -\frac{2H'}{3\alpha' H^3}\frac{d}{dT}, & \text{for } q = 1/2, \\ -\frac{2H'}{3\alpha' H^3}\left(\frac{1-\alpha'(1-2q)\dot{T}^2}{2q}\right)\frac{d}{dT}, & \text{for any arbitrary } q. \end{cases} \tag{5.22}$$

Next we define the following Hubble slow-roll parameters:

$$\epsilon_0 = \frac{H_\star}{H}, \tag{5.23}$$

$$\epsilon_{i+1} = \frac{d\ln|\epsilon_i|}{dN}, \quad i \geq 1 \tag{5.24}$$

where $H_\star$ is the Hubble parameter at the pivot scale. Further using the differential operator identity as mentioned in Eq. (5.22) we get the following Hubble flow equation for tachyonic inflation for $i \geq 0$:

$$\frac{1}{H}\frac{\mathrm{d}\epsilon_i}{\mathrm{d}t}=\frac{\mathrm{d}\epsilon_i}{\mathrm{d}N}=\epsilon_{i+1}\epsilon_i=\begin{cases}-\frac{2H'}{3\alpha' H^3}\frac{\mathrm{d}\epsilon_i}{\mathrm{d}T}, & \text{for } q=1/2,\\ -\frac{2H'}{3\alpha' H^3}\left(\frac{1-\alpha'(1-2q)\dot{T}^2}{2q}\right)\frac{\mathrm{d}\epsilon_i}{\mathrm{d}T}, & \text{for any arbitrary } q.\end{cases} \tag{5.25}$$

For a realistic estimate from the single field tachyonic inflationary model substituting the free index i to $i=0,1,2$ in Eqs. (5.23) and (5.25) we get the contributions from the first three Hubble slow-roll parameter, which can be depicted as

$$\epsilon_1=\frac{\mathrm{d}\ln|\epsilon_0|}{\mathrm{d}N}=-\frac{\dot{H}}{H^2}=\begin{cases}\frac{2}{3\alpha'}\left(\frac{H'}{H^2}\right)^2=\frac{3}{2}\alpha'\dot{T}^2, & \text{for } q=1/2\\ \frac{2}{3\alpha'}\left(\frac{H'}{H^2}\right)^2\left(\frac{1-\alpha'(1-2q)\dot{T}^2}{2q}\right) & \\ \quad=\frac{3}{2}\alpha'\dot{T}^2\left(\frac{2q}{1-\alpha'(1-2q)\dot{T}^2}\right), & \text{for any arbitrary } q,\end{cases} \tag{5.26}$$

$$\epsilon_2=\frac{\mathrm{d}\ln|\epsilon_1|}{\mathrm{d}N}=\frac{\ddot{H}}{H\dot{H}}+2\epsilon_1=\begin{cases}\sqrt{\frac{2}{3\alpha'\epsilon_1}}\frac{\epsilon_1'}{H}=2\frac{\ddot{T}}{H\dot{T}}, & \text{for } q=1/2\\ \sqrt{\frac{2}{3\alpha'\epsilon_1}\left(\frac{1-\alpha'(1-2q)\dot{T}^2}{2q}\right)}\frac{\epsilon_1'}{H} & \\ \quad=\frac{2\ddot{T}}{H\dot{T}\left(1-\alpha'(1-2q)\dot{T}^2\right)}, & \text{for any arbitrary } q,\end{cases} \tag{5.27}$$

$$\begin{aligned}\epsilon_3&=\frac{\mathrm{d}\ln|\epsilon_2|}{\mathrm{d}N}=\frac{1}{\epsilon_2}\left[\frac{\dddot{H}}{H^2\dot{H}}-3\frac{\ddot{H}}{H^3}-\frac{\ddot{H}^2}{H^2\dot{H}^2}+4\frac{\dot{H}^2}{H^4}\right]\\ &=\begin{cases}\sqrt{\frac{2\epsilon_1}{3\alpha'}}\frac{\epsilon_2'}{H}=\left[\frac{2\dddot{T}}{H^2\dot{T}\epsilon_2}+\epsilon_1-\frac{\epsilon_2}{2}\right], & \text{for } q=1/2,\\ \sqrt{\frac{2\epsilon_1}{3\alpha'}\left(\frac{1-\alpha'(1-2q)\dot{T}^2}{2q}\right)}\frac{\epsilon_2'}{H}=\frac{\left[\frac{2\dddot{T}}{H^2\dot{T}\epsilon_2}+\epsilon_1-\frac{\epsilon_2}{2}\right]}{\left(1-\alpha'(1-2q)\dot{T}^2\right)}+\frac{\frac{4\alpha'(1-2q)\ddot{T}^2}{H}}{\left(1-\alpha'(1-2q)\dot{T}^2\right)^2}, & \text{for any arbitrary } q.\end{cases}\end{aligned} \tag{5.28}$$

It is important to note that:

- In the present context ϵ_1 is characterized by the part of the total tachyonic energy density $\dot{T}^2$. Inflation occurs when $\epsilon_1 < 1$ and ends when $\epsilon_1 = 1$, which is exactly the same as the other single field slow-roll inflationary paradigm.
- The slow-roll parameter ϵ_2 characterizes the ratio of the field acceleration relative to the frictional contribution acting on it due to the expansion.
- The third slow-roll parameter ϵ_3 is made up of both ϵ_1 and ϵ_2. More precisely, ϵ_3 is made up of $\dot{T}$, $\ddot{T}$ and $\dddot{T}$. This clearly implies that the third slow-roll parameter ϵ_3 carries the contribution from the part of total tachyonic energy density, field acceleration relative to the frictional contribution and rate of change of field acceleration.
- The slow-roll conditions stated in Eqs. (5.3) and (5.4) are satisfied when the slow-roll parameters satisfy $\epsilon_1 << 1$, $\epsilon_2 << 1$ and $\epsilon_3 << 1$. This also implies that in the slow-roll regime of the tachyonic inflation product of the two slow-roll parameters are also less than unity. For an example from Eq. (5.38) it is clearly observed that to satisfy the slow-roll condition we need to have additionally $\epsilon_2\epsilon_3 << 1$.

Now for the sake of clarity, using Hamilton–Jacobi formalism, the Friedman equations and conservation equation can be rewritten as

$$0 \approx \begin{cases} \left[H'(T)\right]^2 - \frac{9\alpha'}{4} H^4(T) + \frac{\alpha'}{4M_p^4} V^2(T), & \text{for } q = 1/2, \\ H^2(T) \left[1 - \frac{4\left[H'(T)\right]^2}{9\alpha' H^4(T)} \left(\frac{1-\alpha'(1-2q)\dot{T}^2}{2q}\right)^2\right]^{1-q} & \\ -\frac{V(T)}{3M_p^2} \left[1 - \frac{4(1-2q)\left[H'(T)\right]^2}{9\alpha' H^4(T)} \left(\frac{1-\alpha'(1-2q)\dot{T}^2}{2q}\right)^2\right], & \text{for any arbitrary } q, \end{cases} \tag{5.29}$$

and

$$H'(T) \approx \begin{cases} -\frac{3\alpha'}{2} H^2(T)\dot{T}, & \text{for } q = 1/2, \\ -\frac{3\alpha'}{2} H^2(T)\dot{T} \left(\frac{2q}{1-\alpha'(1-2q)\dot{T}^2}\right), & \text{for any arbitrary } q. \end{cases} \tag{5.30}$$

Further using the definition of the first Hubble slow-roll parameter ϵ_1 in Eq. (5.29) we get

$$\begin{cases} H^2(T) \left[1 - \frac{2}{3}\epsilon_1(T)\right]^{1/2} = \frac{V(T)}{3M_p^2}, & \text{for } q = 1/2, \\ H^2(T) \left[1 - \frac{1}{3q}\epsilon_1(T)\right]^{1-q} \approx \frac{V(T)}{3M_p^2} \left[1 - \frac{(1-2q)}{3q}\epsilon_1(T)\right], & \text{for any arbitrary } q, \end{cases} \tag{5.31}$$

where for the arbitrary q we have used the following constraint condition:

$$1 - \underbrace{\alpha'(1-2q)\dot{T}^2}_{<<1} \approx 1. \tag{5.32}$$

Now as in the slow-roll regime of tachyonic inflation $\epsilon_1(T) << 1$, consequently one can expand the exponents appearing in the left hand side of Eq. (5.31), which leads to the following simplified expression:

$$\begin{cases} H^2(T) \left[1 - \frac{1}{3}\epsilon_1(T)\right] + \mathcal{O}(\epsilon_1^2(T)) = \frac{V(T)}{3M_p^2}, & \text{for } q = 1/2, \\ H^2(T) \left[1 - \frac{1-q}{3q}\epsilon_1(T)\right] + \mathcal{O}(\epsilon_1^2(T)) \approx \frac{V(T)}{3M_p^2} \left[1 - \frac{(1-2q)}{3q}\epsilon_1(T)\right], & \text{for any arbitrary } q. \end{cases} \tag{5.33}$$

It is important to mention here that:

- The result for $q = 1/2$ implies that except for the second order correction term in slow-roll i.e., $\mathcal{O}(\epsilon_1^2(T))$ the rest of the contribution exactly matches with the known result for the single field slow-roll inflationary models. But in the non-slow-roll limiting situation truncating at second order in slow-roll is not allowed and in that case for correct computation one needs to consider the full binomial series expansion.
- For $q \neq \frac{1}{2}$, i.e., for any other arbitrary q in the slow-roll regime of tachyonic inflation we have allowed the second order correction term in slow-roll i.e., $\mathcal{O}(\epsilon_1^2(T))$ as appearing for $q \neq \frac{1}{2}$. But the final result implies significant deviation from the result that is well known for single field slow-roll inflationary models in the slow-roll regime. As mentioned earlier in the non-slow-roll limiting situation truncating at a certain order in slow-roll is not allowed and in that case for correct computation one needs to consider the full binomial series expansion.Also for $q \neq \frac{1}{2}$ case, the right hand side of Eq. (5.33) gets modified in the presence of slow-roll parameter ϵ_1.

Our next objective is to express the Hubble slow-roll parameters in terms of the tachyon potential dependent slow-roll parameters. To serve this purpose let us start with writing the expression for the derivatives of the potential in terms of the Hubble slow-roll parameters. Allowing up to the second order contribution in the Hubble slow-roll parameters we get [86]

$$M_p^2\frac{V'(T)}{V(T)H(T)} = -\sqrt{6\epsilon_1}\frac{\left(1-\frac{2}{3}\epsilon_1+\frac{\epsilon_2}{6}\right)}{\left(1-\frac{2}{3}\epsilon_1\right)}, \tag{5.34}$$

$$M_p^4\frac{V''(T)}{V(T)H^2(T)} = 6\epsilon_1\frac{\left(1-\frac{2}{3}\epsilon_1+\frac{\epsilon_2}{6}\right)\left(1-\frac{2}{3}\epsilon_1-\frac{\epsilon_2}{3}\right)}{\left(1-\frac{2}{3}\epsilon_1\right)^2} + \frac{\epsilon_2}{2}\frac{\left(5\epsilon_1-\frac{\epsilon_2}{3}-\epsilon_3\right)}{\left(1-\frac{2}{3}\epsilon_1\right)} + 3\left(\epsilon_1-\frac{\epsilon_2}{2}\right), \tag{5.35}$$

Further using Eqs. (5.36), (5.37), (5.38), (5.34) and (5.35) one can re-express the Hubble slow-roll parameters in terms of the potential dependent slow-roll parameter as

$$\epsilon_1 \approx \begin{cases} \frac{M_p^2}{2\alpha'}\frac{V'^2(T)}{V^3(T)} = \frac{\epsilon_V}{V(T)\alpha'} \equiv \bar{\epsilon}_V, & \text{for } q=1/2,\\ \frac{M_p^2}{4q\alpha'}\frac{V'^2(T)}{V^3(T)} = \frac{\epsilon_V}{2qV(T)\alpha'} \equiv \frac{\bar{\epsilon}_V}{2q}, & \text{for any } q, \end{cases} \tag{5.36}$$

$$\epsilon_2 \approx \begin{cases} \frac{M_p^2}{\alpha'}\left(3\frac{V'^2(T)}{V^3(T)} - 2\frac{V''(T)}{V^2(T)}\right) = \frac{2\,(3\epsilon_V-\eta_V)}{V(T)\alpha'} = 2\,(3\bar{\epsilon}_V-\bar{\eta}_V)\,, & \text{for } q=1/2,\\ \frac{M_p^2}{\sqrt{2q}\alpha'}\left(3\frac{V'^2(T)}{V^3(T)} - 2\frac{V''(T)}{V^2(T)}\right) = \frac{\sqrt{\frac{2}{q}}\,(3\epsilon_V-\eta_V)}{V(T)\alpha'} = \sqrt{\frac{2}{q}}\,(3\bar{\epsilon}_V-\bar{\eta}_V)\,. & \text{for any } q \end{cases} \tag{5.37}$$

$$\epsilon_3\epsilon_2 \approx \begin{cases} \frac{M_p^4}{V^2(T)\alpha'^2}\left(2\frac{V'''(T)V'(T)}{V^2(T)} - 10\frac{V''(T)V'^2(T)}{V^3(T)} + 9\frac{V'^4(T)}{V^4(T)}\right) \\ = \frac{\left(2\xi_V^2-5\eta_V\epsilon_V+36\epsilon_V^2\right)}{V^2(T)\alpha'^2} = \left(2\bar{\xi}_V^2-5\bar{\eta}_V\bar{\epsilon}_V+36\bar{\epsilon}_V^2\right), & \text{for } q=1/2,\\ \frac{M_p^4}{\sqrt{2q}V^2(T)\alpha'^2}\left(2\frac{V'''(T)V'(T)}{V^2(T)} - 10\frac{V''(T)V'^2(T)}{V^3(T)} + 9\frac{V'^4(T)}{V^4(T)}\right) \\ = \frac{\left(2\xi_V^2-5\eta_V\epsilon_V+36\epsilon_V^2\right)}{\sqrt{2q}V^2(T)\alpha'^2} = \frac{\left(2\bar{\xi}_V^2-5\bar{\eta}_V\bar{\epsilon}_V+36\bar{\epsilon}_V^2\right)}{\sqrt{2q}}, & \text{for any } q, \end{cases} \tag{5.38}$$

where the potential dependent slow-roll parameters $\epsilon_V, \eta_V, \xi_V^2, \sigma_V^3$ are defined as

$$\epsilon_V = \frac{M_p^2}{2}\left(\frac{V'(T)}{V(T)}\right)^2, \tag{5.39}$$

$$\eta_V = M_p^2\left(\frac{V''(T)}{V(T)}\right), \tag{5.40}$$

$$\xi_V^2 = M_p^4\left(\frac{V'(T)V'''(T)}{V^2(T)}\right), \tag{5.41}$$

$$\sigma_V^3 = M_p^6\left(\frac{V'^2(T)V''''(T)}{V^3(T)}\right), \tag{5.42}$$

which is exactly similar to the expression for the slow-roll parameter as appearing in the context of single field slow-roll inflationary models. However, for the sake of clarity here we introduce new sets of potential dependent slow-roll parameters for tachyonic inflation by rescaling with the appropriate powers of $\alpha' V(T)$:

$$\bar{\epsilon}_V = \frac{\epsilon_V}{\alpha' V(T)} = \frac{M_p^2}{2\alpha' V(T)}\left(\frac{V'(T)}{V(T)}\right)^2, \tag{5.43}$$

$$\bar{\eta}_V = \frac{\eta_V}{\alpha' V(T)} = \frac{M_p^2}{\alpha' V(T)}\left(\frac{V''(T)}{V(T)}\right), \tag{5.44}$$

$$\bar{\xi}_V^2 = \frac{\xi_V^2}{\alpha'^2 V^2(T)} = \frac{M_p^4}{\alpha'^2 V^2(T)}\left(\frac{V'(T)V'''(T)}{V^2(T)}\right), \tag{5.45}$$

$$\bar{\sigma}_V^3 = \frac{\sigma_V^3}{\alpha'^3 V^3(T)} = \frac{M_p^6}{\alpha'^3 V^3(T)}\left(\frac{V'^2(T)V''''(T)}{V^3(T)}\right). \tag{5.46}$$

Further using Eqs. (5.39)–(5.46) we get the following operator identity for tachyonic inflation:

$$\frac{1}{H}\frac{\mathrm{d}}{\mathrm{d}t} = \frac{\mathrm{d}}{\mathrm{d}N} = \frac{\mathrm{d}}{\mathrm{d}\ln k} \approx \begin{cases} \sqrt{\frac{2\bar{\epsilon}_V}{V(T)\alpha'}}M_p\left(1-\frac{2}{3}\bar{\epsilon}_V\right)^{1/4}\frac{\mathrm{d}}{\mathrm{d}T}, & \text{for} \quad q=1/2,\\ \sqrt{\frac{2\bar{\epsilon}_V}{V(T)\alpha'}}\frac{M_p}{2q}\left(1-\frac{1}{3q}\bar{\epsilon}_V\right)^{1/4}\frac{\mathrm{d}}{\mathrm{d}T}, & \text{for any arbitrary } q. \end{cases} \tag{5.47}$$

Finally using Eq. (5.47) we get the following sets of flow equations in the context of tachyonic inflation:

$$\frac{\mathrm{d}\epsilon_1}{\mathrm{d}N} = \begin{cases} \frac{\mathrm{d}\bar{\epsilon}_V}{\mathrm{d}N} = 2\bar{\epsilon}_V\left(\bar{\eta}_V - 3\bar{\epsilon}_V\right)\left(1-\frac{2}{3}\bar{\epsilon}_V\right)^{1/4}, & \text{for} \quad q=1/2,\\ \frac{1}{2q}\frac{\mathrm{d}\bar{\epsilon}_V}{\mathrm{d}N} = \frac{\bar{\epsilon}_V}{q}\left(\bar{\eta}_V - 3\bar{\epsilon}_V\right)\left(1-\frac{1}{3q}\bar{\epsilon}_V\right)^{1/4}, & \text{for any } q, \end{cases} \tag{5.48}$$

$$\frac{\mathrm{d}\epsilon_2}{\mathrm{d}N} = \begin{cases} 2\left(10\bar{\epsilon}_V\bar{\eta}_V - 18\bar{\epsilon}_V^2 - \bar{\xi}_V^2\right)\left(1-\frac{2}{3}\bar{\epsilon}_V\right)^{1/4}, & \text{for} \quad q=1/2,\\ \sqrt{\frac{2}{q}}\left(10\bar{\epsilon}_V\bar{\eta}_V - 18\bar{\epsilon}_V^2 - \bar{\xi}_V^2\right)\left(1-\frac{1}{3q}\bar{\epsilon}_V\right)^{1/4}, & \text{for any } q, \end{cases} \tag{5.49}$$

$$\frac{\mathrm{d}(\epsilon_2\epsilon_3)}{\mathrm{d}N} = \begin{cases} \left(2\bar{\sigma}_V^3 - 216\bar{\epsilon}_V^3 + 2\bar{\xi}_V^2\bar{\eta}_V - 7\bar{\xi}_V^2\bar{\epsilon}_V + 194\bar{\epsilon}_V^2\bar{\eta}_V - 10\bar{\eta}_V^2\bar{\epsilon}_V\right)\left(1-\frac{2}{3}\bar{\epsilon}_V\right)^{1/4}, & \text{for} \quad q=1/2,\\ \frac{\left(2\bar{\sigma}_V^3 - 216\bar{\epsilon}_V^3 + 2\bar{\xi}_V^2\bar{\eta}_V - 7\bar{\xi}_V^2\bar{\epsilon}_V + 194\bar{\epsilon}_V^2\bar{\eta}_V - 10\bar{\eta}_V^2\bar{\epsilon}_V\right)}{\sqrt{2q}}\left(1-\frac{1}{3q}\bar{\epsilon}_V\right)^{1/4}, & \text{for any } q, \end{cases} \tag{5.50}$$

where we use the following consistency conditions for the rescaled potential dependent slow-roll parameters:

$$\frac{\mathrm{d}\bar{\epsilon}_V}{\mathrm{d}N} = \begin{cases} 2\bar{\epsilon}_V\left(\bar{\eta}_V - 3\bar{\epsilon}_V\right)\left(1-\frac{2}{3}\bar{\epsilon}_V\right)^{1/4}, & \text{for} \quad q=1/2,\\ 2\bar{\epsilon}_V\left(\bar{\eta}_V - 3\bar{\epsilon}_V\right)\left(1-\frac{1}{3q}\bar{\epsilon}_V\right)^{1/4}. & \text{for any } q \end{cases} \tag{5.51}$$

$$\frac{\mathrm{d}\bar{\eta}_V}{\mathrm{d}N} = \begin{cases} \left(\bar{\xi}_V^2 - 4\bar{\epsilon}_V\bar{\eta}_V\right)\left(1-\frac{2}{3}\bar{\epsilon}_V\right)^{1/4}, & \text{for} \quad q=1/2,\\ \left(\bar{\xi}_V^2 - 4\bar{\epsilon}_V\bar{\eta}_V\right)\left(1-\frac{1}{3q}\bar{\epsilon}_V\right)^{1/4}. & \text{for any } q, \end{cases} \tag{5.52}$$

$$\frac{\mathrm{d}\bar{\xi}_V^2}{\mathrm{d}N} = \begin{cases} \left(\bar{\sigma}_V^3 + \bar{\xi}_V^2\bar{\eta}_V - \bar{\xi}_V^2\bar{\epsilon}_V\right)\left(1-\frac{2}{3}\bar{\epsilon}_V\right)^{1/4}, & \text{for} \quad q=1/2,\\ \left(\bar{\sigma}_V^3 + \bar{\xi}_V^2\bar{\eta}_V - \bar{\xi}_V^2\bar{\epsilon}_V\right)\left(1-\frac{1}{3q}\bar{\epsilon}_V\right)^{1/4}. & \text{for any } q \end{cases} \tag{5.53}$$

$$\frac{d\bar{\sigma}_V^3}{dN} = \begin{cases} \bar{\sigma}_V^3\,(\bar{\eta}_V - 12\bar{\epsilon}_V)\left(1-\frac{2}{3}\bar{\epsilon}_V\right)^{1/4}, & \text{for}\quad q=1/2,\\ \bar{\sigma}_V^3\,(\bar{\eta}_V - 12\bar{\epsilon}_V)\left(1-\frac{1}{3q}\bar{\epsilon}_V\right)^{1/4}, & \text{for any } q. \end{cases} \tag{5.54}$$

In terms of the slow-roll parameters, the number of e-foldings can be re-expressed as

$$N(T) = \begin{cases} \sqrt{\frac{3\alpha'}{2}}\int_T^{T_{\mathrm{end}}}\frac{H(T)}{\sqrt{\epsilon_1}}\,dT \\ = \sqrt{\frac{3\alpha'}{2}}\int_T^{T_{\mathrm{end}}}\frac{H(T)}{\sqrt{\bar{\epsilon}_V}}\,dT \\ \approx \frac{\alpha'}{M_p^2}\int_{T_{\mathrm{end}}}^{T}\frac{V^2(T)}{V'(T)}\,dT, & \text{for}\quad q=1/2 \\ 2q\sqrt{\frac{3\alpha'}{2}}\int_T^{T_{\mathrm{end}}}\frac{H(T)}{\sqrt{\epsilon_1}}\,dT \\ = \sqrt{3\alpha' q}\int_T^{T_{\mathrm{end}}}\frac{H(T)}{\sqrt{\bar{\epsilon}_V}}\,dT \\ \approx \frac{\sqrt{2q}\alpha'}{M_p^2}\int_{T_{\mathrm{end}}}^{T}\frac{V^2(T)}{V'(T)}\,dT. & \text{for any } q \end{cases} \tag{5.55}$$

where T_{end} characterizes the tachyonic field value at the end of inflation $t = t_{\mathrm{end}}$. It is important to mention here that in the single field tachyonic inflationary paradigm the field value of the tachyon at the end of inflation is computed from the following condition:

$$\max_{\phi=\phi_e}\left[\epsilon_V, |\eta_V|, |\xi_V^2|, |\sigma_V^3|\right] \equiv 1. \tag{5.56}$$

Let $T_\star$ denote the value of tachyonic field T at which a length scale or more precisely the modes crosses the Hubble radius during inflation, which is given by the momentum at pivot scale $k_\star = a_\star H_\star$. Here $a_\star$ and $H_\star$ signify the scale factor and Hubble parameter at the horizon crossing scale or at the pivot scale. Then the definition of the number of e-foldings as stated in Eqs. (5.335) and (5.55) gives

$$N_\star = N(T_\star) = \ln\left(\frac{a_{\mathrm{end}}}{a_\star}\right), \tag{5.57}$$

where a_{end} is the scale factor at the end of inflation. Then using Eq. (5.57) the corresponding horizon crossing momentum scale or the pivot scale can be computed as

$$c_S k_\star = a_\star H_\star = a_{\mathrm{end}} H_\star \exp(-N_\star). \tag{5.58}$$

Now at any arbitrary momentum scale the number of e-foldings, $N(k)$, between the Hubble exit of the relevant modes and the end of inflation can be expressed as

$$N(k) \approx 71.21 - \ln\left(\frac{k}{k_0}\right) + \frac{1}{4}\ln\left(\frac{V(T_\star)}{M_p^4}\right) + \frac{1}{4}\ln\left(\frac{V(T_\star)}{\rho_{\mathrm{end}}}\right) + \frac{1-3w_{\mathrm{int}}}{12(1+w_{\mathrm{int}})}\ln\left(\frac{\rho_{\mathrm{reh}}}{\rho_{\mathrm{end}}}\right), \tag{5.59}$$

where ρ_{end} is the energy density at the end of inflation, ρ_{reh} is an energy scale during reheating, $c_S k_0 = a_0 H_0$ is the present Hubble scale, $V(T_\star)$ corresponds to the potential energy when the relevant modes left the Hubble patch during inflation corresponding to the momentum scale $c_S k_\star = a_\star H_\star = c_S k_{\mathrm{cmb}}$, and w_{int} characterizes the effective equation of state parameter between the end of inflation and the energy scale during reheating. Further using Eq. (5.59) in Eq. (5.57) we get the following expression:

$$N_\star \approx 71.21 - \ln\left(\frac{k_\star}{k_0}\right) + \frac{1}{4}\ln\left(\frac{V(T_\star)}{M_p^4}\right) + \frac{1}{4}\ln\left(\frac{V(T_\star)}{\rho_{\mathrm{end}}}\right) + \frac{1-3w_{\mathrm{int}}}{12(1+w_{\mathrm{int}})}\ln\left(\frac{\rho_{\mathrm{reh}}}{\rho_{\mathrm{end}}}\right), \tag{5.60}$$

which is very useful to fix the number of e-foldings within $50 < N_\star < 70$ for tachyonic inflation.

5.1.3 Basics of tachyonic perturbations

In this subsection we explicitly discuss the cosmological linear perturbation theory within the framework of tachyonic inflation. Let us clearly mention that here we have various ways of characterizing cosmological perturbations in the context of inflation, which finally depend on the choice of gauge. Let us do the computation in the longitudinal guage, where the scalar metric perturbations of the FLRW background are given by the following infinitesimal line element:

$$ds^2 = -(1+2\Phi(t,\mathbf{x}))\,dt^2 + a^2(t)\,(1-2\Psi(t,\mathbf{x}))\,\delta_{ij}dx^i dx^j, \tag{5.61}$$

where $a(t)$ is the scale factor, $\Phi(t,\mathbf{x})$ and $\Psi(t,\mathbf{x})$ characterizes the gauge invariant metric perturbations. Specifically, the perturbation of the FLRW metric leads to the perturbation in the energy-momentum stress tensor via the Einstein field equation or equivalently through the Friedmann equations. For the perturbed metric as mentioned in Eq. (5.61), the perturbed Einstein field equations can be expressed for the $q = 1/2$ case of the tachyonic inflationary set-up as

$$3H\left(H\Phi(t,\mathbf{k}) + \dot{\Psi}(t,\mathbf{k})\right) + \frac{k^2}{a^2(t)} = -\frac{1}{2M_p^2}\delta\rho, \tag{5.62}$$

$$\ddot{\Psi}(t,\mathbf{k}) + 3H\left(H\Phi(t,\mathbf{k}) + \dot{\Psi}(t,\mathbf{k})\right) + H\dot{\Phi}(t,\mathbf{k}) + 2\dot{H}\Phi(t,\mathbf{k}) + \frac{k^2}{3a^2(t)}\left(\Phi(t,\mathbf{k}) - \Psi(t,\mathbf{k})\right) = \frac{1}{2M_p^2}\delta p, \tag{5.63}$$

$$\dot{\Psi}(t,\mathbf{k}) + H\Phi(t,\mathbf{k}) = -\frac{\alpha' V(T)}{\sqrt{1-\alpha'\dot{T}^2}}\frac{\dot{T}}{M_p^2}\delta T, \tag{5.64}$$

$$\Psi(t,\mathbf{k}) - \Phi(t,\mathbf{k}) = 0. \tag{5.65}$$

Similarly, for any arbitrary q the perturbed Einstein field equations can be expressed as

$$3H\left(H\Phi(t,\mathbf{k}) + \dot{\Psi}(t,\mathbf{k})\right) + \frac{k^2}{a^2(t)} = -\frac{1}{2M_p^2}\delta\rho, \tag{5.66}$$

$$\ddot{\Psi}(t,\mathbf{k}) + 3H\left(H\Phi(t,\mathbf{k}) + \dot{\Psi}(t,\mathbf{k})\right) + H\dot{\Phi}(t,\mathbf{k}) + 2\dot{H}\Phi(t,\mathbf{k}) + \frac{k^2}{3a^2(t)}\left(\Phi(t,\mathbf{k}) - \Psi(t,\mathbf{k})\right) = \frac{1}{2M_p^2}\delta p, \tag{5.67}$$

$$\dot{\Psi}(t,\mathbf{k}) + H\Phi(t,\mathbf{k}) = -\frac{\alpha' V(T)\left[1-\alpha'(1-2q)\dot{T}^2\right]}{\left(1-\alpha'\dot{T}^2\right)^{1-q}}\frac{\dot{T}}{M_p^2}\delta T, \tag{5.68}$$

$$\Psi(t,\mathbf{k}) - \Phi(t,\mathbf{k}) = 0. \tag{5.69}$$

Here $\Phi(t,\mathbf{k})$ and $\Psi(t,\mathbf{k})$ are the two gauge invariant metric perturbations in the Fourier space, defined via the following transformation:

$$\Phi(t,\mathbf{x}) = \int \mathrm{d}^3k\ \Phi(t,\mathbf{k})\ \exp(i\mathbf{k}.\mathbf{x}), \tag{5.70}$$

$$\Psi(t,\mathbf{x}) = \int \mathrm{d}^3k\ \Psi(t,\mathbf{k})\ \exp(i\mathbf{k}.\mathbf{x}). \tag{5.71}$$

Additionally, it is important to note that in Eq. (5.65), the two gauge invariant metric perturbations $\Phi(t,\mathbf{k})$ and $\Psi(t,\mathbf{k})$ are equal in the context of minimally coupled tachyonic string field theoretic model with an Einstein gravity sector. In Eqs. (5.62) and (5.63) the perturbed energy density $\delta\rho$ and pressure δp are given by

$$\delta\rho = \begin{cases} \dfrac{V'(T)\delta T}{\sqrt{1-\alpha'\dot{T}^2}} + \dfrac{\alpha' V(T)\left(\dot{T}\delta\dot{T} + \dot{T}^2\Phi(t,\mathbf{k})\right)}{\left(1-\alpha'\dot{T}^2\right)^{3/2}}, & \text{for } q = 1/2, \\[2ex] \dfrac{\left\{V'(T)\left[1-\alpha'(1-2q)\dot{T}^2\right]\delta T - 4\alpha'(1-2q)V(T)\dot{T}\delta\dot{T}\right\}}{\left(1-\alpha'\dot{T}^2\right)^{1-q}} & \\[2ex] \quad + \dfrac{2\alpha'(1-q)V(T)\left[1-\alpha'(1-2q)\dot{T}^2\right]\left(\dot{T}\delta\dot{T} + \dot{T}^2\Phi(t,\mathbf{k})\right)}{\left(1-\alpha'\dot{T}^2\right)^{2-q}}, & \text{for any arbitrary } q, \end{cases} \tag{5.72}$$

and

$$\delta p = \begin{cases} -V'(T)\sqrt{1-\alpha'\dot{T}^2}\delta T + \dfrac{\alpha' V(T)\left(\dot{T}\delta\dot{T} + \dot{T}^2\Phi(t,\mathbf{k})\right)}{\sqrt{1-\alpha'\dot{T}^2}}, & \text{for } q = 1/2, \\[2ex] -V'(T)\left(1-\alpha'\dot{T}^2\right)^q \delta T + \dfrac{2q\alpha' V(T)\left(\dot{T}\delta\dot{T} + \dot{T}^2\Phi(t,\mathbf{k})\right)}{\left(1-\alpha'\dot{T}^2\right)^{1-q}}, & \text{for any arbitrary } q. \end{cases} \tag{5.73}$$

Similarly after the variation of the tachyoinic field equation motion we get the following expressions for the perturbed equation of motion:

$$0 \approx \begin{cases} \delta\ddot{T} + 3H\delta\dot{T} + \frac{2\alpha'\ddot{T}\left(\dot{T}\delta\dot{T} + \dot{T}^2\Phi(t,\mathbf{k})\right)}{(1-\alpha'\dot{T}^2)} + \frac{M_p\sqrt{1-\alpha'\dot{T}^2}}{\alpha' V(T)}\left[\left(\frac{k^2}{a^2} - 3\dot{H}\right)\Phi(t,\mathbf{k}) - \frac{2k^2}{a^2}\Psi(t,\mathbf{k})\right. \\ \left. -3\left(\ddot{\Psi}(t,\mathbf{k}) + 4H\dot{\Psi}(t,\mathbf{k}) + H\dot{\Phi}(t,\mathbf{k}) + \dot{H}\Phi(t,\mathbf{k}) + 4H^2\Phi(t,\mathbf{k})\right)\right] \\ -\left\{6H\alpha'\dot{T}^3 - \frac{2V'(T)}{\alpha' V(T)}\left(1-\alpha'\dot{T}^2\right)\right\}\Phi(t,\mathbf{k}) - \left(\dot{\Psi}(t,\mathbf{k}) + 3\dot{\Psi}(t,\mathbf{k})\right)\dot{T} - \frac{M_p(1-\alpha'\dot{T}^2)}{\alpha'}\left(\frac{V''(T)}{V(T)} - \frac{V'^2(T)}{V^2(T)}\right), & \text{for } q = 1/2, \\ \delta\ddot{T} + 3H\delta\dot{T} + \frac{2\alpha'\ddot{T}\left(\dot{T}\delta\dot{T} + \dot{T}^2\Phi(t,\mathbf{k})\right)}{(1-\alpha'\dot{T}^2)^{2(1-q)}} + \frac{M_p\left(1-\alpha'\dot{T}^2\right)^{1-q}}{\alpha' V(T)\left[1-\alpha'(1-2q)\dot{T}^2\right]}\left[\left(\frac{k^2}{a^2} - 3\dot{H}\right)\Phi(t,\mathbf{k}) - \frac{2k^2}{a^2}\Psi(t,\mathbf{k})\right. \\ \left. -3\left(\ddot{\Psi}(t,\mathbf{k}) + 4H\dot{\Psi}(t,\mathbf{k}) + H\dot{\Phi}(t,\mathbf{k}) + \dot{H}\Phi(t,\mathbf{k}) + 4H^2\Phi(t,\mathbf{k})\right)\right] - \left\{6H\alpha'\dot{T}^3 - \sqrt{\frac{2}{q}}\frac{V'(T)}{\alpha' V(T)}\left(1-\alpha'\dot{T}^2\right)^{2(1-q)}\right\} \\ \times\Phi(t,\mathbf{k}) - \left(\dot{\Psi}(t,\mathbf{k}) + 3\dot{\Psi}(t,\mathbf{k})\right)\dot{T} - \frac{M_p\left(1-\alpha'\dot{T}^2\right)^{2(1-q)}}{\sqrt{2q}\alpha'}\left(\frac{V''(T)}{V(T)} - \frac{V'^2(T)}{V^2(T)}\right), & \text{for any } q. \end{cases} \tag{5.74}$$

Further we will perform the following steps throughout the next part of the computation:

- First of all we decompose the scalar perturbations into two components-(1) *entropic or isocurvature perturbations* which can be usually treated as the orthogonal projective part to the trajectory and (2) *adiabatic or curvature perturbations* which can be usually treated as the parallel projective part to the trajectory.
- If inflation is governed by a single scalar field then we deal with *adiabatic or curvature perturbations*. On the other hand for multiple scalar fields we deal with *entropic or isocurvature perturbations*.
- In the present context the inflationary dynamics is governed by a single tachyonic field, which implies the surviving part of the cosmological perturbations are governed by the *adiabatic* contribution.
- Within the framework of first order cosmological perturbation theory we define a gauge invariant primordial curvature perturbation on the scales outside the horizon:

$$\zeta = \Psi - \frac{H}{\dot{\rho}}\delta\rho. \tag{5.75}$$

- Next we consider the uniform density hypersurface in which

$$\delta\rho = 0. \tag{5.76}$$

Consequently the curvature perturbation is governed by

$$\zeta = \Psi. \tag{5.77}$$

- Further, the time evolution of the curvature perturbation can be expressed as

$$\dot{\zeta} = H\left(\frac{\delta\bar{p}}{\rho + p}\right), \tag{5.78}$$

where $\delta\bar{p}$ characterizes the non-adiabatic or entropic contribution in the first order linearized cosmological perturbation. In the present context $\delta\bar{p}$ can be expressed as

$$\delta\bar{p} = \Gamma\dot{p}, \tag{5.79}$$

where Γ characterizes the relative displacement between hypersurfaces of uniform pressure and density. Additionally, it is important to note that Eq. (5.375) signifies the change in the *curvature perturbation* on the uniform density hypersurfaces on the large scales. Also from Eq. (5.375) it is clearly observed that the contribution from the time evolution of the *adiabatic or curvature perturbations* are directly proportional to the non-adiabatic contribution which comes from significantly from the isocurvature part of pressure perturbation δp and are completely independent of the specific mathematical structure of the gravitational field equations in the context of Einstein gravity framework. In a generalized prescription the pressure perturbation in arbitrary gauge can be decomposed into the following two contributions:

$$\delta p = c_S^2\delta\rho + \delta\bar{p}, \tag{5.80}$$

where c_S^2 is the effective sound speed, which is mentioned in the earlier section of the paper.

- Now let us consider a situation where the pressure perturbation is completely made up of adiabatic contribution from the cosmological perturbation on large cosmological scales. Consequently we get

$$\delta\bar{p} = \Gamma\dot{p} = 0 \quad \Rightarrow \quad \zeta = \text{Constant}, \tag{5.81}$$

which is consistent with the single field slow-roll conditions in the context of the tachyonic inflationary set-up. Finally, in the uniform density hypersurfaces, the curvature perturbation can be written in terms of the tachyonic field fluctuations on spatially flat hypersurfaces as

$$\zeta = -H\left(\frac{\delta T}{\dot{T}}\right). \tag{5.82}$$

5.1.4 Computation of scalar power spectrum

In this subsection our prime objective is to compute the primordial power spectra of scalar quantum fluctuations from tachyonic inflation and study the cosmological consequences from the previously mentioned string theory originating tachyonic potentials in the light of Planck 2015 data. To serve this purpose let us start with the following canonical variable $v_{\mathbf{k}}$, which can be quantized with the standard techniques:

$$v_{\mathbf{k}} \equiv z\, M_p\, \zeta_{\mathbf{k}}, \tag{5.83}$$

where ζ_k is the curvature perturbation in the momentum space, which can be expressed in terms of the curvature perturbation in position space through the following Fourier transformation:

$$\zeta(t, \mathbf{x}) = \int \mathrm{d}^3k\, \zeta_{\mathbf{k}}(t)\, \exp(i\mathbf{k}.\mathbf{x}). \tag{5.84}$$

Also z is defined as

$$z = \frac{a(t)}{c_S H M_p}\sqrt{\rho + p} = \begin{cases} \dfrac{\sqrt{3\alpha'}a(t)\dot{T}}{\sqrt{1-\alpha'\dot{T}^2}} = \dfrac{a(t)}{c_S}\sqrt{2\epsilon_1} = \dfrac{a(t)}{c_S}\sqrt{2\bar{\epsilon}_V}, & \text{for } q = 1/2, \\ \dfrac{\sqrt{6q\alpha'}a(t)\dot{T}}{\sqrt{1-\alpha'\dot{T}^2}}\sqrt{\dfrac{1+(1-2q)\alpha'\dot{T}^2}{1-(1-2q)\alpha'\dot{T}^2}} = \dfrac{a(t)\sqrt{2\epsilon_1}}{c_S} = \dfrac{a(t)\sqrt{2\bar{\epsilon}_V}}{\sqrt{2q}c_S}, & \text{for any } q. \end{cases} \tag{5.85}$$

Next we use conformal time η instead of using the time t, which is defined via the following infinitesimal transformation:

$$\mathrm{d}t = a\, \mathrm{d}\eta \tag{5.86}$$

using which one can redefine the Hubble parameter in conformal coordinate system as

$$\mathcal{H}(\eta) = \frac{1}{a(\eta)}\frac{\mathrm{d}a(\eta)}{\mathrm{d}\eta} = a\, H(t). \tag{5.87}$$

Further we derive the equation of motion of the scalar fluctuation by extremizing the tachyonic model action as

$$\left[\frac{\mathrm{d}^2}{\mathrm{d}\eta^2} + \left(c_S^2 k^2 - \frac{1}{z}\frac{\mathrm{d}^2 z}{\mathrm{d}\eta^2}\right)\right] v_{\mathbf{k}} = 0 \tag{5.88}$$

where

$$\begin{aligned}\frac{1}{z}\frac{\mathrm{d}^2 z}{\mathrm{d}\eta^2} &= 2a^2H^2 + \overbrace{\frac{2}{3}\frac{\left(\frac{1}{z}\frac{\mathrm{d}z}{\mathrm{d}\eta}\frac{\mathrm{d}\epsilon_1}{\mathrm{d}\eta} + \frac{1}{2}\frac{\mathrm{d}^2\epsilon_1}{\mathrm{d}\eta^2}\right)}{\left(1-\frac{2}{3}\epsilon_1\right)} + \frac{1}{9}\frac{\left(\frac{\mathrm{d}\epsilon_1}{\mathrm{d}\eta}\right)^2}{\left(1-\frac{2}{3}\epsilon_1\right)^2}}^{\text{Higher order slow-roll correction}} \\
&= \begin{cases} 2a^2H^2 + \dfrac{2}{3}\dfrac{\left(\frac{1}{z}\frac{\mathrm{d}z}{\mathrm{d}\eta}\frac{\mathrm{d}\bar{\epsilon}_V}{\mathrm{d}\eta} + \frac{1}{2}\frac{\mathrm{d}^2\bar{\epsilon}_V}{\mathrm{d}\eta^2}\right)}{\left(1-\frac{2}{3}\bar{\epsilon}_V\right)} + \dfrac{1}{9}\dfrac{\left(\frac{\mathrm{d}\bar{\epsilon}_V}{\mathrm{d}\eta}\right)^2}{\left(1-\frac{2}{3}\bar{\epsilon}_V\right)^2} & \\ \quad = a^2H^2\left[2 + 8\bar{\epsilon}_V - 3\bar{\eta}_V + (3\bar{\epsilon}_V - \bar{\eta}_V)^2 + \bar{\epsilon}_V\,(3\bar{\epsilon}_V - \bar{\eta}_V) + \dfrac{1}{2}\left(2\bar{\xi}_V^2 - 5\bar{\eta}_V\bar{\epsilon}_V + 36\bar{\epsilon}_V^2\right)\right] + \cdots, & \text{for } q = 1/2, \\ 2a^2H^2 + \dfrac{1}{3q}\dfrac{\left(\frac{1}{z}\frac{\mathrm{d}z}{\mathrm{d}\eta}\frac{\mathrm{d}\bar{\epsilon}_V}{\mathrm{d}\eta} + \frac{1}{2}\frac{\mathrm{d}^2\bar{\epsilon}_V}{\mathrm{d}\eta^2}\right)}{\left(1-\frac{1}{3q}\bar{\epsilon}_V\right)} + \dfrac{1}{36q^2}\dfrac{\left(\frac{\mathrm{d}\bar{\epsilon}_V}{\mathrm{d}\eta}\right)^2}{\left(1-\frac{1}{3q}\bar{\epsilon}_V\right)^2} & \\ \quad = a^2H^2\left[2 + \left(\dfrac{9}{\sqrt{2q}} - \dfrac{1}{2q}\right)\bar{\epsilon}_V - \dfrac{3}{\sqrt{2q}}\bar{\eta}_V + \dfrac{1}{2q}\,(3\bar{\epsilon}_V - \bar{\eta}_V)^2 + \dfrac{1}{(2q)^{3/2}}\bar{\epsilon}_V\,(3\bar{\epsilon}_V - \bar{\eta}_V)\right. & \\ \quad \left. + \frac{1}{2\sqrt{2q}}\left(2\bar{\xi}_V^2 - 5\bar{\eta}_V\bar{\epsilon}_V + 36\bar{\epsilon}_V^2\right)\right] + \cdots, & \text{for any } q, \end{cases}\end{aligned} \tag{5.89}$$

and the factor aH can be expressed in terms of the conformal time η as

$$\eta \approx \begin{cases} -\frac{1}{aH}\left(1+\bar{\epsilon}_V\right)+\cdots, & \text{for } q=1/2, \\ -\frac{1}{aH}\left(1+\frac{\bar{\epsilon}_V}{2q}\right)+\cdots, & \text{for any arbitrary } q. \end{cases} \tag{5.90}$$

Further replacing the factor aH in Eq. (5.89), we finally get the following simplified expression:

$$\frac{1}{z}\frac{\mathrm{d}^2 z}{\mathrm{d}\eta^2} \approx \begin{cases} \frac{1}{\eta^2}\left[\left(\frac{3}{2}+4\bar{\epsilon}_V-\bar{\eta}_V\right)^2-\frac{1}{4}\right]+\cdots, & \text{for } q=1/2, \\ \frac{1}{\eta^2}\left[\left\{\frac{3}{2}+\left(\frac{1}{2q}+\frac{3}{\sqrt{2q}}\right)\bar{\epsilon}_V-\frac{1}{\sqrt{2q}}\bar{\eta}_V\right\}^2-\frac{1}{4}\right]+\cdots, & \text{for any } q. \end{cases} \tag{5.91}$$

Now for further simplification in the computation of scalar power spectrum we introduce a new factor ν, which is defined as

$$\nu \approx \begin{cases} \left(\frac{3}{2}+4\bar{\epsilon}_V-\bar{\eta}_V\right)+\cdots, & \text{for } q=1/2, \\ \left\{\frac{3}{2}+\left(\frac{1}{2q}+\frac{3}{\sqrt{2q}}\right)\bar{\epsilon}_V-\frac{1}{\sqrt{2q}}\bar{\eta}_V\right\}+\cdots, & \text{for any } q. \end{cases} \tag{5.92}$$

Hence using Eq. (5.100) in Eq. (5.88), we get the following simplified form of the equation of motion:

$$\left[\frac{\mathrm{d}^2}{\mathrm{d}\eta^2}+\left(c_S^2k^2-\frac{\left(\nu^2-\frac{1}{4}\right)}{\eta^2}\right)\right]v_{\mathbf{k}}(\eta)=0, \tag{5.93}$$

and the most general solution of Eq. (5.123) is given by

$$v_{\mathbf{k}}(\eta)=\sqrt{-\eta}\left[C_1H^{(1)}_\nu(-kc_S\eta)+C_2H^{(2)}_\nu(-kc_S\eta)\right], \tag{5.94}$$

where C_1 and C_2 are two arbitrary integration constants, which can be fixed from the appropriate choice of the boundary conditions. Additionally $H^{(1)}_\nu$ and $H^{(2)}_\nu$ represent the Hankel function of the first and second kind with rank ν. Now to impose the well known Bunch–Davies boundary condition at early times we have used:

$$\lim_{kc_S\eta\to-\infty} H^{(1)}_\nu(-kc_S\eta) = \sqrt{\frac{2}{\pi}}\frac{1}{\sqrt{-\eta}}\exp\left(ikc_S\eta\right)\exp\left(i\frac{\pi}{2}\left(\nu+\frac{1}{2}\right)\right), \tag{5.95}$$

$$\lim_{kc_S\eta\to-\infty} H^{(2)}_\nu(-kc_S\eta) = \sqrt{\frac{2}{\pi}}\frac{1}{\sqrt{-\eta}}\exp\left(-ikc_S\eta\right)\exp\left(-i\frac{\pi}{2}\left(\nu+\frac{1}{2}\right)\right). \tag{5.96}$$

As a result the previously mentioned integration constants are fixed at the values $C_1=\sqrt{\frac{\pi}{2}},\ C_2=0$. Consequently the solution of the mode function for scalar fluctuations takes the following form:

$$v_{\mathbf{k}}(\eta)=\sqrt{-\frac{\eta\pi}{2}}H^{(1)}_\nu(-kc_S\eta). \tag{5.97}$$

On the other hand, the solution stated in Eq. (5.94) determines the future evolution of the mode including its super-horizon dynamics at $c_Sk<<aH$ or $|kc_S\eta|<<1$ or $kc_S\eta\to0$ and this is due to

$$\lim_{kc_S\eta\to0} H^{(1)}_\nu(-kc_S\eta)=\frac{i}{\pi}\Gamma(\nu)\left(\frac{-kc_S\eta}{2}\right)^{-\nu}. \tag{5.98}$$

Consequently the solution of the mode function for scalar fluctuations takes the following form:

$$v_{\mathbf{k}}(\eta)=\sqrt{-\frac{\eta\pi}{2}}\frac{i}{\pi}\Gamma(\nu)\left(\frac{-kc_S\eta}{2}\right)^{-\nu}. \tag{5.99}$$

Finally combining the results obtained in Eqs. (5.94), (5.97) and (5.128) we get

$$v_{\mathbf{k}}(\eta)=\begin{cases} \sqrt{-\eta}\Big[C_1H^{(1)}_\nu(-kc_S\eta) \\ \quad +C_2H^{(2)}_\nu(-kc_S\eta)\Big], & \text{for AV}, \\ \sqrt{-\frac{\eta\pi}{2}}H^{(1)}_\nu(-kc_S\eta), & \text{for BD } +|kc_S\eta|>>1, \\ \sqrt{-\frac{\eta\pi}{2}}\frac{i}{\pi}\Gamma(\nu)\left(\frac{-kc_S\eta}{2}\right)^{-\nu}, & \text{for BD } +|kc_S\eta|<<1, \end{cases} \tag{5.100}$$

where AV and BD signify the arbitrary vacuum and the Bunch–Davies vacuum respectively. Finally the two point function from a scalar fluctuation for both AV and BD can be expressed as

$$\begin{aligned}\langle\zeta_{\mathbf{k}}\zeta_{\mathbf{k}'}\rangle &= \left(\frac{H}{\dot{T}}\right)^2\langle\delta T_{\mathbf{k}}\delta T_{\mathbf{k}'}\rangle = \frac{1}{z^2M_p^2}\langle v_{\mathbf{k}}v_{\mathbf{k}'}\rangle \\ &= (2\pi)^3\delta^3(\mathbf{k}+\mathbf{k}')\frac{2\pi^2}{k^3}\Delta_\zeta(k),\end{aligned} \tag{5.101}$$

where the primordial power spectrum for the scalar modes at any arbitrary momentum scale k can be written for both AV and BD with $q=1/2$ as

$$\Delta_\zeta(k) \equiv \frac{k^3 P_\zeta(k)}{2\pi^2} = \frac{k^3|v_k|^2}{2\pi^2 z^2 M_p^2} = \begin{cases} \begin{cases} \dfrac{2^{2\nu-3}\,(-k\eta c_S)^{3-2\nu}\,H^2}{8c_S\bar{\epsilon}_V(1+\bar{\epsilon}_V)^2\pi^2 M_p^2}\left|\dfrac{\Gamma(\nu)}{\Gamma\left(\frac{3}{2}\right)}\right|^2, & \text{for}\quad |kc_S\eta| << 1, \\ \dfrac{2^{2\nu-3}c_S^{2-2\nu}\,(1+\bar{\epsilon}_V)^{1-2\nu}\,H^2}{8\bar{\epsilon}_V\pi^2 M_p^2}\left|\dfrac{\Gamma(\nu)}{\Gamma\left(\frac{3}{2}\right)}\right|^2, & \text{for}\quad |kc_S\eta| = 1, \\ \dfrac{(-k\eta c_S)^3\,H^2|H_\nu^{(1)}(-kc_S\eta)|^2}{8c_S\bar{\epsilon}_V(1+\bar{\epsilon}_V)^2\pi M_p^2}, & \text{for}\quad |kc_S\eta| >> 1, \end{cases} & \underline{\text{for BD}}, \\ \dfrac{(-k\eta c_S)^3\,H^2\left|C_1 H_\nu^{(1)}(-kc_S\eta) + C_2 H_\nu^{(2)}(-kc_S\eta)\right|^2}{4c_S\bar{\epsilon}_V(1+\bar{\epsilon}_V)^2\pi^2 M_p^2}, & \underline{\text{for AV}}, \end{cases} \tag{5.102}$$

and similarly the primordial power spectrum for the scalar modes at any arbitrary momentum scale k can be written for both AV and BD with any arbitrary q as

$$\Delta_\zeta(k) \equiv \frac{k^3 P_\zeta(k)}{2\pi^2} = \frac{k^3|v_k|^2}{2\pi^2 z^2 M_p^2} = \begin{cases} \begin{cases} \dfrac{2^{2\nu-3}q\,(-k\eta c_S)^{3-2\nu}\,H^2}{4c_S\bar{\epsilon}_V\left(1+\frac{1}{2q}\bar{\epsilon}_V\right)^2\pi^2 M_p^2}\left|\dfrac{\Gamma(\nu)}{\Gamma\left(\frac{3}{2}\right)}\right|^2, & \text{for}\quad |kc_S\eta| << 1, \\ \dfrac{2^{2\nu-3}q\,c_S^{2-2\nu}\left(1+\frac{1}{2q}\bar{\epsilon}_V\right)^{1-2\nu}H^2}{4\bar{\epsilon}_V\pi^2 M_p^2}\left|\dfrac{\Gamma(\nu)}{\Gamma\left(\frac{3}{2}\right)}\right|^2, & \text{for}\quad |kc_S\eta| = 1, \\ \dfrac{q\,(-k\eta c_S)^3\,H^2|H_\nu^{(1)}(-kc_S\eta)|^2}{4c_S\bar{\epsilon}_V\left(1+\frac{1}{2q}\bar{\epsilon}_V\right)^2\pi M_p^2}, & \text{for}\quad |kc_S\eta| >> 1. \end{cases} & \underline{\text{for BD}} \\ \dfrac{q\,(-k\eta c_S)^3\,H^2\left|C_1 H_\nu^{(1)}(-kc_S\eta) + C_2 H_\nu^{(2)}(-kc_S\eta)\right|^2}{2c_S\bar{\epsilon}_V\left(1+\frac{1}{2q}\bar{\epsilon}_V\right)^2\pi^2 M_p^2}, & \underline{\text{for AV}}, \end{cases} \tag{5.103}$$

where the effective sound speed c_S is given by

$$c_S = \begin{cases} \sqrt{1-\dfrac{2}{3}\epsilon_1} = \sqrt{1-\dfrac{2}{3}\bar{\epsilon}_V}, & \text{for}\quad q = 1/2, \\ \sqrt{\dfrac{1-\frac{2}{3}\epsilon_1}{1+\frac{2(1-2q)}{3q}\epsilon_1}} = \sqrt{\dfrac{1-\frac{1}{3q}\bar{\epsilon}_V}{1+\frac{(1-2q)}{3q^2}\bar{\epsilon}_V}}, & \text{for any } q. \end{cases} \tag{5.104}$$

Now starting from the expression for primordial power spectrum for the scalar modes one can compute the spectral tilt at any arbitrary momentum scale k for both AV and BD with $q = 1/2$ as

$$n_{\zeta}(k)-1\equiv\frac{d\ln\Delta_{\zeta}(k)}{d\ln k}=\frac{d\ln\Delta_{\zeta}(k)}{dN}$$
$$\approx\begin{cases}\begin{cases}(3-2\nu)\left[1-\frac{2}{3}\bar{\epsilon}_V(\bar{\eta}_V-3\bar{\epsilon}_V)\left(1-\frac{2}{3}\bar{\epsilon}_V\right)^{1/4}\right]+\cdots, & \text{for } |kc_S\eta|<<1\\ (3-2\nu)\left[1-\frac{2}{3}\bar{\epsilon}_V(\bar{\eta}_V-3\bar{\epsilon}_V)\left(1-\frac{2}{3}\bar{\epsilon}_V\right)^{1/4}\right]+\cdots, & \text{for } |kc_S\eta|=1,\\ \bar{\epsilon}_V-\left[\frac{2}{3}\bar{\epsilon}_V(\bar{\eta}_V-3\bar{\epsilon}_V)+2(\bar{\eta}_V-3\bar{\epsilon}_V)\right]\left(1-\frac{2}{3}\bar{\epsilon}_V\right)^{1/4} & \\ \quad+\frac{(-c_S\eta)\left[H^{(1)}_{\nu-1}(-kc_S\eta)-H^{(1)}_{\nu+1}(-kc_S\eta)\right]}{H^{(1)}_{\nu}(-kc_S\eta)}+\cdots, & \text{for } |kc_S\eta|>>1,\end{cases} & \underline{\text{for BD}},\\ \bar{\epsilon}_V-\left[\frac{2}{3}\bar{\epsilon}_V(\bar{\eta}_V-3\bar{\epsilon}_V)+2(\bar{\eta}_V-3\bar{\epsilon}_V)\right]\left(1-\frac{2}{3}\bar{\epsilon}_V\right)^{1/4} & \\ \quad+\frac{(-c_S\eta)\,C_1\left[H^{(1)}_{\nu-1}(-kc_S\eta)-H^{(1)}_{\nu+1}(-kc_S\eta)\right]}{\left[C_1H^{(1)}_{\nu}(-kc_S\eta)+C_2H^{(2)}_{\nu}(-kc_S\eta)\right]} & \\ \quad+\frac{(-c_S\eta)C_2\left[H^{(2)}_{\nu-1}(-kc_S\eta)-H^{(2)}_{\nu+1}(-kc_S\eta)\right]}{\left[C_1H^{(1)}_{\nu}(-kc_S\eta)+C_2H^{(2)}_{\nu}(-kc_S\eta)\right]}+\cdots, & \underline{\text{for AV}}.\end{cases}\tag{5.105}$$

and for both AV and BD with any arbitrary q as

$$n_{\zeta}(k)-1\equiv\frac{d\ln\Delta_{\zeta}(k)}{d\ln k}=\frac{d\ln\Delta_{\zeta}(k)}{dN}$$
$$=\begin{cases}\begin{cases}(3-2\nu)\left[1-\frac{1}{3q}\bar{\epsilon}_V(\bar{\eta}_V-3\bar{\epsilon}_V)\left(1-\frac{1}{3q}\bar{\epsilon}_V\right)^{1/4}\right]+\cdots, & \text{for } |kc_S\eta|<<1,\\ (3-2\nu)\left[1-\frac{1}{3q}\bar{\epsilon}_V(\bar{\eta}_V-3\bar{\epsilon}_V)\left(1-\frac{1}{3q}\bar{\epsilon}_V\right)^{1/4}\right]+\cdots, & \text{for } |kc_S\eta|=1,\\ \frac{\bar{\epsilon}_V}{2q}-\left[\frac{1}{3q}\bar{\epsilon}_V(\bar{\eta}_V-3\bar{\epsilon}_V)+\frac{1}{q}(\bar{\eta}_V-3\bar{\epsilon}_V)\right]\left(1-\frac{2}{3}\bar{\epsilon}_V\right)^{1/4} & \\ \quad+\frac{(-c_S\eta)\left[H^{(1)}_{\nu-1}(-kc_S\eta)-H^{(1)}_{\nu+1}(-kc_S\eta)\right]}{H^{(1)}_{\nu}(-kc_S\eta)}+\cdots, & \text{for } |kc_S\eta|>>1,\end{cases} & \underline{\text{for BD}},\\ \frac{\bar{\epsilon}_V}{2q}-\left[\frac{1}{3q}\bar{\epsilon}_V(\bar{\eta}_V-3\bar{\epsilon}_V)+\frac{1}{q}(\bar{\eta}_V-3\bar{\epsilon}_V)\right]\left(1-\frac{2}{3}\bar{\epsilon}_V\right)^{1/4} & \\ \quad+\frac{(-c_S\eta)\,C_1\left[H^{(1)}_{\nu-1}(-kc_S\eta)-H^{(1)}_{\nu+1}(-kc_S\eta)\right]}{\left[C_1H^{(1)}_{\nu}(-kc_S\eta)+C_2H^{(2)}_{\nu}(-kc_S\eta)\right]} & \\ \quad+\frac{(-c_S\eta)\,C_1\left[H^{(2)}_{\nu-1}(-kc_S\eta)-H^{(2)}_{\nu+1}(-kc_S\eta)\right]}{\left[C_1H^{(1)}_{\nu}(-kc_S\eta)+C_2H^{(2)}_{\nu}(-kc_S\eta)\right]}+\cdots, & \underline{\text{for AV}}.\end{cases}\tag{5.106}$$

One can also consider the following approximations to simplify the final derived form of the primordial scalar power spectrum for the BD vacuum with the $|kc_S\eta|=1$ case:

1. We start with the *Laurent expansion* of the Gamma function:

$$\Gamma(\nu) = \frac{1}{\nu} - \gamma + \frac{1}{2}\left(\gamma^2 + \frac{\pi^2}{6}\right)\nu - \frac{1}{6}\left(\gamma^3 + \frac{\gamma\pi^2}{2} + 2\zeta(3)\right)\nu^2 + \mathcal{O}(\nu^3). \tag{5.107}$$

where γ being the Euler–Mascheroni constant and $\zeta(3)$ characterizing the Riemann zeta function of order 3 originating in the expansion of the gamma function.
2. Hence using the result of Eq. (5.107) for $q = 1/2$ and for arbitrary q we can write:

$$\Gamma(\nu) = \begin{cases} \frac{1}{\left(\frac{3}{2} + 4\bar{\epsilon}_V - \bar{\eta}_V\right)} - \gamma + \frac{1}{2}\left(\gamma^2 + \frac{\pi^2}{6}\right)\left(\frac{3}{2} + 4\bar{\epsilon}_V - \bar{\eta}_V\right) \\ \quad -\frac{1}{6}\left(\gamma^3 + \frac{\gamma\pi^2}{2} + 2\zeta(3)\right)\left(\frac{3}{2} + 4\bar{\epsilon}_V - \bar{\eta}_V\right)^2 + \cdots, & \text{for } q = 1/2, \\ \frac{1}{\left\{\frac{3}{2} + \left(\frac{1}{2q} + \frac{3}{\sqrt{2q}}\right)\bar{\epsilon}_V - \frac{1}{\sqrt{2q}}\bar{\eta}_V\right\}} - \gamma \\ \quad + \frac{1}{2}\left(\gamma^2 + \frac{\pi^2}{6}\right)\left\{\frac{3}{2} + \left(\frac{1}{2q} + \frac{3}{\sqrt{2q}}\right)\bar{\epsilon}_V - \frac{1}{\sqrt{2q}}\bar{\eta}_V\right\} \\ \quad - \frac{1}{6}\left(\gamma^3 + \frac{\gamma\pi^2}{2} + 2\zeta(3)\right)\left\{\frac{3}{2} + \left(\frac{1}{2q} + \frac{3}{\sqrt{2q}}\right)\bar{\epsilon}_V - \frac{1}{\sqrt{2q}}\bar{\eta}_V\right\}^2 + \cdots, & \text{for any } q. \end{cases} \tag{5.108}$$

3. In the slow-roll regime of inflation all the slow-roll parameters satisfy the following constraint:

$$\bar{\epsilon}_V << 1, \tag{5.109}$$
$$|\bar{\eta}_V| << 1, \tag{5.110}$$
$$|\bar{\xi}^2_V| << 1, \tag{5.111}$$
$$|\bar{\sigma}^3_V| << 1. \tag{5.112}$$

Using these approximations the primordial scalar power spectrum can be expressed as

$$\begin{aligned} \Delta_{\zeta,\star} &\approx \left\{\left[1 - (\mathcal{C}_E + 1)\epsilon_1 - \frac{\mathcal{C}_E}{2}\epsilon_2\right]^2 \frac{H^2}{8\pi^2 M_p^2 c_S \epsilon_1}\right\}_{k_\star = a_\star H_\star} \\ &= \begin{cases} \left\{[1 - (\mathcal{C}_E + 1)\bar{\epsilon}_V - \mathcal{C}_E\,(3\bar{\epsilon}_V - \bar{\eta}_V)]^2 \frac{H^2}{8\pi^2 M_p^2 c_S \bar{\epsilon}_V}\right\}_{k_\star = a_\star H_\star}, & \text{for } q = 1/2, \\ \left\{\left[1 - (\mathcal{C}_E + 1)\frac{\bar{\epsilon}_V}{2q} - \frac{\mathcal{C}_E}{\sqrt{2q}}\,(3\bar{\epsilon}_V - \bar{\eta}_V)\right]^2 \frac{qH^2}{4\pi^2 M_p^2 c_S \bar{\epsilon}_V}\right\}_{k_\star = a_\star H_\star}, & \text{for any } q, \end{cases} \end{aligned} \tag{5.113}$$

where $\mathcal{C}_E$ is given by

$$\mathcal{C}_E = -2 + \ln 2 + \gamma \approx -0.72. \tag{5.114}$$

4. Using the slow-roll approximations one can further approximate the expression for the sound speed as

$$c_S^2 = \begin{cases} 1 - \frac{2}{3}\bar{\epsilon}_V + \mathcal{O}(\bar{\epsilon}_V^2) + \cdots, & \text{for } q = 1/2, \\ 1 - \frac{(1-q)}{3q^2}\bar{\epsilon}_V + \mathcal{O}(\bar{\epsilon}_V^2) + \cdots, & \text{for any } q. \end{cases} \tag{5.115}$$

5. Hence using the result in Eq. (5.169) we get the following simplified expression for the primordial scalar power spectrum:

$$\Delta_{\zeta,\star} \approx \begin{cases} \left\{\left[1-\left(\mathcal{C}_E+\frac{5}{6}\right)\bar{\epsilon}_V - \mathcal{C}_E\left(3\bar{\epsilon}_V-\bar{\eta}_V\right)\right]^2 \frac{H^2}{8\pi^2 M_p^2\bar{\epsilon}_V}\right\}_{k_\star=a_\star H_\star}, & \text{for } q=1/2, \\ \left\{\left[1-\left(\mathcal{C}_E+1-\Sigma\right)\frac{\bar{\epsilon}_V}{2q} - \frac{\mathcal{C}_E}{\sqrt{2q}}\left(3\bar{\epsilon}_V-\bar{\eta}_V\right)\right]^2 \frac{qH^2}{4\pi^2 M_p^2\bar{\epsilon}_V}\right\}_{k_\star=a_\star H_\star}, & \text{for any } q, \end{cases} \tag{5.116}$$

where the factor Σ is defined as

$$\Sigma = \begin{cases} \frac{1}{6}, & \text{for } q=1/2 \\ \frac{1-q}{6q}, & \text{for any } q. \end{cases} \tag{5.117}$$

6. Next one can compute the scalar spectral tilt (n_S) of the primordial scalar power spectrum as

$$n_{\zeta,\star}-1 \approx \begin{cases} -2\epsilon_1-\epsilon_2-2\epsilon_1^2-\left(2\mathcal{C}_E+\frac{8}{3}\right)\epsilon_1\epsilon_2-\mathcal{C}_E\epsilon_2\epsilon_3+\cdots & \\ \quad = 2\bar{\eta}_V-8\bar{\epsilon}_V-2\bar{\epsilon}_V^2-2\left(2\mathcal{C}_E+\frac{8}{3}\right)\bar{\epsilon}_V\left(3\bar{\epsilon}_V-\bar{\eta}_V\right) & \\ \quad\quad -\mathcal{C}_E\left(2\bar{\xi}_V^2-5\bar{\eta}_V\bar{\epsilon}_V+36\bar{\epsilon}_V^2\right)+\cdots, & \text{for } q=1/2, \\ -2\epsilon_1-\epsilon_2-2\epsilon_1^2-\left(2\mathcal{C}_E+3-2\Sigma\right)\epsilon_1\epsilon_2-\mathcal{C}_E\epsilon_2\epsilon_3+\cdots & \\ \quad = \sqrt{\frac{2}{q}}\bar{\eta}_V-\left(\frac{1}{q}+3\sqrt{\frac{2}{q}}\right)\bar{\epsilon}_V-\frac{\bar{\epsilon}_V^2}{2q^2}-\frac{2}{(2q)^{3/2}}\left(2\mathcal{C}_E+3-2\Sigma\right)\bar{\epsilon}_V\left(3\bar{\epsilon}_V-\bar{\eta}_V\right) & \\ \quad\quad -\frac{\mathcal{C}_E}{\sqrt{2q}}\left(2\bar{\xi}_V^2-5\bar{\eta}_V\bar{\epsilon}_V+36\bar{\epsilon}_V^2\right)+\cdots, & \text{for any } q. \end{cases} \tag{5.118}$$

7. Next one can compute the running of the scalar spectral tilt (α_S) of the primordial scalar power spectrum as

$$\alpha_{\zeta,\star} = \left(\frac{dn_\zeta(k)}{d\ln k}\right)_{k_\star=a_\star H_\star} = \left(\frac{dn_\zeta(k)}{dN}\right)_{k_\star=a_\star H_\star}$$

$$\approx \begin{cases} -\left\{\left[4\bar{\epsilon}_V(1+\bar{\epsilon}_V)(\bar{\eta}_V-3\bar{\epsilon}_V)+2\left(10\bar{\epsilon}_V\bar{\eta}_V-18\bar{\epsilon}_V^2-\bar{\xi}_V^2\right)\right]\right. & \\ -\mathcal{C}_E\left(2\bar{\sigma}_V^3-216\bar{\epsilon}_V^3+2\bar{\xi}_V^2\bar{\eta}_V-7\bar{\xi}_V^2\bar{\epsilon}_V+194\bar{\epsilon}_V^2\bar{\eta}_V-10\bar{\eta}_V\bar{\epsilon}_V\right) & \\ \left.-\left(2\mathcal{C}_E+\frac{8}{3}\right)\left[2\bar{\epsilon}_V\left(10\bar{\epsilon}_V\bar{\eta}_V-18\bar{\epsilon}_V^2-\bar{\xi}_V^2\right)-4\bar{\epsilon}_V\left(3\bar{\epsilon}_V-\bar{\eta}_V\right)^2\right]\right\}\left(1-\frac{2}{3}\bar{\epsilon}_V\right)^{1/4}+\cdots, & \text{for } q=1/2, \\ -\left\{\left[\sqrt{\frac{2}{q}}\frac{\bar{\epsilon}_V}{q}\left(1+\frac{\bar{\epsilon}_V}{2q}\right)(\bar{\eta}_V-3\bar{\epsilon}_V)+\sqrt{\frac{2}{q}}\left(10\bar{\epsilon}_V\bar{\eta}_V-18\bar{\epsilon}_V^2-\bar{\xi}_V^2\right)\right]\right. & \\ -\frac{\mathcal{C}_E}{\sqrt{2q}}\left(2\bar{\sigma}_V^3-216\bar{\epsilon}_V^3+2\bar{\xi}_V^2\bar{\eta}_V-7\bar{\xi}_V^2\bar{\epsilon}_V+194\bar{\epsilon}_V^2\bar{\eta}_V-10\bar{\eta}_V\bar{\epsilon}_V\right) & \\ \left.-\left(2\mathcal{C}_E+\frac{8}{3}\right)\left[\sqrt{\frac{2}{q}}\bar{\epsilon}_V\left(10\bar{\epsilon}_V\bar{\eta}_V-18\bar{\epsilon}_V^2-\bar{\xi}_V^2\right)-\frac{4}{(2q)^{3/2}}\bar{\epsilon}_V\left(3\bar{\epsilon}_V-\bar{\eta}_V\right)^2\right]\right\} & \\ \times\left(1-\frac{1}{3q}\bar{\epsilon}_V\right)^{1/4}+\cdots, & \text{for any } q. \end{cases} \tag{5.119}$$

8. Finally, one can also compute the running of the running of scalar spectral tilt (κ_S) of the primordial scalar power spectrum as

$$\kappa_{\zeta,\star} = \left(\frac{\mathrm{d}^2 n_\zeta(k)}{\mathrm{d}\ln k^2}\right)_{k_\star = a_\star H_\star} = \left(\frac{\mathrm{d}^2 n_\zeta(k)}{\mathrm{d}N^2}\right)_{k_\star = a_\star H_\star}$$

$$\approx \begin{cases} -\Big[8\bar{\epsilon}_V(1+\bar{\epsilon}_V)(\bar{\eta}_V - 3\bar{\epsilon}_V)^2 + 8\bar{\epsilon}_V^2(\bar{\eta}_V - 3\bar{\epsilon}_V)^2 + 8\bar{\epsilon}_V(1+\bar{\epsilon}_V)\left(\bar{\xi}_V^2 - 10\bar{\epsilon}_V\bar{\eta}_V + 18\bar{\epsilon}_V^2\right) \\ +2\left(20\bar{\epsilon}_V\bar{\eta}_V(\bar{\eta}_V - 3\bar{\epsilon}_V) + 10\bar{\epsilon}_V\left(\bar{\xi}_V^2 - 4\bar{\epsilon}_V\bar{\eta}_V\right) \\ -72\bar{\epsilon}_V^2(\bar{\eta}_V - 3\bar{\epsilon}_V) - \left(\bar{\sigma}_V^3 + \bar{\xi}_V^2\bar{\eta}_V - \bar{\xi}_V^2\bar{\epsilon}_V\right)\right)\Big]\left(1 - \frac{2}{3}\bar{\epsilon}_V\right)^{1/4} + \cdots, & \text{for } q = 1/2, \\ -\left[\left(\frac{2}{q}\right)^{3/2}\bar{\epsilon}_V\left(1 + \frac{\bar{\epsilon}_V}{2q}\right)(\bar{\eta}_V - 3\bar{\epsilon}_V)^2 + \sqrt{\frac{2}{q}}\frac{2}{q^2}\bar{\epsilon}_V^2(\bar{\eta}_V - 3\bar{\epsilon}_V)^2\right. \\ +\sqrt{\frac{2}{q}}\frac{2}{q}\bar{\epsilon}_V\left(1 + \frac{\bar{\epsilon}_V}{2q}\right)\left(\bar{\xi}_V^2 - 10\bar{\epsilon}_V\bar{\eta}_V + 18\bar{\epsilon}_V^2\right) + \sqrt{\frac{2}{q}}\left(\frac{10}{q}\bar{\epsilon}_V\bar{\eta}_V(\bar{\eta}_V - 3\bar{\epsilon}_V) + 10\bar{\epsilon}_V\left(\bar{\xi}_V^2 - 4\bar{\epsilon}_V\bar{\eta}_V\right)\right. \\ \left.\left. -\frac{36}{q}\bar{\epsilon}_V^2(\bar{\eta}_V - 3\bar{\epsilon}_V) - \left(\bar{\sigma}_V^3 + \bar{\xi}_V^2\bar{\eta}_V - \bar{\xi}_V^2\bar{\epsilon}_V\right)\right)\right]\left(1 - \frac{1}{3q}\bar{\epsilon}_V\right)^{1/4} + \cdots, & \text{for any } q. \end{cases} \tag{5.120}$$

5.1.5 Computation of tensor power spectrum

In this subsection our prime objective is to compute the primordial power spectra of tensor quantum fluctuations from tachyonic inflation and study the cosmological consequences from the previously mentioned string theory originating tachyonic potentials in the light of Planck 2015 data. To serve this purpose let us start with the following canonical variable $u_\mathbf{k}$, which can be quantized with the standard techniques:

$$u^\gamma_\mathbf{k} \equiv \frac{a}{\sqrt{2}}\, M_p\, h^\gamma_\mathbf{k}, \tag{5.121}$$

where $h^\gamma_\mathbf{k}$ is the curvature perturbation in the momentum space, which can be expressed in terms of the curvature perturbation in position space through the following Fourier transformation:

$$h^\gamma(t, \mathbf{x}) = \int \mathrm{d}^3k\, h^\gamma_\mathbf{k}(t)\, \exp(i\mathbf{k}.\mathbf{x}). \tag{5.122}$$

Here the superscript γ stands for the helicity index for the transverse and traceless spin-2 graviton degrees of freedom. In general, the tensor modes can be written in terms of the two orthogonal polarization basis vectors.

Further we derive the equation of motion of the tensor fluctuation by extremizing the tachyonic model action as

$$\left[\frac{\mathrm{d}^2}{\mathrm{d}\eta^2} + \left(k^2 - \frac{1}{a}\frac{\mathrm{d}^2 a}{\mathrm{d}\eta^2}\right)\right]u_\mathbf{k} = 0, \tag{5.123}$$

where the helicity index γ is summed over in the Fourier modes for the tensor contribution $u_\mathbf{k}$ and

$$\frac{1}{a}\frac{\mathrm{d}^2 a}{\mathrm{d}\eta^2} = \begin{cases} a^2H^2\left[2 - \bar{\epsilon}_V\right] + \cdots, & \text{for } q = 1/2, \\ a^2H^2\left[2 - \frac{1}{2q}\bar{\epsilon}_V\right] + \cdots, & \text{for any } q. \end{cases} \tag{5.124}$$

Further replacing the factor aH in Eq. (5.89), we finally get the following simplified expression:

$$\frac{1}{a}\frac{\mathrm{d}^2 a}{\mathrm{d}\eta^2} \approx \begin{cases} \frac{1}{\eta^2}\left[\left(\frac{3}{2} + \bar{\epsilon}_V\right)^2 - \frac{1}{4}\right] + \cdots, & \text{for } q = 1/2, \\ \frac{1}{\eta^2}\left[\left\{\frac{3}{2} + \frac{1}{2q}\bar{\epsilon}_V\right\}^2 - \frac{1}{4}\right] + \cdots, & \text{for any } q. \end{cases} \tag{5.125}$$

Now for further simplification in the computation of tensor power spectrum we introduce a new factor μ which is defined as

$$\mu \approx \begin{cases} \left(\frac{3}{2} + \bar{\epsilon}_V\right) + \cdots, & \text{for } q = 1/2, \\ \left\{\frac{3}{2} + \frac{1}{2q}\bar{\epsilon}_V\right\} + \cdots, & \text{for any } q. \end{cases} \tag{5.126}$$

Hence using Eq. (5.126) in Eq. (5.123), we get the following simplified form of the equation of motion:

$$\left[\frac{\mathrm{d}^2}{\mathrm{d}\eta^2} + \left(k^2 - \frac{(\mu^2 - \frac{1}{4})}{\eta^2}\right)\right]u_\mathbf{k}(\eta) = 0, \tag{5.127}$$

and the most general solution of Eq. (5.127) is given by

$$u_\mathbf{k}(\eta) = \sqrt{-\eta}\left[D_1 H^{(1)}_\mu(-k\eta) + D_2 H^{(2)}_\mu(-k\eta)\right], \tag{5.128}$$

where D_1 and D_2 are two arbitrary integration constants, which can be fixed from the appropriate choice of the boundary conditions. Additionally $H^{(1)}_\mu$ and $H^{(2)}_\mu$ represent the Hankel function of the first and second kind with rank μ. Now to impose the well-known Bunch–Davies boundary condition at early times we have used

$$\lim_{k\eta\to-\infty} H^{(1)}_\mu(-k\eta) = \sqrt{\frac{2}{\pi}}\frac{1}{\sqrt{-\eta}}\exp(ik\eta)\exp\left(i\frac{\pi}{2}\left(\mu+\frac{1}{2}\right)\right), \quad (5.129)$$

$$\lim_{k\eta\to-\infty} H^{(2)}_\mu(-k\eta) = \sqrt{\frac{2}{\pi}}\frac{1}{\sqrt{-\eta}}\exp(-ik\eta)\exp\left(-i\frac{\pi}{2}\left(\mu+\frac{1}{2}\right)\right). \quad (5.130)$$

On the other hand, the solution stated in Eq. (5.128) determines the future evolution of the mode including its super-horizon dynamics at $k << aH$ or $|k\eta| << 1$ or $k\eta \to 0$ and this is due to

$$\lim_{k\eta\to 0} H^{(1)}_\mu(-k\eta) = \frac{i}{\pi}\Gamma(\mu)\left(\frac{-k\eta}{2}\right)^{-\mu}. \quad (5.134)$$

Consequently the solution of the mode function for tensor fluctuations takes the following form:

$$u_{\mathbf{k}}(\eta) = \sqrt{-\frac{\eta\pi}{2}}\frac{i}{\pi}\Gamma(\mu)\left(\frac{-k\eta}{2}\right)^{-\mu}. \quad (5.135)$$

Finally combining the results obtained in Eqs. (5.94), (5.97) and (5.128) we get

$$u_{\mathbf{k}}(\eta) = \begin{cases} \sqrt{-\eta}\left[D_1 H^{(1)}_\mu(-k\eta) + D_2 H^{(2)}_\mu(-k\eta)\right], & \text{for AV}, \\ \sqrt{-\frac{\eta\pi}{2}}H^{(1)}_\mu(-k\eta), & \text{for BD} + |k\eta| >> 1, \\ \sqrt{-\frac{\eta\pi}{2}}\frac{i}{\pi}\Gamma(\mu)\left(\frac{-k\eta}{2}\right)^{-\mu}, & \text{for BD} + |k\eta| << 1, \end{cases} \quad (5.136)$$

where AV and BD signify an arbitrary vacuum and the Bunch–Davies vacuum respectively. Finally the two point function from the tensor fluctuations for both AV and BD can be expressed as

$$\langle h_{\mathbf{k}}h_{\mathbf{k}'}\rangle = \left(\frac{4}{M_p^2}\right)\langle\delta\psi_{\mathbf{k}}\delta\psi_{\mathbf{k}'}\rangle = \frac{2}{a^2M_p^2}\langle u_{\mathbf{k}}u_{\mathbf{k}'}\rangle = (2\pi)^3\delta^3(\mathbf{k}+\mathbf{k}')\frac{2\pi^2}{k^3}\Delta_h(k), \quad (5.137)$$

where the primordial power spectrum for tensor modes at any arbitrary momentum scale k can be written for both AV and BD with $q = 1/2$ as

As a result the previously mentioned integration constants are fixed at the following values:

$$D_1 = \sqrt{\frac{\pi}{2}}, \quad (5.131)$$

$$D_2 = 0. \quad (5.132)$$

Consequently the solution of the mode function for tensor fluctuations takes the following form:

$$u_{\mathbf{k}}(\eta) = \sqrt{-\frac{\eta\pi}{2}}H^{(1)}_\mu(-k\eta). \quad (5.133)$$

$$\Delta_h(k) \equiv \overbrace{2}^{\text{Due to graviton helicity}} \times\frac{k^3P_h(k)}{2\pi^2} = \frac{k^3|u_k|^2}{\pi^2a^2M_p^2}$$

$$= \begin{cases} \begin{cases} \frac{2^{2\mu-2}(-k\eta)^{3-2\mu}H^2}{(1+\bar{\epsilon}_V)^2\pi^2M_p^2}\left|\frac{\Gamma(\mu)}{\Gamma\left(\frac{3}{2}\right)}\right|^2, & \text{for } |k\eta| << 1 \\ \frac{2^{2\mu-2}(1+\bar{\epsilon}_V)^{1-2\mu}H^2}{\pi^2M_p^2}\left|\frac{\Gamma(\mu)}{\Gamma\left(\frac{3}{2}\right)}\right|^2, & \text{for } |k\eta| = 1 \\ \frac{(-k\eta)^3H^2|H^{(1)}_\mu(-k\eta)|^2}{(1+\bar{\epsilon}_V)^2\pi M_p^2}, & \text{for } |k\eta| >> 1, \end{cases} & \underline{\text{for BD}}, \\ \frac{2(-k\eta)^3H^2\left|D_1H^{(1)}_\mu(-k\eta) + D_2H^{(2)}_\mu(-k\eta)\right|^2}{(1+\bar{\epsilon}_V)^2\pi^2M_p^2}, & \underline{\text{for AV}}, \end{cases} \quad (5.138)$$

and similarly the primordial power spectrum for tensor modes at any arbitrary momentum scale k can be written for both AV and BD with any arbitrary q as

$$\Delta_h(k) \equiv \overbrace{2}^{\text{Due to graviton helicity}} \times \frac{k^3 P_h(k)}{2\pi^2} = \frac{k^3|u_k|^2}{\pi^2 a^2 M_p^2}$$
$$= \begin{cases} \begin{cases} \dfrac{2^{2\mu-1} q\,(-k\eta)^{3-2\mu}\, H^2}{\left(1+\frac{1}{2q}\bar{\epsilon}_V\right)^2 \pi^2 M_p^2} \left|\dfrac{\Gamma(\mu)}{\Gamma\left(\frac{3}{2}\right)}\right|^2, & \text{for } |k\eta| << 1 \\ \dfrac{2^{2\mu-1} q \left(1+\frac{1}{2q}\bar{\epsilon}_V\right)^{1-2\mu} H^2}{\pi^2 M_p^2} \left|\dfrac{\Gamma(\mu)}{\Gamma\left(\frac{3}{2}\right)}\right|^2, & \text{for } |k\eta| = 1 \qquad \underline{\text{for BD}} \\ \dfrac{2q\,(-k\eta)^3\, H^2 |H^{(1)}_\mu(-k\eta)|^2}{\bar{\epsilon}_V \left(1+\frac{1}{2q}\bar{\epsilon}_V\right)^2 \pi M_p^2}, & \text{for } |k\eta| >> 1. \end{cases} \\ \dfrac{4q\,(-k\eta)^3\, H^2 \left|C_1 H^{(1)}_\mu(-k\eta) + C_2 H^{(2)}_\mu(-k\eta)\right|^2}{\left(1+\frac{1}{2q}\bar{\epsilon}_V\right)^2 \pi^2 M_p^2}, \qquad \underline{\text{for AV}}. \end{cases} \tag{5.139}$$

Now starting from the expression for the primordial power spectrum for the tensor modes one can compute the spectral tilt at any arbitrary momentum scale k for both AV and BD with $q = 1/2$ as

$$n_h(k) \equiv \frac{d\ln\Delta_h(k)}{d\ln k} = \frac{d\ln\Delta_h(k)}{dN}$$
$$\approx \begin{cases} \begin{cases} (3-2\mu)\left[1-\frac{2}{3}\bar{\epsilon}_V(\bar{\eta}_V-3\bar{\epsilon}_V)\left(1-\frac{2}{3}\bar{\epsilon}_V\right)^{1/4}\right]+\cdots, & \text{for } |k\eta| << 1, \\ (3-2\mu)\left[1-\frac{2}{3}\bar{\epsilon}_V(\bar{\eta}_V-3\bar{\epsilon}_V)\left(1-\frac{2}{3}\bar{\epsilon}_V\right)^{1/4}\right]+\cdots, & \text{for } |k\eta| = 1, \qquad \underline{\text{for BD}}, \\ \bar{\epsilon}_V - \frac{2}{3}\bar{\epsilon}_V(\bar{\eta}_V-3\bar{\epsilon}_V)\left(1-\frac{2}{3}\bar{\epsilon}_V\right)^{1/4} - 2(\bar{\eta}_V-3\bar{\epsilon}_V)\left(1-\frac{2}{3}\bar{\epsilon}_V\right)^{1/4} & \\ \dfrac{(-\eta)\left[H^{(1)}_{\mu-1}(-k\eta) - H^{(1)}_{\mu+1}(-k\eta)\right]}{H^{(1)}_\mu(-k\eta)}+\cdots, & \text{for } |k\eta| >> 1, \end{cases} \\ \bar{\epsilon}_V - \frac{2}{3}\bar{\epsilon}_V(\bar{\eta}_V-3\bar{\epsilon}_V)\left(1-\frac{2}{3}\bar{\epsilon}_V\right)^{1/4} - 2(\bar{\eta}_V-3\bar{\epsilon}_V)\left(1-\frac{2}{3}\bar{\epsilon}_V\right)^{1/4} \\ \dfrac{(-\eta)\,C_1\left[H^{(1)}_{\mu-1}(-k\eta) - H^{(1)}_{\mu+1}(-k\eta)\right]}{\left[C_1 H^{(1)}_\mu(-k\eta) + C_2 H^{(2)}_\mu(-k\eta)\right]} \dfrac{(-\eta)\,C_1\left[H^{(2)}_{\mu-1}(-k\eta) - H^{(2)}_{\mu+1}(-k\eta)\right]}{\left[C_1 H^{(1)}_\mu(-k\eta) + C_2 H^{(2)}_\mu(-k\eta)\right]}+\cdots, \qquad \underline{\text{for AV}}, \end{cases} \tag{5.140}$$

and for both AV and BD with any arbitrary q as

$$n_h(k) \equiv \frac{d\ln\Delta_h(k)}{d\ln k} = \frac{d\ln\Delta_h(k)}{dN}$$
$$= \begin{cases} \begin{cases} (3-2\mu)\left[1-\frac{1}{3q}\bar{\epsilon}_V(\bar{\eta}_V-3\bar{\epsilon}_V)\left(1-\frac{1}{3q}\bar{\epsilon}_V\right)^{1/4}\right]+\cdots, & \text{for } |k\eta|<<1, \\ (3-2\mu)\left[1-\frac{1}{3q}\bar{\epsilon}_V(\bar{\eta}_V-3\bar{\epsilon}_V)\left(1-\frac{1}{3q}\bar{\epsilon}_V\right)^{1/4}\right]+\cdots, & \text{for } |k\eta|=1, \\ \frac{\bar{\epsilon}_V}{2q}-\frac{1}{3q}\bar{\epsilon}_V(\bar{\eta}_V-3\bar{\epsilon}_V)\left(1-\frac{1}{3q}\bar{\epsilon}_V\right)^{1/4}-\frac{1}{q}(\bar{\eta}_V-3\bar{\epsilon}_V)\left(1-\frac{2}{3}\bar{\epsilon}_V\right)^{1/4} & \\ \frac{(-\eta)\left[H^{(1)}_{\mu-1}(-k\eta)-H^{(1)}_{\mu+1}(-k\eta)\right]}{H^{(1)}_{\mu}(-k\eta)}+\cdots, & \text{for } |k\eta|>>1, \end{cases} & \underline{\text{for BD}}, \\ \frac{\bar{\epsilon}_V}{2q}-\frac{1}{3q}\bar{\epsilon}_V(\bar{\eta}_V-3\bar{\epsilon}_V)\left(1-\frac{1}{3q}\bar{\epsilon}_V\right)^{1/4}-\frac{1}{q}(\bar{\eta}_V-3\bar{\epsilon}_V)\left(1-\frac{2}{3}\bar{\epsilon}_V\right)^{1/4} & \\ \frac{(-\eta)\,C_1\left[H^{(1)}_{\mu-1}(-k\eta)-H^{(1)}_{\mu+1}(-k\eta)\right]}{\left[C_1H^{(1)}_{\mu}(-k\eta)+C_2H^{(2)}_{\mu}(-k\eta)\right]} & \\ \frac{(-\eta)\,C_1\left[H^{(2)}_{\mu-1}(-k\eta)-H^{(2)}_{\mu+1}(-k\eta)\right]}{\left[C_1H^{(1)}_{\mu}(-k\eta)+C_2H^{(2)}_{\mu}(-k\eta)\right]}+\cdots, & \underline{\text{for AV}}. \end{cases} \tag{5.141}$$

One can also consider the following approximations to simplify the final derived form of the primordial scalar power spectrum for the BD vacuum with $|kc_S\eta|=1$ case:

1. We start with the *Laurent expansion* of the Gamma function:

$$\Gamma(\mu)=\frac{1}{\mu}-\gamma+\frac{1}{2}\left(\gamma^2+\frac{\pi^2}{6}\right)\mu-\frac{1}{6}\left(\gamma^3+\frac{\gamma\pi^2}{2}+2\zeta(3)\right)\mu^2+\mathcal{O}(\mu^3). \tag{5.142}$$

   where γ being the Euler–Mascheroni constant and $\zeta(3)$ characterizing the Riemann zeta function of order 3 originating in the expansion of the gamma function.
2. Hence using the result of Eq. (5.142) for $q=1/2$ and for arbitrary q we can write:

$$\Gamma(\mu)=\begin{cases} \frac{1}{\left(\frac{3}{2}+\bar{\epsilon}_V\right)}-\gamma+\frac{1}{2}\left(\gamma^2+\frac{\pi^2}{6}\right)\left(\frac{3}{2}+\bar{\epsilon}_V\right) & \\ -\frac{1}{6}\left(\gamma^3+\frac{\gamma\pi^2}{2}+2\zeta(3)\right)\left(\frac{3}{2}+\bar{\epsilon}_V\right)^2+\cdots, & \text{for } q=1/2, \\ \frac{1}{\left\{\frac{3}{2}+\frac{1}{2q}\bar{\epsilon}_V\right\}}-\gamma+\frac{1}{2}\left(\gamma^2+\frac{\pi^2}{6}\right)\left\{\frac{3}{2}+\frac{1}{2q}\bar{\epsilon}_V\right\} & \\ -\frac{1}{6}\left(\gamma^3+\frac{\gamma\pi^2}{2}+2\zeta(3)\right)\left\{\frac{3}{2}+\frac{1}{2q}\bar{\epsilon}_V\right\}^2+\cdots, & \text{for any } q. \end{cases} \tag{5.143}$$

3. In the slow-roll regime of inflation all the slow-roll parameters satisfy the following constraint:

$$\bar{\epsilon}_V << 1, \tag{5.144}$$
$$|\bar{\eta}_V| << 1, \tag{5.145}$$
$$|\bar{\xi}_V^2| << 1, \tag{5.146}$$
$$|\bar{\sigma}_V^3| << 1. \tag{5.147}$$

Using these approximations the primordial scalar power spectrum can be expressed as

$$\begin{aligned}\Delta_{\zeta,\star} &\approx \left\{\left[1-(\mathcal{C}_E+1)\epsilon_1-\frac{\mathcal{C}_E}{2}\epsilon_2\right]^2\frac{H^2}{8\pi^2M_p^2c_S\epsilon_1}\right\}_{k_\star=a_\star H_\star}\\ &=\begin{cases}\left\{[1-(\mathcal{C}_E+1)\bar{\epsilon}_V-\mathcal{C}_E\,(3\bar{\epsilon}_V-\bar{\eta}_V)]^2\,\dfrac{H^2}{8\pi^2M_p^2c_S\bar{\epsilon}_V}\right\}_{k_\star=a_\star H_\star}, & \text{for } q=1/2,\\ \left\{\left[1-(\mathcal{C}_E+1)\dfrac{\bar{\epsilon}_V}{2q}-\dfrac{\mathcal{C}_E}{\sqrt{2q}}\,(3\bar{\epsilon}_V-\bar{\eta}_V)\right]^2\dfrac{qH^2}{4\pi^2M_p^2c_S\bar{\epsilon}_V}\right\}_{k_\star=a_\star H_\star}, & \text{for any } q,\end{cases}\end{aligned} \tag{5.148}$$

where $\mathcal{C}_E$ is given by

$$\mathcal{C}_E=-2+\ln 2+\gamma\approx -0.72. \tag{5.149}$$

4. Next one can compute the scalar spectral tilt (n_S) of the primordial scalar power spectrum as

$$n_{h,\star}\approx\begin{cases}-2\epsilon_1\,[1+\epsilon_1+(\mathcal{C}_E+1)\,\epsilon_2]+\cdots\\ =-2\bar{\epsilon}_V\,[1+\bar{\epsilon}_V+2\,(\mathcal{C}_E+1)\,(3\bar{\epsilon}_V-\bar{\eta}_V)]+\cdots, & \text{for } q=1/2,\\ -2\epsilon_1\,[1+\epsilon_1+(\mathcal{C}_E+1)\,\epsilon_2]+\cdots\\ =-\dfrac{\bar{\epsilon}_V}{q}\left[1+\dfrac{\bar{\epsilon}_V}{2q}+\sqrt{\dfrac{2}{q}}\,(\mathcal{C}_E+1)\,(3\bar{\epsilon}_V-\bar{\eta}_V)\right]+\cdots, & \text{for any } q.\end{cases} \tag{5.150}$$

5. Next one can compute the running of the tensor spectral tilt (α_h) of the primordial scalar power spectrum as

$$\alpha_{h,\star}=\left(\frac{dn_h(k)}{d\ln k}\right)_{k_\star=a_\star H_\star}=\left(\frac{dn_h(k)}{dN}\right)_{k_\star=a_\star H_\star} \tag{5.151}$$

$$\approx\begin{cases}-\Big[4\bar{\epsilon}_V(1+\bar{\epsilon}_V)(\bar{\eta}_V-3\bar{\epsilon}_V)+4\bar{\epsilon}_V^2(\bar{\eta}_V-3\bar{\epsilon}_V)-8\,(\mathcal{C}_E+1)\,\bar{\epsilon}_V(\bar{\eta}_V-3\bar{\epsilon}_V)^2\\ \quad-2\bar{\epsilon}_V\left(10\bar{\epsilon}_V\bar{\eta}_V-18\bar{\epsilon}_V^2-\bar{\xi}_V^2\right)\Big]_\star\left(1-\dfrac{2}{3}\bar{\epsilon}_V\right)_\star^{1/4}+\cdots, & \text{for } q=1/2,\\ -\Bigg[2\dfrac{\bar{\epsilon}_V}{q}\left(1+\dfrac{\bar{\epsilon}_V}{2q}\right)(\bar{\eta}_V-3\bar{\epsilon}_V)+\dfrac{1}{q^2}\bar{\epsilon}_V^2(\bar{\eta}_V-3\bar{\epsilon}_V)-\dfrac{8}{(2q)^{5/2}}\,(\mathcal{C}_E+1)\,\bar{\epsilon}_V(\bar{\eta}_V-3\bar{\epsilon}_V)^2\\ \quad-\sqrt{\dfrac{2}{q}}\bar{\epsilon}_V\left(10\bar{\epsilon}_V\bar{\eta}_V-18\bar{\epsilon}_V^2-\bar{\xi}_V^2\right)\Bigg]_\star\left(1-\dfrac{1}{3q}\bar{\epsilon}_V\right)_\star^{1/4}+\cdots, & \text{for any } q.\end{cases} \tag{5.152}$$

6. Finally, one can also compute the running of the running of scalar spectral tilt (κ_S) of the primordial scalar power spectrum as

$$\kappa_{h,\star} = \left(\frac{\mathrm{d}^2 n_h(k)}{\mathrm{d}\ln k^2}\right)_{k_\star=a_\star H_\star} = \left(\frac{\mathrm{d}^2 n_h(k)}{\mathrm{d}N^2}\right)_{k_\star=a_\star H_\star}$$
$$\approx \begin{cases} -\left[8\bar{\epsilon}_V(1+\bar{\epsilon}_V)(\bar{\eta}_V-3\bar{\epsilon}_V)^2+8\bar{\epsilon}_V^2(\bar{\eta}_V-3\bar{\epsilon}_V)^2 \right. \\ -16\,(\mathcal{C}_E+1)\,\bar{\epsilon}_V\left\{(\bar{\eta}_V-3\bar{\epsilon}_V)^3-(\bar{\eta}_V-3\bar{\epsilon}_V)\left(10\bar{\epsilon}_V\bar{\eta}_V-18\bar{\epsilon}_V^2-\bar{\xi}_V^2\right)\right\} \\ \left.-4\bar{\epsilon}_V(1+\bar{\epsilon}_V)\left(10\bar{\epsilon}_V\bar{\eta}_V-18\bar{\epsilon}_V^2-\bar{\xi}_V^2\right)\right]_\star\left(1-\dfrac{2}{3}\bar{\epsilon}_V\right)_\star^{1/4}+\cdots, & \text{for } q=1/2, \\ -\left[\dfrac{4}{q}\bar{\epsilon}_V\left(1+\dfrac{\bar{\epsilon}_V}{2q}\right)(\bar{\eta}_V-3\bar{\epsilon}_V)^2+\dfrac{2}{q^2}\bar{\epsilon}_V^2(\bar{\eta}_V-3\bar{\epsilon}_V)^2+\dfrac{2}{q}\bar{\epsilon}_V\left(1+\dfrac{\bar{\epsilon}_V}{2q}\right)\left(\bar{\xi}_V^2-10\bar{\epsilon}_V\bar{\eta}_V+18\bar{\epsilon}_V^2\right)\right. \\ \left.-\dfrac{8}{q}\,(\mathcal{C}_E+1)\,\bar{\epsilon}_V\left\{(\bar{\eta}_V-3\bar{\epsilon}_V)^3-(\bar{\eta}_V-3\bar{\epsilon}_V)\left(10\bar{\epsilon}_V\bar{\eta}_V-18\bar{\epsilon}_V^2-\bar{\xi}_V^2\right)\right\}\right]_\star\left(1-\frac{1}{3q}\bar{\epsilon}_V\right)_\star^{1/4}+\cdots, & \text{for any } q. \end{cases} \tag{5.153}$$

5.1.6 *Modified consistency relations*

In this subsection we derive the new (modified) consistency relations for single tachyonic field inflation:

1. Let us first start with the tensor-to-scalar ratio r, which can be defined at any arbitrary momentum scale k for the $q=1/2$ case as

$$r(k) \equiv \frac{\Delta_h(k)}{\Delta_\zeta(k)} = 2\frac{P_h(k)}{P_\zeta(k)} = 2\frac{|u_k|^2}{|v_k|^2}\left(\frac{z}{a}\right)^2$$
$$= \begin{cases} \begin{cases} 16\times 2^{2(\mu-\nu)}\bar{\epsilon}_V\,(-k\eta c_S)^{2(\nu-\mu)}\,c_S^{2\mu-2}\left|\dfrac{\Gamma(\mu)}{\Gamma(\nu)}\right|^2, & \text{for } |kc_S\eta|<<1 \\ 16\times 2^{2(\mu-\nu)}\bar{\epsilon}_V\,(1+\bar{\epsilon}_V)^{2(\nu-\mu)}\,c_S^{2\nu-2}\left|\dfrac{\Gamma(\mu)}{\Gamma(\nu)}\right|^2, & \text{for } |kc_S\eta|=1 \\ \dfrac{8\bar{\epsilon}_V}{c_S^2}\times\dfrac{|H_\mu^{(1)}(-k\eta)|^2}{|H_\nu^{(1)}(-kc_S\eta)|^2}, & \text{for } |kc_S\eta|>>1. \end{cases} & \underline{\text{for BD}} \\ \dfrac{8\bar{\epsilon}_V}{c_S^2}\times\dfrac{\left|D_1H_\mu^{(1)}(-k\eta)+D_2H_\mu^{(2)}(-k\eta)\right|^2}{\left|C_1H_\nu^{(1)}(-kc_S\eta)+C_2H_\nu^{(2)}(-kc_S\eta)\right|^2}, & \underline{\text{for AV}}. \end{cases} \tag{5.154}$$

Similarly for arbitrary q one can write the following expression for the tensor-to-scalar ratio r at any arbitrary momentum scale:

$$r(k) \equiv \frac{\Delta_h(k)}{\Delta_\zeta(k)} = 2\frac{P_h(k)}{P_\zeta(k)} = 2\frac{|u_k|^2}{|v_k|^2}\left(\frac{z}{a}\right)^2$$
$$= \begin{cases} \begin{cases} 16\times 2^{2(\mu-\nu)}\bar{\epsilon}_V\,(-k\eta c_S)^{2(\nu-\mu)}\,c_S^{2\mu-2}\left|\dfrac{\Gamma(\mu)}{\Gamma(\nu)}\right|^2, & \text{for } |kc_S\eta|<<1 \\ 16\times 2^{2(\mu-\nu)}\bar{\epsilon}_V\left(1+\dfrac{\bar{\epsilon}_V}{2q}\right)^{2(\nu-\mu)}c_S^{2\nu-2}\left|\dfrac{\Gamma(\mu)}{\Gamma(\nu)}\right|^2, & \text{for } |kc_S\eta|=1 \\ \dfrac{8\bar{\epsilon}_V}{c_S^2}\times\dfrac{|H_\mu^{(1)}(-kc_S\eta)|^2}{|H_\nu^{(1)}(-kc_S\eta)|^2}, & \text{for } |kc_S\eta|>>1. \end{cases} & \underline{\text{for BD}} \\ \dfrac{8\bar{\epsilon}_V}{c_S^2}\times\dfrac{\left|D_1H_\mu^{(1)}(-kc_S\eta)+D_2H_\mu^{(2)}(-kc_S\eta)\right|^2}{\left|C_1H_\nu^{(1)}(-kc_S\eta)+C_2H_\nu^{(2)}(-kc_S\eta)\right|^2}, & \underline{\text{for AV}}. \end{cases} \tag{5.155}$$

2. Next for the BD vacuum with $|kc_S\eta| = 1$ case within the slow-roll regime we can approximately write the following expression for the tensor-to-scalar ratio:

$$r_\star = \frac{\Delta_h(k_\star)}{\Delta_\zeta(k_\star)} = 2\frac{P_h(k_\star)}{P_\zeta(k_\star)} = 2\frac{|u_{k_\star}|^2}{|v_{k_\star}|^2}\left(\frac{z}{a}\right)^2_\star$$
$$= \left[16\epsilon_1 c_S \frac{[1-(\mathcal{C}_E+1)\epsilon_1]^2}{\left[1-(\mathcal{C}_E+1)\epsilon_1 - \frac{\mathcal{C}_E}{2}\epsilon_2\right]^2}\right]_{k_\star=a_\star H_\star} \tag{5.156}$$

$$\approx \begin{cases} \left[16\bar{\epsilon}_V c_S \dfrac{[1-(\mathcal{C}_E+1)\bar{\epsilon}_V]^2}{[1-(\mathcal{C}_E+1)\bar{\epsilon}_V - \mathcal{C}_E\,(3\bar{\epsilon}_V-\bar{\eta}_V)]^2}\right]_{k_\star=a_\star H_\star} \\ = \left[16\bar{\epsilon}_V \dfrac{[1-(\mathcal{C}_E+1)\bar{\epsilon}_V]^2}{\left[1-\left(\mathcal{C}_E+\frac{5}{6}\right)\bar{\epsilon}_V - \mathcal{C}_E\,(3\bar{\epsilon}_V-\bar{\eta}_V)\right]^2}\right]_{k_\star=a_\star H_\star}, & \text{for } q=1/2, \\ \left[\dfrac{8}{q}\bar{\epsilon}_V c_S \dfrac{\left[1-(\mathcal{C}_E+1)\frac{\bar{\epsilon}_V}{2q}\right]^2}{\left[1-(\mathcal{C}_E+1)\frac{\bar{\epsilon}_V}{2q} - \frac{\mathcal{C}_E}{\sqrt{2q}}\,(3\bar{\epsilon}_V-\bar{\eta}_V)\right]^2}\right]_{k_\star=a_\star H_\star} \\ = \left[\dfrac{8}{q}\bar{\epsilon}_V \dfrac{\left[1-(\mathcal{C}_E+1)\frac{\bar{\epsilon}_V}{2q}\right]^2}{\left[1-(\mathcal{C}_E+1-\Sigma)\frac{\bar{\epsilon}_V}{2q} - \frac{\mathcal{C}_E}{\sqrt{2q}}\,(3\bar{\epsilon}_V-\bar{\eta}_V)\right]^2}\right]_{k_\star=a_\star H_\star}, & \text{for any } q. \end{cases} \tag{5.157}$$

3. Hence the consistency relation between the tensor-to-scalar ratio r and spectral tilt n_h for tensor modes for the BD vacuum with the $|kc_S\eta| = 1$ case can be written as

$$r_\star = -8n_{h,\star} \times \left[c_S \frac{[1-(\mathcal{C}_E+1)\epsilon_1]^2}{\left[1-(\mathcal{C}_E+1)\epsilon_1 - \frac{\mathcal{C}_E}{2}\epsilon_2\right]^2 [1+\epsilon_1+(\mathcal{C}_E+1)\,\epsilon_2]}\right]_{k_\star=a_\star H_\star}$$

$$\approx -8n_{h,\star} \times \underbrace{\begin{cases} \left[c_S \dfrac{[1-(\mathcal{C}_E+1)\bar{\epsilon}_V]^2}{[1-(\mathcal{C}_E+1)\bar{\epsilon}_V - \mathcal{C}_E\,(3\bar{\epsilon}_V-\bar{\eta}_V)]^2\,[1+\bar{\epsilon}_V+2\,(\mathcal{C}_E+1)\,(3\bar{\epsilon}_V-\bar{\eta}_V)]}\right]_{k_\star=a_\star H_\star} \\ = \left[\dfrac{[1-(\mathcal{C}_E+1)\bar{\epsilon}_V]^2}{\left[1-\left(\mathcal{C}_E+\frac{5}{6}\right)\bar{\epsilon}_V - \mathcal{C}_E\,(3\bar{\epsilon}_V-\bar{\eta}_V)\right]^2 [1+\bar{\epsilon}_V+2\,(\mathcal{C}_E+1)\,(3\bar{\epsilon}_V-\bar{\eta}_V)]}\right]_{k_\star=a_\star H_\star}, & \text{for } q=1/2, \\ \left[c_S \dfrac{\left[1-(\mathcal{C}_E+1)\frac{\bar{\epsilon}_V}{2q}\right]^2}{\left[1-(\mathcal{C}_E+1)\frac{\bar{\epsilon}_V}{2q} - \frac{\mathcal{C}_E}{\sqrt{2q}}\,(3\bar{\epsilon}_V-\bar{\eta}_V)\right]^2 \left[1+\frac{\bar{\epsilon}_V}{2q}+\sqrt{\frac{2}{q}}\,(\mathcal{C}_E+1)\,(3\bar{\epsilon}_V-\bar{\eta}_V)\right]}\right]_{k_\star=a_\star H_\star} \\ = \left[\dfrac{\left[1-(\mathcal{C}_E+1)\frac{\bar{\epsilon}_V}{2q}\right]^2}{\left[1-(\mathcal{C}_E+1-\Sigma)\frac{\bar{\epsilon}_V}{2q} - \frac{\mathcal{C}_E}{\sqrt{2q}}\,(3\bar{\epsilon}_V-\bar{\eta}_V)\right]^2 \left[1+\frac{\bar{\epsilon}_V}{2q}+\sqrt{\frac{2}{q}}\,(\mathcal{C}_E+1)\,(3\bar{\epsilon}_V-\bar{\eta}_V)\right]}\right]_{k_\star=a_\star H_\star}, & \text{for any } q. \end{cases}}_{\text{Correction factor}} \tag{5.158}$$

4. Next one can express the first two slow-roll parameters $\bar{\epsilon}_V$ and $\bar{\eta}_V$ in terms of the inflationary observables as

$$\bar{\epsilon}_V \approx \begin{cases} \epsilon_1 \approx -\dfrac{n_{h,\star}}{2} + \cdots \approx \dfrac{r_\star}{16} + \cdots, & \text{for } q = 1/2, \\ 2q\epsilon_1 \approx -qn_{h,\star} + \cdots \approx \dfrac{qr_\star}{8} + \cdots, & \text{for any } q, \end{cases}$$

$$\bar{\eta}_V \approx \begin{cases} 3\epsilon_1 - \dfrac{\epsilon_2}{2} \approx \dfrac{1}{2}\left(n_{\zeta,\star} - 1 + \dfrac{r_\star}{2}\right) + \cdots \approx \dfrac{1}{2}\left(n_{\zeta,\star} - 1 - 4n_{h,\star}\right) + \cdots, & \text{for } q = 1/2, \\ 6q\epsilon_1 - \sqrt{\dfrac{q}{2}}\epsilon_2 \approx \sqrt{\dfrac{q}{2}}\left(n_{\zeta,\star} - 1 + \left(\dfrac{1}{q} + 3\sqrt{\dfrac{2}{q}}\right)\dfrac{qr_\star}{8}\right) + \cdots & \\ \quad \approx \sqrt{\dfrac{q}{2}}\left(n_{\zeta,\star} - 1 - q\left(\dfrac{1}{q} + 3\sqrt{\dfrac{2}{q}}\right)n_{h,\star}\right) + \cdots, & \text{for any } q. \end{cases} \tag{5.159}$$

5. Then the connecting consistency relation between tensor and scalar spectral tilt and tensor-to-scalar ratio can be expressed as

$$n_{h,\star} \approx \begin{cases} -\dfrac{r_\star}{8c_S}\left[1 - \dfrac{r_\star}{16} + (1 - n_{\zeta,\star}) - \mathcal{C}_E\left\{\dfrac{r_\star}{8} + (n_{\zeta,\star} - 1)\right\}\right] + \cdots, & \text{for } q = 1/2, \\ -\dfrac{r_\star}{8c_S}\left[1 + \left\{\left(\dfrac{3q}{8}\sqrt{\dfrac{2}{q}} - \left(\sqrt{\dfrac{2}{q}} + 5\right)\dfrac{1}{16}\right)r_\star + \dfrac{(1 - n_{\zeta,\star})}{\sqrt{2q}}\right\}\right. & \\ \left. + \sqrt{\dfrac{2}{q}}\mathcal{C}_E\left(\dfrac{3qr_\star}{8} - \dfrac{1}{2}\left\{n_{\zeta,\star} - 1 + \left(\dfrac{1}{q} + 3\sqrt{\dfrac{2}{q}}\right)\dfrac{qr_\star}{8}\right\}\right)\right] + \cdots, & \text{for any } q. \end{cases} \tag{5.160}$$

Finally, using the approximated version of the expression for c_S in terms of slow-roll parameters, one can recast this consistency condition as

$$n_{h,\star} \approx \begin{cases} -\dfrac{r_\star}{8}\left[1 - \dfrac{r_\star}{24} + (1 - n_{\zeta,\star}) - \mathcal{C}_E\left\{\dfrac{r_\star}{8} + (n_{\zeta,\star} - 1)\right\}\right] + \cdots, & \text{for } q = 1/2, \\ -\dfrac{r_\star}{8}\left[1 + \left\{\left(\dfrac{3q}{8}\sqrt{\dfrac{2}{q}} - \left(\sqrt{\dfrac{2}{q}} + 5\right)\dfrac{1}{16} + \dfrac{\Sigma}{8}\right)r_\star + \dfrac{(1 - n_{\zeta,\star})}{\sqrt{2q}}\right\}\right. & \\ \left. + \sqrt{\dfrac{2}{q}}\mathcal{C}_E\left(\dfrac{3qr_\star}{8} - \dfrac{1}{2}\left\{n_{\zeta,\star} - 1 + \left(\dfrac{1}{q} + 3\sqrt{\dfrac{2}{q}}\right)\dfrac{qr_\star}{8}\right\}\right)\right] + \cdots, & \text{for any } q. \end{cases} \tag{5.161}$$

6. Next the running of the sound speed c_S can be written in terms of slow-roll parameters as

$$S = \frac{\dot{c}_S}{Hc_S} = \frac{\mathrm{d}\ln c_S}{\mathrm{d}N} = \frac{\mathrm{d}\ln c_S}{\mathrm{d}\ln k} = \begin{cases} -\dfrac{2}{3}\bar{\epsilon}_V\left(\bar{\eta}_V - 3\bar{\epsilon}_V\right)\left(1 - \dfrac{2}{3}\bar{\epsilon}_V\right)^{1/4} + \cdots, & \text{for } q = 1/2, \\ -\dfrac{(1-q)}{3q^2}\bar{\epsilon}_V\left(\bar{\eta}_V - 3\bar{\epsilon}_V\right)\left(1 - \dfrac{1}{3q}\bar{\epsilon}_V\right)^{1/4} + \cdots, & \text{for any } q, \end{cases} \tag{5.162}$$

which can be treated as another slow-roll parameter in the present context. One can also recast the slow-roll parameter S in terms of the inflationary observables as

$$S = \frac{\dot{c}_S}{Hc_S} = \frac{\mathrm{d}\ln c_S}{\mathrm{d}N} = \frac{\mathrm{d}\ln c_S}{\mathrm{d}\ln k} = \begin{cases} -\dfrac{r_\star}{48}\left(n_{\zeta,\star} - 1 + \dfrac{r_\star}{8}\right)\left(1 - \dfrac{r_\star}{24}\right)^{1/4} + \cdots, & \text{for } q = 1/2, \\ -\dfrac{(1-q)}{24q^2}\sqrt{\dfrac{q}{2}}r_\star\left(n_{\zeta,\star} - 1 + \dfrac{r_\star}{8}\right)\left(1 - \dfrac{r_\star}{24}\right)^{1/4} + \cdots, & \text{for any } q. \end{cases} \tag{5.163}$$

7. Further the running of the tensor spectral tilt can be written in terms of the inflationary observables as

$$\alpha_{h,\star} = \left(\frac{\mathrm{d}n_h(k)}{\mathrm{d}\ln k}\right)_{k_\star = a_\star H_\star} = \left(\frac{\mathrm{d}n_h(k)}{\mathrm{d}N}\right)_{k_\star = a_\star H_\star} \tag{5.164}$$

$$\approx \begin{cases} -\left[\frac{r_\star}{8}\left(1+\frac{r_\star}{8}\right)\left(n_{\zeta,\star}-1+\frac{r_\star}{8}\right)-\frac{r_\star}{8}\left(n_{\zeta,\star}-1+\frac{r_\star}{8}\right)^2\right. \\ \left.-\mathcal{C}_E\frac{r_\star}{8}\left(n_{\zeta,\star}-1+\frac{r_\star}{8}\right)^2\right]\left(1-\frac{r_\star}{24}\right)^{1/4}+\cdots, & \text{for } q=1/2, \\ -\left[\frac{r_\star}{4}\sqrt{\frac{q}{2}}\left(1+\frac{r_\star}{8}\right)\left(n_{\zeta,\star}-1+\frac{r_\star}{8}\right)\right. \\ \left.-\frac{1}{(2q)^{1/2}}\left(\mathcal{C}_E+1\right)\frac{r_\star}{8}\left(n_{\zeta,\star}-1+\frac{r_\star}{8}\right)^2\right]\left(1-\frac{r_\star}{24}\right)^{1/4}+\cdots, & \text{for any } q. \end{cases} \tag{5.165}$$

8. Next the scalar power spectrum can be expressed in terms of the other inflationary observables as

$$\Delta_{\zeta,\star} \approx \begin{cases} \left[1-\left(\mathcal{C}_E+\frac{5}{6}\right)\frac{r_\star}{16}+\frac{\mathcal{C}_E}{2}\left(n_{\zeta,\star}-1+\frac{r_\star}{8}\right)\right]^2\frac{2H_\star^2}{\pi^2 M_p^2 r_\star}+\cdots, & \text{for } q=1/2, \\ \left[1-\left(\mathcal{C}_E+1-\Sigma\right)\frac{r_\star}{16}+\frac{\mathcal{C}_E}{2}\left(n_{\zeta,\star}-1+\frac{r_\star}{8}\right)\right]^2\frac{2H_\star^2}{\pi^2 M_p^2 r_\star}+\cdots, & \text{for any } q. \end{cases} \tag{5.166}$$

9. Further the tensor power spectrum can be expressed in terms of the other inflationary observables as

$$\Delta_{h,\star} = \begin{cases} \left[1-\left(\mathcal{C}_E+1\right)\frac{r_\star}{16}\right]^2\frac{2H_\star^2}{\pi^2 M_p^2}+\cdots, & \text{for } q=1/2, \\ \left[1-\left(\mathcal{C}_E+1\right)\frac{r_\star}{16}\right]^2\frac{2H_\star^2}{\pi^2 M_p^2}+\cdots, & \text{for any } q. \end{cases} \tag{5.167}$$

10. Next the running of the tensor-to-scalar ratio can be expressed in terms of the inflationary observables as

$$\alpha_{r,\star} = \left(\frac{\mathrm{d}r}{\mathrm{d}\ln k}\right)_\star = \left(\frac{\mathrm{d}r}{\mathrm{d}N}\right)_\star = -8\alpha_{h,\star}+\cdots$$

$$\approx \begin{cases} \left[r_\star\left(1+\frac{r_\star}{8}\right)\left(n_{\zeta,\star}-1+\frac{r_\star}{8}\right)-r_\star\left(n_{\zeta,\star}-1+\frac{r_\star}{8}\right)^2\right. \\ \left.-\mathcal{C}_E r_\star\left(n_{\zeta,\star}-1+\frac{r_\star}{8}\right)^2\right]\left(1-\frac{r_\star}{24}\right)^{1/4}+\cdots, & \text{for } q=1/2, \\ \left[2r_\star\sqrt{\frac{q}{2}}\left(1+\frac{r_\star}{8}\right)\left(n_{\zeta,\star}-1+\frac{r_\star}{8}\right)\right. \\ \left.-\frac{1}{(2q)^{1/2}}\left(\mathcal{C}_E+1\right)r_\star\left(n_{\zeta,\star}-1+\frac{r_\star}{8}\right)^2\right]\left(1-\frac{r_\star}{24}\right)^{1/4}+\cdots, & \text{for any } q. \end{cases} \tag{5.168}$$

11. Finally the scale of single field tachyonic inflation can be expressed in terms of the Hubble parameter and the other inflationary observables as

$$H_{\rm inf} = H_\star \approx \begin{cases} \dfrac{\sqrt{\frac{\Delta_{\zeta,\star} r_\star}{2}}\pi M_p}{\left[1-\left(\mathcal{C}_E+\frac{5}{6}\right)\frac{r_\star}{16}+\frac{\mathcal{C}_E}{2}\left(n_{\zeta,\star}-1+\frac{r_\star}{8}\right)\right]}+\cdots, & \text{for } q=1/2, \\ \dfrac{\sqrt{\frac{\Delta_{\zeta,\star} r_\star}{2}}\pi M_p}{\left[1-(\mathcal{C}_E+1-\Sigma)\frac{r_\star}{16}+\frac{\mathcal{C}_E}{2}\left(n_{\zeta,\star}-1+\frac{r_\star}{8}\right)\right]}+\cdots, & \text{for any } q. \end{cases} \tag{5.169}$$

One can recast this statement in terms of the inflationary potential as

$$\sqrt[4]{V_{\rm inf}} = \sqrt[4]{V_\star} \approx \begin{cases} \dfrac{\sqrt[4]{\frac{3\Delta_{\zeta,\star} r_\star}{2}}\sqrt{\pi} M_p}{\sqrt{\left[1-\left(\mathcal{C}_E+\frac{5}{6}\right)\frac{r_\star}{16}+\frac{\mathcal{C}_E}{2}\left(n_{\zeta,\star}-1+\frac{r_\star}{8}\right)\right]}}+\cdots, & \text{for } q=1/2, \\ \dfrac{\sqrt[4]{\frac{3\Delta_{\zeta,\star} r_\star}{2}}\sqrt{\pi} M_p}{\sqrt{\left[1-(\mathcal{C}_E+1-\Sigma)\frac{r_\star}{16}+\frac{\mathcal{C}_E}{2}\left(n_{\zeta,\star}-1+\frac{r_\star}{8}\right)\right]}}+\cdots, & \text{for any } q. \end{cases} \tag{5.170}$$

5.1.7 Field excursion for tachyon

In this subsection we explicitly derive the expression for the field excursion[4] for tachyonic inflation defined as

$$|\Delta T| = |T_{\rm cmb} - T_{\rm end}| = |T_\star - T_{\rm end}| \tag{5.171}$$

where $T_{\rm cmb}$, $T_{\rm end}$ and $T_\star$ signify the tachyon field value at the time of horizon exit, at end of inflation and at pivot scale respectively. Here we perform the computation for both AV and BD vacuum. For for the sake of simplicity the pivot scale is fixed at the horizon exit scale. To compute the expression for the field excursion we perform the following steps:

1. We start with the operator identity for single field tachyon using which one can write expression for the tachyon field variation with respect to the momentum scale (k) or number of e-foldings (N) in terms of the inflationary observables as

$$\frac{1}{H}\frac{{\rm d}T}{{\rm d}t} = \frac{{\rm d}T}{{\rm d}N} = \frac{{\rm d}T}{{\rm d}\ln k} \approx \begin{cases} \sqrt{\dfrac{r}{8V(T)\alpha'}}M_p\left(1-\dfrac{r}{24}\right)^{1/4}+\cdots, & \text{for } q=1/2, \\ \sqrt{\dfrac{qr}{4V(T)\alpha'}}\dfrac{M_p}{2q}\left(1-\dfrac{r}{24}\right)^{1/4}+\cdots, & \text{for any arbitrary } q, \end{cases} \tag{5.172}$$

   where the tensor-to-scalar ratio r is a function of k or N.
2. Next using Eq. (5.172) we can write the following integral equation:

$$\int_{T_{\rm end}}^{T_\star} {\rm d}T\,\sqrt{V(T)} \approx \begin{cases} \displaystyle\int_{k_{\rm end}}^{k_\star}{\rm d}\ln k\,\sqrt{\frac{r}{8\alpha'}}M_p\left(1-\frac{r}{24}\right)^{1/4}+\cdots \\ \displaystyle\quad = \int_{N_{\rm end}}^{N_\star}{\rm d}N\,\sqrt{\frac{r}{8\alpha'}}M_p\left(1-\frac{r}{24}\right)^{1/4}+\cdots, & \text{for } q=1/2, \\ \displaystyle\int_{k_{\rm end}}^{k_\star}{\rm d}\ln k\,\sqrt{\frac{qr}{4\alpha'}}\frac{M_p}{2q}\left(1-\frac{r}{24}\right)^{1/4}+\cdots \\ \displaystyle\quad = \int_{N_{\rm end}}^{N_\star}{\rm d}N\,\sqrt{\frac{qr}{4\alpha'}}\frac{M_p}{2q}\left(1-\frac{r}{24}\right)^{1/4}+\cdots, & \text{for any arbitrary } q. \end{cases} \tag{5.173}$$

[4] In the context of effective field theory, with a minimally coupled scalar field with Einstein gravity we compute the field excursion formula in Refs. [44,129–132].

3. Next we parametrize the form of the tensor-to-scalar ratio for $q = 1/2$ and for any arbitrary q at any arbitrary scale as

$$r(k) = \begin{cases} \begin{cases} r_\star & \text{for } \underline{\text{Case I}}, \\ r_\star \left(\frac{k}{k_\star}\right)^{n_{h,\star}-n_{\zeta,\star}+1} & \text{for } \underline{\text{Case II}}, \\ r_\star \left(\frac{k}{k_*}\right)^{n_{h,\star}-n_{\zeta,\star}+1+\frac{\alpha_{h,\star}-\alpha_{\zeta,\star}}{2!}\ln\left(\frac{k}{k_\star}\right)+\cdots} & \text{for } \underline{\text{Case III}}, \end{cases} & \text{for BD}, \\ \frac{q r_\star}{2c_S^2} \times \frac{\left|D_1 H_\mu^{(1)}(-kc_S\eta) + D_2 H_\mu^{(2)}(-kc_S\eta)\right|^2}{\left|C_1 H_\nu^{(1)}(-kc_S\eta) + C_2 H_\nu^{(2)}(-kc_S\eta)\right|^2} & \text{for AV}, \end{cases} \tag{5.174}$$

where k_* is the pivot scale of momentum. One can also express Eq. (5.174) in terms of the number of e-foldings (N) as

$$r(N) = \begin{cases} \begin{cases} r_\star & \text{for } \underline{\text{Case I}}, \\ r_\star \exp\left[(N-N_\star)(n_{h,\star}-n_{\zeta,\star}+1)\right] & \text{for } \underline{\text{Case II}}, \\ r_\star \exp\left[(N-N_\star)\left\{(n_{h,\star}-n_{\zeta,\star}+1)\right.\right. & \\ \left.\left. +\frac{\alpha_{h,\star}-\alpha_{\zeta,\star}}{2!}(N-N_\star)+\cdots\right\}\right] & \text{for } \underline{\text{Case III}}, \end{cases} & \text{for BD}, \\ \frac{q r_\star}{2c_S^2} \times \frac{\left|D_1 H_\mu^{(1)}(-k_\star c_S\eta\exp[N-N_\star]) + D_2 H_\mu^{(2)}(-k_\star c_S\eta\exp[N-N_\star])\right|^2}{\left|C_1 H_\nu^{(1)}(-k_\star c_S\eta\exp[N-N_\star]) + C_2 H_\nu^{(2)}(-k_\star c_S\eta\exp[N-N_\star])\right|^2} & \text{for AV} \end{cases} \tag{5.175}$$

where k and N are connected through the following expression: $\frac{k}{k_\star} = \exp\left[(N-N_\star)\right]$. Here the three possibilities for the BD vacuum are:

Case I stands for a situation where the spectrum is scale invariant. This is a similar situation to the one considered in the case of the Lyth bound. This possibility also surmounts to the Harrison & Zeldovich spectrum, which is completely ruled out by Planck 2015+WMAP9 data within 5σ C.L.

Case II stands for a situation where the spectrum shows a power-law feature through the spectral tilt (n_ζ, n_h). This possibility is also tightly constrained by the WMAP9 and Planck 2015+WMAP9 data within 2σ C.L.

Case III signifies a situation where the spectrum shows deviation from power low in the presence of running of the spectral tilt (α_ζ, α_h) along with logarithmic correction in the momentum scale as appearing in the exponent. This possibility is favored by WMAP9 data and tightly constrained within 2σ window by Planck+WMAP9 data.

4. For any value of q including $q = 1/2$ we need to compute the following integral:

$$\int_{k_{\rm end}}^{k_\star} d\ln k\,\sqrt{\frac{qr}{4\alpha^\prime}}\frac{M_p}{2q}\left(1-\frac{r}{24}\right)^{1/4}$$
$$\approx\begin{cases}\sqrt{\frac{qr_\star}{4\alpha^\prime}}\frac{M_p}{2q}\left(1-\frac{r_\star}{24}\right)^{1/4}\ln\left(\frac{k_\star}{k_{\rm end}}\right) & \text{for } \underline{\text{Case I}},\\ \frac{\sqrt{\frac{qr_\star}{4\alpha^\prime}}\frac{M_p}{q}}{3(n_{h,\star}-n_{\zeta,\star}+1)}\left[\left\{{}_2F_1\left[\frac{1}{2},\frac{3}{4};\frac{3}{2};\frac{r_\star}{24}\right]+2\left(1-\frac{r_\star}{24}\right)^{1/4}\right\}\right. & \\ -\left(\frac{k_{\rm end}}{k_\star}\right)^{\frac{n_{h,\star}-n_{\zeta,\star}+1}{2}}\left\{{}_2F_1\left[\frac{1}{2},\frac{3}{4};\frac{3}{2};\frac{r_\star}{24}\left(\frac{k_{\rm end}}{k_\star}\right)^{n_{h,\star}-n_{\zeta,\star}+1}\right]\right. & \\ \left.\left.+2\left(1-\frac{r_\star}{24}\left(\frac{k_{\rm end}}{k_\star}\right)^{n_{h,\star}-n_{\zeta,\star}+1}\right)^{1/4}\right\}\right] & \text{for } \underline{\text{Case II}},\\ \sqrt{\frac{\pi q r_\star}{\alpha^\prime(\alpha_{h,\star}-\alpha_{\zeta,\star})}}\frac{M_p}{48q}e^{-\frac{3(n_{h,\star}-n_{\zeta,\star}+1)^2}{4(\alpha_{h,\star}-\alpha_{\zeta,\star})}} & \\ \left[12e^{\frac{(n_{h,\star}-n_{\zeta,\star}+1)^2}{2(\alpha_{h,\star}-\alpha_{\zeta,\star})}}\left\{{\rm erfi}\left(\frac{n_{h,\star}-n_{\zeta,\star}+1}{2\sqrt{\alpha_{h,\star}-\alpha_{\zeta,\star}}}\right)\right.\right. & \\ \left.-{\rm erfi}\left(\frac{n_{h,\star}-n_{\zeta,\star}+1}{2\sqrt{\alpha_{h,\star}-\alpha_{\zeta,\star}}}+\frac{\sqrt{\alpha_{h,\star}-\alpha_{\zeta,\star}}}{2}\ln\left(\frac{k_{\rm end}}{k_\star}\right)\right)\right\} & \\ -\frac{\sqrt{3}r_\star}{24}\left\{{\rm erfi}\left(\frac{\sqrt{3}(n_{h,\star}-n_{\zeta,\star}+1)}{2\sqrt{\alpha_{h,\star}-\alpha_{\zeta,\star}}}\right)\right. & \\ \left.\left.-{\rm erfi}\left(\frac{\sqrt{3}(n_{h,\star}-n_{\zeta,\star}+1)}{2\sqrt{\alpha_{h,\star}-\alpha_{\zeta,\star}}}+\frac{\sqrt{3(\alpha_{h,\star}-\alpha_{\zeta,\star})}}{2}\ln\left(\frac{k_{\rm end}}{k_\star}\right)\right)\right\}\right] & \text{for } \underline{\text{Case III}},\end{cases}\quad \underline{\text{for BD}}, \tag{5.176}$$

Similarly for AV we get the following result:

$$\int_{k_{\rm end}}^{k_\star} d\ln k\,\sqrt{\frac{qr}{4\alpha^\prime}}\frac{M_p}{2q}\left(1-\frac{r}{24}\right)^{1/4}$$
$$\approx\begin{cases}\sqrt{\frac{r_\star}{8\alpha^\prime}}\frac{M_p}{2c_S}\left(1-\frac{qr_\star}{48c_S^2}\right)^{1/4}\ln\left(\frac{k_\star}{k_{\rm end}}\right) & \text{for } \underline{\text{Case I}},\\ \sqrt{\frac{r_\star}{8\alpha^\prime}}\frac{M_p}{2c_S}\frac{|D|}{|C|}\left(1-\frac{qr_\star}{48c_S^2}\frac{|D|^2}{|C|^2}\right)^{1/4}\ln\left(\frac{k_\star}{k_{\rm end}}\right) & \text{for } \underline{\text{Case II}},\end{cases}\quad \underline{\text{for AV}}. \tag{5.177}$$

In terms of the number of e-foldings N one can re-express Eqs. (5.176) and (5.177) as

$$\int_{k_{\rm end}}^{k_\star} \mathrm{d}\ln k \sqrt{\frac{qr}{4\alpha'}}\frac{M_p}{2q}\left(1-\frac{r}{24}\right)^{1/4}$$
$$\approx \begin{cases} \begin{cases} \sqrt{\frac{qr_\star}{4\alpha'}}\frac{M_p}{2q}\left(1-\frac{r_\star}{24}\right)^{1/4}(N_\star - N_{\rm end}) & \text{for }\underline{\text{Case I}}, \\ \frac{\sqrt{\frac{qr_\star}{4\alpha'}}\frac{M_p}{q}}{3(n_{h,\star}-n_{\zeta,\star}+1)}\left[\left\{{}_2F_1\left[\frac{1}{2},\frac{3}{4};\frac{3}{2};\frac{r_\star}{24}\right]+2\left(1-\frac{r_\star}{24}\right)^{1/4}\right\}\right. \\ -e^{\frac{n_{h,\star}-n_{\zeta,\star}+1}{2}(N_{\rm end}-N_\star)}\left\{{}_2F_1\left[\frac{1}{2},\frac{3}{4};\frac{3}{2};\frac{r_\star}{24}e^{(n_{h,\star}-n_{\zeta,\star}+1)(N_{\rm end}-N_\star)}\right]\right. \\ \left.\left.+2\left(1-\frac{r_\star}{24}e^{(n_{h,\star}-n_{\zeta,\star}+1)(N_{\rm end}-N_\star)}\right)^{1/4}\right\}\right] & \text{for }\underline{\text{Case II}}, \\ \sqrt{\frac{\pi q r_\star}{\alpha'(\alpha_{h,\star}-\alpha_{\zeta,\star})}}\frac{M_p}{48q}e^{-\frac{3(n_{h,\star}-n_{\zeta,\star}+1)^2}{4(\alpha_{h,\star}-\alpha_{\zeta,\star})}} \\ \left[12e^{\frac{(n_{h,\star}-n_{\zeta,\star}+1)^2}{2(\alpha_{h,\star}-\alpha_{\zeta,\star})}}\left\{\mathrm{erfi}\left(\frac{n_{h,\star}-n_{\zeta,\star}+1}{2\sqrt{\alpha_{h,\star}-\alpha_{\zeta,\star}}}\right)\right.\right. \\ \left.-\mathrm{erfi}\left(\frac{n_{h,\star}-n_{\zeta,\star}+1}{2\sqrt{\alpha_{h,\star}-\alpha_{\zeta,\star}}}+\frac{\sqrt{\alpha_{h,\star}-\alpha_{\zeta,\star}}}{2}(N_{\rm end}-N_\star)\right)\right\} \\ -\frac{\sqrt{3}r_\star}{24}\left\{\mathrm{erfi}\left(\frac{\sqrt{3}(n_{h,\star}-n_{\zeta,\star}+1)}{2\sqrt{\alpha_{h,\star}-\alpha_{\zeta,\star}}}\right)\right. \\ \left.\left.-\mathrm{erfi}\left(\frac{\sqrt{3}(n_{h,\star}-n_{\zeta,\star}+1)}{2\sqrt{\alpha_{h,\star}-\alpha_{\zeta,\star}}}+\frac{\sqrt{3(\alpha_{h,\star}-\alpha_{\zeta,\star})}}{2}(N_{\rm end}-N_\star)\right)\right\}\right] & \text{for }\underline{\text{Case III}}, \end{cases} & \underline{\text{for BD}}, \end{cases} \tag{5.178}$$

$$\int_{k_{\rm end}}^{k_\star} \mathrm{d}\ln k \sqrt{\frac{qr}{4\alpha'}}\frac{M_p}{2q}\left(1-\frac{r}{24}\right)^{1/4}$$
$$\approx \begin{cases} \sqrt{\frac{r_\star}{8\alpha'}}\frac{M_p}{2c_S}\left(1-\frac{qr_\star}{48c_S^2}\right)^{1/4}(N_\star-N_{\rm end}) & \text{for }\underline{\text{Case I}}, \\ \sqrt{\frac{r_\star}{8\alpha'}}\frac{M_p}{2c_S}\frac{|D|}{|C|}\left(1-\frac{qr_\star}{48c_S^2}\frac{|D|^2}{|C|^2}\right)^{1/4}(N_\star-N_{\rm end}) & \text{for }\underline{\text{Case II}}, \end{cases} \quad \underline{\text{for AV}}. \tag{5.179}$$

Here the two possibilities for AV vacuum are:
Case I stands for a situation where the spectrum is characterized by the constraint i) $D_1 = D_2 = C_1 = C_2 \neq 0$, ii) $D_1 = D_2$, $C_1 = C_2 = 0$, iii) $D_1 = D_2 = 0$, $C_1 = C_2$.
Case II stands for a situation where the spectrum is characterized by the constraint i) $\mu \approx \nu$, $D_1 = D_2 = D \neq 0$ and $C_1 = C_2 = C \neq 0$, ii) $\mu \approx \nu$, $D_1 = D \neq 0$, $D_2 = 0$ and $C_1 = C \neq 0$, $C_2 = 0$, iii) $\mu \approx \nu$, $D_2 = D \neq 0$, $D_1 = 0$ and $C_2 = C \neq 0$, $C_1 = 0$.

5. Next we assume that the generic tachyonic potential $V(T)$ can be expressed as

$$V(T) = V_0 + \sum_{n=1}^{\infty}\frac{1}{n!}\left(\frac{\mathrm{d}^n V(T)}{\mathrm{d}T^n}\right)_{T=T_0}(T-T_0)^n\,, \tag{5.180}$$

where the contribution from V_0 fix the scale of potential and the higher order Taylor expansion co-efficients characterize the shape of potential.

6. Further we need to compute the following integral:

$$\begin{aligned}\int_{T_{\rm end}}^{T_\star} dT\,\sqrt{V(T)} &\approx \int_{T_{\rm end}}^{T_\star} dT\,\sqrt{V_0+\sum_{n=1}^{\infty}\frac{1}{n!}\left(\frac{d^nV(T)}{dT^n}\right)_{T=T_0}(T-T_0)^n}\\ &\approx \int_{T_{\rm end}}^{T_\star} dT\,\sqrt{V_0}\left\{1+\sum_{n=1}^{\infty}\frac{1}{2n!V_0}\left(\frac{d^nV(T)}{dT^n}\right)_{T=T_0}(T-T_0)^n+\cdots\right\}\\ &\approx \sqrt{V_0}\Delta T\left\{1+\sum_{n=1}^{\infty}\frac{\left(\frac{d^nV(T)}{dT^n}\right)_{T=T_0}}{2(n+1)n!V_0}\frac{\left[(T_\star-T_0)^{n+1}-(T_{\rm end}-T_0)^{n+1}\right]}{\Delta T}+\cdots\right\}\end{aligned} \tag{5.181}$$

7. Next we assume that

$$\frac{1}{V_0}\left(\frac{d^nV(T)}{dT^n}\right)_{T=T_0}\frac{\left[(T_\star-T_0)^{n+1}-(T_{\rm end}-T_0)^{n+1}\right]}{\Delta T}<<1. \tag{5.182}$$

Consequently from Eq. (5.181) we get

$$\int_{T_{\rm end}}^{T_\star} dT\,\sqrt{V(T)}\approx\sqrt{V_0}\Delta T \tag{5.183}$$

8. Finally using Eqs. (5.178), (5.179), (5.183) and (5.173) we get

$$\frac{\Delta T}{M_p}\approx\begin{cases}\sqrt{\frac{qr_\star}{4\alpha' V_0}}\frac{1}{2q}\left(1-\frac{r_\star}{24}\right)^{1/4}(N_\star-N_{\rm end}) & \text{for }\underline{\text{Case I}},\\ \frac{\sqrt{\frac{qr_\star}{4\alpha' V_0}}\frac{1}{q}}{3(n_{h,\star}-n_{\zeta,\star}+1)}\left[\left\{{}_2F_1\left[\frac{1}{2},\frac{3}{4};\frac{3}{2};\frac{r_\star}{24}\right]+2\left(1-\frac{r_\star}{24}\right)^{1/4}\right\}\right.\\ -e^{\frac{n_{h,\star}-n_{\zeta,\star}+1}{2}(N_{\rm end}-N_\star)}\left\{{}_2F_1\left[\frac{1}{2},\frac{3}{4};\frac{3}{2};\frac{r_\star}{24}e^{(n_{h,\star}-n_{\zeta,\star}+1)(N_{\rm end}-N_\star)}\right]\right.\\ \left.\left.+2\left(1-\frac{r_\star}{24}e^{(n_{h,\star}-n_{\zeta,\star}+1)(N_{\rm end}-N_\star)}\right)^{1/4}\right\}\right] & \text{for }\underline{\text{Case II}},\\ \sqrt{\frac{\pi q r_\star}{\alpha'(\alpha_{h,\star}-\alpha_{\zeta,\star})V_0}}\frac{1}{48q}e^{-\frac{3(n_{h,\star}-n_{\zeta,\star}+1)^2}{4(\alpha_{h,\star}-\alpha_{\zeta,\star})}} & \underline{\text{for BD}},\\ \left[12e^{\frac{(n_{h,\star}-n_{\zeta,\star}+1)^2}{2(\alpha_{h,\star}-\alpha_{\zeta,\star})}}\left\{\mathrm{erfi}\left(\frac{n_{h,\star}-n_{\zeta,\star}+1}{2\sqrt{\alpha_{h,\star}-\alpha_{\zeta,\star}}}\right)\right.\right.\\ \left.-\mathrm{erfi}\left(\frac{n_{h,\star}-n_{\zeta,\star}+1}{2\sqrt{\alpha_{h,\star}-\alpha_{\zeta,\star}}}+\frac{\sqrt{\alpha_{h,\star}-\alpha_{\zeta,\star}}}{2}(N_{\rm end}-N_\star)\right)\right\}\\ -\frac{\sqrt{3}r_\star}{24}\left\{\mathrm{erfi}\left(\frac{\sqrt{3}(n_{h,\star}-n_{\zeta,\star}+1)}{2\sqrt{\alpha_{h,\star}-\alpha_{\zeta,\star}}}\right)\right.\\ \left.\left.-\mathrm{erfi}\left(\frac{\sqrt{3}(n_{h,\star}-n_{\zeta,\star}+1)}{2\sqrt{\alpha_{h,\star}-\alpha_{\zeta,\star}}}+\frac{\sqrt{3(\alpha_{h,\star}-\alpha_{\zeta,\star})}}{2}(N_{\rm end}-N_\star)\right)\right\}\right] & \text{for }\underline{\text{Case III}},\end{cases} \tag{5.184}$$

$$\frac{\Delta T}{M_p}\approx\begin{cases}\sqrt{\frac{r_\star}{8\alpha' V_0}}\frac{1}{2c_S}\left(1-\frac{qr_\star}{48c_S^2}\right)^{1/4}(N_\star-N_{\rm end}) & \text{for }\underline{\text{Case I}},\\ \sqrt{\frac{r_\star}{8\alpha' V_0}}\frac{|D|}{2c_S|C|}\left(1-\frac{qr_\star}{48c_S^2}\frac{|D|^2}{|C|^2}\right)^{1/4}(N_\star-N_{\rm end}) & \text{for }\underline{\text{Case II}},\end{cases}\quad\underline{\text{for AV}}. \tag{5.185}$$

9. Next using Eq. (5.170) in Eqs. (5.184) and (5.185) we get

$$\frac{\Delta T}{M_p} \approx \begin{cases} \sqrt{\frac{qr_\star}{4\alpha'}}\frac{1}{2q\sqrt{\frac{3\Delta_{\zeta,\star}r_\star}{2}}\pi M_p^2}\left(1-\frac{r_\star}{24}\right)^{1/4}(N_\star - N_{\text{end}}) \\ \left[1-(\mathcal{C}_E+1-\Sigma)\frac{r_\star}{16}+\frac{\mathcal{C}_E}{2\sqrt{2q}}\left(n_{\zeta,\star}-1\right.\right. \\ \left.\left.+\left(1+3\sqrt{2q}-6q\right)\frac{r_\star}{8}\right)\right] & \text{for } \underline{\text{Case I}}, \\ \frac{\sqrt{\frac{qr_\star}{4\alpha'}}\frac{1}{q\sqrt{\frac{3\Delta_{\zeta,\star}r_\star}{2}}\pi M_p^2}}{3(n_{h,\star}-n_{\zeta,\star}+1)}\left[\left\{{}_2F_1\left[\frac{1}{2},\frac{3}{4};\frac{3}{2};\frac{r_\star}{24}\right]+2\left(1-\frac{r_\star}{24}\right)^{1/4}\right\}\right. \\ -e^{\frac{n_{h,\star}-n_{\zeta,\star}+1}{2}(N_{\text{end}}-N_\star)}\left\{{}_2F_1\left[\frac{1}{2},\frac{3}{4};\frac{3}{2};\frac{r_\star}{24}e^{(n_{h,\star}-n_{\zeta,\star}+1)(N_{\text{end}}-N_\star)}\right]\right. \\ \left.\left.+2\left(1-\frac{r_\star}{24}e^{(n_{h,\star}-n_{\zeta,\star}+1)(N_{\text{end}}-N_\star)}\right)^{1/4}\right\}\right] \\ \left[1-(\mathcal{C}_E+1-\Sigma)\frac{r_\star}{16}+\frac{\mathcal{C}_E}{2\sqrt{2q}}\left(n_{\zeta,\star}-1\right.\right. \\ \left.\left.+\left(1+3\sqrt{2q}-6q\right)\frac{r_\star}{8}\right)\right] & \text{for } \underline{\text{Case II}}, \quad \underline{\text{for BD}}, \\ \frac{\sqrt{\frac{\pi q r_\star}{\alpha'(\alpha_{h,\star}-\alpha_{\zeta,\star})}}}{48q\sqrt{\frac{3\Delta_{\zeta,\star}r_\star}{2}}\pi M_p^2}e^{-\frac{3(n_{h,\star}-n_{\zeta,\star}+1)^2}{4(\alpha_{h,\star}-\alpha_{\zeta,\star})}} \\ \left[12e^{\frac{(n_{h,\star}-n_{\zeta,\star}+1)^2}{2(\alpha_{h,\star}-\alpha_{\zeta,\star})}}\left\{\text{erfi}\left(\frac{n_{h,\star}-n_{\zeta,\star}+1}{2\sqrt{\alpha_{h,\star}-\alpha_{\zeta,\star}}}\right)\right.\right. \\ \left.-\text{erfi}\left(\frac{n_{h,\star}-n_{\zeta,\star}+1}{2\sqrt{\alpha_{h,\star}-\alpha_{\zeta,\star}}}+\frac{\sqrt{\alpha_{h,\star}-\alpha_{\zeta,\star}}}{2}(N_{\text{end}}-N_\star)\right)\right\} \\ -\frac{\sqrt{3}r_\star}{24}\left\{\text{erfi}\left(\frac{\sqrt{3}(n_{h,\star}-n_{\zeta,\star}+1)}{2\sqrt{\alpha_{h,\star}-\alpha_{\zeta,\star}}}\right)\right. \\ \left.\left.-\text{erfi}\left(\frac{\sqrt{3}(n_{h,\star}-n_{\zeta,\star}+1)}{2\sqrt{\alpha_{h,\star}-\alpha_{\zeta,\star}}}+\frac{\sqrt{3(\alpha_{h,\star}-\alpha_{\zeta,\star})}}{2}(N_{\text{end}}-N_\star)\right)\right\}\right] \\ \left[1-(\mathcal{C}_E+1-\Sigma)\frac{r_\star}{16}+\frac{\mathcal{C}_E}{2\sqrt{2q}}\left(n_{\zeta,\star}-1\right.\right. \\ \left.\left.+\left(1+3\sqrt{2q}-6q\right)\frac{r_\star}{8}\right)\right] & \text{for } \underline{\text{Case III}}, \end{cases} \tag{5.186}$$

$$\frac{\Delta T}{M_p} \approx \begin{cases} \sqrt{\frac{r_\star}{8\alpha'}}\frac{\left(1-\frac{qr_\star}{48c_S^2}\right)^{1/4}(N_\star - N_{\text{end}})}{2c_S\sqrt{\frac{3\Delta_{\zeta,\star}r_\star}{2}}\pi M_p^2} \\ \left[1-(\mathcal{C}_E+1-\Sigma)\frac{r_\star}{16}+\frac{\mathcal{C}_E}{2\sqrt{2q}}\left(n_{\zeta,\star}-1+\left(1+3\sqrt{2q}-6q\right)\frac{r_\star}{8}\right)\right] & \text{for } \underline{\text{Case I}}, \\ \sqrt{\frac{r_\star}{8\alpha'}}\frac{|D|\left(1-\frac{qr_\star}{48c_S^2}\frac{|D|^2}{|C|^2}\right)^{1/4}(N_\star - N_{\text{end}})}{2c_S\,|C|\sqrt{\frac{3\Delta_{\zeta,\star}r_\star}{2}}\pi M_p^2} \\ \left[1-(\mathcal{C}_E+1-\Sigma)\frac{r_\star}{16}+\frac{\mathcal{C}_E}{2\sqrt{2q}}\left(n_{\zeta,\star}-1+\left(1+3\sqrt{2q}-6q\right)\frac{r_\star}{8}\right)\right] & \text{for } \underline{\text{Case II}}, \end{cases} \quad \underline{\text{for AV}}. \tag{5.187}$$

Further using the approximated form of the sound speed c_S the expression for the field excursion for AV can be rewritten as

$$\frac{\Delta T}{M_p} \approx \left\{\begin{array}{ll} \sqrt{\frac{r_\star}{8\alpha'}}\frac{\left(1-\frac{qr_\star}{48\left[1-\frac{(1-q)}{3q}\frac{r_\star}{8}\right]}\right)^{1/4}(N_\star - N_{\rm end})}{2\sqrt{1-\frac{(1-q)}{3q}\frac{r_\star}{8}}\sqrt{\frac{3\Delta_{\zeta,\star}r_\star}{2}\pi M_p^2}} & \\ \left[1-(\mathcal{C}_E+1-\Sigma)\frac{r_\star}{16}+\frac{\mathcal{C}_E}{2\sqrt{2q}}\left(n_{\zeta,\star}-1+\left(1+3\sqrt{2q}-6q\right)\frac{r_\star}{8}\right)\right] & \text{for }\underline{\text{Case I}}, \\ \sqrt{\frac{r_\star}{8\alpha'}}\frac{|D|\left(1-\frac{qr_\star}{48\left[1-\frac{(1-q)}{3q}\frac{r_\star}{8}\right]}\frac{|D|^2}{|C|^2}\right)^{1/4}(N_\star - N_{\rm end})}{2\sqrt{1-\frac{(1-q)}{3q}\frac{r_\star}{8}}\,|C|\sqrt{\frac{3\Delta_{\zeta,\star}r_\star}{2}\pi M_p^2}} & \\ \left[1-(\mathcal{C}_E+1-\Sigma)\frac{r_\star}{16}+\frac{\mathcal{C}_E}{2\sqrt{2q}}\left(n_{\zeta,\star}-1+\left(1+3\sqrt{2q}-6q\right)\frac{r_\star}{8}\right)\right] & \text{for }\underline{\text{Case II}}, \end{array}\right. \quad \underline{\text{for AV}}. \tag{5.188}$$

5.1.8 Semi-analytical study and cosmological parameter estimation

In this subsection our prime objective are:

- To compute various inflationary observables from variants of tachyonic single field potentials as mentioned earlier in this paper.
- To estimate the relevant cosmological parameters from the proposed models.
- Next to compare the effectiveness of all of these models in the light of recent Planck 2015 data alongwith other combined constraints.
- Finally to check the compatibility of all of these models with the CMB TT, TE and EE angular power spectra as observed by Planck 2015.

Model I: inverse cosh potential

For the single field case the first model of the tachyonic potential is given by

$$V(T) = \frac{\lambda}{\cosh\left(\frac{T}{T_0}\right)}, \tag{5.189}$$

where λ characterizes the scale of inflation and T_0 is the parameter of the model. In Fig. 1 we have depicted the symmetric behavior of the inverse cosh potential with respect to scaled field coordinate T/T_0 in dimensionless units around the origin fixed at $T/T_0 = 0$. In this case the tachyon field started rolling down from the top height of the potential and takes part in the inflationary dynamics.

Next using specified form of the potential the potential dependent slow-roll parameters are computed as

$$\bar{\epsilon}_V = \frac{1}{2g}\frac{\sinh^2\left(\frac{T}{T_0}\right)}{\cosh\left(\frac{T}{T_0}\right)}, \tag{5.190}$$

$$\bar{\eta}_V = \frac{1}{g}\left[\frac{\sinh^2\left(\frac{T}{T_0}\right)}{\cosh\left(\frac{T}{T_0}\right)} - \mathrm{sech}\left(\frac{T}{T_0}\right)\right], \tag{5.191}$$

$$\bar{\xi}^2_V = \frac{1}{g^2}\frac{\sinh^2\left(\frac{T}{T_0}\right)}{\cosh\left(\frac{T}{T_0}\right)}\left[\frac{\sinh^2\left(\frac{T}{T_0}\right)}{\cosh\left(\frac{T}{T_0}\right)} - 5\,\mathrm{sech}\left(\frac{T}{T_0}\right)\right], \tag{5.192}$$

$$\bar{\sigma}^3_V = \frac{1}{g^3}\frac{\sinh^2\left(\frac{T}{T_0}\right)}{\cosh\left(\frac{T}{T_0}\right)}\left[\frac{\sinh^2\left(\frac{T}{T_0}\right)}{\cosh\left(\frac{T}{T_0}\right)}\right. \times\left.\left\{\frac{\sinh^2\left(\frac{T}{T_0}\right)}{\cosh\left(\frac{T}{T_0}\right)} - 18\,\mathrm{sech}\left(\frac{T}{T_0}\right)\right\} + 5\,\mathrm{sech}^2\left(\frac{T}{T_0}\right)\right], \tag{5.193}$$

where the factor g is defined as

$$g = \frac{\alpha'\lambda T_0^2}{M_p^2} = \frac{M_s^4}{(2\pi)^3 g_s}\frac{\alpha' T_0^2}{M_p^2}. \tag{5.194}$$

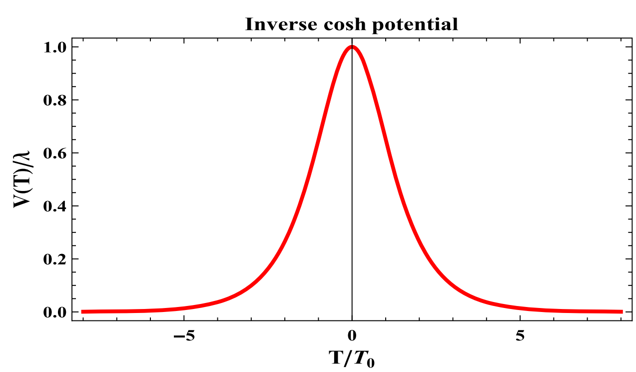

Fig. 1 Variation of the inverse cosh potential $V(T)/\lambda$ with field T/T_0 in dimensionless units

Next we compute the number of e-foldings from this model:

$$N(T)=\begin{cases} g\ \ln\left[\dfrac{\tanh\left(\frac{T_{\rm end}}{2T_0}\right)}{\tanh\left(\frac{T}{2T_0}\right)}\right], & \text{for}\quad q=1/2,\\ \sqrt{2q}\ g\ \ln\left[\dfrac{\tanh\left(\frac{T_{\rm end}}{2T_0}\right)}{\tanh\left(\frac{T}{2T_0}\right)}\right], & \text{for any arbitrary } q. \end{cases} \tag{5.195}$$

Further using the condition to end inflation:

$$\bar{\epsilon}_V(T_{\rm end})=1, \tag{5.196}$$
$$|\bar{\eta}_V(T_{\rm end})|=1, \tag{5.197}$$

we get the following field value at the end of inflation:

$$T_{\rm end}=T_0\ {\rm sech}^{-1}(g). \tag{5.198}$$

Next using $N=N_{\rm cmb}=N_\star$ and $T=T_{\rm cmb}=T_\star$ at the horizon crossing we get

$$T_\star=2T_0\times\begin{cases} \tanh^{-1}\left[\exp\left(-\dfrac{N_\star}{g}\right)\tanh\left(\dfrac{1}{2}{\rm sech}^{-1}(g)\right)\right], & \text{for}\quad q=1/2\\ \tanh^{-1}\left[\exp\left(-\dfrac{N_\star}{\sqrt{2q}g}\right)\tanh\left(\dfrac{1}{2}{\rm sech}^{-1}(g)\right)\right], & \text{for any arbitrary } q. \end{cases} \tag{5.199}$$

Consequently the field excursion can be computed as

$$|\Delta T|=T_0\times\begin{cases} \left|2\tanh^{-1}\left[\exp\left(-\dfrac{N_\star}{g}\right)\tanh\left(\dfrac{1}{2}{\rm sech}^{-1}(g)\right)\right]-{\rm sech}^{-1}(g)\right|, & \text{for}\quad q=1/2,\\ \left|2\tanh^{-1}\left[\exp\left(-\dfrac{N_\star}{\sqrt{2q}g}\right)\tanh\left(\dfrac{1}{2}{\rm sech}^{-1}(g)\right)\right]-{\rm sech}^{-1}(g)\right|, & \text{for any } q. \end{cases} \tag{5.200}$$

In the slow-roll regime of inflation the following approximations hold good:

$$\cosh\left(\frac{T_\star}{T_0}\right)\approx\begin{cases} \dfrac{1}{\tanh\left(\frac{N_\star}{g}\right)}, & \text{for}\quad q=1/2,\\ \dfrac{1}{\tanh\left(\frac{N_\star}{\sqrt{2q}g}\right)}, & \text{for any arbitrary } q, \end{cases} \tag{5.201}$$

$$\sinh\left(\frac{T_\star}{T_0}\right)\approx\begin{cases} \dfrac{1}{\sinh\left(\frac{N_\star}{g}\right)}, & \text{for}\quad q=1/2,\\ \dfrac{1}{\sinh\left(\frac{N_\star}{\sqrt{2q}g}\right)}, & \text{for any arbitrary } q. \end{cases} \tag{5.202}$$

Using Eqs. (5.201) and (5.202) in the definition of potential dependent slow-roll parameter finally we compute the following inflationary observables:

$$\Delta_{\zeta,\star}\approx\frac{g\lambda}{12\pi^2M_p^4}\times\begin{cases} \sinh^2\left(\dfrac{N_\star}{g}\right), & \text{for}\quad q=1/2,\\ 2q\ \sinh^2\left(\dfrac{N_\star}{\sqrt{2q}g}\right), & \text{for any arbitrary } q, \end{cases} \tag{5.203}$$

$$n_{\zeta,\star}-1\approx-\frac{2}{g}\times\begin{cases}\dfrac{1}{\tanh\left(\frac{N_\star}{g}\right)}, & \text{for} \quad q=1/2,\\[2ex] \dfrac{1}{\sqrt{2q}\tanh\left(\frac{N_\star}{\sqrt{2q}g}\right)}, & \text{for any arbitrary } q,\end{cases} \tag{5.204}$$

$$\alpha_{\zeta,\star}\approx-\frac{2}{g^2}\times\begin{cases}\dfrac{1}{\sinh^2\left(\frac{N_\star}{g}\right)}, & \text{for} \quad q=1/2,\\[2ex] \dfrac{1}{2q\sinh^2\left(\frac{N_\star}{\sqrt{2q}g}\right)}, & \text{for any arbitrary } q,\end{cases} \tag{5.205}$$

$$\kappa_{\zeta,\star}\approx-\frac{4}{g^3}\times\begin{cases}\dfrac{\cosh\left(\frac{N_\star}{g}\right)}{\sinh^3\left(\frac{N_\star}{g}\right)}, & \text{for} \quad q=1/2,\\[2ex] \dfrac{\cosh\left(\frac{N_\star}{2qg}\right)}{(2q)^{3/2}\sinh^3\left(\frac{N_\star}{\sqrt{2q}g}\right)}, & \text{for any arbitrary } q,\end{cases} \tag{5.206}$$

$$r_\star\approx\frac{16}{g}\times\begin{cases}\dfrac{1}{\sinh\left(\frac{2N_\star}{g}\right)}, & \text{for} \quad q=1/2,\\[2ex] \dfrac{1}{2q\sinh\left(\frac{2N_\star}{\sqrt{2q}g}\right)}, & \text{for any arbitrary } q.\end{cases} \tag{5.207}$$

For the inverse cosh potential we get the following consistency relations:

$$r_\star\approx 4(1-n_{\zeta,\star})\times\begin{cases}\dfrac{1}{\cosh^2\left(\frac{N_\star}{g}\right)}, & \text{for} \quad q=1/2,\\[2ex] \dfrac{\sqrt{2q}}{\cosh^2\left(\frac{N_\star}{2qg}\right)}, & \text{for any arbitrary } q,\end{cases} \tag{5.208}$$

$$\Delta_{\zeta,\star}\approx\frac{\lambda}{12\pi^2M_p^4(1-n_{\zeta,\star})}\times\begin{cases}\sinh\left(\dfrac{2N_\star}{g}\right), & \text{for} \quad q=1/2,\\[2ex] \sqrt{2q}\sinh\left(\dfrac{2N_\star}{\sqrt{2q}g}\right), & \text{for any arbitrary } q,\end{cases} \tag{5.209}$$

$$\Delta_{\zeta,\star}\approx\frac{2\lambda}{3\pi^2M_p^4r_\star}\times\begin{cases}\tanh\left(\dfrac{N_\star}{g}\right), & \text{for} \quad q=1/2,\\[2ex] \tanh\left(\dfrac{N_\star}{\sqrt{2q}g}\right), & \text{for any arbitrary } q,\end{cases} \tag{5.210}$$

$$\alpha_{\zeta,\star}\approx\frac{2}{g}\times\left(n_{\zeta,\star}-1\right)\times\begin{cases}\dfrac{1}{\sinh\left(\frac{2N_\star}{g}\right)}, & \text{for} \quad q=1/2,\\[2ex] \dfrac{1}{\sqrt{2q}\sinh\left(\frac{2N_\star}{\sqrt{2q}g}\right)}, & \text{for any arbitrary } q,\end{cases} \tag{5.211}$$

$$\kappa_{\zeta,\star}\approx\frac{2}{g^2}\times\left(n_{\zeta,\star}-1\right)\times\begin{cases}\dfrac{1}{\sinh^2\left(\frac{N_\star}{g}\right)}, & \text{for} \quad q=1/2,\\[2ex] \dfrac{1}{2q\sinh^2\left(\frac{N_\star}{\sqrt{2q}g}\right)}, & \text{for any arbitrary } q.\end{cases} \tag{5.212}$$

Let us now discuss the general constraints on the parameters of tachyonic string theory including the factor q and on the parameters appearing in the expression for the inverse cosh potential. In Fig. 2a, b, we have shown the behavior of the tensor-to-scalar ratio r with respect to the scalar spectral index n_ζ and the model parameter g for the inverse cosh potential respectively. In both the figures the purple and blue colored line represent the upper bound of the tensor-to-scalar ratio allowed by Planck+ BICEP2+Keck Array joint constraint and only Planck 2015 data respectively. For both the figures the red, green, brown, orange colored curves represent $q=1/2$, $q=1$, $q=3/2$ and $q=2$, respectively. The cyan color shaded region bounded by two vertical black colored lines in Fig. 2a represent the Planck 2σ allowed region and the rest of the light gray shaded region shows the 1σ allowed range, which is at present disfavored by the Planck 2015 data and Planck+ BICEP2+Keck Array joint constraint. The rest of the region is completely ruled out by the present observational constraints. From Fig. 2a, b, it is also observed that, within $50<N_\star<70$, the inverse cosh potential is favored only for the characteristic index $1/2<q<2$, by Planck 2015 data and Planck+ BICEP2+Keck Array joint analysis. Also in Fig. 2a for $q=1/2$, $q=1$, $q=3/2$ and $q=2$ we fix $N_\star/g\sim 0.8$. This implies that for $50<N_\star<70$, the prescribed window for g from the r–n_ζ plot is given by $63<g<88$. In Fig. 2b, we have explicitly shown that the in r–g plane the observationally favored lower bound for the characteristic index is $q\geq 1/2$. It is additionally important to note that, for $q>>2$, the tensor-to-scalar ratio computed from the model is negligibly small for the inverse cosh potential. This implies that if the inflationary tensor mode is detected close to its present upper bound on tensor-to-scalar ratio then all $q>>2$ possibilities for tachyonic inflation can be discarded for the inverse cosh

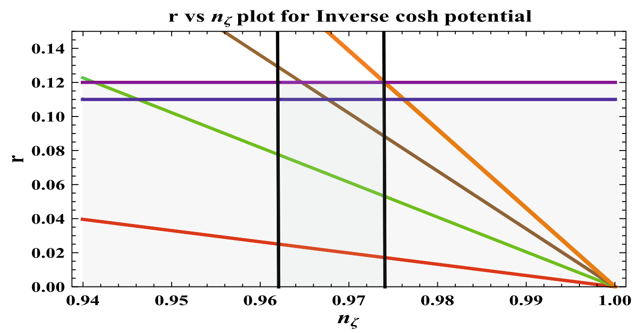

(a) r vs n_ζ.

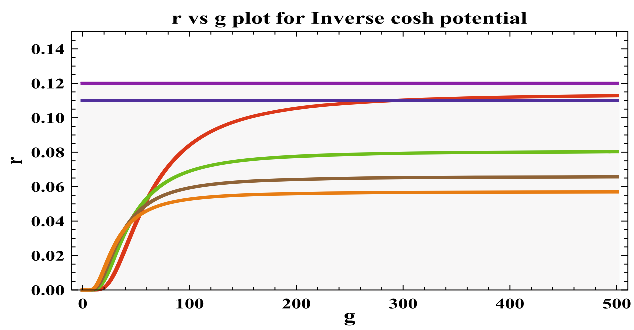

(b) r vs g.

Fig. 2 Behavior of the tensor-to-scalar ratio r with respect to **a** the scalar spectral index n_ζ and **b** the parameter g for the inverse cosh potential. The *purple* and *blue colored line* represent the *upper* bound of tensor-to-scalar ratio allowed by Planck+ BICEP2+Keck Array joint constraint and only Planck 2015 data respectively. For both the figures the *red*, *green*, *brown*, *orange colored curves* represent $q = 1/2, q = 1$, $q = 3/2$ and $q = 2$ respectively. The *cyan color shaded* region bounded by two *vertical black colored lines* in **a** represents the Planck 2σ allowed region and the rest of the *light gray shaded* region shows the 1σ allowed range, which is at present disfavored by the Planck data and Planck+ BICEP2+Keck Array joint constraint. From **a** and **b**, it is also observed that, within $50 < N_\star < 70$, the inverse cosh potential is favored only for the characteristic index $1/2 < q < 2$, by Planck 2015 data and Planck+ BICEP2+Keck Array joint analysis. In **b**, we have explicitly shown that in the r–g plane the observationally favored lower bound for the characteristic index is $q \geq 1/2$

potential. On the contrary, if inflationary tensor modes are never detected by any of the future observational probes then the $q >> 2$ possibilities for tachyonic inflation in the case of the inverse cosh potential are highly prominent. Also it is important to mention that, in Fig. 2b within the window $0 < g < 100$, if we take a smaller value of g, then the inflationary tensor-to-scalar ratio also gradually decreases. To analyze the results more clearly let us describe the cosmological features from Fig. 2a in detail. Let us first start with the $q = 1/2$ situation, in which the 2σ constraint on the scalar spectral tilt is satisfied within the window of tensor-to-scalar ratio, $0.015 < r < 0.025$ for $50 < N_\star < 70$. Next for the $q = 1$ case, the same constraint is satisfied within the window of the tensor-to-scalar ratio, $0.050 < r < 0.075$ for $50 < N_\star < 70$. Further for the $q = 3/2$ case, the same constraint on scalar spectral tilt is satisfied within the window of the tensor-to-scalar ratio, $0.090 < r < 0.12$ for $50 < N_\star < 70$. Finally, for the $q = 2$ situation, the value for the tensor-to-scalar ratio is $r < 0.12$, which is tightly constrained from the upper bound of the spectral tilt from Planck 2015 observational data.

In Fig. 3a–c, we have depicted the behavior of the scalar power spectrum Δ_ζ vs. the stringy parameter g, scalar spectral tilt n_ζ vs. the stringy parameter g and scalar power spectrum Δ_ζ vs. scalar spectral index n_ζ for the inverse cosh potential respectively. It is important to note that, for all of the figures the red, green, brown, orange colored curves represent $q = 1/2$, $q = 1$, $q = 3/2$ and $q = 2$ respectively. The purple and blue colored line represent the upper and lower bound allowed by WMAP+Planck 2015 data respectively. The cyan color shaded region bounded by two vertical black colored lines represent the Planck 2σ allowed region and the rest of the light gray shaded region is the 1σ region, which is presently disfavored by the joint Planck+WMAP constraints. The rest of the region is completely ruled out by the present observational constraints. From Fig. 3a it is clearly observed that the observational constraints on the amplitude of the scalar mode fluctuations satisfy within the window $80 < g < 100$. For $g > 100$ the corresponding amplitude falls down in a non-trivial fashion by following the exact functional form as stated in Eq. (5.203). Next using the behavior as shown in Fig. 3b, the lower bound on the stringy parameter g is constrained by $g > 50$ by using the non-trivial relationship as stated in Eq. (5.204). But at this lower bound of the parameter g the amplitude of the scalar power spectrum is larger compared to the present observational constraints. This implies that, to satisfy both the constraints from the amplitude of the scalar power spectrum and its spectral tilt, within 2σ CL the constrained numerical value of the stringy parameter is lying within the window $80 < g < 100$. Also in Fig. 3c for $q = 1/2, q = 1, q = 3/2$ and $q = 2$ we fix $N_\star/g \sim 0.8$, which further implies that for $50 < N_\star < 70$, the prescribed window for g from Δ_ζ–n_ζ plot is given by $63 < g < 88$. If we additionally impose the constraint from the upper bound on tensor-to-scalar ratio then also the allowed parameter range is lying within a similar window, i.e., $88 < g < 100$.

In Fig. 4a, b, we have shown the behavior of the running of the scalar spectral tilt α_ζ and running of the running of the scalar spectral tilt κ_ζ with respect to the scalar spectral index n_ζ for the inverse cosh potential with $g = 88$, respectively. For both the figures the red, green, brown, orange colored curves represent $q = 1/2, q = 1, q = 3/2$ and $q = 2$, respectively. The cyan color shaded region bounded by two vertical black colored lines in both the plots represent the Planck 2σ allowed region and the rest of the light gray shaded region shows the 1σ allowed range, which is at present disfavored by the Planck data and Planck+ BICEP2+Keck Array joint

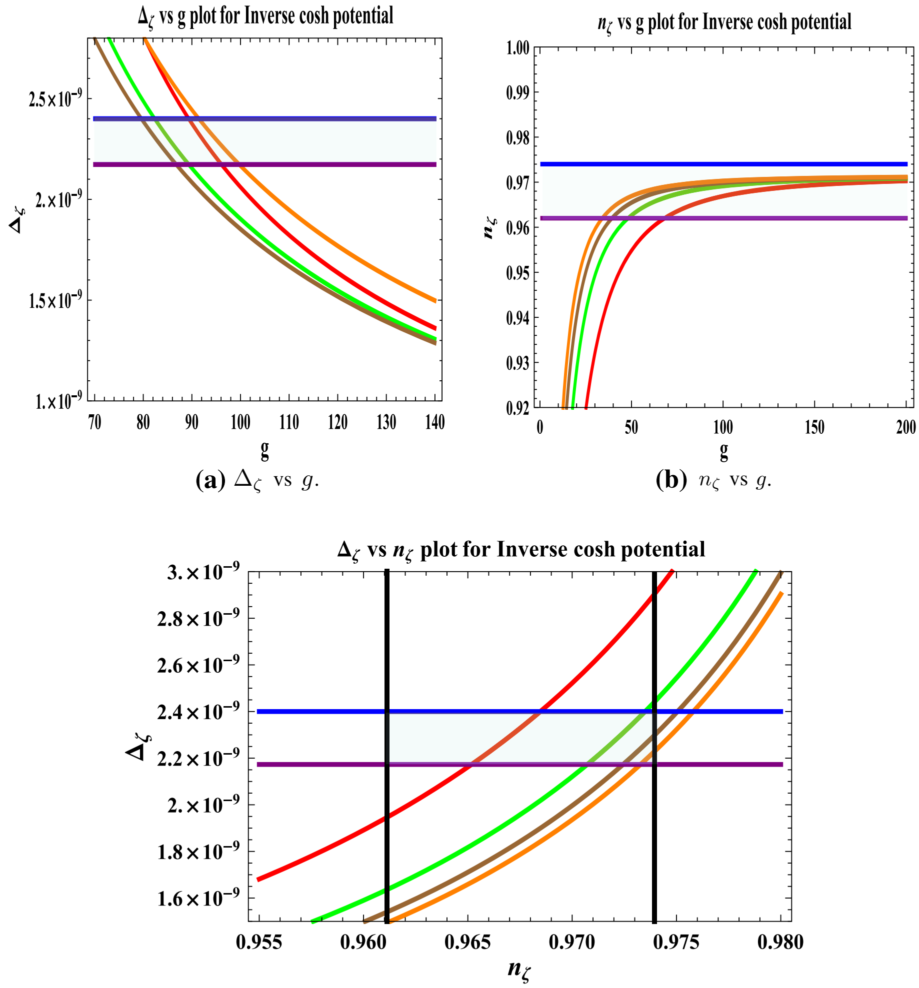

(a) Δ_ζ vs g. **(b)** n_ζ vs g. **(c)** Δ_ζ vs n_ζ.

Fig. 3 Variation of the **a** scalar power spectrum Δ_ζ vs. scalar spectral index n_ζ, **b** scalar power spectrum Δ_ζ vs. the stringy parameter g and **c** scalar spectral tilt n_ζ vs. the stringy parameter g. The *purple* and *blue colored line* represent the *upper* and *lower* bound allowed by WMAP+Planck 2015 data respectively. The *green dotted* region bounded by two *vertical black colored lines* represent the Planck 2σ allowed region and the rest of the *light gray shaded* region is disfavored by the Planck+WMAP constraint

constraint. From both of these figures, it is also observed that, within $50 < N_\star < 70$, the inverse cosh potential is favored for the characteristic index $1/2 < q < 2$, by Planck 2015 data and Planck+ BICEP2+Keck Array joint analysis. From Fig. 4a, b, it is observed that within the 2σ observed range of the scalar spectral tilt n_ζ, as the value of the characteristic parameter q increases, the value of the running α_ζ and running of the running κ_ζ decreases for the inverse cosh potential. It is also important to note that for $1/2 < q < 2$, the numerical value of the running $\alpha_\zeta \sim \mathcal{O}(-10^{-4})$ and running of the running $\kappa_\zeta \sim \mathcal{O}(-10^{-6})$, which are perfectly consistent with the 1.5σ constraints on running and running of the running as obtained from Planck 2015 data.

Model II: logarithmic potential

For single field case the second model of tachyonic potential is given by

$$V(T) = \lambda \left\{ \left(\frac{T}{T_0}\right)^2 \left[\ln\left(\frac{T}{T_0}\right)\right]^2 + 1 \right\}, \tag{5.213}$$

where λ characterize the scale of inflation and T_0 is the parameter of the model. In Fig. 5 we have depicted the behavior of the logarithmic potential with respect to scaled field coordinate T/T_0 in dimensionless units. In this case the tachyon field started rolling down from the top height of the potential either from the left or right hand side and takes part in the inflationary dynamics.

Next using specified form of the potential the potential dependent slow-roll parameters are computed as

$$\bar{\epsilon}_V = \frac{1}{2g} \frac{4\left(\frac{T}{T_0}\right)^2 \ln^2\left(\frac{T}{T_0}\right)\left[1+\ln\left(\frac{T}{T_0}\right)\right]^2}{\left[1+\left(\frac{T}{T_0}\right)^2 \ln^2\left(\frac{T}{T_0}\right)\right]^3}, \tag{5.214}$$

$$\bar{\eta}_V = \frac{1}{g} \frac{2\left\{\ln\left(\frac{T}{T_0}\right)+\left[1+\ln\left(\frac{T}{T_0}\right)\right]^2\right\}}{\left[1+\left(\frac{T}{T_0}\right)^2 \ln^2\left(\frac{T}{T_0}\right)\right]^2}, \tag{5.215}$$

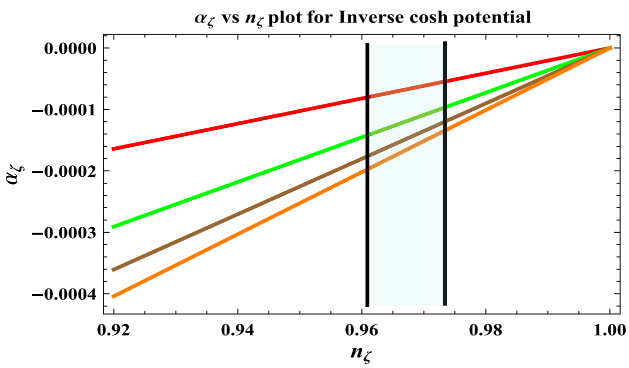

(a) α_ζ vs n_ζ.

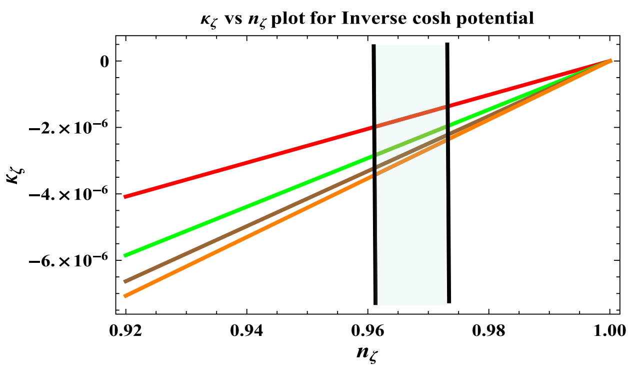

(b) κ_ζ vs n_ζ.

Fig. 4 Behavior of the **a** running of the scalar spectral tilt α_ζ and **b** running of the running of the scalar spectral tilt κ_ζ with respect to the scalar spectral index n_ζ for the inverse cosh potential with $g = 88$. For both figures the *red*, *green*, *brown*, *orange colored curves* represent $q = 1/2$, $q = 1$, $q = 3/2$ and $q = 2$ respectively. The *cyan color shaded* region bounded by two *vertical black colored lines* in **a** represent the Planck 2σ allowed region and the rest of the *light gray shaded* region shows the 1σ allowed range, which is at present disfavored by the Planck data and Planck+ BICEP2+Keck Array joint constraint. From **a** and **b**, it is also observed that, within $50 < N_\star < 70$, the inverse cosh potential is favored for the characteristic index $1/2 < q < 2$, by Planck 2015 data and Planck+ BICEP2+Keck Array joint analysis

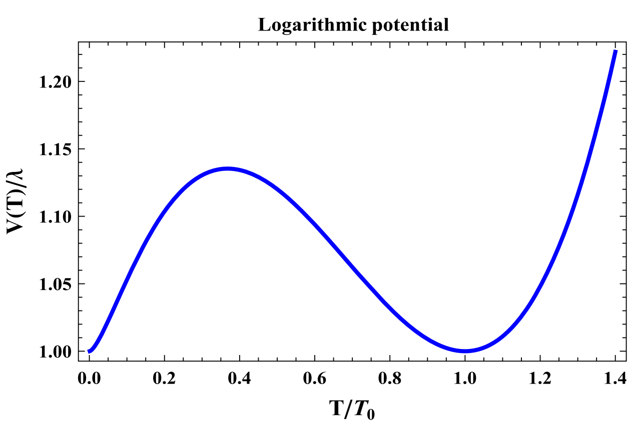

Fig. 5 Variation of the logarithmic potential $V(T)/\lambda$ with field T/T_0 in dimensionless units

$$\bar{\xi}_V^2 = \frac{1}{g^2}\frac{4\ln\left(\frac{T}{T_0}\right)\left[1+\ln\left(\frac{T}{T_0}\right)\right]\left[3+2\ln\left(\frac{T}{T_0}\right)\right]}{\left[1+\left(\frac{T}{T_0}\right)^2\ln^2\left(\frac{T}{T_0}\right)\right]^4}, \quad (5.216)$$

$$\bar{\sigma}_V^3 = -\frac{1}{g^3}\frac{4\ln^2\left(\frac{T}{T_0}\right)\left[1+\ln\left(\frac{T}{T_0}\right)\right]^2\left[1+2\ln\left(\frac{T}{T_0}\right)\right]}{\left[1+\left(\frac{T}{T_0}\right)^2\ln^2\left(\frac{T}{T_0}\right)\right]^6}, \quad (5.217)$$

where the factor g is defined as

$$g = \frac{\alpha'\lambda T_0^2}{M_p^2} = \frac{M_s^4}{(2\pi)^3 g_s}\frac{\alpha' T_0^2}{M_p^2}. \quad (5.218)$$

Next we compute the number of e-foldings from this model:

$$N(T) = \begin{cases} \frac{g}{2}\left\{-\frac{2\mathrm{Ei}\left[2\left(\ln\left(\frac{T}{T_0}\right)+1\right)\right]}{e^2} - \frac{\mathrm{Ei}\left[4\left(\ln\left(\frac{T}{T_0}\right)+1\right)\right]}{e^4} \right. \\ +\left(\frac{T}{T_0}\right)^4\left[\frac{11}{32}-\frac{3}{8}\ln\left(\frac{T}{T_0}\right)+\frac{1}{4}\ln^2\left(\frac{T}{T_0}\right)\right] \\ \left.+\left(\frac{T}{T_0}\right)^2+\ln\left(\frac{\ln\left(\frac{T}{T_0}\right)}{1+\ln\left(\frac{T}{T_0}\right)}\right)\right\}_{T_{\mathrm{end}}}^{T}, & \text{for } q=1/2, \\ \sqrt{2q}\,\frac{g}{2}\left\{-\frac{2\mathrm{Ei}\left[2\left(\ln\left(\frac{T}{T_0}\right)+1\right)\right]}{e^2}\right. \\ -\frac{\mathrm{Ei}\left[4\left(\ln\left(\frac{T}{T_0}\right)+1\right)\right]}{e^4} \\ +\left(\frac{T}{T_0}\right)^4\left[\frac{11}{32}-\frac{3}{8}\ln\left(\frac{T}{T_0}\right)+\frac{1}{4}\ln^2\left(\frac{T}{T_0}\right)\right] \\ \left.+\left(\frac{T}{T_0}\right)^2+\ln\left(\frac{\ln\left(\frac{T}{T_0}\right)}{1+\ln\left(\frac{T}{T_0}\right)}\right)\right\}_{T_{\mathrm{end}}}^{T}, & \text{for any arbitrary } q. \end{cases} \quad (5.219)$$

Further using the condition to end inflation:

$$\bar{\epsilon}_V(T_{\mathrm{end}}) = 1, \quad (5.220)$$

$$|\bar{\eta}_V(T_{\mathrm{end}})| = 1, \quad (5.221)$$

we get the following transcendental equation:

$$\left[1+\ln\left(\frac{T_{\mathrm{end}}}{T_0}\right)\right]^2\left\{\left(\frac{T_{\mathrm{end}}}{T_0}\right)^2\ln^2\left(\frac{T_{\mathrm{end}}}{T_0}\right)-1\right\} = \ln\left(\frac{T_{\mathrm{end}}}{T_0}\right), \quad (5.222)$$

from which we get the following sets of real solutions for the field value:

$$T_{\mathrm{end}} = (0.07\ T_0,\ 0.69\ T_0,\ 1.83\ T_0)\,. \quad (5.223)$$

Then using this result we need to numerically solve the transcendental equation of $T_\star$ which involves $N_\star$ explicitly. However, in the slow-roll regime of inflation we get the following simplified expression for the field value $T_\star$ in terms of $N_\star$, T_{end} and T_0:

$$T_\star \approx T_0 \times \begin{cases} \sqrt{\frac{2N_\star}{g} + \left(\frac{T_{\rm end}}{T_0}\right)^2}, & \text{for} \quad q = 1/2, \\ \sqrt{\frac{2N_\star}{\sqrt{2q}g} + \left(\frac{T_{\rm end}}{T_0}\right)^2}, & \text{for any arbitrary } q, \end{cases} \tag{5.224}$$

where we have explicitly used the fact that in the slow-roll regime the quadratic term gives the dominant contribution in $N_\star$.

Also the field excursion can be computed as

$$|\Delta T| = T_0 \times \begin{cases} \left|\sqrt{\frac{2N_\star}{g} + c^2} - c\right|, & \text{for} \quad q = 1/2, \\ \left|\sqrt{\frac{2N_\star}{\sqrt{2q}g} + c^2} - c\right|, & \text{for any arbitrary } q, \end{cases} \tag{5.225}$$

where $c = 0.07, 0.69, 1.83$. During the numerical estimation we have taken $c = 0.07$ as it is compatible with the observational constraints from Planck 2015 data.

Finally using the previously mentioned definition of potential dependent slow-roll parameter we compute the following inflationary observables:

$$\Delta_{\zeta,\star} \approx \frac{g\lambda}{48\pi^2 M_p^4} \times \begin{cases} \dfrac{\left[1 + \frac{1}{4}\left(\frac{2N_\star}{g} + \left(\frac{T_{\rm end}}{T_0}\right)^2\right)\ln^2\left(\frac{2N_\star}{g} + \left(\frac{T_{\rm end}}{T_0}\right)^2\right)\right]^4}{\left(\frac{2N_\star}{g} + \left(\frac{T_{\rm end}}{T_0}\right)^2\right)\ln^2\left(\frac{2N_\star}{g} + \left(\frac{T_{\rm end}}{T_0}\right)^2\right)\left[1 + \frac{1}{2}\ln\left(\frac{2N_\star}{g} + \left(\frac{T_{\rm end}}{T_0}\right)^2\right)\right]^2}, & \text{for} \quad q = 1/2, \\ \dfrac{2q\left[1 + \frac{1}{4}\left(\frac{2N_\star}{\sqrt{2q}g} + \left(\frac{T_{\rm end}}{T_0}\right)^2\right)\ln^2\left(\frac{2N_\star}{\sqrt{2q}g} + \left(\frac{T_{\rm end}}{T_0}\right)^2\right)\right]^4}{\left(\frac{2N_\star}{\sqrt{2q}g} + \left(\frac{T_{\rm end}}{T_0}\right)^2\right)\ln^2\left(\frac{2N_\star}{\sqrt{2q}g} + \left(\frac{T_{\rm end}}{T_0}\right)^2\right)\left[1 + \frac{1}{2}\ln\left(\frac{2N_\star}{\sqrt{2q}g} + \left(\frac{T_{\rm end}}{T_0}\right)^2\right)\right]^2}. & \text{for any } q \end{cases} \tag{5.226}$$

$$n_{\zeta,\star} - 1 \approx \frac{4}{g} \times \begin{cases} \dfrac{\vartheta_\star}{\left[1 + \frac{1}{4}\left(\frac{2N_\star}{g} + \left(\frac{T_{\rm end}}{T_0}\right)^2\right)\ln^2\left(\frac{2N_\star}{g} + \left(\frac{T_{\rm end}}{T_0}\right)^2\right)\right]^3}, & \text{for} \quad q = 1/2, \\ \dfrac{\vartheta_\star}{\left[1 + \frac{1}{4}\left(\frac{2N_\star}{\sqrt{2q}g} + \left(\frac{T_{\rm end}}{T_0}\right)^2\right)\ln^2\left(\frac{2N_\star}{\sqrt{2q}g} + \left(\frac{T_{\rm end}}{T_0}\right)^2\right)\right]^3}. & \text{for any } q \end{cases} \tag{5.227}$$

$$r_\star \approx \frac{32}{g} \times \begin{cases} \dfrac{\left(\frac{2N_\star}{g} + \left(\frac{T_{\rm end}}{T_0}\right)^2\right)\ln^2\left(\frac{2N_\star}{g} + \left(\frac{T_{\rm end}}{T_0}\right)^2\right)\left[1 + \frac{1}{2}\ln\left(\frac{2N_\star}{g} + \left(\frac{T_{\rm end}}{T_0}\right)^2\right)\right]^2}{\left[1 + \frac{1}{4}\left(\frac{2N_\star}{g} + \left(\frac{T_{\rm end}}{T_0}\right)^2\right)\ln^2\left(\frac{2N_\star}{g} + \left(\frac{T_{\rm end}}{T_0}\right)^2\right)\right]^3}, & \text{for} \quad q = 1/2, \\ \dfrac{1}{2q}\dfrac{\left(\frac{2N_\star}{\sqrt{2q}g} + \left(\frac{T_{\rm end}}{T_0}\right)^2\right)\ln^2\left(\frac{2N_\star}{\sqrt{2q}g} + \left(\frac{T_{\rm end}}{T_0}\right)^2\right)\left[1 + \frac{1}{2}\ln\left(\frac{2N_\star}{\sqrt{2q}g} + \left(\frac{T_{\rm end}}{T_0}\right)^2\right)\right]^2}{\left[1 + \frac{1}{4}\left(\frac{2N_\star}{\sqrt{2q}g} + \left(\frac{T_{\rm end}}{T_0}\right)^2\right)\ln^2\left(\frac{2N_\star}{\sqrt{2q}g} + \left(\frac{T_{\rm end}}{T_0}\right)^2\right)\right]^3}, & \text{for any arbitrary } q, \end{cases} \tag{5.228}$$

where

$$\vartheta_\star \approx \begin{cases} \left[1-\frac{3}{4}\left(\frac{2N_\star}{g}+\left(\frac{T_{\rm end}}{T_0}\right)^2\right)\ln^2\left(\frac{2N_\star}{g}+\left(\frac{T_{\rm end}}{T_0}\right)^2\right)\right]\left[1+\frac{1}{2}\ln\left(\frac{2N_\star}{g}+\left(\frac{T_{\rm end}}{T_0}\right)^2\right)\right]^2 \\ \quad +\frac{1}{2}\ln\left(\frac{2N_\star}{g}+\left(\frac{T_{\rm end}}{T_0}\right)^2\right)\left[1+\frac{1}{4}\left(\frac{2N_\star}{g}+\left(\frac{T_{\rm end}}{T_0}\right)^2\right)\ln^2\left(\frac{2N_\star}{g}+\left(\frac{T_{\rm end}}{T_0}\right)^2\right)\right], & \text{for } q=1/2, \\ \left[1-\frac{G}{4}\left(\frac{N_\star}{qg}\right)\ln^2\left(\frac{2N_\star}{\sqrt{2q}g}+\left(\frac{T_{\rm end}}{T_0}\right)^2\right)\right]\left[1+\frac{1}{2}\ln\left(\frac{2N_\star}{\sqrt{2q}g}+\left(\frac{T_{\rm end}}{T_0}\right)^2\right)\right]^2 \\ \quad +\frac{P}{2}\ln\left(\frac{2N_\star}{\sqrt{2q}g}+\left(\frac{T_{\rm end}}{T_0}\right)^2\right)\left[1+\frac{1}{4}\left(\frac{2N_\star}{\sqrt{2q}g}+\left(\frac{T_{\rm end}}{T_0}\right)^2\right)\ln^2\left(\frac{2N_\star}{\sqrt{2q}g}+\left(\frac{T_{\rm end}}{T_0}\right)^2\right)\right], & \text{for any arbitrary } q. \end{cases} \tag{5.229}$$

Here the constants G and P are defined as

$$G=\frac{1}{2q}\left(1+2\sqrt{2q}\right), \tag{5.230}$$

$$P=\frac{1}{\sqrt{2q}}. \tag{5.231}$$

For the inverse cosh potential we get the following consistency relations:

$$r_\star \approx 8(1-n_{\zeta,\star})\times \begin{cases} \frac{\left(\frac{2N_\star}{g}+\left(\frac{T_{\rm end}}{T_0}\right)^2\right)\ln^2\left(\frac{2N_\star}{g}+\left(\frac{T_{\rm end}}{T_0}\right)^2\right)\left[1+\frac{1}{2}\ln\left(\frac{2N_\star}{g}+\left(\frac{T_{\rm end}}{T_0}\right)^2\right)\right]^2}{|\vartheta_\star|}, & \text{for } q=1/2, \\ \frac{\left(\frac{2N_\star}{\sqrt{2q}g}+\left(\frac{T_{\rm end}}{T_0}\right)^2\right)\ln^2\left(\frac{2N_\star}{\sqrt{2q}g}+\left(\frac{T_{\rm end}}{T_0}\right)^2\right)\left[1+\frac{1}{2}\ln\left(\frac{2N_\star}{\sqrt{2q}g}+\left(\frac{T_{\rm end}}{T_0}\right)^2\right)\right]^2}{2q|\vartheta_\star|}, & \text{for any } q \end{cases} \tag{5.232}$$

$$\Delta_{\zeta,\star} \approx \frac{\lambda}{12\pi^2 M_p^4}\times \begin{cases} \frac{|\vartheta_\star|}{(n_{\zeta,\star}-1)\left(\frac{2N_\star}{g}+\left(\frac{T_{\rm end}}{T_0}\right)^2\right)\ln^2\left(\frac{2N_\star}{g}+\left(\frac{T_{\rm end}}{T_0}\right)^2\right)\left[1+\frac{1}{2}\ln\left(\frac{2N_\star}{g}+\left(\frac{T_{\rm end}}{T_0}\right)^2\right)\right]^2}, & \text{for } q=1/2, \\ \frac{2q|\vartheta_\star|}{(n_{\zeta,\star}-1)\left(\frac{2N_\star}{\sqrt{2q}g}+\left(\frac{T_{\rm end}}{T_0}\right)^2\right)\ln^2\left(\frac{2N_\star}{\sqrt{2q}g}+\left(\frac{T_{\rm end}}{T_0}\right)^2\right)\left[1+\frac{1}{2}\ln\left(\frac{2N_\star}{\sqrt{2q}g}+\left(\frac{T_{\rm end}}{T_0}\right)^2\right)\right]^2}. & \text{for any } q \end{cases} \tag{5.233}$$

$$\Delta_{\zeta,\star} \approx \frac{2\lambda}{3\pi^2 M_p^4 r_\star}\times \begin{cases} \left[1+\frac{1}{4}\left(\frac{2N_\star}{g}+\left(\frac{T_{\rm end}}{T_0}\right)^2\right)\ln^2\left(\frac{2N_\star}{g}+\left(\frac{T_{\rm end}}{T_0}\right)^2\right)\right], & \text{for } q=1/2, \\ \left[1+\frac{1}{4}\left(\frac{2N_\star}{\sqrt{2q}g}+\left(\frac{T_{\rm end}}{T_0}\right)^2\right)\ln^2\left(\frac{2N_\star}{\sqrt{2q}g}+\left(\frac{T_{\rm end}}{T_0}\right)^2\right)\right], & \text{for any arbitrary } q. \end{cases} \tag{5.234}$$

Let us now discuss the general constraints on the parameters of tachyonic string theory including the factor q and on the paramters appearing in the expression for the logarithmic potential. In Fig. 6a, b, we have shown the behavior of the tensor-to-scalar ratio r with respect to the scalar spectral index n_ζ and the model parameter g for the logarithmic potential respectively. In both the figures the purple and blue colored line represent the upper bound of the tensor-to-scalar ratio allowed by Planck+ BICEP2+Keck Array joint constraint and only Planck 2015 data respectively. For both the figures the red, green, brown, orange colored curves represent $q=1/2$, $q=1$, $q=3/2$ and $q=2$, respectively. The cyan color shaded region bounded by two vertical black colored lines in Fig. 6a represent the Planck 2σ allowed region and the rest of the light gray shaded region shows the 1σ allowed range, which is at present disfavored by the Planck 2015 data and Planck+ BICEP2+Keck Array joint constraint. The rest of the region is completely ruled out by the present observational constraints. From Fig. 6a, b, it is also observed that, within $50<N_\star<70$, the logarithmic potential is favored for the characteristic index $1/2<q<2$, by Planck 2015 data and Planck+ BICEP2+Keck Array joint analysis. Also in Fig. 6a for $q=1/2$, $q=1$, $q=3/2$ and $q=2$ we fix $N_\star/g\sim 0.7$. This implies that for $50<N_\star<70$, the prescribed window for g from r–n_ζ plot is given by $71.4<g<100$. In Fig. 6b, we have explicitly shown that the in $r-g$ plane the observationally favored lower bound for

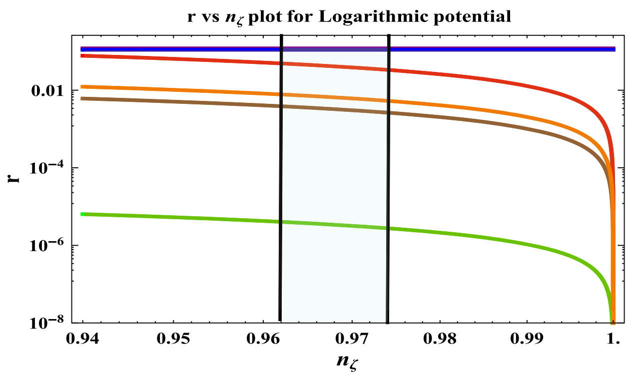

(a) r vs n_ζ.

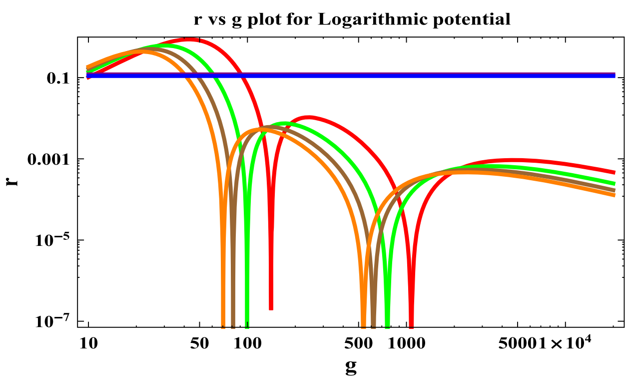

(b) r vs g.

Fig. 6 Behavior of the tensor-to-scalar ratio r with respect to **a** the scalar spectral index n_ζ and **b** the parameter g for the logarithmic potential. The *purple and blue colored line* represent the *upper* bound of tensor-to-scalar ratio allowed by Planck+ BICEP2+Keck Array joint constraint and only Planck 2015 data respectively. For both figures the *red*, *green*, *brown*, *orange colored curves* represent $q = 1/2$, $q = 1$, $q = 3/2$ and $q = 2$, respectively. The *cyan color shaded* region bounded by two *vertical black colored lines* in **a** represent the Planck 2σ allowed region and the rest of the *light gray shaded* region shows the 1σ allowed range, which is at present disfavored by the Planck data and Planck+ BICEP2+Keck Array joint constraint. From **a** and **b**, it is also observed that, within $50 < N_\star < 70$, the logarithmic potential is favored for the characteristic index $1/2 < q < 2$, by Planck 2015 data and Planck+ BICEP2+Keck Array joint analysis. In **a**, we have explicitly shown that in the r–n_ζ plane the observationally favored lower bound for the characteristic index is $q \geq 1/2$

the characteristic index is $q \geq 1/2$. It is additionally important to note that, for $q >> 2$, the tensor-to-scalar ratio computed from the model is negligibly small for the logarithmic potential. This implies that if the inflationary tensor mode is detected close to its present upper bound on tensor-to-scalar ratio then all $q >> 2$ possibilities for tachyonic inflation can be discarded for the logarithmic potential. On the contrary, if inflationary tensor modes are never detected by any of the future observational probes then the $q >> 2$ possibilities for tachyonic inflation in the case of a logarithmic potential are highly prominent. Also it is important to mention that, in Fig. 6b within the window $40 < g < 150$, if we increase the value of g, then the inflationary tensor-to-scalar ratio also gradually decreases. After that within $71 < g < 300$ the value of the tensor-to-scalar ratio slightly increases and again it falls down to lower value within the the interval $120 < g < 1000$.

In Fig. 7a–c, we have depicted the behavior of the scalar power spectrum Δ_ζ vs. the stringy parameter g, scalar spectral tilt n_ζ vs. the stringy parameter g and scalar power spectrum Δ_ζ vs. scalar spectral index n_ζ for the logarithmic potential respectively. It is important to note that, for all of the figures the red, green, brown, orange colored curves represent $q = 1/2$, $q = 1$, $q = 3/2$ and $q = 2$ respectively. The purple and blue colored line represent the upper and lower bound allowed by WMAP+Planck 2015 data respectively. The cyan color shaded region bounded by two vertical black colored lines represent the Planck 2σ allowed region and the rest of the light gray shaded region is the 1σ region, which is presently disfavored by the joint Planck+WMAP constraints. The rest of the region is completely ruled out by the present observational constraints. From Fig. 7a it is clearly observed that the observational constraints on the amplitude of the scalar mode fluctuations satisfy within the window $g = (26, 90)$ for $q = 1/2$, $g = (20, 60)$ for $q = 1$, $g = (18, 48)$ for $q = 3/2$ and $g = (16, 38)$ for $q = 2$. For all the cases outside the mentioned window for the parameter g the corresponding amplitude gradually increases in a non-trivial fashion by following the exact functional form as stated in Eq. (5.226). Next using the behavior as shown in Fig. 7b, the lower bound on the stringy parameter g is constrained by $g > 45$ by using the non-trivial relationship as stated in Eq. (5.227) for $q = 2$. Similarly by observing the Fig. 7b one can find the other lower bounds on g from different value of q. But at this lower bound of the parameter g the amplitude of the scalar power spectrum is very larger compared to the present observational constraints. This implies that, to satisfy both the constraints from the amplitude of the scalar power spectrum and its spectral tilt within 2σ CL the constrained numerical value of the stringy parameter is lying within the window $48 < g < 90$ in which $q = 2$ case is slightly disfavored compared to the other lower values of q studied in the present context. Also in Fig. 7c for $q = 1/2$, and $q = 1$ we fix $N_\star/g \sim 0.7$, which further implies that for $50 < N_\star < 70$, the prescribed window for g from the Δ_ζ–n_ζ plot is given by $71.4 < g < 100$. If we additionally impose the constraint from the upper bound on tensor-to-scalar ratio then also the allowed parameter range is lying within a similar window, i.e., $71.4 < g < 90$ and combining all the constraints the allowed value of the characteristic index is lying within $1/2 < q < 1$. However, $q = 1/2$ is tightly constrained as depicted in Fig. 7c.

Model III: exponential potential Type I

For the single field case the third model of the tachyonic potential is given by

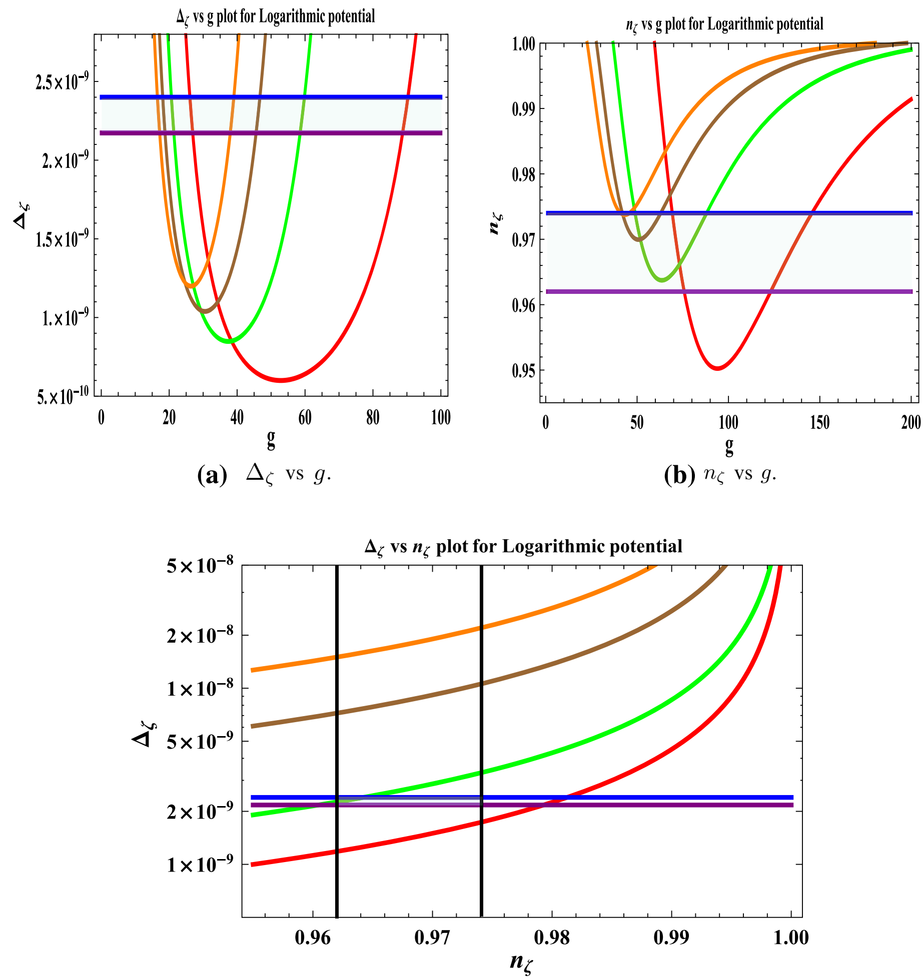

(a) Δ_ζ vs g.

(b) n_ζ vs g.

(c) Δ_ζ vs n_ζ.

Fig. 7 Variation of the **a** scalar power spectrum Δ_ζ vs. scalar spectral index n_ζ, **b** scalar power spectrum Δ_ζ vs. the stringy parameter g and **c** scalar spectral tilt n_ζ vs. the stringy parameter g. The *purple and blue colored line* represent the *upper* and *lower* bound allowed by WMAP+Planck 2015 data respectively. The *green dotted* region bounded by two *vertical black colored lines* represent the Planck 2σ allowed region and the rest of the *light gray shaded* region is disfavored by the Planck+WMAP constraint

$$V(T) = \lambda \exp\left(-\frac{T}{T_0}\right), \tag{5.235}$$

where λ characterizes the scale of inflation and T_0 is the parameter of the model. In Fig. 8 we have depicted the behavior of the exponential potential Type-I with respect to the scaled field coordinate T/T_0 in dimensionless units. In this case the tachyon field started rolling down from the top height of the potential from the left hand side and takes part in the inflationary dynamics.

Next using specified form of the potential the potential dependent slow-roll parameters are computed as

$$\bar{\epsilon}_V = \frac{1}{2g}\exp\left(\frac{T}{T_0}\right), \tag{5.236}$$

$$\bar{\eta}_V = \frac{1}{g}\exp\left(\frac{T}{T_0}\right), \tag{5.237}$$

$$\bar{\xi}_V^2 = \frac{1}{g^2}\exp\left(\frac{2T}{T_0}\right), \tag{5.238}$$

$$\bar{\sigma}_V^3 = \frac{1}{g^3}\exp\left(\frac{3T}{T_0}\right), \tag{5.239}$$

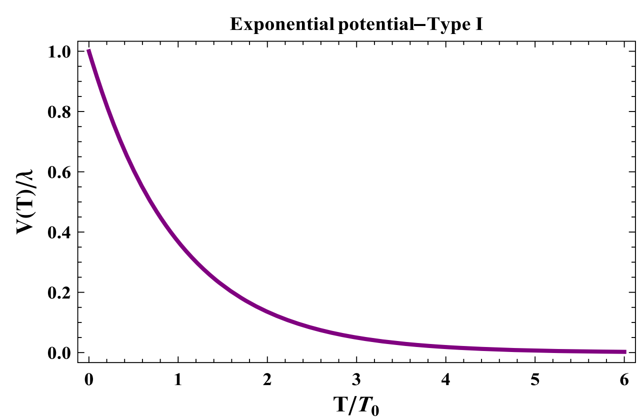

Fig. 8 Variation of the exponential potential Type-I $V(T)/\lambda$ with field T/T_0 in dimensionless units

where the factor g is defined as

$$g = \frac{\alpha'\lambda T_0^2}{M_p^2} = \frac{M_s^4}{(2\pi)^3 g_s}\frac{\alpha' T_0^2}{M_p^2}. \tag{5.240}$$

Next we compute the number of e-foldings from this model:

$$N(T)=\begin{cases} g\left[\exp\left(-\frac{T}{T_0}\right)-\exp\left(-\frac{T_{\rm end}}{T_0}\right)\right], & \text{for} \quad q=1/2,\\ \sqrt{2q}\,g\left[\exp\left(-\frac{T}{T_0}\right)-\exp\left(-\frac{T_{\rm end}}{T_0}\right)\right], & \text{for any arbitrary } q. \end{cases} \tag{5.241}$$

Further using the condition to end inflation:

$$\bar{\epsilon}_V(T_{\rm end})=1, \tag{5.242}$$

we get the following field value at the end of inflation:

$$T_{\rm end}=T_0\,\ln(2g). \tag{5.243}$$

Next using $N=N_{\rm cmb}=N_\star$ and $T=T_{\rm cmb}=T_\star$ at the horizon crossing we get

$$T_\star=T_0\times\begin{cases} \ln\left[\frac{g}{\frac{1}{2}+N_\star}\right], & \text{for} \quad q=1/2,\\ \ln\left[\frac{g}{\frac{1}{2}+\frac{N_\star}{\sqrt{2q}}}\right], & \text{for any arbitrary } q. \end{cases} \tag{5.244}$$

Also the field excursion can be computed as

$$|\Delta T|=T_0\times\begin{cases} \left|\ln\left[\frac{1}{1+2N_\star}\right]\right|, & \text{for} \quad q=1/2,\\ \left|\ln\left[\frac{1}{1+\frac{2N_\star}{\sqrt{2q}}}\right]\right|, & \text{for any arbitrary } q. \end{cases} \tag{5.245}$$

Finally we compute the following inflationary observables:

$$\Delta_{\zeta,\star}\approx\frac{g\lambda}{12\pi^2M_p^4}\times\begin{cases} \left(\frac{N_\star+\frac{1}{2}}{g}\right)^2, & \text{for} \quad q=1/2,\\ 2q\left(\frac{\frac{N_\star}{\sqrt{2q}}+\frac{1}{2}}{g}\right)^2, & \text{for any arbitrary } q, \end{cases} \tag{5.246}$$

$$n_{\zeta,\star}-1\approx\begin{cases} -\frac{2}{N_\star+\frac{1}{2}}, & \text{for} \quad q=1/2,\\ -\frac{2}{\sqrt{2q}\left(\frac{N_\star}{\sqrt{2q}}+\frac{1}{2}\right)}, & \text{for any arbitrary } q, \end{cases} \tag{5.247}$$

$$\alpha_{\zeta,\star}\approx\begin{cases} -\frac{2}{\left(N_\star+\frac{1}{2}\right)^2}, & \text{for} \quad q=1/2,\\ -\frac{2}{2q\left(\frac{N_\star}{\sqrt{2q}}+\frac{1}{2}\right)^2}, & \text{for any arbitrary } q, \end{cases} \tag{5.248}$$

$$\kappa_{\zeta,\star}\approx\begin{cases} -\frac{4}{\left(N_\star+\frac{1}{2}\right)^3}, & \text{for} \quad q=1/2,\\ -\frac{4}{(2q)^{3/2}\left(\frac{N_\star}{\sqrt{2q}}+\frac{1}{2}\right)^3}, & \text{for any arbitrary } q, \end{cases} \tag{5.249}$$

$$r_\star\approx\begin{cases} \frac{8}{\left(N_\star+\frac{1}{2}\right)}, & \text{for} \quad q=1/2,\\ \frac{8}{2q\left(\frac{N_\star}{\sqrt{2q}}+\frac{1}{2}\right)}, & \text{for any arbitrary } q. \end{cases} \tag{5.250}$$

For the inverse cosh potential we get the following consistency relations:

$$r_\star\approx 4(1-n_{\zeta,\star})\times\begin{cases} 1, & \text{for} \quad q=1/2,\\ \frac{1}{\sqrt{2q}}, & \text{for any arbitrary } q, \end{cases} \tag{5.251}$$

$$\Delta_{\zeta,\star}\approx\frac{\lambda}{3g\pi^2M_p^4(1-n_{\zeta,\star})^2}\times\begin{cases} 1, & \text{for} \quad q=1/2,\\ 1, & \text{for any arbitrary } q, \end{cases} \tag{5.252}$$

$$\Delta_{\zeta,\star}\approx\frac{2\lambda}{3g\pi^2M_p^4r_\star}\times\begin{cases} \left(N_\star+\frac{1}{2}\right), & \text{for} \quad q=1/2,\\ \left(\frac{N_\star}{\sqrt{2q}}+\frac{1}{2}\right), & \text{for any arbitrary } q, \end{cases} \tag{5.253}$$

$$\alpha_{\zeta,\star}\approx-\frac{1}{2}\left(n_{\zeta,\star}-1\right)^2\times\begin{cases} 1, & \text{for} \quad q=1/2,\\ 1, & \text{for any arbitrary } q, \end{cases} \tag{5.254}$$

$$\kappa_{\zeta,\star}\approx\frac{1}{2}\left(n_{\zeta,\star}-1\right)^3\times\begin{cases} 1, & \text{for} \quad q=1/2,\\ 1, & \text{for any arbitrary } q. \end{cases} \tag{5.255}$$

Let us now discuss the general constraints on the parameters of tachyonic string theory including the factor q and on the parameters appearing in the expression for exponential potential Type-I. In Fig. 9a, we have shown the behavior of the tensor-to-scalar ratio r with respect to the scalar spectral index n_ζ for exponential potential Type-I respectively. In both the figures the purple and blue colored line represent the upper bound of the tensor-to-scalar ratio allowed by Planck+ BICEP2+Keck Array joint constraint and only Planck 2015 data respectively. For both the figures the red, green, brown, orange colored curve represent $q=1/2$, $q=1$, $q=3/2$ and $q=2$, respectively. The cyan color shaded region bounded by two vertical black colored lines in Fig. 9a represent the Planck 2σ allowed region and the rest of the light gray shaded region shows the 1σ allowed range, which is at present disfavored by the Planck 2015 data

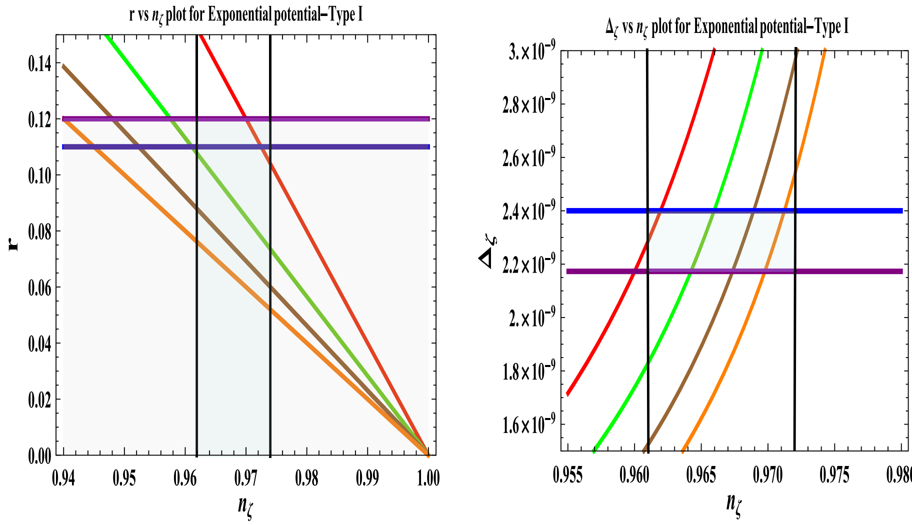

(a) r vs n_ζ. **(b)** Δ_ζ vs n_ζ.

Fig. 9 In **a** the behavior of the tensor-to-scalar ratio r with respect to the scalar spectral index n_ζ and **b** the parameter g for exponential potential Type-I. The *purple* and *blue colored line* represent the *upper* bound of the tensor-to-scalar ratio allowed by Planck+ BICEP2+Keck Array joint constraint and only Planck 2015 data respectively. For both figures the *red*, *green*, *brown*, *orange colored curves* represent $q = 1/2$, $q = 1$, $q = 3/2$ and $q = 2$, respectively. The *cyan color shaded* region bounded by two *vertical black colored lines* in **a** represent the Planck 2σ allowed region and the rest of the *light gray shaded* region shows the 1σ allowed range, which is at present disfavored by the Planck data and Planck+ BICEP2+Keck Array joint constraint. In **a**, we have explicitly shown that in $r - n_\zeta$ plane the observationally favored *lower* bound for the characteristic index is $q \geq 1/2$. Variation of the scalar power spectrum Δ_ζ vs. scalar spectral index n_ζ is shown in **b**. The *purple* and *blue colored line* represent the *upper* and *lower* bounds allowed by WMAP+Planck 2015 data respectively. The *green dotted* region bounded by two *vertical black colored lines* represents the Planck 2σ allowed region and the rest of the light gray shaded region is disfavored by the Planck+WMAP constraint. From **a** and **b**, it is also observed that, within $50 < N_\star < 70$, the exponential potential Type-I is favored for the characteristic index $1 < q < 2$, by Planck 2015 data and Planck+ BICEP2+Keck Array joint analysis

and Planck+ BICEP2+Keck Array joint constraint. The rest of the region is completely ruled out by the present observational constraints. From Fig. 9a, it is also observed that, within $50 < N_\star < 70$, the exponential potential Type-I is favored for the characteristic index $1/2 < q < 2$, by Planck 2015 data and Planck+ BICEP2+Keck Array joint analysis. Also in Fig. 9a for $q = 1/2$, $q = 1$, $q = 3/2$ and $q = 2$ we fix $N_\star/g \sim 0.8$. This implies that for $50 < N_\star < 70$, the prescribed window for g from r–n_ζ plot is given by $63 < g < 88$. To analyze the results more clearly let us describe the cosmological features from Fig. 9a in detail. Let us first start with the $q = 1/2$ situation, in which the 2σ constraint on the scalar spectral tilt is satisfied within the window of the tensor-to-scalar ratio, $0.10 < r < 0.12$ for $50 < N_\star < 70$. Next for the $q = 1$ case, the same constraint is satisfied within the window of the tensor-to-scalar ratio, $0.07 < r < 0.11$ for $50 < N_\star < 70$. Further for the $q = 3/2$ case, the same constraint on scalar spectral tilt is satisfied within the window of the tensor-to-scalar ratio, $0.06 < r < 0.085$ for $50 < N_\star < 70$. Finally, for $q = 2$ situation, the value for the tensor-to-scalar ratio is $0.05 < r < 0.075$.

In Fig. 9b, we have depicted the behavior of the scalar power spectrum Δ_ζ vs. scalar spectral tilt n_ζ for exponential potential Type-I respectively. It is important to note that, for all of the figures the red, green, brown, orange colored curves represent $q = 1/2$, $q = 1$, $q = 3/2$ and $q = 2$ respectively. The purple and blue colored line represent the upper and lower bound allowed by WMAP+Planck 2015 data respectively. The cyan color shaded region bounded by two vertical black colored lines represent the Planck 2σ allowed region and the rest of the light gray shaded region is the 1σ region, which is presently disfavored by the joint Planck+WMAP constraints. The rest of the region is completely ruled out by the present observational constraints. Also in Fig. 9b for $q = 1/2$, $q = 1$, $q = 3/2$ and $q = 2$ we fix $N_\star \sim 70$. But the plots can be reproduced for $50 < N_\star < 70$ also considering the present observational constraints from Planck 2015 data. It is important to mention here that if we combine the constraints obtained from Fig. 9a, b, then by comparing the behavior of the GTachyon in the r–n_ζ and Δ_ζ–n_ζ planes we clearly observe that the $q = 1/2$ case is almost discarded as it is not consistent with both of the 2σ constraints simultaneously.

In Fig. 10a, b, we have shown the behavior of the running of the scalar spectral tilt α_ζ and running of the running of the scalar spectral tilt κ_ζ with respect to the scalar spectral index n_ζ for exponential potential Type I respectively. For both the figures the red colored curve represent the behavior for any arbitrary values of q. The cyan color

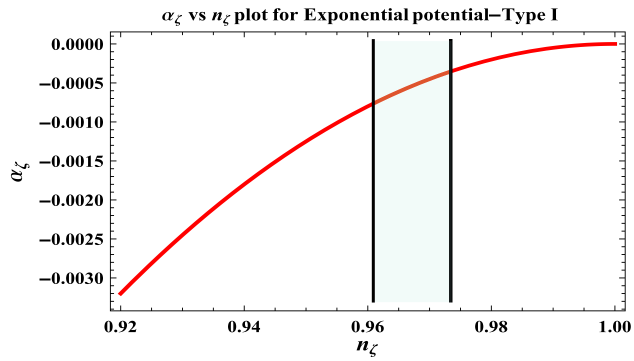

(a) α_ζ vs n_ζ.

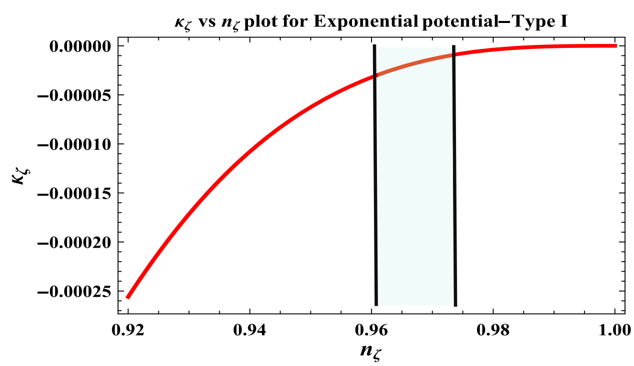

(b) κ_ζ vs n_ζ.

Fig. 10 Behavior of the **a** running of the scalar spectral tilt α_ζ and **b** running of the running of the scalar spectral tilt κ_ζ with respect to the scalar spectral index n_ζ for exponential potential Type-I. For both the figures *red colored curves* represent for any value of q, respectively. The *cyan color shaded* region bounded by two *vertical black colored lines* in **a** represent the Planck 2σ allowed region and the rest of the *light gray shaded* region shows the 1σ allowed range, which is at present disfavored by the Planck data and Planck+ BICEP2+Keck Array joint constraint. From **a** and **b**, it is also observed that, within $50 < N_\star < 70$, the exponential potential Type-I is favored for the characteristic index $1 < q < 2$, by Planck 2015 data and Planck+ BICEP2+Keck Array joint analysis

shaded region bounded by two vertical black colored lines in both the plots represent the Planck 2σ allowed region and the rest of the light gray shaded region shows the 1σ allowed range, which is at present disfavored by the Planck data and Planck+ BICEP2+Keck Array joint constraint. From both of these figures, it is also observed that, within $50 < N_\star < 70$, the exponential potential Type-I is favored for the characteristic index $1 < q < 2$, by Planck 2015 data and Planck+ BICEP2+Keck Array joint analysis. It is also important to note that for any values of q, the numerical value of the running $\alpha_\zeta \sim \mathcal{O}(-10^{-4})$ and running of the running $\kappa_\zeta \sim \mathcal{O}(-10^{-5})$, which are perfectly consistent with the 1.5σ constraints on running and running of the running as obtained from Planck 2015 data. For $q = 1/2$, $q = 1$, $q = 3/2$ and $q = 2$ g is not explicitly appearing in the various inflationary observables except the amplitude of scalar

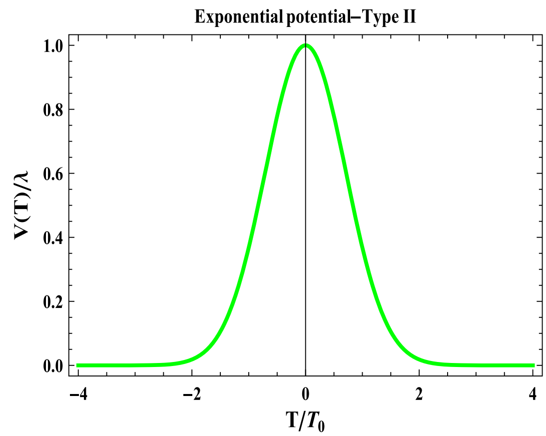

Fig. 11 Variation of the exponential potential Type-II $V(T)/\lambda$ with field T/T_0 in dimensionless units

power spectrum in this case. To produce the correct value of the amplitude of the scalar power spectra we fix the parameter $360 < g < 400$.

Model IV: exponential potential-type II

For the single field case the first model of the tachyonic potential is given by

$$V(T) = \lambda \exp\left[-\left(\frac{T}{T_0}\right)^2\right], \tag{5.256}$$

where λ characterize the scale of inflation and T_0 is the parameter of the model. In Fig. 11 we have depicted the symmetric behavior of the exponential potential Type-I with respect to the scaled field coordinate T/T_0 in dimensionless units. In this case the tachyon field started rolling down from the top height of the potential situated at the origin and takes part in the inflationary dynamics.

Next using specified form of the potential the potential dependent slow-roll parameters are computed as

$$\bar{\epsilon}_V = \frac{1}{2g}4\left(\frac{T}{T_0}\right)^2 \exp\left[\left(\frac{T}{T_0}\right)^2\right], \tag{5.257}$$

$$\bar{\eta}_V = \frac{1}{g}\left[2\left(\frac{T}{T_0}\right)^2 - 1\right] \exp\left[\left(\frac{T}{T_0}\right)^2\right], \tag{5.258}$$

$$\bar{\xi}_V^2 = \frac{1}{g^2}8\left(\frac{T}{T_0}\right)^2\left[2\left(\frac{T}{T_0}\right)^2 - 3\right] \exp\left[2\left(\frac{T}{T_0}\right)^2\right], \tag{5.259}$$

$$\bar{\sigma}_V^3 = \frac{1}{g^3}16\left(\frac{T}{T_0}\right)^2\left[4\left(\frac{T}{T_0}\right)^4 - 12\left(\frac{T}{T_0}\right)^2 + 3\right] \times \exp\left[3\left(\frac{T}{T_0}\right)^2\right], \tag{5.260}$$

where the factor g is defined as

$$g = \frac{\alpha' \lambda T_0^2}{M_p^2} = \frac{M_s^4}{(2\pi)^3 g_s} \frac{\alpha' T_0^2}{M_p^2}. \quad (5.261)$$

Next we compute the number of e-foldings from this model:[5]

$$N(T) \approx \begin{cases} g\left[\ln\left(\frac{T}{T_0}\right) - \ln\left(\frac{T_{\rm end}}{T_0}\right)\right], & \text{for} \quad q = 1/2, \\ \sqrt{2q}\, g\left[\ln\left(\frac{T}{T_0}\right) - \ln\left(\frac{T_{\rm end}}{T_0}\right)\right], & \text{for any arbitrary } q. \end{cases} \quad (5.263)$$

Further using the condition to end inflation:

$$\bar{\epsilon}_V(T_{\rm end}) = 1. \quad (5.264)$$

we get the following transcendental equation to determine the field value at the end of inflation:

$$\left(\frac{T_{\rm end}}{T_0}\right)^2 \exp\left[\left(\frac{T_{\rm end}}{T_0}\right)^2\right] = \frac{g}{2} \quad (5.265)$$

which we need to solve numerically for a given value of g. For the sake of simplicity in the further computation one can consider the following possibilities:

$$T_{\rm end} \approx \begin{cases} T_0, & \text{for } \frac{g}{2} \sim e \\ \sqrt{\frac{g}{2}}\, T_0, & \text{for } \frac{g}{2} << 1 \end{cases} \quad (5.266)$$

Next using $N = N_{\rm cmb} = N_\star$ and $T = T_{\rm cmb} = T_\star$ at the horizon crossing we get

$$T_\star = T_0 \times \begin{cases} \exp\left[\frac{N_\star}{g} + \ln\left(\frac{T_{\rm end}}{T_0}\right)\right], & \text{for} \quad q = 1/2, \\ \exp\left[\frac{N_\star}{\sqrt{2q}g} + \ln\left(\frac{T_{\rm end}}{T_0}\right)\right], & \text{for any arbitrary } q. \end{cases} \quad (5.267)$$

Also the field excursion can be computed as

$$|\Delta T| = T_0 \times \begin{cases} \left|\exp\left[\frac{N_\star}{g} + \ln p\right] - p\right|, & \text{for } q = 1/2, \\ \left|\exp\left[\frac{N_\star}{\sqrt{2q}g} + \ln p\right] - p\right|, & \text{for any arbitrary } q \end{cases} \quad (5.268)$$

where $p = 1, \sqrt{\frac{g}{2}}$. But during numerical estimation we only take $p = \sqrt{\frac{g}{2}}$ because $p = 1$ is disfavored by the Planck 2015 data.

Finally we compute the following inflationary observables:

$$\Delta_{\zeta,\star} \approx \frac{g\lambda}{48\pi^2 M_p^4} \times \begin{cases} \frac{\exp\left(-2\exp\left[\frac{2N_\star}{g} + 2\ln\left(\frac{T_{\rm end}}{T_0}\right)\right]\right)}{\exp\left[\frac{2N_\star}{g} + 2\ln\left(\frac{T_{\rm end}}{T_0}\right)\right]}, & \text{for} \quad q = 1/2, \\ 2q\, \frac{\exp\left(-2\exp\left[\frac{2N_\star}{\sqrt{2q}g} + 2\ln\left(\frac{T_{\rm end}}{T_0}\right)\right]\right)}{\exp\left[\frac{2N_\star}{\sqrt{2q}g} + 2\ln\left(\frac{T_{\rm end}}{T_0}\right)\right]}, & \text{for any arbitrary } q, \end{cases} \quad (5.269)$$

$$n_{\zeta,\star} - 1 \approx \begin{cases} -\frac{2}{g}\left\{1 + 2\left(\frac{T_{\rm end}}{T_0}\right)^2 \exp\left[\frac{2N_\star}{g}\right]\right\}, & \text{for} \quad q = 1/2, \\ -\frac{2}{\sqrt{2q}\,g}\left\{1 + 2\left(\frac{T_{\rm end}}{T_0}\right)^2 \exp\left[\frac{2N_\star}{\sqrt{2q}g}\right]\right\}, & \text{for any arbitrary } q. \end{cases} \quad (5.270)$$

[5] It is important to note that here we have used the following approximation:

$$\mathrm{Ei}\left[-\left(\frac{T}{T_0}\right)^2\right] \approx \gamma + 2\ln\left(\frac{T}{T_0}\right) + \cdots \quad (5.262)$$

where all the terms represented via $\cdots$ are negligibly small in the series expansion. Here γ represents the Euler constant, with the numerical value $\gamma \simeq 0.577216$.

$$\alpha_{\zeta,\star} \approx \frac{8}{g^2} \times \begin{cases} \left(\frac{T_{\rm end}}{T_0}\right)^2 \ \exp\left[\frac{2N_\star}{g}\right], & \text{for} \quad q = 1/2, \\ \frac{1}{2q}\left(\frac{T_{\rm end}}{T_0}\right)^2 \ \exp\left[\frac{2N_\star}{\sqrt{2qg}}\right], & \text{for any arbitrary } q, \end{cases} \tag{5.271}$$

$$\kappa_{\zeta,\star} \approx -\frac{16}{g^3} \times \begin{cases} \left(\frac{T_{\rm end}}{T_0}\right)^2 \ \exp\left[\frac{2N_\star}{g}\right], & \text{for} \quad q = 1/2, \\ \frac{1}{(2q)^{3/2}}\left(\frac{T_{\rm end}}{T_0}\right)^2 \ \exp\left[\frac{2N_\star}{\sqrt{2qg}}\right], & \text{for any arbitrary } q, \end{cases} \tag{5.272}$$

$$r_\star \approx \frac{32}{g} \times \begin{cases} \left(\frac{T_{\rm end}}{T_0}\right)^2 \exp\left[\frac{2N_\star}{g} + \left(\frac{T_{\rm end}}{T_0}\right)^2 \exp\left[\frac{2N_\star}{g}\right]\right], & \text{for} \quad q = 1/2, \\ \frac{1}{2q}\left(\frac{T_{\rm end}}{T_0}\right)^2 \exp\left[\frac{2N_\star}{\sqrt{2qg}} + \left(\frac{T_{\rm end}}{T_0}\right)^2 \exp\left[\frac{2N_\star}{\sqrt{2qg}}\right]\right], & \text{for any arbitrary } q. \end{cases} \tag{5.273}$$

For the inverse cosh potential we get the following consistency relations:

$$r_\star \approx \frac{16}{g} \times \begin{cases} \left[\frac{g}{2}\left(1 - n_{\zeta,\star}\right) - 1\right] \exp\left[\frac{1}{2}\left(\frac{g}{2}\left(1 - n_{\zeta,\star}\right) - 1\right)\right], & \text{for} \quad q = 1/2, \\ \frac{1}{2q}\left[\frac{\sqrt{2qg}}{2}\left(1 - n_{\zeta,\star}\right) - 1\right] \exp\left[\frac{1}{2}\left(\frac{\sqrt{2qg}}{2}\left(1 - n_{\zeta,\star}\right) - 1\right)\right], & \text{for any arbitrary } q, \end{cases} \tag{5.274}$$

$$\Delta_{\zeta,\star} \approx \frac{g\lambda}{24\pi^2 M_p^4} \times \begin{cases} \frac{\exp\left(-\left[\frac{g}{2}\left(1 - n_{\zeta,\star}\right) - 1\right]\right)}{\left[\frac{g}{2}\left(1 - n_{\zeta,\star}\right) - 1\right]}, & \text{for} \quad q = 1/2, \\ 2q \ \frac{\exp\left(-\left[\frac{\sqrt{2qg}}{2}\left(1 - n_{\zeta,\star}\right) - 1\right]\right)}{\left[\frac{\sqrt{2qg}}{2}\left(1 - n_{\zeta,\star}\right) - 1\right]}, & \text{for any arbitrary } q, \end{cases} \tag{5.275}$$

$$\Delta_{\zeta,\star} \approx \frac{2\lambda}{3\pi^2 M_p^4 r_\star} \times \begin{cases} \exp\left[-\left(\frac{T_{\rm end}}{T_0}\right)^2 \ \exp\left[\frac{2N_\star}{g}\right]\right], & \text{for} \quad q = 1/2, \\ \exp\left[-\left(\frac{T_{\rm end}}{T_0}\right)^2 \ \exp\left[\frac{2N_\star}{\sqrt{2qg}}\right]\right], & \text{for any arbitrary } q, \end{cases} \tag{5.276}$$

$$\alpha_{\zeta,\star} \approx \frac{4}{g^2} \times \begin{cases} \left[\frac{g}{2}\left(1 - n_{\zeta,\star}\right) - 1\right], & \text{for} \quad q = 1/2, \\ \frac{1}{2q}\left[\frac{\sqrt{2qg}}{2}\left(1 - n_{\zeta,\star}\right) - 1\right], & \text{for any arbitrary } q, \end{cases} \tag{5.277}$$

$$\kappa_{\zeta,\star} \approx -\frac{8}{g^3} \times \begin{cases} \left[\frac{g}{2}\left(1 - n_{\zeta,\star}\right) - 1\right], & \text{for} \quad q = 1/2, \\ \frac{1}{(2q)^{3/2}}\left[\frac{\sqrt{2qg}}{2}\left(1 - n_{\zeta,\star}\right) - 1\right], & \text{for any arbitrary } q. \end{cases} \tag{5.278}$$

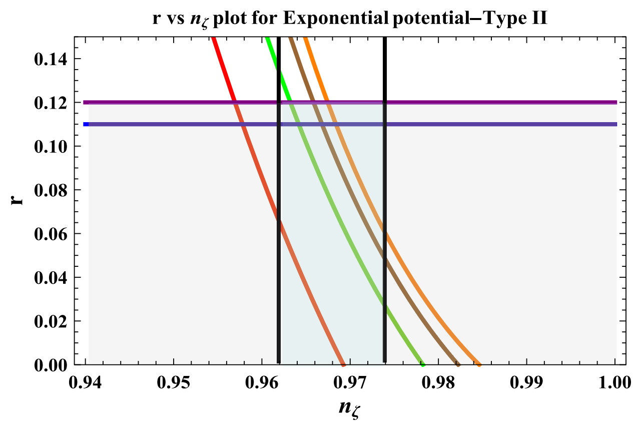

(a) r vs n_ζ.

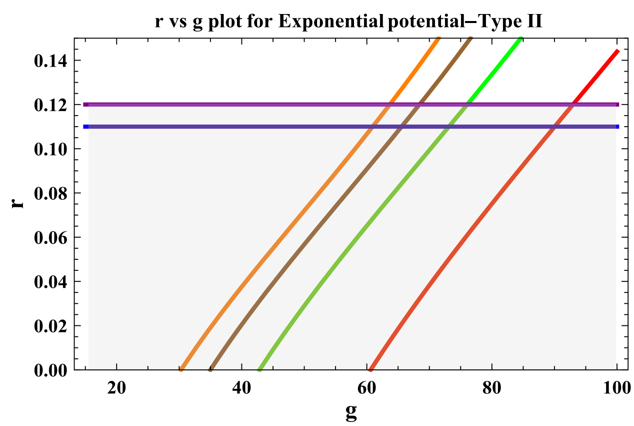

(b) r vs g.

Fig. 12 Behavior of the tensor-to-scalar ratio r with respect to **a** the scalar spectral index n_ζ and **b** the parameter g for exponential potential Type-II. The *purple* and *blue colored line* represent the *upper* bound of the tensor-to-scalar ratio allowed by Planck+ BICEP2+Keck Array joint constraint and only Planck 2015 data respectively. For both figures the *red*, *green*, *brown*, *orange colored curves* represent $q = 1/2, q = 1$, $q = 3/2$ and $q = 2$, respectively. The *cyan color shaded* region bounded by two *vertical black colored lines* in **a** represent the Planck 2σ allowed region and the rest of the light gray shaded region shows the 1σ allowed range, which is at present disfavored by the Planck data and Planck+ BICEP2+Keck Array joint constraint. From **a** and **b**, it is also observed that, within $50 < N_\star < 70$, the logarithmic potential is favored for the characteristic index $1/2 < q < 2$, by Planck 2015 data and Planck+ BICEP2+Keck Array joint analysis

Let us now discuss the general constraints on the parameters of tachyonic string theory including the factor q and on the parameters appearing in the expression for exponential potential Type-II. In Fig. 12a, b, we have shown the behavior of the tensor-to-scalar ratio r with respect to the scalar spectral index n_ζ and the model parameter g for exponential potential Type-II respectively. In both the figures the purple and blue colored line represent the upper bound of tensor-to-scalar ratio allowed by Planck+ BICEP2+Keck Array joint constraint and only Planck 2015 data respectively. For both the figures the red, green, brown, orange colored curve represent $q = 1/2$, $q = 1$, $q = 3/2$ and $q = 2$, respectively. The cyan color shaded region bounded by two vertical black colored lines in Fig. 12a represent the Planck 2σ allowed region and the rest of the light gray shaded region shows the 1σ allowed range, which is at present disfavored by the Planck 2015 data and Planck+ BICEP2+Keck Array joint constraint. The rest of the region is completely ruled out by the present observational constraints. From Fig. 12a, b, it is also observed that, within $50 < N_\star < 70$, the exponential potential Type-II is favored only for the characteristic index $1/2 < q < 2$, by Planck 2015 data and Planck+ BICEP2+Keck Array joint analysis. Also in Fig. 12a for $q = 1/2$, $q = 1$, $q = 3/2$ and $q = 2$ we fix $N_\star/g \sim 0.85$. This implies that for $50 < N_\star < 70$, the prescribed window for g from r–n_ζ plot is given by $59 < g < 82.3$ considering $1/2 < q < 2$. It is additionally important to note that, for $q << 1/2$, the tensor-to-scalar ratio computed from the model is negligibly small for exponential potential Type-II. This implies that if the inflationary tensor mode is detected near its present upper bound on the tensor-to-scalar ratio then all $q << 1/2$ possibilities for tachyonic inflation can be discarded for exponential potential Type-II. On the contrary, if inflationary tensor modes are never detected by any of the future observational probes then $q << 1/2$ possibilities for tachyonic inflation in the case of an exponential potential Type-II is highly prominent. Also it is important to mention that, in Fig. 12b within the window $30 < g < 93$, if we take a smaller value of g, then the inflationary tensor-to-scalar ratio also gradually decreases. To analyze the results more clearly let us describe the cosmological features from Fig. 12a in detail. Let us first start with the $q = 1/2$ situation, in which the 2σ constraint on the scalar spectral tilt is satisfied within the window of the tensor-to-scalar ratio, $0 < r < 0.065$ for $50 < N_\star < 70$. Next for the $q = 1$ case, the same constraint is satisfied within the window of the tensor-to-scalar ratio, $0.030 < r < 0.12$ for $50 < N_\star < 70$. Further for the $q = 3/2$ case, the same constraint on scalar spectral tilt is satisfied within the window of the tensor-to-scalar ratio, $0.045 < r < 0.12$ for $50 < N_\star < 70$. Finally, for the $q = 2$ situation, the value for the tensor-to-scalar ratio is $0.060 < r < 0.12$, which is tightly constrained from the upper bound of spectral tilt from Planck 2015 observational data.

In Fig. 13a–c, we have depicted the behavior of the scalar power spectrum Δ_ζ vs. the stringy parameter g, scalar spectral tilt n_ζ vs. the stringy parameter g and scalar power spectrum Δ_ζ vs. scalar spectral index n_ζ for exponential potential, Type-II respectively. It is important to note that, for all of the figures the red, green, brown, orange colored curves represent $q = 1/2$, $q = 1$, $q = 3/2$ and $q = 2$ respectively. The purple and blue colored line represent the upper and lower bound allowed by WMAP+Planck 2015 data respectively. The cyan color shaded region bounded by two vertical

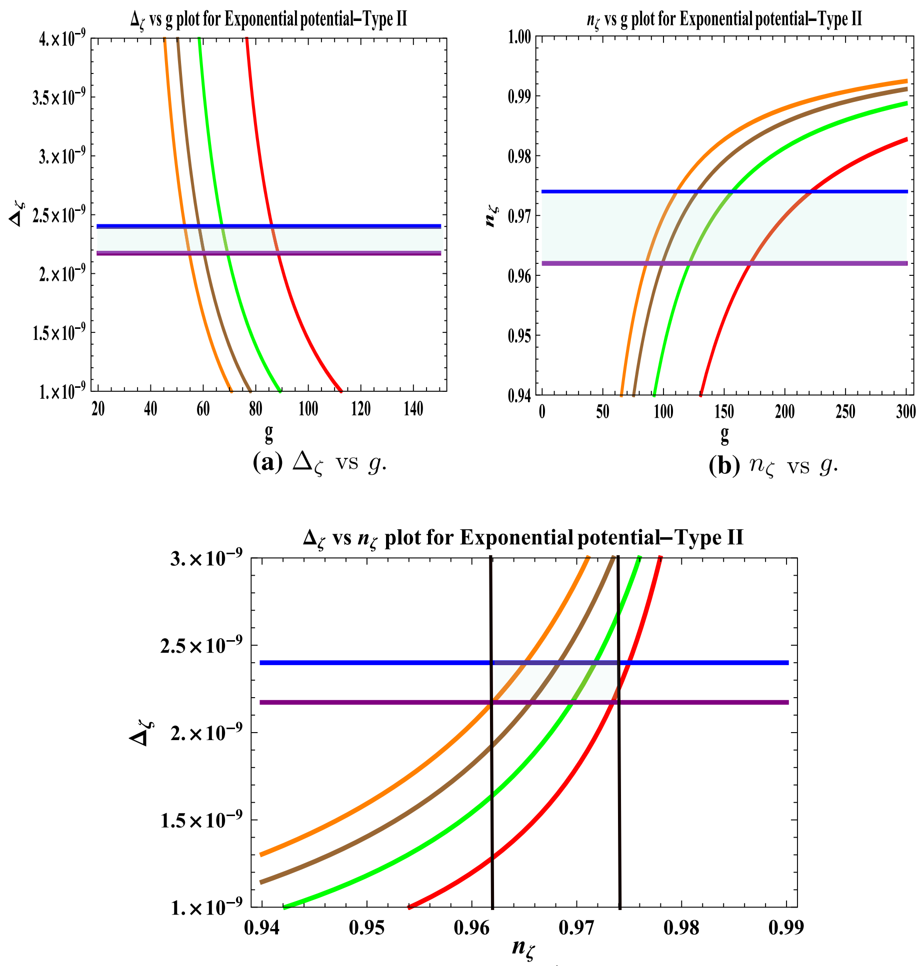

(a) Δ_ζ vs g. **(b)** n_ζ vs g. **(c)** Δ_ζ vs n_ζ.

Fig. 13 Variation of the **a** scalar power spectrum Δ_ζ vs. scalar spectral index n_ζ, **b** scalar power spectrum Δ_ζ vs. the stringy parameter g and **c** scalar spectral tilt n_ζ vs. the stringy parameter g. The *purple* and *blue colored line* represent the *upper* and *lower* bound allowed by WMAP+Planck 2015 data respectively. The *green dotted* region bounded by two *vertical black colored lines* represent the Planck 2σ allowed region and the rest of the *light gray shaded* region is disfavored by the Planck+WMAP constraint

black colored lines represent the Planck 2σ allowed region and the rest of the light gray shaded region is the 1σ region, which is presently disfavored by the joint Planck+WMAP constraints. The rest of the region is completely ruled out by the present observational constraints. From Fig. 13a it is clearly observed that the observational constraints on the amplitude of the scalar mode fluctuations satisfy within the window $55 < g < 93$ considering $1/2 < q < 2$. For $g > 93$ the corresponding amplitude falls down in a non-trivial fashion by following the exact functional form as stated in Eq. (5.269). Next using the behavior as shown in Fig. 13b, the lower bound on the stringy parameter g is constrained by $g > 73$ by using the non-trivial relationship as stated in Eq. (5.270). But at this lower bound of the parameter g the amplitude of the scalar power spectrum is slightly outside to the present observational constraints. This implies that, to satisfy both the constraints from the amplitude of the scalar power spectrum and its spectral tilt, within 2σ CL the constrained numerical value of the stringy parameter is lying within the window $73 < g < 93$. Also in Fig. 13c for $q = 1/2$, $q = 1$, $q = 3/2$ and $q = 2$ we fix $N_\star/g \sim 0.85$, which further implies that for $50 < N_\star < 70$, the prescribed window for g from Δ_ζ–n_ζ plot is given by $59 < g < 82.3$. If we additionally impose the constraint from the upper bound on the tensor-to-scalar ratio then also the allowed parameter range is lying within the window, i.e., $73 < g < 82.3$.

In Fig. 14a, b, we have shown the behavior of the running of the scalar spectral tilt α_ζ and running of the running of the scalar spectral tilt κ_ζ with respect to the scalar spectral index n_ζ for exponential potential Type II with $g = 76$, respectively. For both the figures the red, green, brown, orange colored curves represent $q = 1/2$, $q = 1$, $q = 3/2$ and $q = 2$, respectively. The cyan color shaded region bounded by two vertical black colored lines in both plots represent the Planck 2σ allowed region and the rest of the light gray shaded region shows the 1σ allowed range, which is at present disfavored by the Planck data and Planck+ BICEP2+Keck Array joint constraint. From both of these figures, it is also observed that, within $50 < N_\star < 70$, the exponential potential Type-II is favored for the characteristic index $1/2 < q < 2$, by the Planck 2015 data and Planck+ BICEP2+Keck Array joint analysis. From Fig. 14a, b, it is observed that within the 2σ

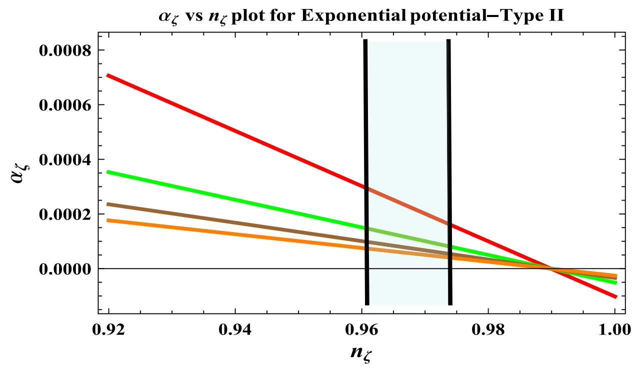

(a) α_ζ vs n_ζ.

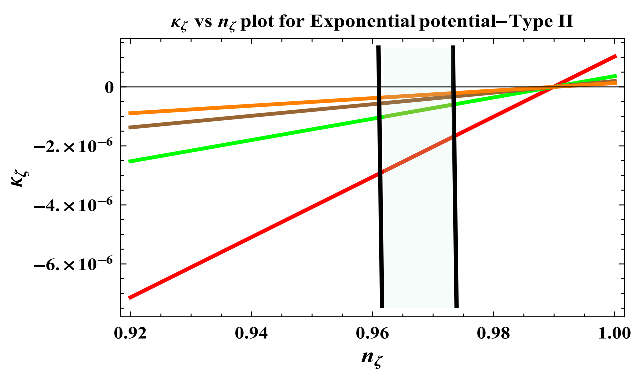

(b) κ_ζ vs n_ζ.

Fig. 14 Behavior of the **a** running of the scalar spectral tilt α_ζ and **b** running of the running of the scalar spectral tilt κ_ζ with respect to the scalar spectral index n_ζ for the inverse cosh potential with $g = 88$. For both figures the *red*, *green*, *brown*, *orange colored curves* represent $q = 1/2$, $q = 1$, $q = 3/2$ and $q = 2$ respectively. The *cyan color shaded* region bounded by two *vertical black colored lines* in **a** represent the Planck 2σ allowed region and the rest of the *light gray shaded* region shows the 1σ allowed range, which is at present disfavored by the Planck data and Planck+ BICEP2+Keck Array joint constraint. From **a** and **b**, it is also observed that, within $50 < N_\star < 70$, the inverse cosh potential is favored for the characteristic index $1/2 < q < 2$, by Planck 2015 data and Planck+ BICEP2+Keck Array joint analysis

observed range of the scalar spectral tilt n_ζ, as the value of the characteristic parameter q increases, the value of the running α_ζ decreases and running of the running κ_ζ increases for exponential potential Type-II. It is also important to note that for $1/2 < q < 2$, the numerical value of the running $\alpha_\zeta \sim \mathcal{O}(10^{-4})$ and running of the running $\kappa_\zeta \sim \mathcal{O}(-10^{-6})$, which are perfectly consistent with the 1.5σ constraints on running and running of the running as obtained from the Planck 2015 data.

Model V: inverse power-law potential

For single field case the first model of tachyonic potential is given by

$$V(T) = \frac{\lambda}{\left[1+\left(\frac{T}{T_0}\right)^4\right]}, \tag{5.279}$$

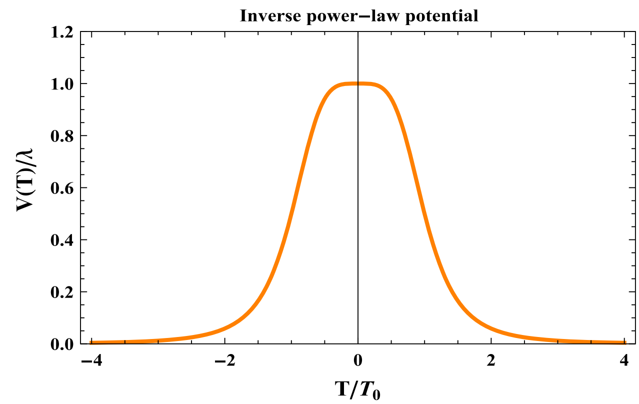

Fig. 15 Variation of the inverse power-law potential $V(T)/\lambda$ with the field T/T_0 in dimensionless units

where λ characterize the scale of inflation and T_0 is the parameter of the model. In Fig. 15 we have depicted the symmetric behavior of the inverse power-law potential with respect to the scaled field coordinate T/T_0 in dimensionless units. In this case the tachyon field started rolling down from the top height of the potential situated at the origin and takes part in the inflationary dynamics.

Next using specified form of the potential the potential dependent slow-roll parameters are computed as

$$\bar{\epsilon}_V = \frac{1}{2g}\frac{16\left(\frac{T}{T_0}\right)^6}{\left[1+\left(\frac{T}{T_0}\right)^4\right]}, \tag{5.280}$$

$$\bar{\eta}_V = \frac{1}{g}\frac{4\left[5\left(\frac{T}{T_0}\right)^4-3\right]}{\left[1+\left(\frac{T}{T_0}\right)^4\right]}, \tag{5.281}$$

$$\bar{\xi}^2_V = \frac{1}{g^2}\frac{96\left(\frac{T}{T_0}\right)^2\left[5\left(\frac{T}{T_0}\right)^8-10\left(\frac{T}{T_0}\right)^4+1\right]}{\left[1+\left(\frac{T}{T_0}\right)^4\right]^2}, \tag{5.282}$$

$$\bar{\sigma}^3_V = \frac{1}{g^3}\frac{384\left(\frac{T}{T_0}\right)^6\left[5\left(\frac{T}{T_0}\right)^4\left(7\left(\frac{T}{T_0}\right)^8-31\left(\frac{T}{T_0}\right)^4+13\right)-1\right]}{\left[1+\left(\frac{T}{T_0}\right)^4\right]^3}, \tag{5.283}$$

where the factor g is defined as

$$g = \frac{\alpha'\lambda T_0^2}{M_p^2} = \frac{M_s^4}{(2\pi)^3 g_s}\frac{\alpha' T_0^2}{M_p^2}. \tag{5.284}$$

Next we compute the number of e-foldings from this model:

$$N(T)=\begin{cases}\frac{g}{8}\left[\frac{1}{\left(\frac{T}{T_0}\right)^2}-\frac{1}{\left(\frac{T_{\rm end}}{T_0}\right)^2}\right], & \text{for}\quad q=1/2,\\ \sqrt{2q}\,\frac{g}{8}\left[\frac{1}{\left(\frac{T}{T_0}\right)^2}-\frac{1}{\left(\frac{T_{\rm end}}{T_0}\right)^2}\right], & \text{for any arbitrary } q.\end{cases} \tag{5.285}$$

Further using the condition to end inflation:

$$\bar{\epsilon}_V(T_{\rm end})=1, \tag{5.286}$$

we get the following field values at the end of inflation:

$$T_{\rm end}\sim\sqrt{\frac{g}{8}}\,T_0. \tag{5.287}$$

Next using $N=N_{\rm cmb}=N_\star$ and $T=T_{\rm cmb}=T_\star$ at the horizon crossing we get

$$T_\star=T_0\times\begin{cases}\frac{1}{\sqrt{\frac{8}{g}\left(N_\star+1\right)}}, & \text{for}\quad q=1/2,\\ \frac{1}{\sqrt{\frac{8}{g}\left(\frac{N_\star}{\sqrt{2q}}+1\right)}}, & \text{for any arbitrary } q,\end{cases} \tag{5.288}$$

Also the field excursion can be computed as

$$|\Delta T|=T_0\times\begin{cases}\left|\frac{1}{\sqrt{\frac{8}{g}\left(N_\star+1\right)}}-\sqrt{\frac{g}{8}}\right|, & \text{for}\quad q=1/2,\\ \left|\frac{1}{\sqrt{\frac{8}{g}\left(\frac{N_\star}{\sqrt{2q}}+1\right)}}-\sqrt{\frac{g}{8}}\right|, & \text{for any arbitrary } q.\end{cases} \tag{5.289}$$

Finally we compute the following inflationary observables:

$$\Delta_{\zeta,\star}\approx\frac{g\lambda}{12\pi^2M_p^4}\times\begin{cases}\frac{1}{16\left(\frac{8}{g}\left(N_\star+1\right)\right)^3}, & \text{for}\quad q=1/2,\\ \frac{2q}{16\left(\frac{8}{g}\left(\frac{N_\star}{\sqrt{2q}}+1\right)\right)^3}, & \text{for any arbitrary } q,\end{cases} \tag{5.290}$$

$$n_{\zeta,\star}-1\approx\begin{cases}-\frac{3}{(N_\star+1)}, & \text{for}\quad q=1/2,\\ -\frac{3}{\left(\frac{N_\star}{\sqrt{2q}}+1\right)}, & \text{for any arbitrary } q.\end{cases} \tag{5.291}$$

$$\alpha_{\zeta,\star}\approx\begin{cases}-\frac{3}{(N_\star+1)^2}, & \text{for}\quad q=1/2,\\ -\frac{3}{\sqrt{2q}\left(\frac{N_\star}{\sqrt{2q}}+1\right)^2}, & \text{for any arbitrary } q,\end{cases} \tag{5.292}$$

$$\kappa_{\zeta,\star}\approx\begin{cases}-\frac{6}{(N_\star+1)^3}, & \text{for}\quad q=1/2,\\ -\frac{6}{2q\left(\frac{N_\star}{\sqrt{2q}}+1\right)^3}, & \text{for any arbitrary } q,\end{cases} \tag{5.293}$$

$$r_\star\approx\begin{cases}\frac{16}{(N_\star+1)}, & \text{for}\quad q=1/2,\\ \frac{16}{2q\left(\frac{N_\star}{\sqrt{2q}}+1\right)}, & \text{for any arbitrary } q.\end{cases} \tag{5.294}$$

For the inverse cosh potential we get the following consistency relations:

$$r_\star\approx\frac{16}{3}(1-n_{\zeta,\star})\times\begin{cases}1, & \text{for}\quad q=1/2,\\ \frac{1}{2q}, & \text{for any arbitrary } q,\end{cases} \tag{5.295}$$

$$\Delta_{\zeta,\star}\approx\frac{g^4\lambda(1-n_{\zeta,\star})^3}{12\pi^2M_p^4}\times\begin{cases}\frac{1}{221184}, & \text{for}\quad q=1/2,\\ \frac{2q}{221184}, & \text{for any arbitrary } q,\end{cases} \tag{5.296}$$

$$\Delta_{\zeta,\star}\approx\frac{g^4\lambda r_\star^3}{12\pi^2M_p^4}\times\begin{cases}\frac{1}{33554432}, & \text{for}\quad q=1/2,\\ \frac{(2q)^3}{33554432}, & \text{for any arbitrary } q,\end{cases} \tag{5.297}$$

$$\alpha_{\zeta,\star}\approx-\frac{1}{3}\left(n_{\zeta,\star}-1\right)^2\times\begin{cases}1, & \text{for}\quad q=1/2,\\ \frac{1}{\sqrt{2q}}, & \text{for any arbitrary } q,\end{cases} \tag{5.298}$$

$$\kappa_{\zeta,\star}\approx\frac{2}{9}\left(n_{\zeta,\star}-1\right)^3\times\begin{cases}1, & \text{for}\quad q=1/2,\\ \frac{1}{2q}, & \text{for any arbitrary } q.\end{cases} \tag{5.299}$$

Let us now discuss the general constraints on the parameters of tachyonic string theory including the factor q and on the parameters appearing in the expression for inverse power-law potential. In Fig. 16a, we have shown the behavior of the tensor-to-scalar ratio r with respect to the scalar

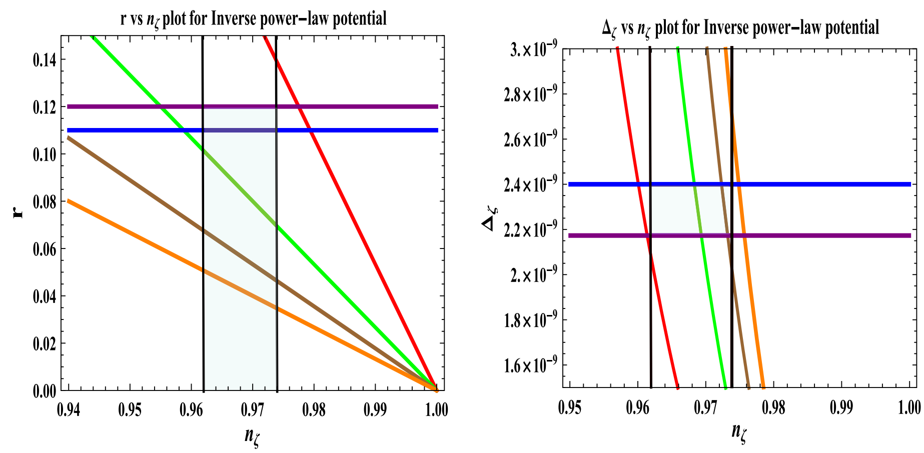

(a) r vs n_ζ **(b)** Δ_ζ vs n_ζ

Fig. 16 In **a** the behavior of the tensor-to-scalar ratio r with respect to the scalar spectral index n_ζ and **b** the parameter g for inverse power-law potential. The *purple* and *blue colored line* represent the *upper* bound of the tensor-to-scalar ratio allowed by Planck+ BICEP2+Keck Array joint constraint and only Planck 2015 data respectively. For both figures the *red*, *green*, *brown*, *orange colored curves* represent $q = 1/2, q = 1$, $q = 3/2$ and $q = 2$, respectively. The *cyan color shaded* region bounded by two *vertical black colored lines* in **a** represent the Planck 2σ allowed region and the rest of the *light gray shaded* region shows the 1σ allowed range, which is at present disfavored by the Planck data and Planck+ BICEP2+Keck Array joint constraint. In **a**, we have explicitly shown that in r–n_ζ plane the observationally disfavored value of the characteristic index is $q \geq 1/2$. Variation of the scalar power spectrum Δ_ζ vs. scalar spectral index n_ζ is shown in **b**. The *purple* and *blue colored line* represent the *upper* and *lower* bound allowed by WMAP+Planck 2015 data respectively. The *green dotted* region bounded by two *vertical black colored lines* represent the Planck 2σ allowed region and the rest of the *light gray shaded* region is disfavored by the Planck+WMAP constraint. In **b**, we have explicitly shown that in $\Delta_\zeta - n_\zeta$ plane the observationally favored value of the characteristic index is $q = 1$ and $q = 3/2$. From **a** and **b**, it is also observed that, within $50 < N_\star < 70$, the inverse power-law potential is favored for the characteristic index $3/2 < q < 1$, by Planck 2015 data and Planck+ BICEP2+Keck Array joint analysis

spectral index n_ζ for inverse power-law potential respectively. In both the figures the purple and blue colored line represent the upper bound of the tensor-to-scalar ratio allowed by Planck+ BICEP2+Keck Array joint constraint and only Planck 2015 data respectively. For both the figures the red, green, brown, orange colored curve represent $q = 1/2$, $q = 1$, $q = 3/2$ and $q = 2$, respectively. The cyan color shaded region bounded by two vertical black colored lines in Fig. 16a represent the Planck 2σ allowed region and the rest of the light gray shaded region shows the 1σ allowed range, which is at present disfavored by the Planck 2015 data and Planck+ BICEP2+Keck Array joint constraint. The rest of the region is completely ruled out by the present observational constraints. From Fig. 16a, it is also observed that, within $50 < N_\star < 70$, the inverse power-law potential is favored for the characteristic index $1 < q < 2$, by Planck 2015 data and Planck+ BICEP2+Keck Array joint analysis. Also in Fig. 16a for $q = 1/2$, $q = 1$, $q = 3/2$ and $q = 2$ we fix $N_\star \sim 70$. One can draw similar characteristic curves for any value of the number of e-foldings lying within the window $50 < N_\star < 70$ also. To analyze the results more clearly let us describe the cosmological features from Fig. 16a in detail. Let us first start with the $q = 1/2$ situation, in which the 2σ constraint on the scalar spectral tilt is disfavored for $50 < N_\star < 70$. Next for the $q = 1$ case, the same constraint is satisfied within the window of the tensor-to-scalar ratio, $0.07 < r < 0.10$ for $50 < N_\star < 70$. Further for the $q = 3/2$ case, the same constraint on scalar spectral tilt is satisfied within the window of the tensor-to-scalar ratio, $0.05 < r < 0.07$ for $50 < N_\star < 70$. Finally, for the $q = 2$ situation, the value for the tensor-to-scalar ratio is $0.035 < r < 0.05$.

In Fig. 16b, we have depicted the behavior of the scalar power spectrum Δ_ζ vs. scalar spectral tilt n_ζ for inverse power-law potential respectively. It is important to note that, for all of the figures the red, green, brown, orange colored curves represent $q = 1/2$, $q = 1$, $q = 3/2$ and $q = 2$ respectively. The purple and blue colored line represent the upper and lower bound allowed by WMAP+Planck 2015 data respectively. The cyan color shaded region bounded by two vertical black colored lines represent the Planck 2σ allowed region and the rest of the light gray shaded region is the 1σ region, which is presently disfavored by the joint Planck+WMAP constraints. The rest of the region is completely ruled out by the present observational constraints. Also in Fig. 16b for $q = 1/2$, $q = 1$, $q = 3/2$ and $q = 2$ we fix $N_\star \sim 70$. But the plots can be reproduced for $50 < N_\star < 70$ also considering the present observational constraints from Planck 2015 data. It is clearly observed from Fig. 16b that the Planck 2015 constraint on amplitude of the scalar power spectrum Δ_ζ and the scalar spectral tilt n_ζ disfavor $q = 1/2$ and $q = 2$ values for inverse power-law potential.

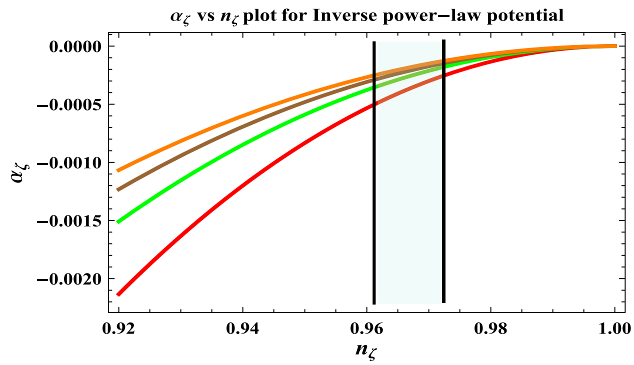

(a) α_ζ vs n_ζ.

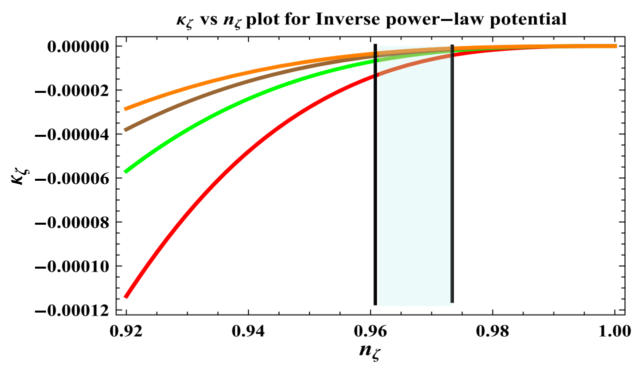

(b) κ_ζ vs n_ζ.

Fig. 17 Behavior of the **a** running of the scalar spectral tilt α_ζ and **b** running of the running of the scalar spectral tilt κ_ζ with respect to the scalar spectral index n_ζ for the inverse cosh potential with $g = 88$. For both figures the *red*, *green*, *brown*, *orange colored curves* represent $q = 1/2$, $q = 1$, $q = 3/2$ and $q = 2$ respectively. The *cyan color shaded* region bounded by two *vertical black colored lines* in **a** and **a** represent the Planck 2σ allowed region and the rest of the *light gray shaded* region shows the 1σ allowed range, which is at present disfavored by the Planck data and Planck+ BICEP2+Keck Array joint constraint. From **a** and **b**, it is also observed that, within $50 < N_\star < 70$, the inverse cosh potential is favored for the characteristic index $1/2 < q < 2$, by Planck 2015 data and Planck+ BICEP2+Keck Array joint analysis

In Fig. 17a, b, we show the behavior of the running of the scalar spectral tilt α_ζ and running of the running of the scalar spectral tilt κ_ζ with respect to the scalar spectral index n_ζ for inverse power-law potential respectively. For both the figures the red, green, brown, and orange colored curves represent $q = 1/2, q = 1, q = 3/2$, and $q = 2$, respectively. The cyan color shaded region bounded by two vertical black colored lines in both plots represent the Planck 2σ allowed region and the rest of the light gray shaded region shows the 1σ allowed range, which is at present disfavored by the Planck data and Planck+ BICEP2+Keck Array joint constraint. From both of these figures, it is also observed that, within $50 < N_\star < 70$, the inverse power-law potential is favored for the characteristic index $1/2 < q < 2$, by Planck 2015 data and a Planck+ BICEP2+Keck Array joint analysis. If we additionally impose the constraints from the r–n_ζ and the Δ_ζ–n_ζ plane then the stringent window on the characteristic index of GTachyon is lying within $1 < q < 3/2$. It is also important to note that for any values of q, the numerical value of the running $\alpha_\zeta \sim \mathcal{O}(-10^{-4})$ and running of the running $\kappa_\zeta \sim \mathcal{O}(-10^{-5})$, which are perfectly consistent with the 1.5σ constraints on running and running of the running as obtained from Planck 2015 data. For $q = 1/2$, $q = 1$, $q = 3/2$ and $q = 2$ g does not explicitly appear in the various inflationary observables except the amplitude of scalar power spectrum in this case. To produce the correct value of the amplitude of the scalar power spectra we fix the parameter $600 < g < 700$.

5.1.9 Analyzing CMB power spectrum

In this section we explicitly study the cosmological consequences from the CMB TT, TE, EE, BB angular power spectrum computed from all the proposed models of inflation.[6] The angular power spectra or equivalently the two point correlator of the X and Y fields are defined as [10]

$$C_\ell^{XY} \equiv \frac{1}{2\ell+1}\sum_{m=-l}^{l}\langle a^*_{X,\ell m}a_{Y,\ell m}\rangle, \qquad X, Y = T, E, B. \tag{5.300}$$

Here l characterizes the CMB multipole and m signifies the magnetic quantum number, which runs from $m = -l, \ldots, +l$. In general, the field $X(\hat{n})$ and $Y(\hat{n})$ can be expressed in terms of the following harmonic expansion:

$$X(\hat{n}), Y(\hat{n}) = \begin{cases} \displaystyle\sum_{l=0}^{\infty}\sum_{m=-l}^{+l} a_{T,lm}V_{lm}(\hat{n}), & \text{for } X = T, \\ \displaystyle\sum_{l=0}^{\infty}\sum_{m=-l}^{+l} a_{E,lm}V_{lm}(\hat{n}), & \text{for } X = E, \\ \displaystyle\sum_{l=0}^{\infty}\sum_{m=-l}^{+l} a_{B,lm}V_{lm}(\hat{n}), & \text{for } X = B, \end{cases} \tag{5.301}$$

where $\hat{n}$ is the arbitrary directional unit vector in CMB map. Here $V_{lm}(\hat{n})$ are the spherical harmonics which are chosen to be the basis of the harmonic expansion of the temperature anisotropy and the E and B polarization. Further using the inflationary power spectra at any momentum scale k:

$$\Delta(k) \equiv \{\Delta_\zeta(k), \Delta_h(k)\} \tag{5.302}$$

[6] In this work we have not considered the possibility of other cross correlators, i.e., TB, EB as there is no observational evidence of such contributions in the CMB map. Also till date there is no observational evidence for inflationary origin of BB angular power spectrum except from CMB lensing [133]. However, for the sake of completeness in this paper we show the theoretical BB angular power spectra from the various models of the tachyonic potential.

the angular power spectra for CMB temperature fluctuations and polarization can be expressed as [10]

$$C_\ell^{XY} = \frac{2}{\pi}\int k^2 \mathrm{d}k \underbrace{\Delta(k)}_{\text{Inflation}} \underbrace{\Theta_{X\ell}(k)\Theta_{Y\ell}(k)}_{\text{Anisotropies}}, \tag{5.303}$$

where the anisotropic integral kernel can be written as [10]

$$\Theta_{X\ell}(k) = \int_0^{\eta_0} \mathrm{d}\eta \underbrace{S_X(k,\eta)}_{\text{Sources}} \underbrace{P_{X\ell}(k[\eta_0-\eta])}_{\text{Projection}}. \tag{5.304}$$

The integral (5.303) relates the inhomogeneities predicted by inflation, $\Delta(k)$, to the anisotropies observed in the CMB, C_ℓ^{XY}. The correlations between the different X and Y modes are related by the transfer functions $\Theta_{X\ell}(k)$ and $\Theta_{Y\ell}(k)$. The transfer functions may be written as the line-of-sight integral Eq. (5.304) which factorizes into physical source terms $S_X(k,\eta)$ and geometric projection factors $P_{X\ell}(k[\eta_0-\eta])$ through combinations of Bessel functions.

Further expressing Eq. (5.303) in terms of TT, TE, EE, BB correlation we get

For curvature perturbation

$$C_\ell^{TT} = \frac{2}{\pi}\int k^2 \mathrm{d}k\ \Delta_S(k)\ \Theta_{T\ell}(k)\Theta_{T\ell}(k), \tag{5.305}$$

$$C_\ell^{TE} = (4\pi)^2\int k^2 \mathrm{d}k\ \Delta_S(k)\ \Theta_{T\ell}(k)\Theta_{E\ell}(k), \tag{5.306}$$

$$C_\ell^{EE} = (4\pi)^2\int k^2 \mathrm{d}k\ \Delta_S(k)\ \Theta_{E\ell}(k)\Theta_{E\ell}(k), \tag{5.307}$$

For tensor perturbation

$$C_\ell^{BB} = (4\pi)^2\int k^2 \mathrm{d}k\ \Delta_h(k)\ \Theta_{B\ell}(k)\Theta_{B\ell}(k) \tag{5.308}$$

$$C_\ell^{TT} = \frac{2}{\pi}\int k^2 \mathrm{d}k\ \Delta_h(k)\ \Theta_{T\ell}(k)\Theta_{T\ell}(k), \tag{5.309}$$

$$C_\ell^{TE} = (4\pi)^2\int k^2 \mathrm{d}k\ \Delta_h(k)\ \Theta_{T\ell}(k)\Theta_{E\ell}(k), \tag{5.310}$$

$$C_\ell^{EE} = (4\pi)^2\int k^2 \mathrm{d}k\ \Delta_h(k)\ \Theta_{E\ell}(k)\Theta_{E\ell}(k), \tag{5.311}$$

where the inflationary power spectra $\{\Delta_\zeta(k), \Delta_h(k)\}$ are parametrized at any arbitrary momentum scale k as[7]

$$\Delta_\zeta(k) = \Delta_{\zeta,\star}\left(\frac{k}{c_S k_\star}\right)^{n_{\zeta,\star}-1+\frac{\alpha_{\zeta,\star}}{2}\ln\left(\frac{k}{c_S k_\star}\right)+\frac{\kappa_{\zeta,\star}}{6}\ln^2\left(\frac{k}{c_S k_\star}\right)+\cdots}, \tag{5.312}$$

$$\Delta_h(k) = r(k)\Delta_\zeta(k)$$
$$= \Delta_{h,\star}\left(\frac{k}{k_\star}\right)^{n_{h,\star}+\frac{\alpha_{h,\star}}{2}\ln\left(\frac{k}{k_\star}\right)+\frac{\kappa_{h,\star}}{6}\ln^2\left(\frac{k}{k_\star}\right)+\cdots}. \tag{5.313}$$

It is important to note that the cosmological significance of the E and B decomposition of CMB polarization carries the following significant features:

- Curvature (density) perturbations create only polarizing E-modes.
- Vector (vorticity) perturbations create mainly B-modes. However, it is important to note that here the contributions of vector modes decay with the expansion of the universe and are therefore sub-dominant at the epoch of recombination. For this reason we have neglected such sub-dominant effects from our rest of the analysis.
- Tensor (gravitational wave) perturbations create both E-modes and B-modes. But to quantify the exact contribution of the primordial gravitational waves, specifically in the inflationary B modes, one needs to separate all the other significant contributions in the B modes, i.e., the primordial magnetic field, gravitational lensing, non-Gaussianity, etc., But at present in the cosmological literature no such sophisticated techniques or algorithms are available using which one can separate all of these significant contributions completely.

To compute the momentum integrals numerically and to analyze the various features of CMB angular power spectra from all of the inflationary models mentioned in the last section, here we use a semi-analytical code "CAMB". For the numerical analysis we use here the best fit model parameters corresponding to all of the five tachyonic models, which are compatible with Planck 2015 data. Additionally we take the ΛCDM background. Further we put all these inputs to "CAMB" and modify the inbuilt parameterization of the power spectrum for scalar and tensor modes accordingly. After performing all the numerical computations via "CAMB" finally from our analysis we have generated all the theoretical CMB angular power spectra from which we observed the following significant features:

- In Fig. 18, at low ℓ region ($2 < l < 49$) the contributions from the running (α_ζ, α_h), and running of running (κ_ζ, κ_h) are very small. Their additional contribution to the CMB power spectrum for scalar and tensor modes becomes unity ($\mathcal{O}(1)$) within low-l region and the original power spectrum becomes unchanged. As a result the tachyonic models will be well fitted with the CMB TT spectrum at low-l region within high cosmic variance as observed by Planck except for a few outliers according

[7] However, it is important to mention here that if we know the mode scalar and tensor mode functions, which are obtained from the exact solution of Mukhanov–Sasaki equation for exactly Bunch–Davies vacuum or for any arbitrary vacuum then one can implement the exact structural form of the primordial power spectra. But within the slow-roll regime of inflation the presented version of the parametrization of the power spectra is exactly compatible with the exact power spectrum from the solution of the Mukhanov–Sasaki equation.

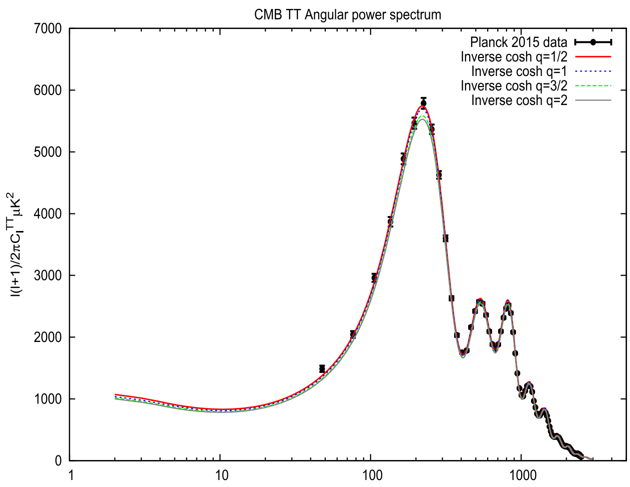

(a) $l(l+1)C_l^{TT}/2\pi$ vs l (scalar)

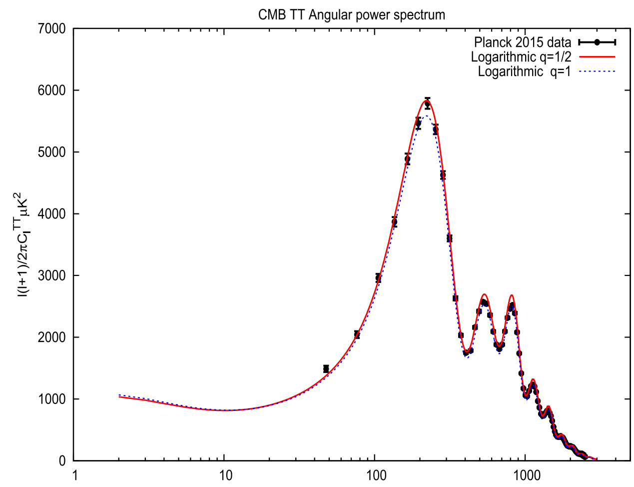

(b) $l(l+1)C_l^{TT}/2\pi$ vs l (scalar)

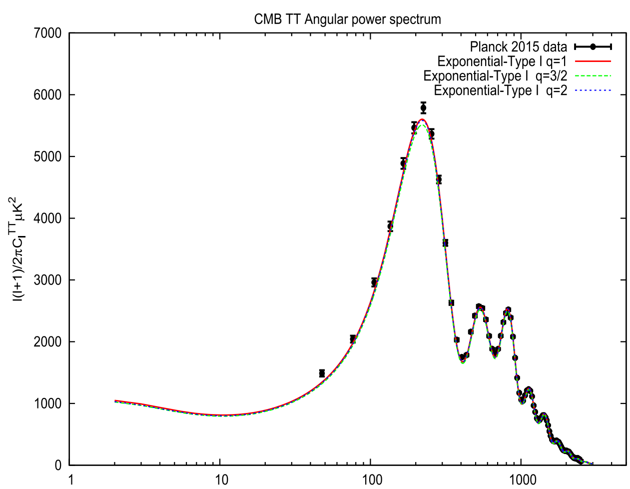

(c) $l(l+1)C_l^{TT}/2\pi$ vs l (scalar)

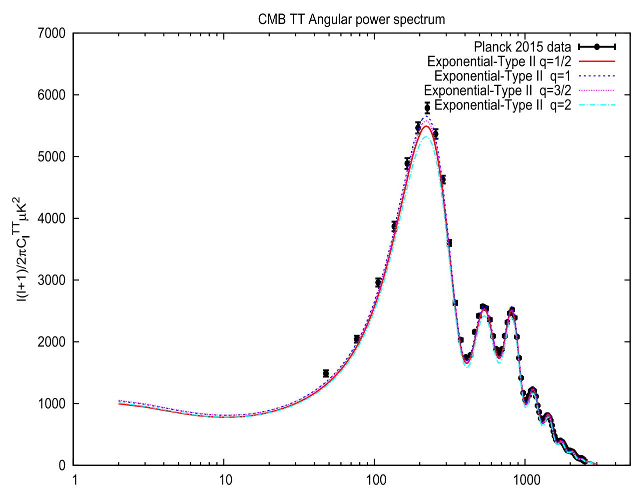

(d) $l(l+1)C_l^{TT}/2\pi$ vs l (scalar)

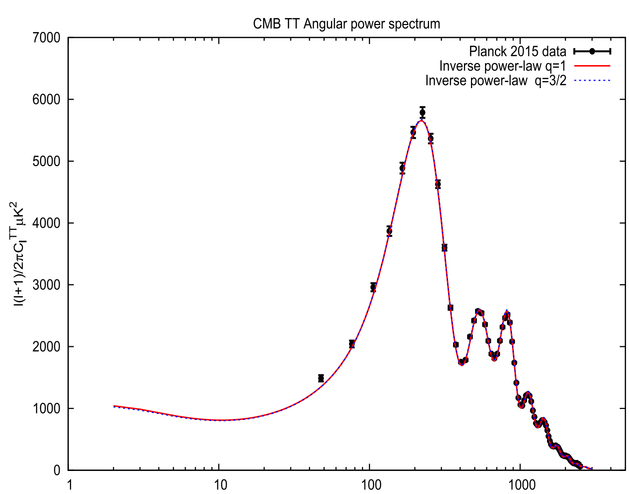

(e) $l(l+1)C_l^{TT}/2\pi$ vs l (scalar)

Fig. 18 We show the variation of CMB TT angular power spectrum with respect to the multipole, l, for scalar modes for all five tachyonic models to the Planck 2013 data release.[8] But to update our analysis with the latest Planck 2015 data set we have not shown such high cosmic variance explicitly. In case of WMAP9 data for CMB TT spectrum the cosmic variance in the low-l region is not very large compared to the Planck low-l data. But our tachyonic models are also well fitted with WMAP9 low-l data, which we have not shown explicitly in the plot to update the analysis using Planck 2015 data. It is also important to mention that if we incorporate the uncertainties in the scanning multipole l for the measurement of CMB TT spectrum, then also our prescribed analysis is fairly consistent with the Planck 2015 data. Further if we move toward the high ℓ regime ($47 < l < 2500$) the contributions of running and running of running become stronger, and this will enhance the power spectrum to a permissible value such that it will accurately fit high-l data within very a small cosmic variance as observed by Planck. In this way one can easily scan over all the multipoles starting from low-l to high-l using the same momentum dependent parameterization of the tensor-to-scalar ratio.

- From Fig. 18, we see that the Sachs–Wolfe plateau obtained from our proposed tachyonic models is non-flat, confirming the appearance of running, and running of the running in the spectrum observed for low l region ($l < 47$). For larger values of the multipole ($47 < l < 2500$), the CMB anisotropy spectrum is dominated by the baryon acoustic oscillations (BAO), giving rise to several ups and downs in the CMB TT spectrum. In the low l region due to the presence of very large cosmic variance there may be other pre-inflationary scenarios which might be able to describe the TT-power spectrum better. In our study we have considered only the possibility for which the behavior of tachyonic models is analyzed for both low and high l regions.
- From Figs. 18, 19, 20, we observe that if we include the uncertainties in multipole l as well in the observed CMB angular power spectra then the proposed tachyonic models is fairly consistent with the CMB TT, TE, EE for scalar mode from Planck 2015 data.
- In Figs. 21, 22, 23 and 24 we have explicitly shown the theoretical CMB BB, TT, TE and EE angular power spectra from the tensor mode. Most importantly, if the inflationary paradigm is responsible for the nearly de Sitter expansion of the early universe then the CMB BB spectra for tensor modes is one of the prime components through which one can detect the contribution for primordial gravitational waves via the tensor-to-scalar ratio. But till date only the contribution from the lensing B-modes are detected via South Pole Telescope and Planck 2015 +BICEP2/Keck Array joint mission. But confirming the sole inflationary origin from the detection of the de-lensed version of the signal is not sufficient to draw any final conclusion.[9] There are other possibilities as well through which it is possible to generate CMB B-modes—those components are the primordial magnetic field, gravitational lensing, CP asymmetry in the lepton sector of particle physics, etc.

5.2 Computation for assisted inflation

In the case of assisted inflation [134–137] all the tachyons would follow a similar trajectory with a unique late time attractor.[10] In more technical language one can state that

$$T_1 \sim T_2 \sim \cdots T_M \equiv T_i = T \quad \forall\, i = 1, 2, \ldots, M. \tag{5.314}$$

Most importantly the detailed computation of the density and tensor perturbation responsible for the anisotropy of CMB depends on this late time attractor behavior of the fields.

5.2.1 *Condition for inflation*

For assisted tachyonic inflation, the prime condition for inflation is given by

$$\dot{H} + H^2 = \left(\frac{\ddot{a}}{a}\right) = -\sum_{i=1}^{M} \frac{(\rho_i + 3p_i)}{6M_p^2} = \frac{(\rho + 3p)}{6M_p^2} > 0 \tag{5.315}$$

which can be re-expressed in terms of the following constraint condition in the context of assisted tachyonic inflation:

$$\sum_{i=1}^{M} \frac{V(T_i)}{3M_p^2\sqrt{1-\alpha'\dot{T}_i^2}}\left(1 - \frac{3}{2}\alpha'\dot{T}_i^2\right) = \frac{MV(T)}{3M_p^2\sqrt{1-\alpha'\dot{T}^2}}\left(1 - \frac{3}{2}\alpha'\dot{T}^2\right) > 0. \tag{5.316}$$

Here Eq. (5.316) implies that to satisfy inflationary constraints in the slow-roll regime the following constraint always holds good:

$$\dot{T} < \sqrt{\frac{2}{3\alpha'}} \quad \forall\, i = 1, 2, \ldots, M, \tag{5.317}$$

$$\ddot{T} < 3H\dot{T} < \sqrt{\frac{6}{\alpha'}}H \quad \forall\, i = 1, 2, \ldots, M. \tag{5.318}$$

[8] From Fig. 18 it is observed that for the inverse cosh and logarithmic model $q = 1/2$, exponential Type-I and Type-II model $q = 1$, inverse power-law model $q = 1$ and $q = 3/2$ generalized characteristic indices are well fitted with Planck 2015 data.

[9] In this respect one may consider the alternative frameworks of inflationary paradigm as well.

[10] We also suggest the reader to read Ref. [138] for completeness.

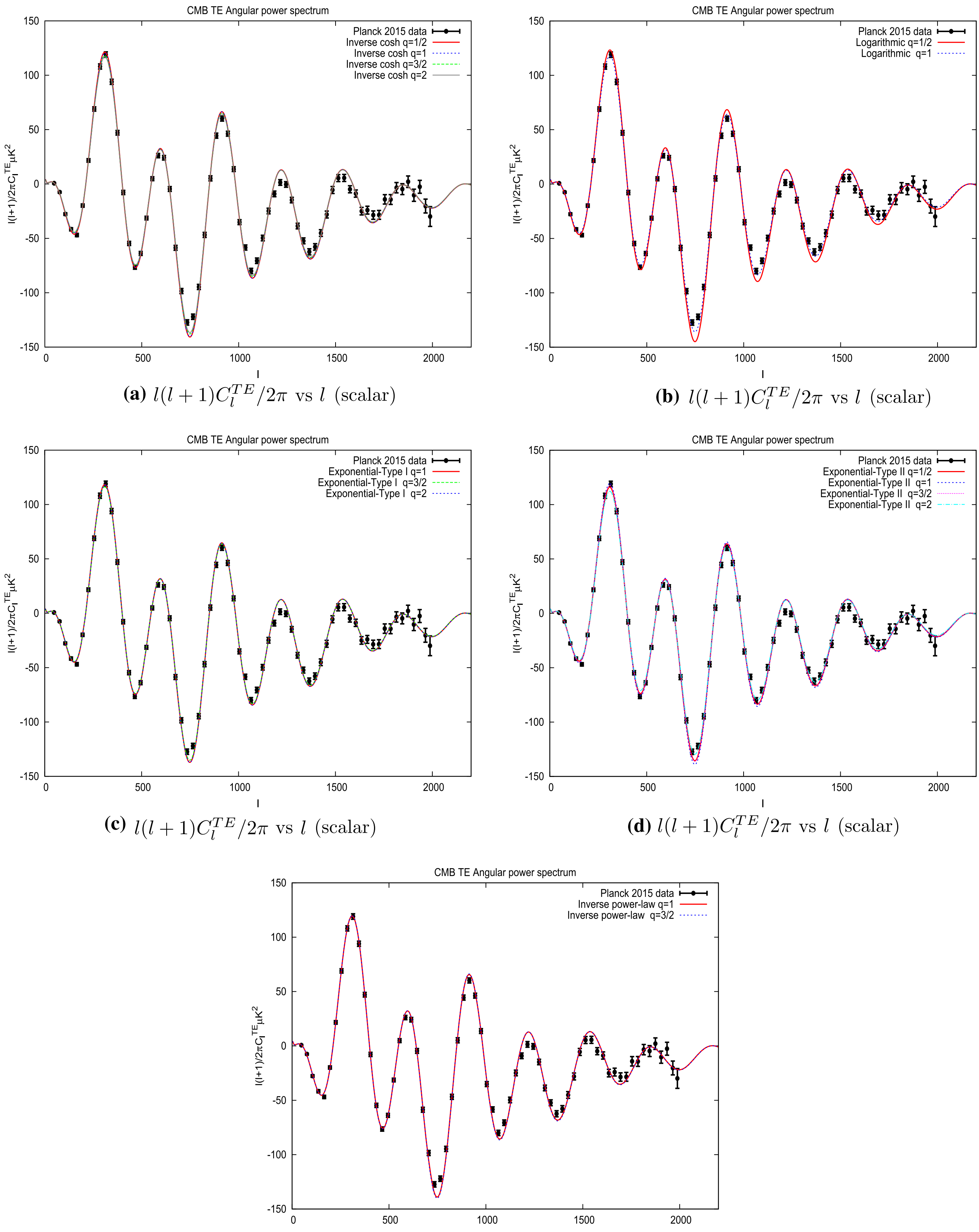

(a) $l(l+1)C_l^{TE}/2\pi$ vs l (scalar)

(b) $l(l+1)C_l^{TE}/2\pi$ vs l (scalar)

(c) $l(l+1)C_l^{TE}/2\pi$ vs l (scalar)

(d) $l(l+1)C_l^{TE}/2\pi$ vs l (scalar)

(e) $l(l+1)C_l^{TE}/2\pi$ vs l (scalar)

Fig. 19 We show the variation of CMB TE angular power spectrum with respect to the multipole, l, for scalar modes for all five tachyonic models

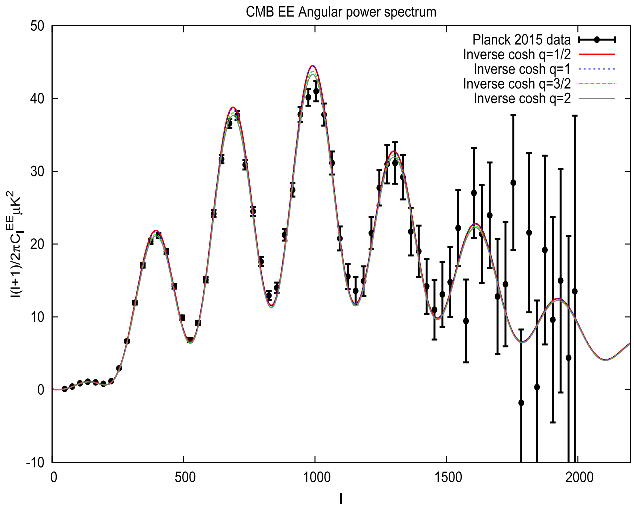

(a) $l(l+1)C_l^{EE}/2\pi$ vs l (scalar)

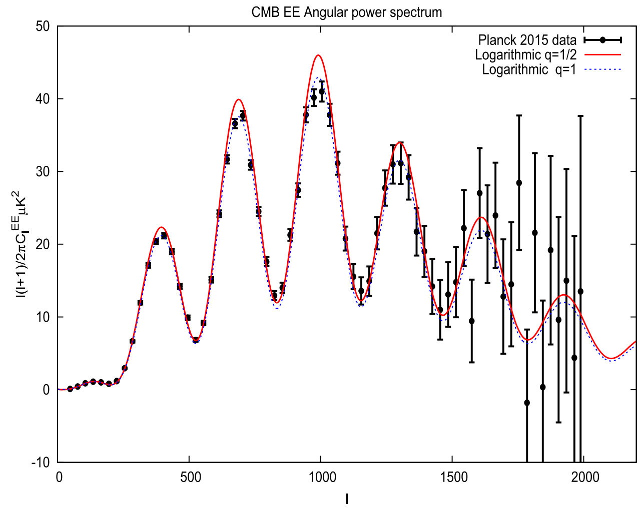

(b) $l(l+1)C_l^{EE}/2\pi$ vs l (scalar)

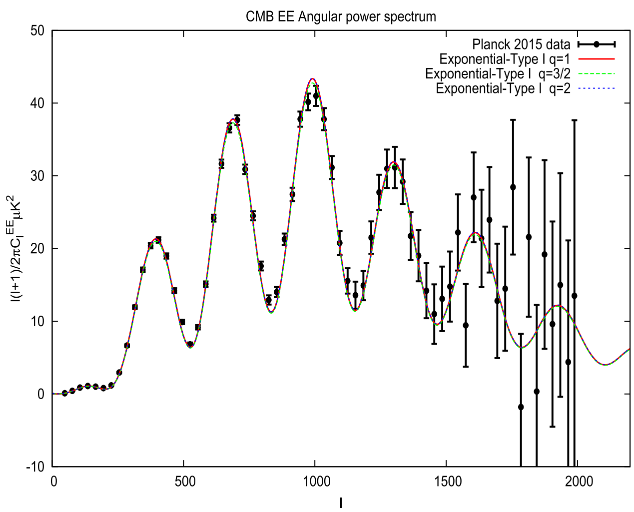

(c) $l(l+1)C_l^{EE}/2\pi$ vs l (scalar)

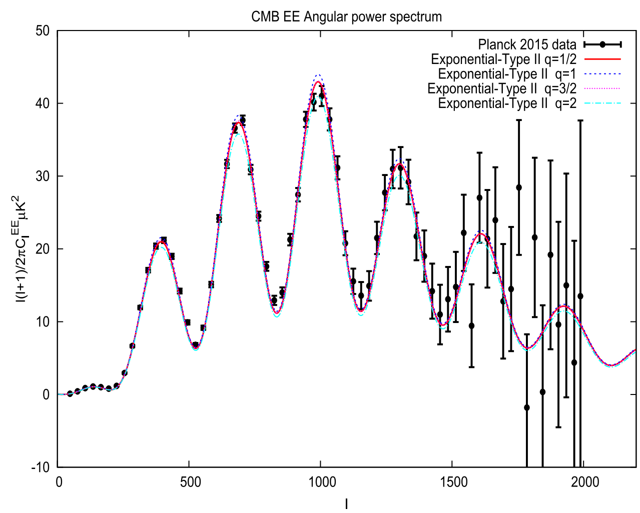

(d) $l(l+1)C_l^{EE}/2\pi$ vs l (scalar)

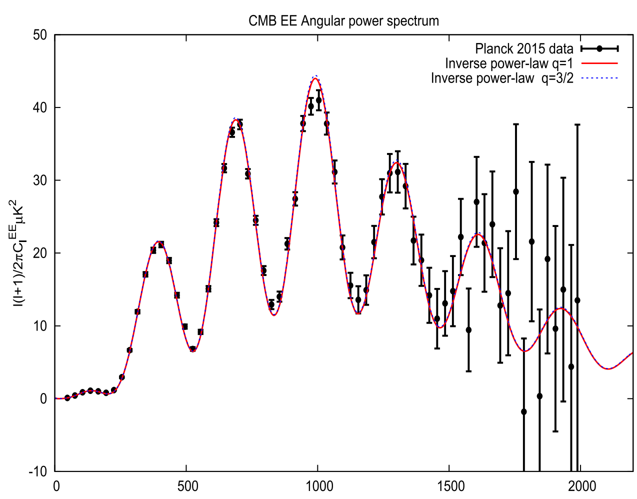

(e) $l(l+1)C_l^{EE}/2\pi$ vs l (scalar)

Fig. 20 We show the variation of CMB EE angular power spectrum with respect to the multipole, l, for scalar modes for all five tachyonic models

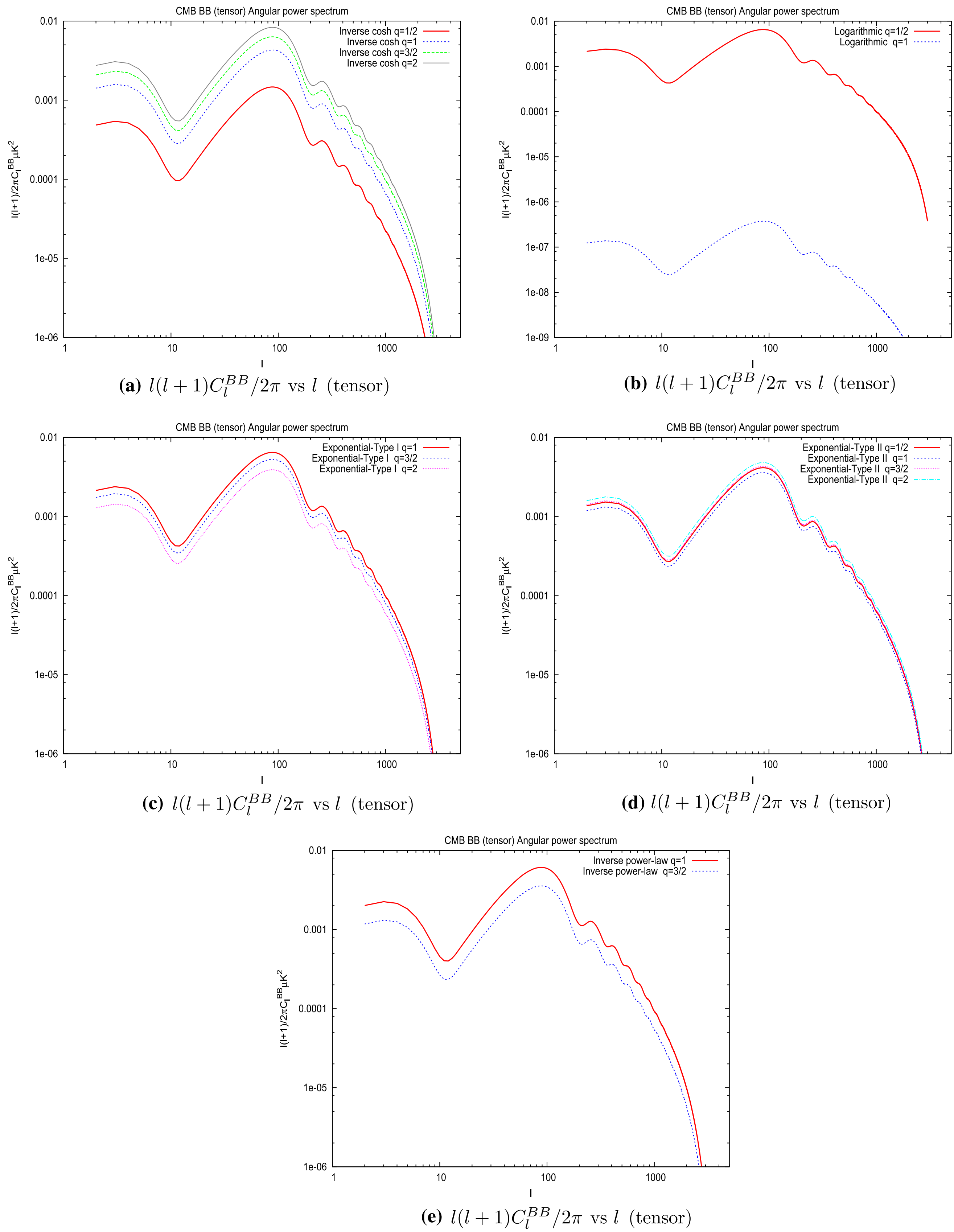

(a) $l(l+1)C_l^{BB}/2\pi$ vs l (tensor)

(b) $l(l+1)C_l^{BB}/2\pi$ vs l (tensor)

(c) $l(l+1)C_l^{BB}/2\pi$ vs l (tensor)

(d) $l(l+1)C_l^{BB}/2\pi$ vs l (tensor)

(e) $l(l+1)C_l^{BB}/2\pi$ vs l (tensor)

Fig. 21 We show the variation of CMB BB angular power spectrum with respect to the multipole, l, for tensor modes for all five tachyonic models

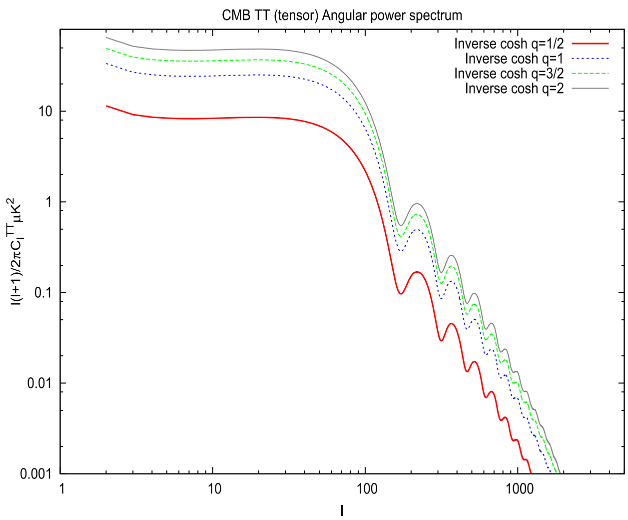

(a) $l(l+1)C_l^{TT}/2\pi$ vs l (tensor)

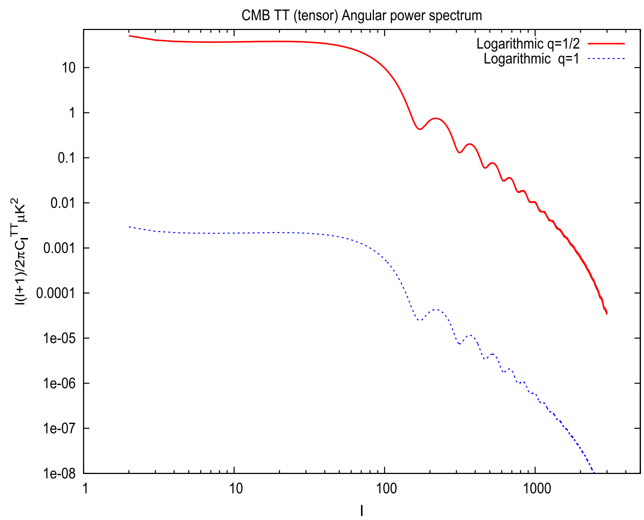

(b) $l(l+1)C_l^{TT}/2\pi$ vs l (tensor)

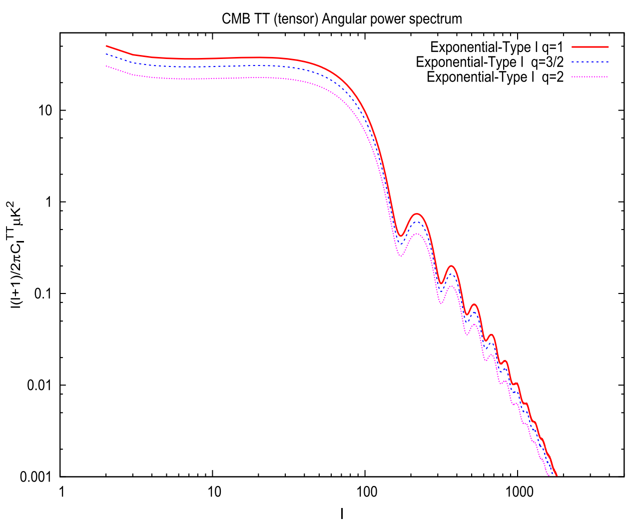

(c) $l(l+1)C_l^{TT}/2\pi$ vs l (tensor)

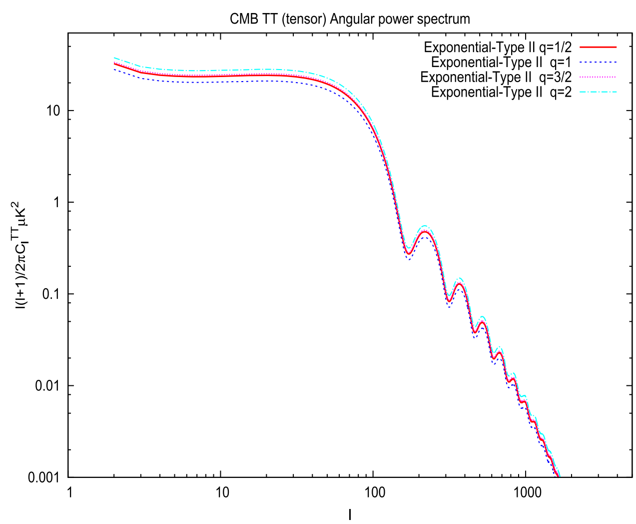

(d) $l(l+1)C_l^{TT}/2\pi$ vs l (tensor)

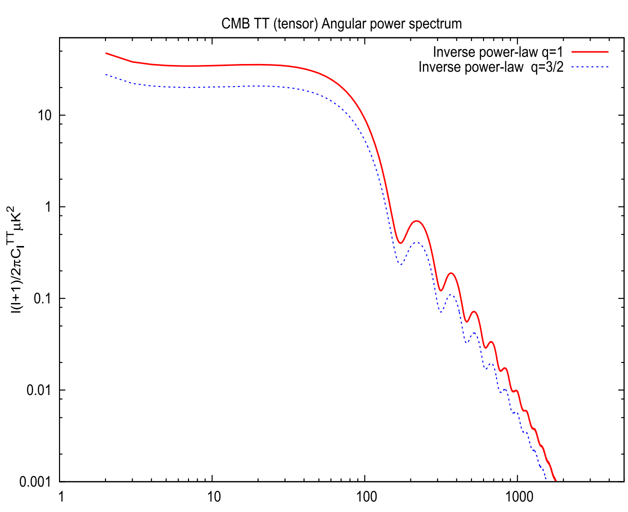

(e) $l(l+1)C_l^{TT}/2\pi$ vs l (tensor)

Fig. 22 We show the variation of CMB TT angular power spectrum with respect to the multipole, l, for tensor modes for all five tachyonic models

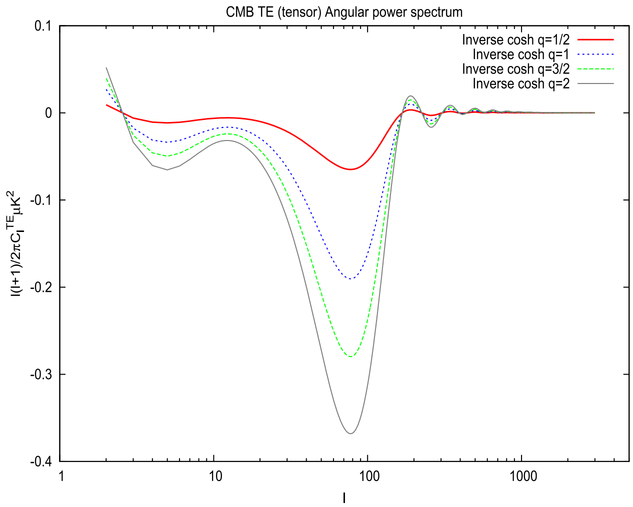

(a) $l(l+1)C_l^{TE}/2\pi$ vs l (tensor)

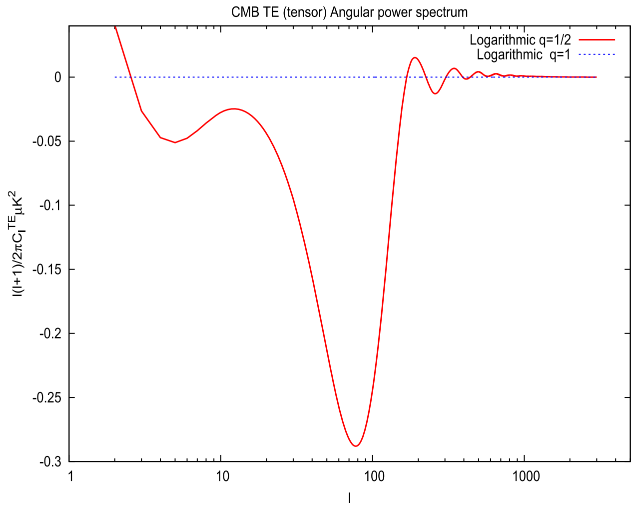

(b) $l(l+1)C_l^{TE}/2\pi$ vs l (tensor)

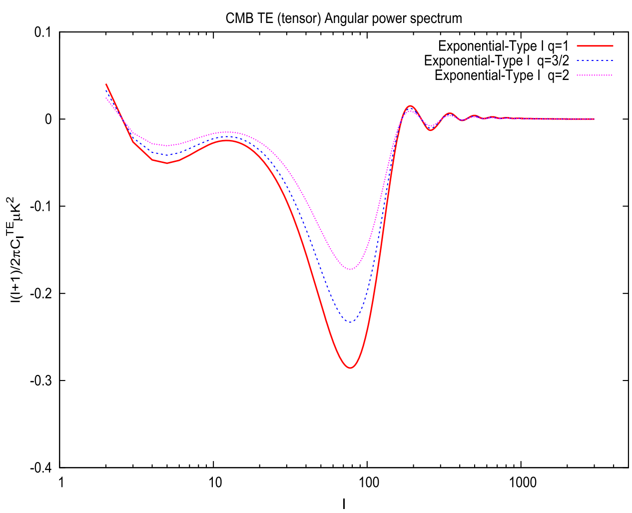

(c) $l(l+1)C_l^{TE}/2\pi$ vs l (tensor)

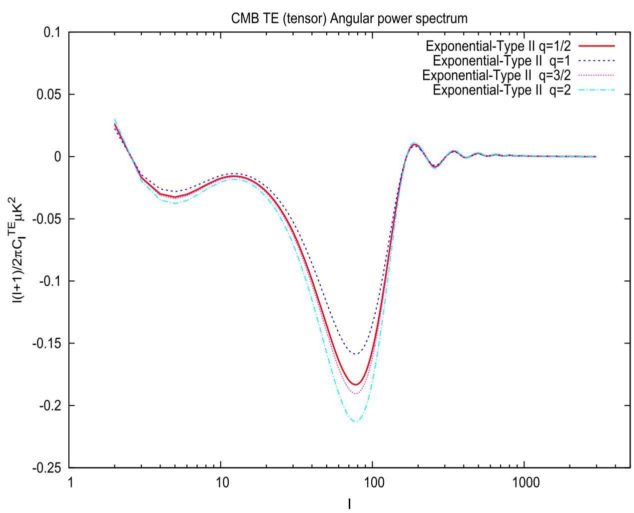

(d) $l(l+1)C_l^{TE}/2\pi$ vs l (tensor)

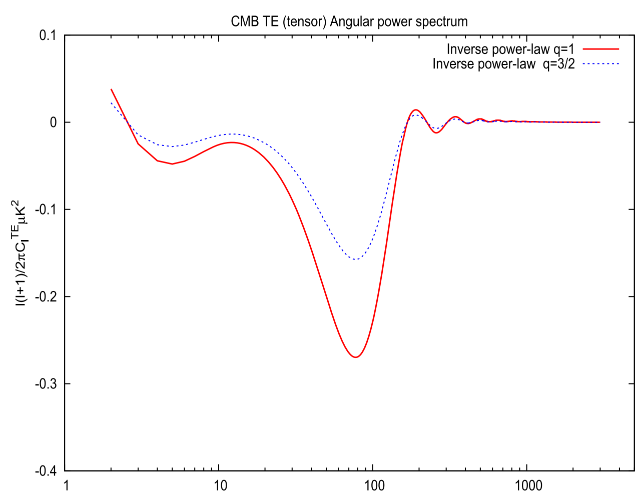

(e) $l(l+1)C_l^{TE}/2\pi$ vs l (tensor)

Fig. 23 We show the variation of CMB TE angular power spectrum with respect to the multipole, l, for tensor modes for all five tachyonic models

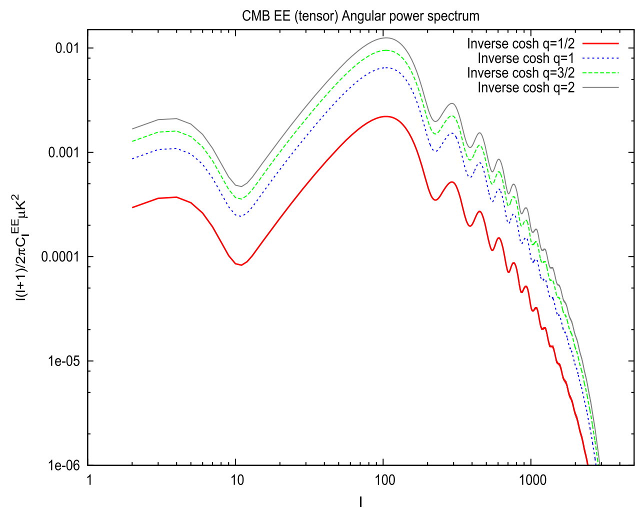

(a) $l(l+1)C_l^{EE}/2\pi$ vs l (tensor)

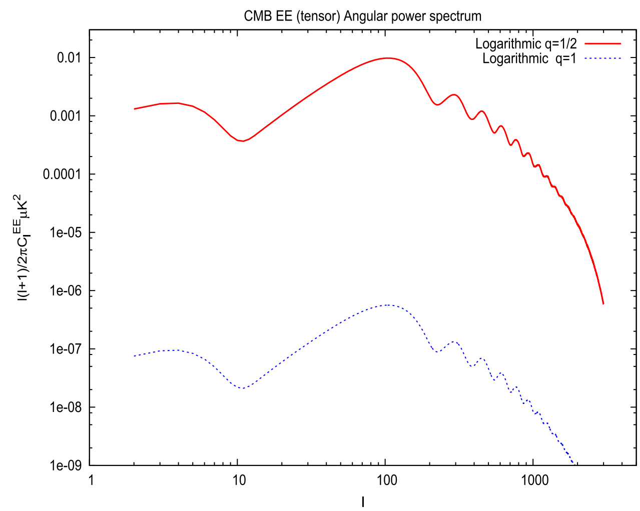

(b) $l(l+1)C_l^{EE}/2\pi$ vs l (tensor)

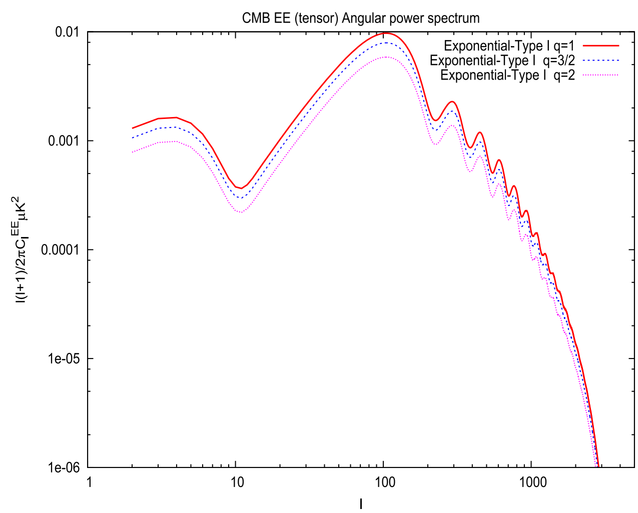

(c) $l(l+1)C_l^{EE}/2\pi$ vs l (tensor)

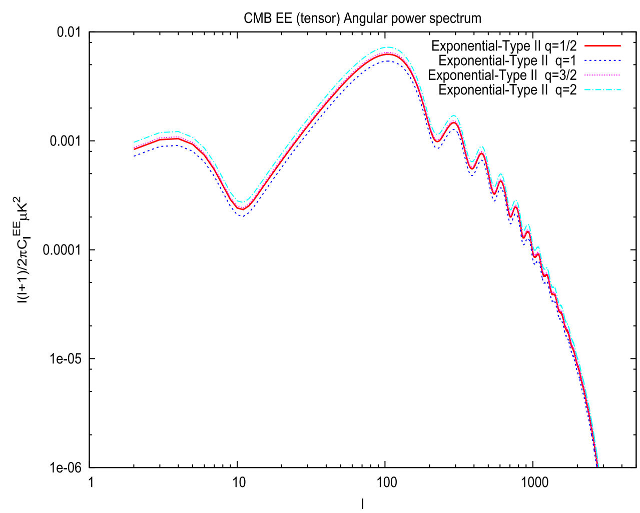

(d) $l(l+1)C_l^{EE}/2\pi$ vs l (tensor)

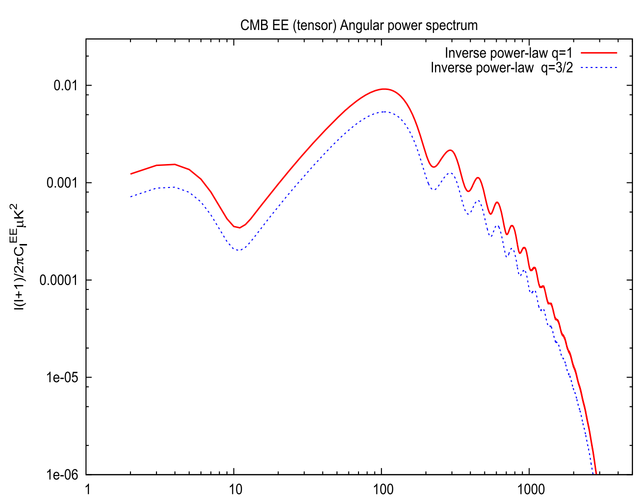

(e) $l(l+1)C_l^{EE}/2\pi$ vs l (tensor)

Fig. 24 We show the variation of CMB EE angular power spectrum with respect to the multipole, l, for tensor modes for all five tachyonic models

$$0=\begin{cases}\frac{1}{\sqrt{-g}}\partial_\mu\left(\sqrt{-g}V_{eff}(T_1,\chi_i)\sqrt{1+g^{\alpha\beta}\partial_\alpha\chi_i\partial_\beta\chi_i}\right)\\ \quad=\frac{\alpha'\ddot{\chi}_i}{(1-\alpha'\dot{\chi}_i^2)}+3H\alpha'\dot{\chi}_i+\frac{\mathrm{d}V_{eff}(T_1,\chi_i)}{V_{eff}(T_1,\chi_i)\mathrm{d}\chi_i}, & \text{for}\quad q=1/2,\\ \frac{1}{\sqrt{-g}}\partial_\mu\left(\sqrt{-g}V_{eff}(T_1,\chi_i)\left(1+g^{\alpha\beta}\partial_\alpha\chi_i\partial_\beta\chi_i\right)^q\right)\\ \quad=\frac{2q\alpha'\ddot{\chi}_i}{(1-\alpha'\dot{\chi}_i^2)}+6q\alpha'H\frac{\dot{\chi}_i}{1-\alpha'(1-2q)\dot{\chi}_i^2}+\frac{\mathrm{d}V_{eff}(T_1,\chi_i)}{V_{eff}(T_1,\chi_i)\mathrm{d}\chi_i}, & \text{for any}\ q,\end{cases} \tag{5.328}$$

Consequently the field equations are approximated by

$$3H\alpha'\dot{T}_i+\frac{\mathrm{d}V(T_i)}{V(T_i)\mathrm{d}T_i}\approx 0\quad\forall\, i=1,2,\ldots,M, \tag{5.319}$$

Similarly, in the most generalized case,

$$\sum_{i=1}^{M}\frac{V(T_i)}{3M_p^2\left(1-\alpha'\dot{T}_i^2\right)^{1-q}}\left(1-(1+q)\alpha'\dot{T}_i^2\right)=\frac{MV(T)}{3M_p^2\left(1-\alpha'\dot{T}^2\right)^{1-q}}\left(1-(1+q)\alpha'\dot{T}^2\right)>0. \tag{5.320}$$

Here Eq. (5.320) implies that to satisfy inflationary constraints in the slow-roll regime the following constraint always holds good:

$$\dot{T}<\sqrt{\frac{1}{\alpha'(1+q)}}\quad\forall\, i=1,2,\ldots,M, \tag{5.321}$$

$$\ddot{T}<3H\dot{T}<\sqrt{\frac{9}{\alpha'(1+q)}}H\quad\forall\, i=1,2,\ldots,M. \tag{5.322}$$

Consequently the field equations are approximated by

$$6q\alpha'H\dot{T}_i+\frac{\mathrm{d}V(T_i)}{V(T_i)\mathrm{d}T_i}\approx 0\quad\forall\, i=1,2,\ldots,M. \tag{5.323}$$

Also for both cases in the slow-roll regime the Friedmann equation is modified as

$$H^2\approx\sum_{i=1}^{M}\frac{V(T_i)}{3M_p^2}=\frac{MV(T)}{3M_p^2}. \tag{5.324}$$

The equation of motions can be mapped to the equations of a model with a single tachyonic field using the following redefinitions:

$$\tilde{T}=\sqrt{M}T, \tag{5.325}$$

$$\tilde{V}=V(\tilde{T})=MV(T)=\sum_{i=1}^{M}V(T_i). \tag{5.326}$$

Now to show the late time attractor behavior of the solution of scalar fields we keep T_1, but we replace the rest with the redefined fields:

$$\chi_i=T_i-T_1\quad\forall\, i=2,\ldots,M. \tag{5.327}$$

Using Eq. (5.327), at late times the equation of motion can be recast as

where $V_{eff}(T_1,\chi_i)$ represents the effective potential. The minimum in the χ_i direction is always appearing at $\chi_i=0$, regardless of the explicit behavior of the tachyon field T_1. Consequently the late time solution has all the T_i equal. From this analysis it is also observed that the length of the time interval to reach this attractor behavior will depend on the initial separation, i.e., the tachyon field value χ_i and the extent of the frictional contribution coming from the expansion rate H.

It is important to mention that, for assisted inflation, the equation of motion for each tachyon fields follows the following simple relationship:

$$\frac{\mathrm{d}\ln T_i}{\mathrm{d}t}\simeq\frac{\mathrm{d}\ln T}{\mathrm{d}t}\quad\forall\, i=1,2,\ldots,M. \tag{5.329}$$

Further substituting Eq. (5.324) in Eqs. (5.319) and (5.323) we get

$$\frac{\sqrt{3MV(T)}}{M_p}\alpha'\dot{T}_i+\frac{\mathrm{d}V(T_i)}{V(T_i)\mathrm{d}T_i}\approx 0, \tag{5.330}$$

$$6q\frac{\sqrt{MV(T)}}{\sqrt{3}M_p}\alpha'\dot{T}_i+\frac{\mathrm{d}V(T_i)}{V(T_i)\mathrm{d}T_i}\approx 0. \tag{5.331}$$

Finally the general solution for both cases can be expressed in terms of the single field tachyonic potential $V(T)$ as

$$t-t_{in}\approx-\frac{\sqrt{3M}\alpha'}{M_p}\int_{T_{in}}^{T_i}\mathrm{d}T_i\,\frac{\sqrt{V(T)}V(T_i)}{V'(T_i)}, \tag{5.332}$$

$$t-t_{in}\approx-\frac{6q\sqrt{M}\alpha'}{\sqrt{3}M_p}\int_{T_{in}}^{T_i}\mathrm{d}T_i\,\frac{\sqrt{V(T)}V(T_i)}{V'(T_i)}. \tag{5.333}$$

Further using Eqs. (5.15), (5.16) and (5.324) we get the following solution for the scale factor in terms of the tachyonic field for the usual $q=1/2$ and for a generalized value of q:

$$a=a_{in}\times\begin{cases}\exp\left[-\frac{\alpha'M}{M_p^2}\int_{T_{in}}^{T_i}\mathrm{d}T_i\,\frac{V(T)V(T_i)}{V'(T_i)}\right], & \text{for}\quad q=1/2,\\ \exp\left[-\frac{2q\alpha'M}{M_p^2}\int_{T_{in}}^{T_i}\mathrm{d}T_i\,\frac{V(T)V(T_i)}{V'(T_i)}\right], & \text{for any arbitrary}\ q.\end{cases} \tag{5.334}$$

5.2.2 Analysis using slow-roll formalism

Here our prime objective is to define slow-roll parameters for tachyon inflation in terms of the Hubble parameter and the assisted tachyonic inflationary potential. Using the slow-roll approximation one can expand various cosmological observables in terms of small dynamical quantities derived from the appropriate derivatives of the Hubble parameter and of the inflationary potential. To start with here we use the horizon-flow parameters based on the derivatives of the Hubble parameter with respect to the number of e-foldings N, defined as

$$N(t) = \int_{t}^{t_{\rm end}} H(t)\, {\rm d}t, \tag{5.335}$$

where $t_{\rm end}$ signifies the end of inflation. Further, using Eqs. (5.5), (5.9), (5.10) and (5.335), we get

$$\frac{{\rm d}T_i}{{\rm d}N} = \frac{\dot{T}_i}{H} = \begin{cases} -\dfrac{2H'}{3\alpha' H^3}, & \text{for} \quad q = 1/2, \\ -\dfrac{2H'}{3\alpha' H^3}\left(\dfrac{1-\alpha'(1-2q)\dot{T}_i^2}{2q}\right), & \text{for any arbitrary } q, \end{cases} \tag{5.336}$$

where $H' > 0$, which makes always $\dot{T}_i > 0$ during inflationary phase. Further using Eq. (5.336) we get the following differential operator identity for tachyonic inflation:

$$\frac{1}{H}\frac{\rm d}{{\rm d}t} = \frac{\rm d}{{\rm d}N} = \frac{\rm d}{{\rm d}\ln k} = \begin{cases} -\dfrac{2H'}{3\alpha' H^3}\dfrac{\rm d}{{\rm d}T_i}, & \text{for} \quad q = 1/2, \\ -\dfrac{2H'}{3\alpha' H^3}\left(\dfrac{1-\alpha'(1-2q)\dot{T}_i^2}{2q}\right)\dfrac{\rm d}{{\rm d}T_i}, & \text{for any arbitrary } q. \end{cases} \tag{5.337}$$

Further using the differential operator identity as mentioned in Eq. (5.337) we get the following Hubble flow equation for tachyonic inflation for $j \geq 0$:

$$\frac{1}{H}\frac{{\rm d}\epsilon_i}{{\rm d}t} = \frac{{\rm d}\epsilon_j}{{\rm d}N} = \epsilon_{j+1}\epsilon_j = \begin{cases} -\dfrac{2H'}{3\alpha' H^3}\dfrac{{\rm d}\epsilon_j}{{\rm d}T_i}, & \text{for} \quad q = 1/2, \\ -\dfrac{2H'}{3\alpha' H^3}\left(\dfrac{1-\alpha'(1-2q)\dot{T}_i^2}{2q}\right)\dfrac{{\rm d}\epsilon_j}{{\rm d}T_i}, & \text{for any arbitrary } q. \end{cases} \tag{5.338}$$

For a realistic estimate from the single field tachyonic inflationary model substituting the free index j to $j = 0, 1, 2$ in Eqs. (5.23) and (5.338) we get the contributions from the first three Hubble slow-roll parameters, which can be represented as

$$\epsilon_1 = \frac{{\rm d}\ln|\epsilon_0|}{{\rm d}N} = -\frac{\dot{H}}{H^2} = \begin{cases} \dfrac{2}{3\alpha'}\left(\dfrac{H'}{H^2}\right)^2 = \dfrac{3}{2}\alpha'\dot{T}_i^2, & \text{for} \quad q = 1/2, \\ \dfrac{2}{3\alpha'}\left(\dfrac{H'}{H^2}\right)^2\left(\dfrac{1-\alpha'(1-2q)\dot{T}_i^2}{2q}\right) & \\ \quad = \dfrac{3}{2}\alpha'\dot{T}_i^2\left(\dfrac{2q}{1-\alpha'(1-2q)\dot{T}_i^2}\right), & \text{for any arbitrary } q, \end{cases} \tag{5.339}$$

$$\epsilon_2 = \frac{{\rm d}\ln|\epsilon_1|}{{\rm d}N} = \frac{\ddot{H}}{H\dot{H}} + 2\epsilon_1 = \begin{cases} \sqrt{\dfrac{2}{3\alpha'\epsilon_1}}\dfrac{\epsilon_1'}{H} = 2\dfrac{\ddot{T}_i}{H\dot{T}_i}, & \text{for} \quad q = 1/2, \\ \sqrt{\dfrac{2}{3\alpha'\epsilon_1}\left(\dfrac{1-\alpha'(1-2q)\dot{T}_i^2}{2q}\right)}\dfrac{\epsilon_1'}{H} & \\ \quad = \dfrac{2\ddot{T}_i}{H\dot{T}\left(1-\alpha'(1-2q)\dot{T}_i^2\right)}, & \text{for any arbitrary } q, \end{cases} \tag{5.340}$$

$$\epsilon_3 = \frac{\mathrm{d}\ln|\epsilon_2|}{\mathrm{d}N} = \frac{1}{\epsilon_2}\left[\frac{\dddot{H}}{H^2\dot{H}} - 3\frac{\ddot{H}}{H^3} - \frac{\ddot{H}^2}{H^2\dot{H}^2} + 4\frac{\dot{H}^2}{H^4}\right]$$

$$= \begin{cases} \sqrt{\frac{2\epsilon_1}{3\alpha'}}\frac{\epsilon_2'}{H} = \left[\frac{2\dddot{T}_i}{H^2\dot{T}_i\epsilon_2} + \epsilon_1 - \frac{\epsilon_2}{2}\right], & \text{for} \quad q = 1/2, \\ \sqrt{\frac{2\epsilon_1}{3\alpha'}\left(\frac{1-\alpha'(1-2q)\dot{T}_i^2}{2q}\right)}\frac{\epsilon_2'}{H} & \\ \quad = \frac{\left[\frac{2\dddot{T}_i}{H^2\dot{T}_i\epsilon_2} + \epsilon_1 - \frac{\epsilon_2}{2}\right]}{\left(1-\alpha'(1-2q)\dot{T}_i^2\right)} + \frac{\frac{4\alpha'(1-2q)\ddot{T}_i^2}{H}}{\left(1-\alpha'(1-2q)\dot{T}_i^2\right)^2}, & \text{for any arbitrary } q. \end{cases} \tag{5.341}$$

Further using Eqs. (5.339), (5.340), (5.343), (5.34) and (5.35) one can re-express the Hubble slow-roll parameters in terms of the potential dependent slow-roll parameter as

$$\epsilon_1 \approx \begin{cases} \frac{M_p^2}{2\alpha'}\frac{V'^2(T_i)}{MV(T)V^2(T_i)} = \frac{\epsilon_V(T_i)}{MV(T)\alpha'} \equiv \bar{\epsilon}_V(T_i), & \text{for} \quad q = 1/2, \\ \frac{M_p^2}{4q\alpha'}\frac{V'^2(T_i)}{MV(T)V^2(T_i)} = \frac{\epsilon_V(T_i)}{2qMV(T)\alpha'} \equiv \frac{\bar{\epsilon}_V(T_i)}{2q}, & \text{for any } q, \end{cases} \tag{5.342}$$

$$\epsilon_2 \approx \begin{cases} \frac{M_p^2}{\alpha' M}\left(3\frac{V'^2(T_i)}{V(T)V^2(T_i)} - 2\frac{V''(T_i)}{V(T)V(T_i)}\right) & \\ \quad = \frac{2\left(3\epsilon_V(T_i) - \eta_V(T_i)\right)}{MV(T)\alpha'} = 2\left(3\bar{\epsilon}_V(T_i) - \bar{\eta}_V(T_i)\right), & \text{for} \quad q = 1/2, \\ \frac{M_p^2}{\sqrt{2q}\alpha' M}\left(3\frac{V'^2(T_i)}{V(T)V^2(T_i)} - 2\frac{V''(T_i)}{V(T)V(T_i)}\right) & \\ \quad = \frac{\sqrt{\frac{2}{q}}\left(3\epsilon_V(T_i) - \eta_V(T_i)\right)}{MV(T)\alpha'} = \sqrt{\frac{2}{q}}\left(3\bar{\epsilon}_V(T_i) - \bar{\eta}_V(T_i)\right), & \text{for any } q \end{cases}$$

$$\epsilon_3\epsilon_2 \approx \begin{cases} \frac{M_p^4}{M^2V^2(T)\alpha'^2}\left(2\frac{V'''(T_i)V'(T_i)}{V^2(T_i)} - 10\frac{V''(T_i)V'^2(T_i)}{V^3(T_i)} + 9\frac{V'^4(T_i)}{V^4(T_i)}\right) & \\ \quad = \frac{\left(2\xi_V^2(T_i) - 5\eta_V(T_i)\epsilon_V(T_i) + 36\epsilon_V^2(T_i)\right)}{M^2V^2(T)\alpha'^2} & \\ \quad = \left(2\bar{\xi}_V^2(T_i) - 5\bar{\eta}_V(T_i)\bar{\epsilon}_V(T_i) + 36\bar{\epsilon}_V^2(T_i)\right), & \text{for} \quad q = 1/2, \\ \frac{M_p^4}{M^2\sqrt{2q}V^2(T)\alpha'^2}\left(2\frac{V'''(T_i)V'(T_i)}{V^2(T_i)} - 10\frac{V''(T_i)V'^2(T_i)}{V^3(T_i)} + 9\frac{V'^4(T_i)}{V^4(T_i)}\right) & \\ \quad = \frac{\left(2\xi_V^2(T_i) - 5\eta_V(T_i)\epsilon_V(T_i) + 36\epsilon_V^2(T_i)\right)}{M^2\sqrt{2q}V^2(T)\alpha'^2} & \\ \quad = \frac{\left(2\bar{\xi}_V^2(T_i) - 5\bar{\eta}_V(T_i)\bar{\epsilon}_V(T_i) + 36\bar{\epsilon}_V^2(T_i)\right)}{\sqrt{2q}}, & \text{for any } q, \end{cases} \tag{5.343}$$

where $' = \mathrm{d}/\mathrm{d}T_i$ and the potential dependent slow-roll parameters $\epsilon_V, \eta_V, \xi^2_V, \sigma^3_V$ are defined as

$$\epsilon_V(T_i) = \frac{M_p^2}{2}\left(\frac{V'(T_i)}{V(T_i)}\right)^2, \tag{5.344}$$

$$\eta_V(T_i) = M_p^2\left(\frac{V''(T_i)}{V(T_i)}\right), \tag{5.345}$$

$$\xi^2_V(T_i) = M_p^4\left(\frac{V'(T_i)V'''(T_i)}{V^2(T_i)}\right), \tag{5.346}$$

$$\sigma^3_V(T_i) = M_p^6\left(\frac{V'^2(T_i)V''''(T_i)}{V^3(T_i)}\right), \tag{5.347}$$

which is exactly similar to the expression for the slow-roll parameter as appearing in the context of single field slow-roll inflationary models. However, for the sake of clarity here we introduce new sets of potential dependent slow-roll parameters for tachyonic inflation by rescaling with the appropriate powers of $\alpha' V(T)$:

$$\bar{\epsilon}_V(T_i) = \frac{\epsilon_V(T_i)}{M\alpha' V(T)} = \frac{M_p^2}{2M\alpha' V(T)}\left(\frac{V'(T_i)}{V(T_i)}\right)^2 = \frac{\bar{\epsilon}_V}{M}, \tag{5.348}$$

$$\bar{\eta}_V(T_i) = \frac{\eta_V(T_i)}{M\alpha' V(T)} = \frac{M_p^2}{M\alpha' V(T)}\left(\frac{V''(T_i)}{V(T_i)}\right) = \frac{\bar{\eta}_V}{M}, \tag{5.349}$$

$$\bar{\xi}^2_V(T_i) = \frac{\xi^2_V(T_i)}{M^2\alpha'^2 V^2(T)} = \frac{M_p^4}{M^2\alpha'^2 V^2(T)}\left(\frac{V'(T_i)V'''(T_i)}{V^2(T_i)}\right) = \frac{\bar{\xi}^2_V}{M^2}, \tag{5.350}$$

$$\bar{\sigma}^3_V(T_i) = \frac{\sigma^3_V(T_i)}{M^3\alpha'^3 V^3(T)} = \frac{M_p^6}{M^2\alpha'^3 V^3(T)}\left(\frac{V'^2(T_i)V''''(T_i)}{V^3(T_i)}\right) = \frac{\bar{\sigma}^3_V}{M^3}. \tag{5.351}$$

where $\bar{\epsilon}_V, \bar{\eta}_V, \bar{\xi}^2_V$ and $\bar{\sigma}^3_V$ are the single field tachyonic slow-roll parameters. Further using Eqs. (5.344)–(5.470) we get the following operator identity for tachyonic inflation:

$$\frac{1}{H}\frac{\mathrm{d}}{\mathrm{d}t} = \frac{\mathrm{d}}{\mathrm{d}N} = \frac{\mathrm{d}}{\mathrm{d}\ln k} \approx \begin{cases} \sqrt{\dfrac{2\bar{\epsilon}_V(T_i)}{MV(T)\alpha'}}M_p\left(1-\dfrac{2}{3}\bar{\epsilon}_V(T_i)\right)^{1/4}\dfrac{\mathrm{d}}{\mathrm{d}T_i}, & \text{for } \quad q = 1/2, \\ \sqrt{\dfrac{2\bar{\epsilon}_V(T_i)}{MV(T)\alpha'}}\dfrac{M_p}{2q}\left(1-\dfrac{1}{3q}\bar{\epsilon}_V(T_i)\right)^{1/4}\dfrac{\mathrm{d}}{\mathrm{d}T_i}, & \text{for any arbitrary } q. \end{cases} \tag{5.352}$$

Finally using Eq. (5.352) we get the following sets of flow equations in the context of tachyonic inflation:

$$\frac{\mathrm{d}\epsilon_1}{\mathrm{d}N} = \begin{cases} \dfrac{\mathrm{d}\bar{\epsilon}_V(T_i)}{\mathrm{d}N} = \dfrac{2}{M^2}\bar{\epsilon}_V\left(\bar{\eta}_V - 3\bar{\epsilon}_V\right)\left(1-\dfrac{2}{3}\dfrac{\bar{\epsilon}_V}{M}\right)^{1/4}, & \text{for } \quad q = 1/2, \\ \dfrac{1}{2q}\dfrac{\mathrm{d}\bar{\epsilon}_V(T_i)}{\mathrm{d}N} = \dfrac{\bar{\epsilon}_V}{qM^2}\left(\bar{\eta}_V - 3\bar{\epsilon}_V\right)\left(1-\dfrac{1}{3q}\dfrac{\bar{\epsilon}_V}{M}\right)^{1/4}, & \text{for any } q, \end{cases} \tag{5.353}$$

$$\frac{\mathrm{d}\epsilon_2}{\mathrm{d}N} = \begin{cases} \dfrac{2}{M^2}\left(10\bar{\epsilon}_V\bar{\eta}_V - 18\bar{\epsilon}^2_V - \bar{\xi}^2_V\right)\left(1-\dfrac{2}{3}\dfrac{\bar{\epsilon}_V}{M}\right)^{1/4}, & \text{for } \quad q = 1/2, \\ \dfrac{\sqrt{\frac{2}{q}}}{M^2}\left(10\bar{\epsilon}_V\bar{\eta}_V - 18\bar{\epsilon}^2_V - \bar{\xi}^2_V\right)\left(1-\dfrac{1}{3q}\dfrac{\bar{\epsilon}_V}{M}\right)^{1/4}, & \text{for any } q, \end{cases} \tag{5.354}$$

$$\frac{d(\epsilon_2\epsilon_3)}{dN} = \begin{cases} \frac{1}{M^3}\Big(2\bar{\sigma}_V^3 - 216\bar{\epsilon}_V^3 + 2\bar{\xi}_V^2\bar{\eta}_V - 7\bar{\xi}_V^2\bar{\epsilon}_V \\ \quad + 194\bar{\epsilon}_V^2\bar{\eta}_V - 10\bar{\eta}_V\bar{\epsilon}_V\Big)\left(1 - \frac{2}{3}\bar{\epsilon}_V\frac{\bar{\epsilon}_V}{M}\right)^{1/4}, & \text{for } q = 1/2, \\ \frac{1}{M^3\sqrt{2q}}\Big(2\bar{\sigma}_V^3 - 216\bar{\epsilon}_V^3 + 2\bar{\xi}_V^2\bar{\eta}_V - 7\bar{\xi}_V^2\bar{\epsilon}_V \\ \quad + 194\bar{\epsilon}_V^2\bar{\eta}_V - 10\bar{\eta}_V\bar{\epsilon}_V\Big)\left(1 - \frac{1}{3q}\frac{\bar{\epsilon}_V}{M}\right)^{1/4}, & \text{for any } q, \end{cases} \tag{5.355}$$

where we use the following consistency conditions for the rescaled potential dependent slow-roll parameters:

$$\frac{d\bar{\epsilon}_V}{dN} = \begin{cases} \frac{2}{M^2}\bar{\epsilon}_V\,(\bar{\eta}_V - 3\bar{\epsilon}_V)\left(1 - \frac{2}{3}\frac{\bar{\epsilon}_V}{M}\right)^{1/4}, & \text{for } q = 1/2, \\ \frac{2}{M^2}\bar{\epsilon}_V\,(\bar{\eta}_V - 3\bar{\epsilon}_V)\left(1 - \frac{1}{3q}\frac{\bar{\epsilon}_V}{M}\right)^{1/4}, & \text{for any } q, \end{cases} \tag{5.356}$$

$$\frac{d\bar{\eta}_V}{dN} = \begin{cases} \frac{1}{M^2}\left(\bar{\xi}_V^2 - 4\bar{\epsilon}_V\bar{\eta}_V\right)\left(1 - \frac{2}{3}\frac{\bar{\epsilon}_V}{M}\right)^{1/4}, & \text{for } q = 1/2, \\ \frac{1}{M^2}\left(\bar{\xi}_V^2 - 4\bar{\epsilon}_V\bar{\eta}_V\right)\left(1 - \frac{1}{3q}\frac{\bar{\epsilon}_V}{M}\right)^{1/4}, & \text{for any } q, \end{cases} \tag{5.357}$$

$$\frac{d\bar{\xi}_V^2}{dN} = \begin{cases} \frac{1}{M^3}\left(\bar{\sigma}_V^3 + \bar{\xi}_V^2\bar{\eta}_V - \bar{\xi}_V^2\bar{\epsilon}_V\right)\left(1 - \frac{2}{3}\frac{\bar{\epsilon}_V}{M}\right)^{1/4}, & \text{for } q = 1/2, \\ \frac{1}{M^3}\left(\bar{\sigma}_V^3 + \bar{\xi}_V^2\bar{\eta}_V - \bar{\xi}_V^2\bar{\epsilon}_V\right)\left(1 - \frac{1}{3q}\frac{\bar{\epsilon}_V}{M}\right)^{1/4}, & \text{for any } q, \end{cases} \tag{5.358}$$

$$\frac{d\bar{\sigma}_V^3}{dN} = \begin{cases} \frac{1}{M^4}\bar{\sigma}_V^3\,(\bar{\eta}_V - 12\bar{\epsilon}_V)\left(1 - \frac{2}{3}\frac{\bar{\epsilon}_V}{M}\right)^{1/4}, & \text{for } q = 1/2, \\ \frac{1}{M^4}\bar{\sigma}_V^3\,(\bar{\eta}_V - 12\bar{\epsilon}_V)\left(1 - \frac{1}{3q}\frac{\bar{\epsilon}_V}{M}\right)^{1/4}, & \text{for any } q. \end{cases} \tag{5.359}$$

In terms of the slow-roll parameters, the number of e-foldings can be re-expressed as

$$N = \begin{cases} \sqrt{\frac{3\alpha'}{2}}\int_{T_i}^{T_{i,end}}\frac{H(T)}{\sqrt{\epsilon_1}}\,dT_i = \sqrt{\frac{3\alpha'}{2}}\int_{T_i}^{T_{\rm end}}\frac{H(T)}{\sqrt{\bar{\epsilon}_V(T_i)}}\,dT \\ \quad\approx \frac{\alpha' M}{M_p^2}\int_{T_{i,end}}^{T_i}\frac{V(T)V(T_i)}{V'(T_i)}\,dT_i, & \text{for } q = 1/2, \\ 2q\sqrt{\frac{3\alpha'}{2}}\int_{T_i}^{T_{i,end}}\frac{H(T)}{\sqrt{\epsilon_1}}\,dT_i = \sqrt{3\alpha' q}\int_{T_i}^{T_{i,end}}\frac{H(T)}{\sqrt{\bar{\epsilon}_V(T_i)}}\,dT_i \\ \quad\approx \frac{\sqrt{2q}\alpha' M}{M_p^2}\int_{T_{i,end}}^{T_i}\frac{V(T)V(T_i)}{V'(T_i)}\,dT_i, & \text{for any arbitrary } q, \end{cases}$$

where $T_{i,end}$ characterizes the tachyonic field value at the end of inflation $t = t_{\rm end}$ for all i fields participating in assisted inflation. As in the case of assisted inflation all the M fields are identical; then one can re-express the number of e-foldings as

$$N = \begin{cases} \frac{\alpha' M}{M_p^2}\int_{T_{i,end}}^{T_i}\frac{V^2(T_i)}{V'(T_i)}\,dT_i = \frac{\alpha' M}{M_p^2}\int_{T_{\rm end}}^{T}\frac{V^2(T)}{V'(T)}\,dT, & \text{for } q = 1/2, \\ \frac{\sqrt{2q}\alpha' M}{M_p^2}\int_{T_{i,end}}^{T_i}\frac{V^2(T_i)}{V'(T_i)}\,dT_i = \frac{\sqrt{2q}\alpha' M}{M_p^2}\int_{T_{\rm end}}^{T}\frac{V^2(T)}{V'(T)}\,dT, & \text{for any arbitrary } q. \end{cases} \tag{5.360}$$

5.2.3 Basics of tachyonic perturbations

In this subsection we explicitly discuss the cosmological linear perturbation theory within the framework of assisted tachyonic inflation. Let us clearly mention that here we have various ways of characterizing cosmological perturbations in the context of inflation, which finally depend on the choice of gauge. Let us do the computation in the longitudinal gauge, where the scalar metric perturbations of the FLRW background are given by the following infinitesimal line element:

$$ds^2 = -(1+2\Phi(t,x))\,dt^2 + a^2(t)\,(1-2\Psi(t,x))\,\delta_{ij}dx^i dx^j, \tag{5.361}$$

where $a(t)$ is the scale factor, $\Phi(t,x)$ and $\Psi(t,x)$ characterizes the gauge invariant metric perturbations. Specifically, the perturbation of the FLRW metric leads to the perturbation in the energy-momentum stress tensor via the Einstein field equation or equivalently through the Friedmann equations. For the perturbed metric as mentioned in Eq. (5.361), the perturbed Einstein field equations can be expressed for the $q = 1/2$ case of the tachyonic inflationary set-up as

$$3H\left(H\Phi(t,\mathbf{k}) + \dot{\Psi}(t,\mathbf{k})\right) + \frac{k^2}{a^2(t)} = -\frac{1}{2M_p^2}\delta\rho_i, \tag{5.362}$$

$$\ddot{\Psi}(t,\mathbf{k}) + 3H\left(H\Phi(t,\mathbf{k}) + \dot{\Psi}(t,\mathbf{k})\right) + H\dot{\Phi}(t,\mathbf{k}) + 2\dot{H}\Phi(t,\mathbf{k}) + \frac{k^2}{3a^2(t)}\left(\Phi(t,\mathbf{k}) - \Psi(t,\mathbf{k})\right) = \frac{1}{2M_p^2}\delta p_i, \tag{5.363}$$

$$\dot{\Psi}(t,\mathbf{k}) + H\Phi(t,\mathbf{k}) = -\frac{\alpha' V(T_i)}{\sqrt{1-\alpha'\dot{T}_i^2}}\frac{\dot{T}_i}{M_p^2}\delta T_i, \tag{5.364}$$

$$\Psi(t,\mathbf{k}) - \Phi(t,\mathbf{k}) = 0. \tag{5.365}$$

Similarly, for any arbitrary q the perturbed Einstein field equations can be expressed as

$$3H\left(H\Phi(t,\mathbf{k}) + \dot{\Psi}(t,\mathbf{k})\right) + \frac{k^2}{a^2(t)} = -\frac{1}{2M_p^2}\delta\rho_i, \tag{5.366}$$

$$\ddot{\Psi}(t,\mathbf{k}) + 3H\left(H\Phi(t,\mathbf{k}) + \dot{\Psi}(t,\mathbf{k})\right) + H\dot{\Phi}(t,\mathbf{k}) + 2\dot{H}\Phi(t,\mathbf{k}) + \frac{k^2}{3a^2(t)}\left(\Phi(t,\mathbf{k}) - \Psi(t,\mathbf{k})\right) = \frac{1}{2M_p^2}\delta p_i, \tag{5.367}$$

$$\dot{\Psi}(t,\mathbf{k}) + H\Phi(t,\mathbf{k}) = -\frac{\alpha' V(T_i)\left[1-\alpha'(1-2q)\dot{T}_i^2\right]}{\left(1-\alpha'\dot{T}_i^2\right)^{1-q}}\frac{\dot{T}_i}{M_p^2}\delta T_i, \tag{5.368}$$

$$\Psi(t,\mathbf{k}) - \Phi(t,\mathbf{k}) = 0. \tag{5.369}$$

Here $\Phi(t,\mathbf{k})$ and $\Psi(t,\mathbf{k})$ are the two gauge invariant metric perturbations in the Fourier space. Additionally, it is important to note that in Eq. (5.65), the two gauge invariant metric perturbations $\Phi(t,\mathbf{k})$ and $\Psi(t,\mathbf{k})$ are equal in the context of a minimally coupled tachyonic string field theoretic model with an Einstein gravity sector. In Eqs. (5.62) and (5.63) the perturbed energy density $\delta\rho$ and pressure δp are given by

$$\delta\rho_i = \begin{cases} \dfrac{V'(T_i)\delta T_i}{\sqrt{1-\alpha'\dot{T}_i^2}} + \dfrac{\alpha' V(T_i)\left(\dot{T}_i\delta\dot{T}_i + \dot{T}_i^2\Phi(t,\mathbf{k})\right)}{\left(1-\alpha'\dot{T}_i^2\right)^{3/2}}, & \text{for } q = 1/2, \\[2ex] \dfrac{\left\{V'(T_i)\left[1-\alpha'(1-2q)\dot{T}_i^2\right]\delta T_i - 4\alpha'(1-2q)V(T_i)\dot{T}_i\delta\dot{T}_i\right\}}{\left(1-\alpha'\dot{T}_i^2\right)^{1-q}} & \\ \quad + \dfrac{2\alpha'(1-q)V(T_i)\left[1-\alpha'(1-2q)\dot{T}_i^2\right]\left(\dot{T}_i\delta\dot{T}_i + \dot{T}_i^2\Phi(t,\mathbf{k})\right)}{\left(1-\alpha'\dot{T}_i^2\right)^{2-q}}, & \text{for any arbitrary } q. \end{cases} \tag{5.370}$$

$$\delta p_i = \begin{cases} -V'(T_i)\sqrt{1-\alpha'\dot{T}_i^2}\,\delta T_i + \dfrac{\alpha' V(T_i)\left(\dot{T}_i\delta\dot{T}_i + \dot{T}^2\Phi(t,\mathbf{k})\right)}{\sqrt{1-\alpha'\dot{T}^2}}, & \text{for } q = 1/2, \\[2ex] -V'(T_i)\left(1-\alpha'\dot{T}_i^2\right)^q\delta T_i + \dfrac{2q\alpha' V(T_i)\left(\dot{T}_i\delta\dot{T}_i + \dot{T}_i^2\Phi(t,\mathbf{k})\right)}{\left(1-\alpha'\dot{T}_i^2\right)^{1-q}}, & \text{for any arbitrary } q. \end{cases}$$

Similarly after the variation of the tachyonic field we get the following expressions for the perturbed equation of motion:

$$0 \approx \begin{cases} \delta\ddot{T}_i + 3H\delta\dot{T}_i + \dfrac{2\alpha'\ddot{T}_i\left(\dot{T}_i\delta\dot{T}_i + \dot{T}_i^2\Phi(t,\mathbf{k})\right)}{\left(1-\alpha'\dot{T}_i^2\right)} \\ \quad + \dfrac{M_p\sqrt{1-\alpha'\dot{T}_i^2}}{\alpha' V(T_i)}\left[\left(\dfrac{k^2}{a^2} - 3\dot{H}\right)\Phi(t,\mathbf{k}) - \dfrac{2k^2}{a^2}\Psi(t,\mathbf{k})\right. \\ \quad \left. -3\left(\ddot{\Psi}(t,\mathbf{k}) + 4H\dot{\Psi}(t,\mathbf{k}) + H\dot{\Phi}(t,\mathbf{k}) + \dot{H}\Phi(t,\mathbf{k}) + 4H^2\Phi(t,\mathbf{k})\right)\right] \\ \quad - \left\{6H\alpha'\dot{T}_i^3 - \dfrac{2V'(T_i)}{\alpha' V(T_i)}\left(1-\alpha'\dot{T}_i^2\right)\right\}\Phi(t,\mathbf{k}) - \left(\dot{\Psi}(t,\mathbf{k}) + 3\dot{\Psi}(t,\mathbf{k})\right)\dot{T}_i \\ \quad - \dfrac{M_p\left(1-\alpha'\dot{T}_i^2\right)}{\alpha'}\left(\dfrac{V''(T_i)}{V(T_i)} - \dfrac{V'^2(T_i)}{V^2(T_i)}\right), & \text{for } q = 1/2, \\ \delta\ddot{T}_i + 3H\delta\dot{T}_i + \dfrac{2\alpha'\ddot{T}_i\left(\dot{T}_i\delta\dot{T}_i + \dot{T}_i^2\Phi(t,\mathbf{k})\right)}{\left(1-\alpha'\dot{T}_i^2\right)^{2(1-q)}} \\ \quad + \dfrac{M_p\left(1-\alpha'\dot{T}_i^2\right)^{1-q}}{\alpha' V(T_i)\left[1-\alpha'(1-2q)\dot{T}_i^2\right]}\left[\left(\dfrac{k^2}{a^2} - 3\dot{H}\right)\Phi(t,\mathbf{k}) - \dfrac{2k^2}{a^2}\Psi(t,\mathbf{k})\right. \\ \quad \left. -3\left(\ddot{\Psi}(t,\mathbf{k}) + 4H\dot{\Psi}(t,\mathbf{k}) + H\dot{\Phi}(t,\mathbf{k}) + \dot{H}\Phi(t,\mathbf{k}) + 4H^2\Phi(t,\mathbf{k})\right)\right] \\ \quad - \left\{6H\alpha'\dot{T}_i^3 - \sqrt{\dfrac{2}{q}}\dfrac{V'(T_i)}{\alpha' V(T_i)}\left(1-\alpha'\dot{T}_i^2\right)^{2(1-q)}\right\}\Phi(t,\mathbf{k}) - \left(\dot{\Psi}(t,\mathbf{k}) + 3\dot{\Psi}(t,\mathbf{k})\right)\dot{T}_i \\ \quad - \dfrac{M_p\left(1-\alpha'\dot{T}_i^2\right)^{2(1-q)}}{\sqrt{2q}\,\alpha'}\left(\dfrac{V''(T_i)}{V(T_i)} - \dfrac{V'^2(T_i)}{V^2(T_i)}\right), & \text{for any } q. \end{cases} \tag{5.371}$$

Further we will perform the following steps throughout the next part of the computation:

- First of all we decompose the scalar perturbations into two components-(1) *entropic or isocurvature perturbations* which can be usually treated as the orthogonal projective part to the trajectory and (2) *adiabatic or curvature perturbations* which can be usually treated as the parallel projective part to the trajectory.
- Within the framework of first order cosmological perturbation theory we define a gauge invariant primordial curvature perturbation on the scales outside the horizon:

$$\zeta = \sum_{i=1}^{M}\left(\zeta_r + \zeta_{\tilde{T}_i}\right) = \Psi - \sum_{i=1}^{M}\frac{H}{\dot{\rho}_i}\delta\rho_i. \tag{5.372}$$

- Next we consider the uniform density hypersurface in which

$$\delta\rho_i = 0 \quad \forall\, i = 1, 2, \ldots, M. \tag{5.373}$$

Consequently the curvature perturbation is governed by

$$\zeta = \sum_{i=1}^{M}\left(\zeta_r + \zeta_{\tilde{T}_i}\right) = \Psi. \tag{5.374}$$

- Further, the time evolution of the curvature perturbation can be expressed as

$$\dot{\zeta} = H\sum_{i=1}^{M}\left(\frac{\delta\bar{p}_i}{\rho_i + p_i}\right), \tag{5.375}$$

where $\delta\bar{p}_i$ characterizes the non-adiabatic or entropic contribution in the first order linearized cosmological perturbation. In the present context $\delta\bar{p}_i$ can be expressed as

$$\delta\bar{p}_i = \Gamma\dot{p}_i = \left(\frac{\partial p_i}{\partial S}\right)_S \delta S, \tag{5.376}$$

where Γ characterizes the relative displacement between hypersurfaces of uniform pressure and density. In the case of the assisted or multi-component fluid dynamical system, there are two contributions to the $\delta\bar{p}$ appearing in the computation:

$$\delta\bar{p}_i = \delta\bar{p}_{rel,\tilde{T}_i} + \delta\bar{p}_{\rm int}, \tag{5.377}$$

where $\delta\bar{p}_{rel,i}$ and $\delta\bar{p}_{\rm int}$ characterize the relative and intrinsic contributions to the multi-component fluid system given by

$$\delta\bar{p}_{rel,\tilde{T}_i} = \frac{1}{3H\dot{\rho}}\dot{\rho}_r\dot{\rho}_{\tilde{T}_i}\left(c_r^2 - c_{S,\tilde{T}_i}^2\right)\mathcal{S}_{r\tilde{T}_i} \propto \dot{\rho}_r, \tag{5.378}$$

$$\delta\bar{p}_{\rm int} = \delta\bar{p}_{int,\tilde{T}_i} + \delta\bar{p}_{int,r} = \sum_{\alpha=r,\tilde{T}_i}\left(\delta p_\alpha - c_\alpha^2\delta\rho_\alpha\right). \tag{5.379}$$

Here $c^2_{S,\tilde{T}_i}$ and c_r^2 are the effective adiabatic sound speed and sound speed due to radiation. Also the relative entropic perturbation is defined as

$$\begin{aligned}\mathcal{S}_{r\tilde{T}_i} &= 3\left(\zeta_r - \zeta_{\tilde{T}_i}\right) = -3H\left(\frac{\delta\rho_r}{\dot{\rho}_r} - \frac{\delta\rho_{\tilde{T}_i}}{\dot{\rho}_{\tilde{T}_i}}\right)\\ &= \frac{\delta_r}{1+w_r} - \frac{\delta_{\tilde{T}_i}}{1+w_{\tilde{T}_i}},\end{aligned} \tag{5.380}$$

where w_r and $w_{\tilde{T}_i}$ signify the equation of state parameters due to radiation and tachyonic matter, δ_r and $\delta_{\tilde{T}_i}$ characterize the energy density contrasts due to radiation and tachyonic matter; M is the number of tachyonic matter contents, defined by

$$\delta_\alpha = \frac{\delta\rho_\alpha}{\rho_\alpha} \quad \forall\ \alpha = r, \tilde{T}_i (\forall i = 1, 2, \ldots, M). \tag{5.381}$$

In a generalized prescription the pressure perturbation in arbitrary gauge can be decomposed into the following contributions:

$$\begin{aligned}\delta p &= \sum_{i=1}^{M}\delta p_i = c_S^2\delta\rho + \frac{1}{3H\dot{\rho}}\dot{\rho}_r\sum_{i=1}^{M}\dot{\rho}_{\tilde{T}_i}\left(c_r^2 - c^2_{S,\tilde{T}_i}\right)\mathcal{S}_{r\tilde{T}_i}\\ &\quad + \sum_{i=1}^{M}\sum_{\alpha=r,\tilde{T}_i}\left(\delta p_\alpha - c_\alpha^2\delta\rho_\alpha\right).\end{aligned} \tag{5.382}$$

As $\delta\bar{p}_{rel,\tilde{T}_i} \propto \dot{\rho}_r$, the relative non-adiabatic pressure perturbation is heavily suppressed in the computation and one can safely ignore such contributions during the epoch of inflation. Here the relative entropic perturbation $\mathcal{S}_{r\tilde{T}_i}$ remains small and finite in the limit of small $\dot{\rho}_r$ due to the smallness of the curvature perturbations ζ_r and $\zeta_{\tilde{T}_i}$.

- Now let us consider a situation where the equation of state parameter corresponding to radiation is

$$w_r = c_r^2 = \text{Constant}. \tag{5.383}$$

Consequently the fluctuation in pressure due to radiation can be expressed in terms of the fluctuation of the density:

$$\delta p_r = w_r\delta\rho_r = c_r^2\delta\rho_r = \text{Constant}\times\delta\rho_r \propto \delta\rho_r. \tag{5.384}$$

This clearly implies that

$$\delta\bar{p}_{int,r} = \left(\delta p_r - c_r^2\delta\rho_r\right) = 0 \tag{5.385}$$

i.e., the intrinsic non-adiabatic pressure vanishes identically. However, in terms of the effective tachyonic field $\tilde{T}$ this situation is not very simple, as the equation of state parameter and the intrinsic sound speed changes with the number of component fields M. During the inflationary epoch all M fields obey the following equation of state:

$$w_{\tilde{T}_i} = \frac{p_{\tilde{T}_i}}{\rho_{\tilde{T}_i}} \simeq -1 = c^2_{S,\tilde{T}_i} = \text{Constant} \quad \forall\ i = 1, 2, \ldots, M. \tag{5.386}$$

For all M effective tachyon fields the fluctuation in the pressure can be expressed as

$$\delta p_{\tilde{T}_i} \simeq w_{\tilde{T}_i}\delta\rho_{\tilde{T}_i} = c^2_{S,\tilde{T}_i}\delta\rho_{\tilde{T}_i} \simeq -\delta\rho_{\tilde{T}_i}. \tag{5.387}$$

Consequently the intrinsic non-adiabatic pressure within each tachyonic field amongst M fields can be expressed as

$$\delta p_{int,\tilde{T}_i} = \delta p_{\tilde{T}_i} - c^2_{S,\tilde{T}_i}\delta\rho_{\tilde{T}_i} \simeq 0. \tag{5.388}$$

Now in the present context the relative contributions to the non-adiabatic pressure of M tachyonic fields in this context can be expressed as

$$\delta p_{rel,\tilde{T}_i\tilde{T}_j} \propto \left(c^2_{S,\tilde{T}_i} - c^2_{S,\tilde{T}_j}\right) \simeq 0, \tag{5.389}$$

since

$$c^2_{S,\tilde{T}_i} \simeq c^2_{S,\tilde{T}_j} \simeq -1 \quad \forall\ i, j = 1, 2, \ldots, M. \tag{5.390}$$

This implies that the total non-adiabatic pressure is negligible during inflation, i.e.,

$$\delta\bar{p}_{\rm int} = \delta\bar{p}_{int,\tilde{T}_i} + \delta\bar{p}_{int,r} = \sum_{\alpha=r,\tilde{T}_i}\left(\delta p_\alpha - c_\alpha^2\delta\rho_\alpha\right) = 0. \tag{5.391}$$

and it is completely justified to write the fluctuation in the pressure for M individual tachyonic field contents as

$$\delta\bar{p}_i = \delta\bar{p}_{rel,\tilde{T}_i} = \frac{1}{3H\dot{\rho}}\dot{\rho}_r\dot{\rho}_{\tilde{T}_i}\left(c_r^2 - c^2_{S,\tilde{T}_i}\right)\mathcal{S}_{r\tilde{T}_i} \propto \dot{\rho}_r. \tag{5.392}$$

Using these results the total fluctuation in the pressure can be re-expressed as

$$\delta p = \sum_{i=1}^{M} \delta p_i = c_S^2 \delta\rho + \sum_{i=1}^{M} \delta \bar{p}_i = c_S^2 \delta\rho + AM\dot{\rho}_r \simeq c_S^2 \delta\rho, \tag{5.393}$$

where A is the proportionality constant and we have safely ignored the contribution from the isocurvatrure modes due to its smallness in the case of assisted tachyonic inflation. Consequently we get

$$\delta \bar{p}_i = \Gamma \dot{p}_i = AM\dot{\rho}_r \simeq 0 \Rightarrow \rho_r = \text{Constant} \quad \Rightarrow \quad \zeta = \text{Constant}, \tag{5.394}$$

which is exactly similar with the usual single field slow-roll conditions in the context of the tachyonic inflationary set-up discussed earlier. Finally, in the uniform density hypersurfaces, the curvature perturbation can be written in terms of the tachyonic field fluctuations on spatially flat hypersurfaces as

$$\zeta = -H \sum_{i=1}^{M} \left(\frac{\delta T_i}{\dot{T}_i}\right) = -HM\left(\frac{\delta T}{\dot{T}}\right) = -HM\left(\frac{\delta \tilde{T}}{\dot{\tilde{T}}}\right). \tag{5.395}$$

perturbation rapidly becomes adiabatic perturbation of the same amplitude, as local pressure differences, due to the local fluctuations in the equation of state, re-distribute the energy density. However, this change is slightly less efficient during the epoch of radiation compared to the tachyonic matter dominated epoch and can only occur after the decoupling between the photons and baryons, in the specific case of baryonic isocurvature perturbation. Causality precludes this re-distribution on scales bigger than the Hubble radius, and thus any entropy perturbation on these scales remains with a constant amplitude. Also it is important to note that the entropic or isocurvature perturbations are not affected by Silk damping, which is exactly contrary to the curvature or adiabatic perturbations.

5.2.4 *Computation of scalar power spectrum*

In this subsection we will not derive the results for assisted inflation as it is exactly the same as derived in the case of single tachyonic inflation. But we will state the results for the BD vacuum where the changes will appear due to the presence of M identical copies of the tachyon field. One can similarly write down the detailed expressions for AV as well. The changes will appear in the expressions for the following inflationary observables at the horizon crossing:

- In the present context amplitude of scalar power spectrum can be computed as

$$\Delta_{\zeta,\star} = \begin{cases} \left\{\left[1-(\mathcal{C}_E+1)\frac{\bar{\epsilon}_V}{M} - \frac{\mathcal{C}_E}{M}(3\bar{\epsilon}_V - \bar{\eta}_V)\right]^2 \frac{MH^2}{8\pi^2 M_p^2 c_S \bar{\epsilon}_V}\right\}_{k_\star = a_\star H_\star}, & \text{for } q = 1/2, \\ \left\{\left[1-(\mathcal{C}_E+1)\frac{\bar{\epsilon}_V}{2qM} - \frac{\mathcal{C}_E}{\sqrt{2q}M}(3\bar{\epsilon}_V - \bar{\eta}_V)\right]^2 \frac{qMH^2}{4\pi^2 M_p^2 c_S \bar{\epsilon}_V}\right\}_{k_\star = a_\star H_\star}, & \text{for any } q, \end{cases} \tag{5.396}$$

- But in the case of multi-tachyonic inflation where the M number of fields are not identical with each other the situation is not simpler like assisted inflation. In that case during the short time intervals when fields decay in a very much faster rate and its corresponding equation of state changes rapidly then it would be really interesting to investigate the production of isocurvature perturbations. On the scale smaller than the Hubble radius any entropy

where $H^2 = MV/3M_p^2$ and $\mathcal{C}_E = -2 + \ln 2 + \gamma \approx -0.72$. Using the slow-roll approximations one can further approximate the expression for the sound speed as

$$c_S^2 = \begin{cases} 1 - \frac{2}{3}\frac{\bar{\epsilon}_V}{M} + \mathcal{O}\left(\frac{\bar{\epsilon}_V^2}{M^2}\right) + \cdots, & \text{for } q = 1/2, \\ 1 - \frac{(1-q)}{3q^2 M}\bar{\epsilon}_V + \mathcal{O}\left(\frac{\bar{\epsilon}_V^2}{M^2}\right) + \cdots, & \text{for any } q. \end{cases} \tag{5.397}$$

Hence using the result in Eq. (5.408) we get the following simplified expression for the primordial scalar power spectrum:

$$\Delta_{\zeta,\star} \approx \begin{cases} \left\{\left[1-\left(\mathcal{C}_E+\frac{5}{6}\right)\frac{\bar{\epsilon}_V}{M}-\frac{\mathcal{C}_E}{M}\left(3\bar{\epsilon}_V-\bar{\eta}_V\right)\right]^2\frac{MH^2}{8\pi^2M_p^2\bar{\epsilon}_V}\right\}_{k_\star=a_\star H_\star}, & \text{for } q=1/2,\\ \left\{\left[1-\left(\mathcal{C}_E+1-\Sigma\right)\frac{\bar{\epsilon}_V}{2qM}-\frac{\mathcal{C}_E}{\sqrt{2q}M}\left(3\bar{\epsilon}_V-\bar{\eta}_V\right)\right]^2\frac{qMH^2}{4\pi^2M_p^2\bar{\epsilon}_V}\right\}_{k_\star=a_\star H_\star}, & \text{for any } q. \end{cases} \tag{5.398}$$

- Next one can compute the scalar spectral tilt (n_S) of the primordial scalar power spectrum as

$$n_{\zeta,\star}-1 \approx \begin{cases} \frac{1}{M}\left(2\bar{\eta}_V-8\bar{\epsilon}_V\right)-\frac{2}{M^2}\bar{\epsilon}_V^2-\frac{2}{M^2}\left(2\mathcal{C}_E+\frac{8}{3}\right)\bar{\epsilon}_V\left(3\bar{\epsilon}_V-\bar{\eta}_V\right) & \\ \quad -\frac{\mathcal{C}_E}{M^2}\left(2\bar{\xi}_V^2-5\bar{\eta}_V\bar{\epsilon}_V+36\bar{\epsilon}_V^2\right)+\cdots, & \text{for } q=1/2,\\ \frac{1}{M}\sqrt{\frac{2}{q}}\bar{\eta}_V-\frac{1}{M}\left(\frac{1}{q}+3\sqrt{\frac{2}{q}}\right)\bar{\epsilon}_V-\frac{\bar{\epsilon}_V^2}{2q^2M^2} & \\ \quad -\frac{2}{(2q)^{3/2}M^2}\left(2\mathcal{C}_E+3-2\Sigma\right)\bar{\epsilon}_V\left(3\bar{\epsilon}_V-\bar{\eta}_V\right) & \\ \quad -\frac{\mathcal{C}_E}{\sqrt{2q}M^2}\left(2\bar{\xi}_V^2-5\bar{\eta}_V\bar{\epsilon}_V+36\bar{\epsilon}_V^2\right)+\cdots, & \text{for any } q. \end{cases} \tag{5.399}$$

- Next one can compute the running of the scalar spectral tilt (α_S) of the primordial scalar power spectrum as

$$\alpha_{\zeta,\star} \approx \begin{cases} -\left\{\left[\frac{4}{M^2}\bar{\epsilon}_V\left(1+\frac{\bar{\epsilon}_V}{M}\right)\left(\bar{\eta}_V-3\bar{\epsilon}_V\right)+\frac{2}{M^2}\left(10\bar{\epsilon}_V\bar{\eta}_V-18\bar{\epsilon}_V^2-\bar{\xi}_V^2\right)\right]\right. & \\ \quad -\frac{\mathcal{C}_E}{M^3}\left(2\bar{\sigma}_V^3-216\bar{\epsilon}_V^3+2\bar{\xi}_V^2\bar{\eta}_V-7\bar{\xi}_V^2\bar{\epsilon}_V+194\bar{\epsilon}_V^2\bar{\eta}_V-10\bar{\eta}_V\bar{\epsilon}_V\right) & \\ \quad -\frac{1}{M^3}\left(2\mathcal{C}_E+\frac{8}{3}\right)\left[2\bar{\epsilon}_V\left(10\bar{\epsilon}_V\bar{\eta}_V-18\bar{\epsilon}_V^2-\bar{\xi}_V^2\right)\right. & \\ \quad \left.\left.-4\bar{\epsilon}_V\left(3\bar{\epsilon}_V-\bar{\eta}_V\right)^2\right]\right\}\left(1-\frac{2}{3}\frac{\bar{\epsilon}_V}{M}\right)^{1/4}+\cdots, & \text{for } q=1/2,\\ -\left\{\left[\sqrt{\frac{2}{q}}\frac{\bar{\epsilon}_V}{qM^2}\left(1+\frac{\bar{\epsilon}_V}{2qM}\right)\left(\bar{\eta}_V-3\bar{\epsilon}_V\right)+\frac{1}{M^2}\sqrt{\frac{2}{q}}\left(10\bar{\epsilon}_V\bar{\eta}_V-18\bar{\epsilon}_V^2-\bar{\xi}_V^2\right)\right]\right. & \\ \quad -\frac{\mathcal{C}_E}{\sqrt{2q}M^3}\left(2\bar{\sigma}_V^3-216\bar{\epsilon}_V^3+2\bar{\xi}_V^2\bar{\eta}_V-7\bar{\xi}_V^2\bar{\epsilon}_V+194\bar{\epsilon}_V^2\bar{\eta}_V-10\bar{\eta}_V\bar{\epsilon}_V\right) & \\ \quad -\frac{1}{M^3}\left(2\mathcal{C}_E+\frac{8}{3}\right)\left[\sqrt{\frac{2}{q}}\bar{\epsilon}_V\left(10\bar{\epsilon}_V\bar{\eta}_V-18\bar{\epsilon}_V^2-\bar{\xi}_V^2\right)\right. & \\ \quad \left.\left.-\frac{4}{(2q)^{3/2}}\bar{\epsilon}_V\left(3\bar{\epsilon}_V-\bar{\eta}_V\right)^2\right]\right\}\left(1-\frac{1}{3q}\frac{\bar{\epsilon}_V}{M}\right)^{1/4}+\cdots, & \text{for any } q. \end{cases}$$

- Finally, one can also compute the running of the running of scalar spectral tilt (κ_S) of the primordial scalar power spectrum as

$$
\kappa_{\zeta,\star} \approx \begin{cases}
-\frac{1}{M^3}\Big[8\bar{\epsilon}_V(1+\bar{\epsilon}_V)(\bar{\eta}_V-3\bar{\epsilon}_V)^2+c\bar{\epsilon}_V^2(\bar{\eta}_V-3\bar{\epsilon}_V)^2 \\
+8\bar{\epsilon}_V(1+\bar{\epsilon}_V)\left(\bar{\xi}_V^2-10\bar{\epsilon}_V\bar{\eta}_V+18\bar{\epsilon}_V^2\right) \\
+2\left(20\bar{\epsilon}_V\bar{\eta}_V\left(\bar{\eta}_V-3\bar{\epsilon}_V\right)+10\bar{\epsilon}_V\left(\bar{\xi}_V^2-4\bar{\epsilon}_V\bar{\eta}_V\right)\right. \\
\left.\left.-72\bar{\epsilon}_V^2\left(\bar{\eta}_V-3\bar{\epsilon}_V\right)-\left(\bar{\sigma}_V^3+\bar{\xi}_V^2\bar{\eta}_V-\bar{\xi}_V^2\bar{\epsilon}_V\right)\right)\Big]\left(1-\frac{2}{3}\frac{\bar{\epsilon}_V}{M}\right)^{1/4}+\cdots, & \text{for } q=1/2, \\
-\frac{1}{M^3}\Bigg[\left(\frac{2}{q}\right)^{3/2}\bar{\epsilon}_V\left(1+\frac{\bar{\epsilon}_V}{2qM}\right)(\bar{\eta}_V-3\bar{\epsilon}_V)^2+\sqrt{\frac{2}{q}}\frac{2}{q^2M}\bar{\epsilon}_V^2(\bar{\eta}_V-3\bar{\epsilon}_V)^2 \\
+\sqrt{\frac{2}{q}}\frac{2}{q}\bar{\epsilon}_V\left(1+\frac{\bar{\epsilon}_V}{2q}\right)\left(\bar{\xi}_V^2-10\bar{\epsilon}_V\bar{\eta}_V+18\bar{\epsilon}_V^2\right) \\
+\sqrt{\frac{2}{q}}\left(\frac{10}{q}\bar{\epsilon}_V\bar{\eta}_V\left(\bar{\eta}_V-3\bar{\epsilon}_V\right)+10\bar{\epsilon}_V\left(\bar{\xi}_V^2-4\bar{\epsilon}_V\bar{\eta}_V\right)\right. \\
\left.\left.-\frac{36}{q}\bar{\epsilon}_V^2\left(\bar{\eta}_V-3\bar{\epsilon}_V\right)-\left(\bar{\sigma}_V^3+\bar{\xi}_V^2\bar{\eta}_V-\bar{\xi}_V^2\bar{\epsilon}_V\right)\right)\Bigg]\left(1-\frac{1}{3q}\frac{\bar{\epsilon}_V}{M}\right)^{1/4}+\cdots, & \text{for any } q.
\end{cases} \tag{5.400}
$$

5.2.5 Computation of tensor power spectrum

In this subsection we will not derive the results for assisted inflation as it is exactly the same as derived in the case of single tachyonic inflation. But we will state the results for the BD vacuum where the changes will appear due to the presence of M identical copies of the tachyon field. One can similarly write down the detailed expressions for AV as well. The changes will appear in the expressions for the following inflationary observables at the horizon crossing:

- In the present context amplitude of tensor power spectrum can be computed as

$$
\Delta_{h,\star} = \begin{cases}
\left\{\left[1-(\mathcal{C}_E+1)\frac{\bar{\epsilon}_V}{M}\right]^2\frac{2H^2}{\pi^2M_p^2}\right\}_{k_\star=a_\star H_\star}, & \text{for } q=1/2, \\
\left\{\left[1-(\mathcal{C}_E+1)\frac{\bar{\epsilon}_V}{2qM}\right]^2\frac{2H^2}{\pi^2M_p^2}\right\}_{k_\star=a_\star H_\star}, & \text{for any } q,
\end{cases} \tag{5.401}
$$

  where $\mathcal{C}_E=-2+\ln 2+\gamma\approx -0.72$.
- Next one can compute the scalar spectral tilt (n_S) of the primordial scalar power spectrum as

$$
n_{h,\star} \approx \begin{cases}
-\frac{2}{M}\bar{\epsilon}_V\left[1+\frac{\bar{\epsilon}_V}{M}+\frac{2}{M}\left(\mathcal{C}_E+1\right)\left(3\bar{\epsilon}_V-\bar{\eta}_V\right)\right]+\cdots, & \text{for } q=1/2, \\
-\frac{\bar{\epsilon}_V}{qM}\left[1+\frac{\bar{\epsilon}_V}{2qM}+\frac{1}{M}\sqrt{\frac{2}{q}}\left(\mathcal{C}_E+1\right)\left(3\bar{\epsilon}_V-\bar{\eta}_V\right)\right]+\cdots, & \text{for any } q.
\end{cases} \tag{5.402}
$$

- Next one can compute the running of the tensor spectral tilt (α_h) of the primordial scalar power spectrum as

$$\alpha_{h,\star} \approx \begin{cases} -\left[\frac{4}{M^2}\bar{\epsilon}_V\left(1+\frac{\bar{\epsilon}_V}{M}\right)(\bar{\eta}_V-3\bar{\epsilon}_V)+\frac{4}{M^3}\bar{\epsilon}_V^2(\bar{\eta}_V-3\bar{\epsilon}_V)\right. \\ -\frac{8}{M^3}\left(\mathcal{C}_E+1\right)\bar{\epsilon}_V(\bar{\eta}_V-3\bar{\epsilon}_V)^2 \\ \left.-\frac{2}{M^3}\bar{\epsilon}_V\left(10\bar{\epsilon}_V\bar{\eta}_V-18\bar{\epsilon}_V^2-\bar{\xi}_V^2\right)\right]_\star\left(1-\frac{2}{3}\frac{\bar{\epsilon}_V}{M}\right)_\star^{1/4}+\cdots, & \text{for } q=1/2, \\ -\left[2\frac{\bar{\epsilon}_V}{qM^2}\left(1+\frac{\bar{\epsilon}_V}{2qM}\right)(\bar{\eta}_V-3\bar{\epsilon}_V)+\frac{1}{q^2M^3}\bar{\epsilon}_V^2(\bar{\eta}_V-3\bar{\epsilon}_V)\right. \\ -\frac{8}{(2q)^{5/2}M^3}\left(\mathcal{C}_E+1\right)\bar{\epsilon}_V(\bar{\eta}_V-3\bar{\epsilon}_V)^2 \\ \left.-\frac{1}{M^3}\sqrt{\frac{2}{q}}\bar{\epsilon}_V\left(10\bar{\epsilon}_V\bar{\eta}_V-18\bar{\epsilon}_V^2-\bar{\xi}_V^2\right)\right]_\star\left(1-\frac{1}{3q}\frac{\bar{\epsilon}_V}{M}\right)_\star^{1/4}+\cdots, & \text{for any } q. \end{cases} \tag{5.403}$$

- Finally, one can also compute the running of the running of scalar spectral tilt (κ_S) of the primordial scalar power spectrum as

$$\kappa_{h,\star} \approx \begin{cases} -\left[\frac{8}{M^3}\bar{\epsilon}_V(1+\bar{\epsilon}_V)(\bar{\eta}_V-3\bar{\epsilon}_V)^2+\frac{8}{M^4}\bar{\epsilon}_V^2(\bar{\eta}_V-3\bar{\epsilon}_V)^2\right. \\ -\frac{16}{M^4}\left(\mathcal{C}_E+1\right)\bar{\epsilon}_V\left\{(\bar{\eta}_V-3\bar{\epsilon}_V)^3-(\bar{\eta}_V-3\bar{\epsilon}_V)\left(10\bar{\epsilon}_V\bar{\eta}_V-18\bar{\epsilon}_V^2-\bar{\xi}_V^2\right)\right\} \\ \left.-\frac{4}{M^3}\bar{\epsilon}_V\left(1+\frac{\bar{\epsilon}_V}{M}\right)\left(10\bar{\epsilon}_V\bar{\eta}_V-18\bar{\epsilon}_V^2-\bar{\xi}_V^2\right)\right]_\star\left(1-\frac{2}{3}\frac{\bar{\epsilon}_V}{M}\right)_\star^{1/4}+\cdots, & \text{for } q=1/2, \\ -\left[\frac{4}{qM^3}\bar{\epsilon}_V\left(1+\frac{\bar{\epsilon}_V}{2qM}\right)(\bar{\eta}_V-3\bar{\epsilon}_V)^2+\frac{2}{q^2M^4}\bar{\epsilon}_V^2(\bar{\eta}_V-3\bar{\epsilon}_V)^2\right. \\ +\frac{2}{qM^3}\bar{\epsilon}_V\left(1+\frac{\bar{\epsilon}_V}{2q}\right)\left(\bar{\xi}_V^2-10\bar{\epsilon}_V\bar{\eta}_V+18\bar{\epsilon}_V^2\right) \\ \left.-\frac{8}{qM^4}\left(\mathcal{C}_E+1\right)\bar{\epsilon}_V\left\{(\bar{\eta}_V-3\bar{\epsilon}_V)^3-(\bar{\eta}_V-3\bar{\epsilon}_V)\left(10\bar{\epsilon}_V\bar{\eta}_V-18\bar{\epsilon}_V^2-\bar{\xi}_V^2\right)\right\}\right]_\star \\ \times\left(1-\frac{1}{3q}\frac{\bar{\epsilon}_V}{M}\right)_\star^{1/4}+\cdots, & \text{for any } q. \end{cases} \tag{5.404}$$

5.2.6 Modified consistency relations

In this subsection we derive the new (modified) consistency relations for single tachyonic field inflation:

1. Next for the BD vacuum with $|kc_S\eta| = 1$ case within slow-roll regime we can approximately write the following expression for the tensor-to-scalar ratio:

$$r_\star \approx \begin{cases} \left[\frac{16}{M}\bar{\epsilon}_V c_S \frac{\left[1-(\mathcal{C}_E+1)\frac{\bar{\epsilon}_V}{M}\right]^2}{\left[1-(\mathcal{C}_E+1)\frac{\bar{\epsilon}_V}{M}-\frac{\mathcal{C}_E}{M}(3\bar{\epsilon}_V-\bar{\eta}_V)\right]^2}\right]_{k_\star=a_\star H_\star} \\ =\left[\frac{16}{M}\bar{\epsilon}_V \frac{\left[1-(\mathcal{C}_E+1)\frac{\bar{\epsilon}_V}{M}\right]^2}{\left[1-\left(\mathcal{C}_E+\frac{5}{6}\right)\frac{\bar{\epsilon}_V}{M}-\frac{\mathcal{C}_E}{M}(3\bar{\epsilon}_V-\bar{\eta}_V)\right]^2}\right]_{k_\star=a_\star H_\star}, & \text{for } q=1/2, \\ \left[\frac{8}{qM}\bar{\epsilon}_V c_S \frac{\left[1-(\mathcal{C}_E+1)\frac{\bar{\epsilon}_V}{2qM}\right]^2}{\left[1-(\mathcal{C}_E+1)\frac{\bar{\epsilon}_V}{2qM}-\frac{\mathcal{C}_E}{M\sqrt{2q}}(3\bar{\epsilon}_V-\bar{\eta}_V)\right]^2}\right]_{k_\star=a_\star H_\star} \\ =\left[\frac{8}{qM}\bar{\epsilon}_V \frac{\left[1-(\mathcal{C}_E+1)\frac{\bar{\epsilon}_V}{2qM}\right]^2}{\left[1-(\mathcal{C}_E+1-\Sigma)\frac{\bar{\epsilon}_V}{2qM}-\frac{\mathcal{C}_E}{M\sqrt{2q}}(3\bar{\epsilon}_V-\bar{\eta}_V)\right]^2}\right]_{k_\star=a_\star H_\star}, & \text{for any } q. \end{cases} \tag{5.405}$$

2. Hence the consistency relation between the tensor-to-scalar ratio r and spectral tilt n_T for tensor modes for BD vacuum with $|kc_S\eta|=1$ case can be written as

$$r_\star \approx -8n_{h,\star}\times \underbrace{\begin{cases} \left[c_S \frac{\left[1-(\mathcal{C}_E+1)\frac{\bar{\epsilon}_V}{M}\right]^2}{\left[1-(\mathcal{C}_E+1)\frac{\bar{\epsilon}_V}{M}-\frac{\mathcal{C}_E}{M}(3\bar{\epsilon}_V-\bar{\eta}_V)\right]^2\left[1+\frac{\bar{\epsilon}_V}{M}+\frac{2}{M}(\mathcal{C}_E+1)(3\bar{\epsilon}_V-\bar{\eta}_V)\right]}\right]_{k_\star=a_\star H_\star} \\ =\left[\frac{\left[1-(\mathcal{C}_E+1)\frac{\bar{\epsilon}_V}{M}\right]^2}{\left[1-\left(\mathcal{C}_E+\frac{5}{6}\right)\frac{\bar{\epsilon}_V}{M}-\frac{\mathcal{C}_E}{M}(3\bar{\epsilon}_V-\bar{\eta}_V)\right]^2\left[1+\frac{\bar{\epsilon}_V}{M}+\frac{2}{M}(\mathcal{C}_E+1)(3\bar{\epsilon}_V-\bar{\eta}_V)\right]}\right]_{k_\star}, & \text{for } q=1/2, \\ \left[c_S \frac{\left[1-(\mathcal{C}_E+1)\frac{\bar{\epsilon}_V}{2qM}\right]^2}{\left[1-(\mathcal{C}_E+1)\frac{\bar{\epsilon}_V}{2qM}-\frac{\mathcal{C}_E}{M\sqrt{2q}}(3\bar{\epsilon}_V-\bar{\eta}_V)\right]^2\left[1+\frac{\bar{\epsilon}_V}{2qM}+\frac{1}{M}\sqrt{\frac{2}{q}}(\mathcal{C}_E+1)(3\bar{\epsilon}_V-\bar{\eta}_V)\right]}\right]_{k_\star=a_\star H_\star} \\ =\left[\frac{\left[1-(\mathcal{C}_E+1)\frac{\bar{\epsilon}_V}{2qM}\right]^2}{\left[1-(\mathcal{C}_E+1-\Sigma)\frac{\bar{\epsilon}_V}{2qM}-\frac{\mathcal{C}_E}{M\sqrt{2q}}(3\bar{\epsilon}_V-\bar{\eta}_V)\right]^2\left[1+\frac{\bar{\epsilon}_V}{2qM}+\frac{1}{M}\sqrt{\frac{2}{q}}(\mathcal{C}_E+1)(3\bar{\epsilon}_V-\bar{\eta}_V)\right]}\right]_{k_\star}, & \text{for any } q. \end{cases}}_{\text{Correction factor}} \tag{5.406}$$

3. Next one can express the first two slow-roll parameters $\bar{\epsilon}_V$ and $\bar{\eta}_V$ in terms of the inflationary observables as

$$\bar{\epsilon}_V \approx \begin{cases} \epsilon_1 \approx -\frac{n_{h,\star}M}{2}+\cdots \approx \frac{r_\star M}{16}+\cdots, & \text{for } q=1/2, \\ 2q\epsilon_1 \approx -qn_{h,\star}M+\cdots \approx \frac{qr_\star M}{8}+\cdots, & \text{for any } q, \end{cases} \tag{5.407}$$

$$\bar{\eta}_V \approx \begin{cases} 3\epsilon_1-\frac{\epsilon_2}{2} \approx \frac{M}{2}\left(n_{\zeta,\star}-1+\frac{r_\star}{2}\right)+\cdots \approx \frac{M}{2}\left(n_{\zeta,\star}-1-4n_{h,\star}\right)+\cdots, & \text{for } q=1/2, \\ 6q\epsilon_1-\sqrt{\frac{q}{2}}\epsilon_2 \approx M\sqrt{\frac{q}{2}}\left(n_{\zeta,\star}-1+\left(\frac{1}{q}+3\sqrt{\frac{2}{q}}\right)\frac{qr_\star}{8}\right)+\cdots \\ \approx M\sqrt{\frac{q}{2}}\left(n_{\zeta,\star}-1-q\left(\frac{1}{q}+3\sqrt{\frac{2}{q}}\right)n_{h,\star}\right)+\cdots, & \text{for any } q. \end{cases} \tag{5.408}$$

4. Then the connecting consistency relation between tensor and scalar spectral tilt and tensor-to-scalar ratio can be expressed as

$$n_{h,\star} \approx \begin{cases} -\frac{r_\star}{8c_S}\left[1-\frac{r_\star}{16}+\left(1-n_{\zeta,\star}\right)-\mathcal{C}_E\left\{\frac{r_\star}{8}+\left(n_{\zeta,\star}-1\right)\right\}\right]+\cdots, & \text{for } q=1/2, \\ -\frac{r_\star}{8c_S}\left[1+\left\{\left(\frac{3q}{8}\sqrt{\frac{2}{q}}-\left(\sqrt{\frac{2}{q}}+5\right)\frac{1}{16}\right)r_\star+\frac{\left(1-n_{\zeta,\star}\right)}{\sqrt{2q}}\right\}\right. & \\ \left.+\sqrt{\frac{2}{q}}\mathcal{C}_E\left(\frac{3qr_\star}{8}-\frac{1}{2}\left\{n_{\zeta,\star}-1+\left(\frac{1}{q}+3\sqrt{\frac{2}{q}}\right)\frac{qr_\star}{8}\right\}\right)\right]+\cdots, & \text{for any } q. \end{cases} \tag{5.409}$$

Finally using the approximated version of the expression for c_S in terms of slow-roll parameters one can recast this consistency condition as

$$n_{h,\star} \approx \begin{cases} -\frac{r_\star}{8}\left[1-\frac{r_\star}{24}+\left(1-n_{\zeta,\star}\right)-\mathcal{C}_E\left\{\frac{r_\star}{8}+\left(n_{\zeta,\star}-1\right)\right\}\right]+\cdots, & \text{for } q=1/2, \\ -\frac{r_\star}{8}\left[1+\left\{\left(\frac{3q}{8}\sqrt{\frac{2}{q}}-\left(\sqrt{\frac{2}{q}}+5\right)\frac{1}{16}+\frac{\Sigma}{8}\right)r_\star+\frac{\left(1-n_{\zeta,\star}\right)}{\sqrt{2q}}\right\}\right. & \\ \left.+\sqrt{\frac{2}{q}}\mathcal{C}_E\left(\frac{3qr_\star}{8}-\frac{1}{2}\left\{n_{\zeta,\star}-1+\left(\frac{1}{q}+3\sqrt{\frac{2}{q}}\right)\frac{qr_\star}{8}\right\}\right)\right]+\cdots, & \text{for any } q. \end{cases} \tag{5.410}$$

5. Next the running of the sound speed c_S can be written in terms of slow-roll parameters as

$$\begin{aligned} S &= \frac{\dot{c}_S}{Hc_S}=\frac{\mathrm{d}\ln c_S}{\mathrm{d}N}=\frac{\mathrm{d}\ln c_S}{\mathrm{d}\ln k} \\ &= \begin{cases} -\frac{2}{3M^2}\bar{\epsilon}_V\left(\bar{\eta}_V-3\bar{\epsilon}_V\right)\left(1-\frac{2}{3}\frac{\bar{\epsilon}_V}{M}\right)^{1/4}+\cdots, & \text{for } q=1/2, \\ -\frac{(1-q)}{3q^2M^2}\bar{\epsilon}_V\left(\bar{\eta}_V-3\bar{\epsilon}_V\right)\left(1-\frac{1}{3q}\frac{\bar{\epsilon}_V}{M}\right)^{1/4}+\cdots, & \text{for any } q, \end{cases} \end{aligned} \tag{5.411}$$

which can be treated as another slow-roll parameter in the present context. One can also recast the slow-roll parameter S in terms of the inflationary observables as

$$S = \begin{cases} -\frac{r_\star}{48}\left(n_{\zeta,\star}-1+\frac{r_\star}{8}\right)\left(1-\frac{r_\star}{24}\right)^{1/4}+\cdots, & \text{for } q=1/2, \\ -\frac{(1-q)}{24q^2}\sqrt{\frac{q}{2}}r_\star\left(n_{\zeta,\star}-1+\frac{r_\star}{8}\right)\left(1-\frac{r_\star}{24}\right)^{1/4}+\cdots, & \text{for any } q. \end{cases} \tag{5.412}$$

6. Further the running of the tensor spectral tilt can be written in terms of the inflationary observables as

$$\alpha_{h,\star} = \begin{cases} -\left[\frac{r_\star}{8}\left(1+\frac{r_\star}{8}\right)\left(n_{\zeta,\star}-1+\frac{r_\star}{8}\right)-\frac{r_\star}{8}\left(n_{\zeta,\star}-1+\frac{r_\star}{8}\right)^2\right. & \\ \left.-\mathcal{C}_E\frac{r_\star}{8}\left(n_{\zeta,\star}-1+\frac{r_\star}{8}\right)^2\right]\left(1-\frac{r_\star}{24}\right)^{1/4}+\cdots, & \text{for } q=1/2, \\ -\left[\frac{r_\star}{4}\sqrt{\frac{q}{2}}\left(1+\frac{r_\star}{8}\right)\left(n_{\zeta,\star}-1+\frac{r_\star}{8}\right)\right. & \\ \left.-\frac{1}{(2q)^{1/2}}\left(\mathcal{C}_E+1\right)\frac{r_\star}{8}\left(n_{\zeta,\star}-1+\frac{r_\star}{8}\right)^2\right]\left(1-\frac{r_\star}{24}\right)^{1/4}+\cdots, & \text{for any } q. \end{cases} \tag{5.413}$$

7. Next the scalar power spectrum can be expressed in terms of the other inflationary observables as

$$\Delta_{\zeta,\star} \approx \begin{cases} \left[1-\left(\mathcal{C}_E+\frac{5}{6}\right)\frac{r_\star}{16}+\frac{\mathcal{C}_E}{2}\left(n_{\zeta,\star}-1+\frac{r_\star}{8}\right)\right]^2 \frac{2H_\star^2}{\pi^2 M_p^2 r_\star}+\cdots, & \text{for } q=1/2, \\ \left[1-(\mathcal{C}_E+1-\Sigma)\frac{r_\star}{16}+\frac{\mathcal{C}_E}{2}\left(n_{\zeta,\star}-1+\frac{r_\star}{8}\right)\right]^2 \frac{2H_\star^2}{\pi^2 M_p^2 r_\star}+\cdots, & \text{for any } q. \end{cases} \quad (5.414)$$

8. Further the tensor power spectrum can be expressed in terms of the other inflationary observables as

$$\Delta_{h,\star} = \begin{cases} \left[1-(\mathcal{C}_E+1)\frac{r_\star}{16}\right]^2 \frac{2H_\star^2}{\pi^2 M_p^2}+\cdots, & \text{for } q=1/2, \\ \left[1-(\mathcal{C}_E+1)\frac{r_\star}{16}\right]^2 \frac{2H_\star^2}{\pi^2 M_p^2}+\cdots, & \text{for any } q. \end{cases} \quad (5.415)$$

9. Next the running of the tensor-to-scalar ratio can be expressed in terms of the inflationary observables as

$$\begin{aligned} \alpha_{r,\star} &= -8\alpha_{h,\star}+\cdots \\ &\approx \begin{cases} \left[r_\star\left(1+\frac{r_\star}{8}\right)\left(n_{\zeta,\star}-1+\frac{r_\star}{8}\right)-r_\star\left(n_{\zeta,\star}-1+\frac{r_\star}{8}\right)^2 \right. \\ \left. -\mathcal{C}_E r_\star\left(n_{\zeta,\star}-1+\frac{r_\star}{8}\right)^2\right]\left(1-\frac{r_\star}{24}\right)^{1/4}+\cdots, & \text{for } q=1/2, \\ \left[2r_\star\sqrt{\frac{q}{2}}\left(1+\frac{r_\star}{8}\right)\left(n_{\zeta,\star}-1+\frac{r_\star}{8}\right) \right. \\ \left. -\frac{1}{(2q)^{1/2}}(\mathcal{C}_E+1)\,r_\star\left(n_{\zeta,\star}-1+\frac{r_\star}{8}\right)^2\right]\left(1-\frac{r_\star}{24}\right)^{1/4}+\cdots, & \text{for any } q. \end{cases} \end{aligned} \quad (5.416)$$

10. Finally the scale of single field tachyonic inflation can be expressed in terms of the Hubble parameter and the other inflationary observables as

$$H_{\rm inf}=H_\star \approx \begin{cases} \dfrac{\sqrt{\frac{\Delta_{\zeta,\star}r_\star}{2}}\,\pi M_p}{\left[1-\left(\mathcal{C}_E+\frac{5}{6}\right)\frac{r_\star}{16}+\frac{\mathcal{C}_E}{2}\left(n_{\zeta,\star}-1+\frac{r_\star}{8}\right)\right]}+\cdots, & \text{for } q=1/2, \\ \dfrac{\sqrt{\frac{\Delta_{\zeta,\star}r_\star}{2}}\,\pi M_p}{\left[1-(\mathcal{C}_E+1-\Sigma)\frac{r_\star}{16}+\frac{\mathcal{C}_E}{2}\left(n_{\zeta,\star}-1+\frac{r_\star}{8}\right)\right]}+\cdots, & \text{for any } q. \end{cases} \quad (5.417)$$

One can recast this statement in terms of the inflationary potential as

$$\sqrt[4]{V_{\rm inf}}=\sqrt[4]{V_\star} \approx \begin{cases} \dfrac{\sqrt[4]{\frac{3\Delta_{\zeta,\star}r_\star}{2}}\sqrt{\pi}\,M_p}{\sqrt{\left[1-\left(\mathcal{C}_E+\frac{5}{6}\right)\frac{r_\star}{16}+\frac{\mathcal{C}_E}{2}\left(n_{\zeta,\star}-1+\frac{r_\star}{8}\right)\right]}}+\cdots, & \text{for } q=1/2, \\ \dfrac{\sqrt[4]{\frac{3\Delta_{\zeta,\star}r_\star}{2}}\sqrt{\pi}\,M_p}{\sqrt{\left[1-(\mathcal{C}_E+1-\Sigma)\frac{r_\star}{16}+\frac{\mathcal{C}_E}{2}\left(n_{\zeta,\star}-1+\frac{r_\star}{8}\right)\right]}}+\cdots, & \text{for any } q. \end{cases} \quad (5.418)$$

5.2.7 Field excursion for tachyon

In this subsection we explicitly derive the expression for the field excursion for tachyonic inflation defined as

$$|\Delta T| = |T_{\rm cmb}-T_{\rm end}| = |T_\star - T_{\rm end}| \quad (5.419)$$

where $T_{\rm cmb}$, $T_{\rm end}$ and $T_\star$ signify the tachyon field value at the time of horizon exit, at end of inflation and at pivot scale respectively. Here we perform the computation for both AV and BD vacuum. For for the sake of simplicity the pivot scale is fixed at the horizon exit scale. To compute the expression for the field excursion we perform the following steps:

1. We start with the operator identity for single field tachyon using which one can write expression for the tachyon field variation with respect to the momentum scale (k) or number of e-foldings (N) in terms of the inflationary observables as

$$\frac{1}{H}\frac{dT}{dt} = \frac{dT}{dN} = \frac{dT}{d\ln k} \approx \begin{cases} \sqrt{\frac{r}{8MV(T)\alpha'}}M_p\left(1-\frac{r}{24}\right)^{1/4}+\cdots, & \text{for} \quad q=1/2,\\ \sqrt{\frac{qr}{4MV(T)\alpha'}}\frac{M_p}{2q}\left(1-\frac{r}{24}\right)^{1/4}+\cdots, & \text{for any arbitrary } q, \end{cases} \tag{5.420}$$

   where the tensor-to-scalar ratio r is a function of k or N.
2. Next using Eq. (5.172) we can write the following integral equation:

$$\int_{T_{\rm end}}^{T_\star} dT\,\sqrt{V(T)} \approx \begin{cases} \int_{k_{\rm end}}^{k_\star} d\ln k\,\sqrt{\frac{r}{8M\alpha'}}M_p\left(1-\frac{r}{24}\right)^{1/4}+\cdots \\ \quad = \int_{N_{\rm end}}^{N_\star} dN\,\sqrt{\frac{r}{8M\alpha'}}M_p\left(1-\frac{r}{24}\right)^{1/4}+\cdots, & \text{for} \quad q=1/2,\\ \int_{k_{\rm end}}^{k_\star} d\ln k\,\sqrt{\frac{qr}{4M\alpha'}}\frac{M_p}{2q}\left(1-\frac{r}{24}\right)^{1/4}+\cdots \\ \quad = \int_{N_{\rm end}}^{N_\star} dN\,\sqrt{\frac{qr}{4M\alpha'}}\frac{M_p}{2q}\left(1-\frac{r}{24}\right)^{1/4}+\cdots, & \text{for any arbitrary } q. \end{cases} \tag{5.421}$$

3. Next we use the same parametrization of the tensor-to-scalar ratio for $q=1/2$ and for any arbitrary q at any arbitrary scale as mentioned earlier for the single tachyonic field case.
4. For any value of q including $q=1/2$ we need to compute the following integral:

$$\begin{aligned}&\int_{k_{\rm end}}^{k_\star} d\ln k\,\sqrt{\frac{qr}{4M\alpha'}}\frac{M_p}{2q}\left(1-\frac{r}{24}\right)^{1/4}\\ &\approx \begin{cases} \sqrt{\frac{qr_\star}{4M\alpha'}}\frac{M_p}{2q}\left(1-\frac{r_\star}{24}\right)^{1/4}\ln\left(\frac{k_\star}{k_{\rm end}}\right) & \text{for } \underline{\text{Case I}},\\ \frac{\sqrt{\frac{qr_\star}{4M\alpha'}}\frac{M_p}{q}}{3(n_{h,\star}-n_{\zeta,\star}+1)}\left[\left\{{}_2F_1\left[\frac{1}{2},\frac{3}{4};\frac{3}{2};\frac{r_\star}{24}\right]+2\left(1-\frac{r_\star}{24}\right)^{1/4}\right\}\right.\\ \quad -\left(\frac{k_{\rm end}}{k_\star}\right)^{\frac{n_{h,\star}-n_{\zeta,\star}+1}{2}}\left\{{}_2F_1\left[\frac{1}{2},\frac{3}{4};\frac{3}{2};\frac{r_\star}{24}\left(\frac{k_{\rm end}}{k_\star}\right)^{n_{h,\star}-n_{\zeta,\star}+1}\right]\right.\\ \quad \left.\left.+2\left(1-\frac{r_\star}{24}\left(\frac{k_{\rm end}}{k_\star}\right)^{n_{h,\star}-n_{\zeta,\star}+1}\right)^{1/4}\right\}\right] & \text{for } \underline{\text{Case II}},\\ \sqrt{\frac{\pi q r_\star}{M\alpha'(\alpha_{h,\star}-\alpha_{\zeta,\star})}}\frac{M_p}{48q}e^{-\frac{3(n_{h,\star}-n_{\zeta,\star}+1)^2}{4(\alpha_{h,\star}-\alpha_{\zeta,\star})}}\\ \quad \left[12e^{\frac{(n_{h,\star}-n_{\zeta,\star}+1)^2}{2(\alpha_{h,\star}-\alpha_{\zeta,\star})}}\left\{\mathrm{erfi}\left(\frac{n_{h,\star}-n_{\zeta,\star}+1}{2\sqrt{\alpha_{h,\star}-\alpha_{\zeta,\star}}}\right)\right.\right.\\ \quad \left.-\mathrm{erfi}\left(\frac{n_{h,\star}-n_{\zeta,\star}+1}{2\sqrt{\alpha_{h,\star}-\alpha_{\zeta,\star}}}+\frac{\sqrt{\alpha_{h,\star}-\alpha_{\zeta,\star}}}{2}\ln\left(\frac{k_{\rm end}}{k_\star}\right)\right)\right\}\\ \quad -\frac{\sqrt{3}r_\star}{24}\left\{\mathrm{erfi}\left(\frac{\sqrt{3}(n_{h,\star}-n_{\zeta,\star}+1)}{2\sqrt{\alpha_{h,\star}-\alpha_{\zeta,\star}}}\right)\right.\\ \quad \left.\left.-\mathrm{erfi}\left(\frac{\sqrt{3}(n_{h,\star}-n_{\zeta,\star}+1)}{2\sqrt{\alpha_{h,\star}-\alpha_{\zeta,\star}}}+\frac{\sqrt{3(\alpha_{h,\star}-\alpha_{\zeta,\star})}}{2}\ln\left(\frac{k_{\rm end}}{k_\star}\right)\right)\right\}\right] & \text{for } \underline{\text{Case III}}, \end{cases} \quad \underline{\text{for BD}}.\end{aligned} \tag{5.422}$$

Similarly for AV we get the following result:

$$\int_{k_{\rm end}}^{k_\star} d\ln k\,\sqrt{\frac{qr}{4M\alpha'}}\frac{M_p}{2q}\left(1-\frac{r}{24}\right)^{1/4} \approx \begin{cases} \sqrt{\frac{r_\star}{8M\alpha'}}\frac{M_p}{2c_S}\left(1-\frac{qr_\star}{48c_S^2}\right)^{1/4}\ln\left(\frac{k_\star}{k_{\rm end}}\right) & \text{for } \underline{\text{Case I}}, \\ \sqrt{\frac{r_\star}{8M\alpha'}}\frac{M_p}{2c_S}\frac{|D|}{|C|}\left(1-\frac{qr_\star}{48c_S^2}\frac{|D|^2}{|C|^2}\right)^{1/4}\ln\left(\frac{k_\star}{k_{\rm end}}\right) & \text{for } \underline{\text{Case II}}, \end{cases} \quad \underline{\text{for AV}}. \tag{5.423}$$

In terms of the number of e-foldings N one can re-express Eqs. (5.422) and (5.423) as

$$\int_{k_{\rm end}}^{k_\star} d\ln k\,\sqrt{\frac{qr}{4M\alpha'}}\frac{M_p}{2q}\left(1-\frac{r}{24}\right)^{1/4}$$

$$\approx \begin{cases} \sqrt{\frac{qr_\star}{4M\alpha'}}\frac{M_p}{2q}\left(1-\frac{r_\star}{24}\right)^{1/4}(N_\star-N_{\rm end}) & \text{for } \underline{\text{Case I}}, \\ \frac{\sqrt{\frac{qr_\star}{4M\alpha'}}\frac{M_p}{q}}{3(n_{h,\star}-n_{\zeta,\star}+1)}\left[\left\{{}_2F_1\left[\frac{1}{2},\frac{3}{4};\frac{3}{2};\frac{r_\star}{24}\right]+2\left(1-\frac{r_\star}{24}\right)^{1/4}\right\}\right. & \\ -e^{\frac{n_{h,\star}-n_{\zeta,\star}+1}{2}(N_{\rm end}-N_\star)}\left\{{}_2F_1\left[\frac{1}{2},\frac{3}{4};\frac{3}{2};\frac{r_\star}{24}e^{(n_{h,\star}-n_{\zeta,\star}+1)(N_{\rm end}-N_\star)}\right]\right. & \\ \left.\left.+2\left(1-\frac{r_\star}{24}e^{(n_{h,\star}-n_{\zeta,\star}+1)(N_{\rm end}-N_\star)}\right)^{1/4}\right\}\right] & \text{for } \underline{\text{Case II}}, \\ \sqrt{\frac{\pi q r_\star}{M\alpha'(\alpha_{h,\star}-\alpha_{\zeta,\star})}}\frac{M_p}{48q}e^{-\frac{3(n_{h,\star}-n_{\zeta,\star}+1)^2}{4(\alpha_{h,\star}-\alpha_{\zeta,\star})}} & \underline{\text{for BD}}, \\ \left[12e^{\frac{(n_{h,\star}-n_{\zeta,\star}+1)^2}{2(\alpha_{h,\star}-\alpha_{\zeta,\star})}}\left\{\text{erfi}\left(\frac{n_{h,\star}-n_{\zeta,\star}+1}{2\sqrt{\alpha_{h,\star}-\alpha_{\zeta,\star}}}\right)\right.\right. & \\ \left.-\text{erfi}\left(\frac{n_{h,\star}-n_{\zeta,\star}+1}{2\sqrt{\alpha_{h,\star}-\alpha_{\zeta,\star}}}+\frac{\sqrt{\alpha_{h,\star}-\alpha_{\zeta,\star}}}{2}(N_{\rm end}-N_\star)\right)\right\} & \\ -\frac{\sqrt{3}r_\star}{24}\left\{\text{erfi}\left(\frac{\sqrt{3}(n_{h,\star}-n_{\zeta,\star}+1)}{2\sqrt{\alpha_{h,\star}-\alpha_{\zeta,\star}}}\right)\right. & \\ \left.\left.-\text{erfi}\left(\frac{\sqrt{3}(n_{h,\star}-n_{\zeta,\star}+1)}{2\sqrt{\alpha_{h,\star}-\alpha_{\zeta,\star}}}+\frac{\sqrt{3(\alpha_{h,\star}-\alpha_{\zeta,\star})}}{2}(N_{\rm end}-N_\star)\right)\right\}\right] & \text{for } \underline{\text{Case III}}, \end{cases} \tag{5.424}$$

$$\int_{k_{\rm end}}^{k_\star} d\ln k\,\sqrt{\frac{qr}{4\alpha'}}\frac{M_p}{2q}\left(1-\frac{r}{24}\right)^{1/4} \approx \begin{cases} \sqrt{\frac{r_\star}{8M\alpha'}}\frac{M_p}{2c_S}\left(1-\frac{qr_\star}{48c_S^2}\right)^{1/4}(N_\star-N_{\rm end}) & \text{for } \underline{\text{Case I}}, \\ \sqrt{\frac{r_\star}{8M\alpha'}}\frac{M_p}{2c_S}\frac{|D|}{|C|}\left(1-\frac{qr_\star}{48c_S^2}\frac{|D|^2}{|C|^2}\right)^{1/4}(N_\star-N_{\rm end}) & \text{for } \underline{\text{Case II}}, \end{cases} \quad \underline{\text{for AV}}. \tag{5.425}$$

Here the two possibilities for AV vacuum as appearing for the assisted inflationary framework are:

Case I stands for a situation where the spectrum is characterized by the constraint i) $D_1 = D_2 = C_1 = C_2 \neq 0$, ii) $D_1 = D_2, C_1 = C_2 = 0$, iii) $D_1 = D_2 = 0, C_1 = C_2$.

Case II stands for a situation where the spectrum is characterized by the constraint i) $\mu \approx \nu$, $D_1 = D_2 = D \neq 0$ and $C_1 = C_2 = C \neq 0$, ii) $\mu \approx \nu$, $D_1 = D \neq 0$, $D_2 = 0$ and $C_1 = C \neq 0$, $C_2 = 0$, iii) $\mu \approx \nu$, $D_2 = D \neq 0$, $D_1 = 0$ and $C_2 = C \neq 0$, $C_1 = 0$.

5. Next following exactly the same steps for single field inflation and also using Eqs. (5.424), (5.425) and (5.421) we get

$$\frac{\Delta T}{M_p} \approx \begin{cases} \sqrt{\frac{q r_\star}{4M\alpha' V_0}}\frac{1}{2q}\left(1-\frac{r_\star}{24}\right)^{1/4}(N_\star - N_{\text{end}}) & \text{for } \underline{\text{Case I}}, \\ \frac{\sqrt{\frac{q r_\star}{4M\alpha' V_0}}\frac{1}{q}}{3(n_{h,\star}-n_{\zeta,\star}+1)}\left[\left\{{}_2F_1\left[\frac{1}{2},\frac{3}{4};\frac{3}{2};\frac{r_\star}{24}\right]+2\left(1-\frac{r_\star}{24}\right)^{1/4}\right\}\right. & \\ -e^{\frac{n_{h,\star}-n_{\zeta,\star}+1}{2}(N_{\text{end}}-N_\star)}\left\{{}_2F_1\left[\frac{1}{2},\frac{3}{4};\frac{3}{2};\frac{r_\star}{24}e^{(n_{h,\star}-n_{\zeta,\star}+1)(N_{\text{end}}-N_\star)}\right]\right. & \\ \left.\left.+2\left(1-\frac{r_\star}{24}e^{(n_{h,\star}-n_{\zeta,\star}+1)(N_{\text{end}}-N_\star)}\right)^{1/4}\right\}\right] & \text{for } \underline{\text{Case II}}, \\ \sqrt{\frac{\pi q r_\star}{M\alpha'(\alpha_{h,\star}-\alpha_{\zeta,\star})V_0}}\frac{1}{48q}e^{-\frac{3(n_{h,\star}-n_{\zeta,\star}+1)^2}{4(\alpha_{h,\star}-\alpha_{\zeta,\star})}} & \underline{\text{for BD}}, \\ \left[12e^{\frac{(n_{h,\star}-n_{\zeta,\star}+1)^2}{2(\alpha_{h,\star}-\alpha_{\zeta,\star})}}\left\{\text{erfi}\left(\frac{n_{h,\star}-n_{\zeta,\star}+1}{2\sqrt{\alpha_{h,\star}-\alpha_{\zeta,\star}}}\right)\right.\right. & \\ \left.-\text{erfi}\left(\frac{n_{h,\star}-n_{\zeta,\star}+1}{2\sqrt{\alpha_{h,\star}-\alpha_{\zeta,\star}}}+\frac{\sqrt{\alpha_{h,\star}-\alpha_{\zeta,\star}}}{2}(N_{\text{end}}-N_\star)\right)\right\} & \\ -\frac{\sqrt{3}r_\star}{24}\left\{\text{erfi}\left(\frac{\sqrt{3}(n_{h,\star}-n_{\zeta,\star}+1)}{2\sqrt{\alpha_{h,\star}-\alpha_{\zeta,\star}}}\right)\right. & \\ \left.\left.-\text{erfi}\left(\frac{\sqrt{3}(n_{h,\star}-n_{\zeta,\star}+1)}{2\sqrt{\alpha_{h,\star}-\alpha_{\zeta,\star}}}+\frac{\sqrt{3(\alpha_{h,\star}-\alpha_{\zeta,\star})}}{2}(N_{\text{end}}-N_\star)\right)\right\}\right] & \text{for } \underline{\text{Case III}}, \end{cases} \tag{5.426}$$

$$\frac{\Delta T}{M_p} \approx \begin{cases} \sqrt{\frac{r_\star}{8M\alpha' V_0}}\frac{1}{2c_S}\left(1-\frac{q r_\star}{48 c_S^2}\right)^{1/4}(N_\star - N_{\text{end}}) & \text{for } \underline{\text{Case I}}, \\ \sqrt{\frac{r_\star}{8M\alpha' V_0}}\frac{|D|}{2c_S\,|C|}\left(1-\frac{q r_\star}{48 c_S^2}\frac{|D|^2}{|C|^2}\right)^{1/4}(N_\star - N_{\text{end}}) & \text{for } \underline{\text{Case II}}, \end{cases} \quad \underline{\text{for AV}}. \tag{5.427}$$

6. Next using Eq. (5.418) in Eqs. (5.426) and (5.427) we get

$$\frac{\Delta T}{M_p} \approx \begin{cases} \sqrt{\frac{q r_\star}{4M\alpha'}} \frac{1}{2q\sqrt{\frac{3\Delta_{\zeta,\star} r_\star}{2}} \pi M_p^2} \left(1 - \frac{r_\star}{24}\right)^{1/4} (N_\star - N_{\text{end}}) \\ \left[1 - (\mathcal{C}_E + 1 - \Sigma)\frac{r_\star}{16} + \frac{\mathcal{C}_E}{2\sqrt{2q}}\left(n_{\zeta,\star} - 1 + \frac{r_\star}{8}\right)\right] & \text{for } \underline{\text{Case I}}, \\ \frac{\sqrt{\frac{q r_\star}{4M\alpha'}} \frac{1}{q\sqrt{\frac{3\Delta_{\zeta,\star} r_\star}{2}} \pi M_p^2}}{3(n_{h,\star} - n_{\zeta,\star} + 1)} \left[\left\{ {}_2F_1\left[\frac{1}{2}, \frac{3}{4}; \frac{3}{2}; \frac{r_\star}{24}\right] + 2\left(1 - \frac{r_\star}{24}\right)^{1/4}\right\}\right. \\ -e^{\frac{n_{h,\star} - n_{\zeta,\star} + 1}{2}(N_{\text{end}} - N_\star)} \left\{ {}_2F_1\left[\frac{1}{2}, \frac{3}{4}; \frac{3}{2}; \frac{r_\star}{24} e^{(n_{h,\star} - n_{\zeta,\star} + 1)(N_{\text{end}} - N_\star)}\right]\right. \\ \left.\left. +2\left(1 - \frac{r_\star}{24} e^{(n_{h,\star} - n_{\zeta,\star} + 1)(N_{\text{end}} - N_\star)}\right)^{1/4}\right\}\right] \\ \left[1 - (\mathcal{C}_E + 1 - \Sigma)\frac{r_\star}{16} + \frac{\mathcal{C}_E}{2}\left(n_{\zeta,\star} - 1 + \frac{r_\star}{8}\right)\right] & \text{for } \underline{\text{Case II}}, \\ \frac{\sqrt{\frac{\pi q r_\star}{M\alpha'(\alpha_{h,\star} - \alpha_{\zeta,\star})}}}{48q\sqrt{\frac{3\Delta_{\zeta,\star} r_\star}{2}} \pi M_p^2} e^{-\frac{3(n_{h,\star} - n_{\zeta,\star} + 1)^2}{4(\alpha_{h,\star} - \alpha_{\zeta,\star})}} \\ \left[12 e^{\frac{(n_{h,\star} - n_{\zeta,\star} + 1)^2}{2(\alpha_{h,\star} - \alpha_{\zeta,\star})}} \left\{ \text{erfi}\left(\frac{n_{h,\star} - n_{\zeta,\star} + 1}{2\sqrt{\alpha_{h,\star} - \alpha_{\zeta,\star}}}\right)\right.\right. \\ \left. -\text{erfi}\left(\frac{n_{h,\star} - n_{\zeta,\star} + 1}{2\sqrt{\alpha_{h,\star} - \alpha_{\zeta,\star}}} + \frac{\sqrt{\alpha_{h,\star} - \alpha_{\zeta,\star}}}{2}(N_{\text{end}} - N_\star)\right)\right\} \\ -\frac{\sqrt{3} r_\star}{24} \left\{ \text{erfi}\left(\frac{\sqrt{3}(n_{h,\star} - n_{\zeta,\star} + 1)}{2\sqrt{\alpha_{h,\star} - \alpha_{\zeta,\star}}}\right)\right. \\ \left.\left. -\text{erfi}\left(\frac{\sqrt{3}(n_{h,\star} - n_{\zeta,\star} + 1)}{2\sqrt{\alpha_{h,\star} - \alpha_{\zeta,\star}}} + \frac{\sqrt{3(\alpha_{h,\star} - \alpha_{\zeta,\star})}}{2}(N_{\text{end}} - N_\star)\right)\right\}\right] \\ \left[1 - (\mathcal{C}_E + 1 - \Sigma)\frac{r_\star}{16} + \frac{\mathcal{C}_E}{2}\left(n_{\zeta,\star} - 1 + \frac{r_\star}{8}\right)\right] & \text{for } \underline{\text{Case III}}, \end{cases} \quad \underline{\text{for BD}}, \tag{5.428}$$

$$\frac{\Delta T}{M_p} \approx \begin{cases} \sqrt{\frac{r_\star}{8M\alpha'}} \frac{\left(1 - \frac{q r_\star}{48 c_S^2}\right)^{1/4} (N_\star - N_{\text{end}})}{2c_S\sqrt{\frac{3\Delta_{\zeta,\star} r_\star}{2}} \pi M_p^2} \\ \left[1 - (\mathcal{C}_E + 1 - \Sigma)\frac{r_\star}{16} + \frac{\mathcal{C}_E}{2}\left(n_{\zeta,\star} - 1 + \frac{r_\star}{8}\right)\right] & \text{for } \underline{\text{Case I}}, \\ \sqrt{\frac{r_\star}{8M\alpha'}} \frac{|D|\left(1 - \frac{q r_\star}{48 c_S^2}\frac{|D|^2}{|C|^2}\right)^{1/4} (N_\star - N_{\text{end}})}{2c_S\,|C|\sqrt{\frac{3\Delta_{\zeta,\star} r_\star}{2}} \pi M_p^2} \\ \left[1 - (\mathcal{C}_E + 1 - \Sigma)\frac{r_\star}{16} + \frac{\mathcal{C}_E}{2}\left(n_{\zeta,\star} - 1 + \frac{r_\star}{8}\right)\right] & \text{for } \underline{\text{Case II}}, \end{cases} \quad \underline{\text{for AV}}. \tag{5.429}$$

Further using the approximated form of the sound speed c_S the expression for the field excursion for AV can be rewritten as

$$\frac{\Delta T}{M_p} \approx \begin{cases} \sqrt{\frac{r_\star}{8M\alpha'}}\,\frac{\left(1-\frac{q r_\star}{48\left[1-\frac{(1-q)}{3q}\frac{r_\star}{8}\right]}\right)^{1/4}(N_\star - N_{\text{end}})}{2\sqrt{1-\frac{(1-q)}{3q}\frac{r_\star}{8}}\sqrt{\frac{3\Delta_{\zeta,\star}r_\star}{2}}\,\pi M_p^2} \\ \left[1-(\mathcal{C}_E+1-\Sigma)\frac{r_\star}{16}+\frac{\mathcal{C}_E}{2}\left(n_{\zeta,\star}-1+\frac{r_\star}{8}\right)\right] & \text{for } \underline{\text{Case I}}, \\ \sqrt{\frac{r_\star}{8M\alpha'}}\,\frac{|D|\left(1-\frac{q r_\star}{48\left[1-\frac{(1-q)}{3q}\frac{r_\star}{8}\right]}\frac{|D|^2}{|C|^2}\right)^{1/4}(N_\star - N_{\text{end}})}{2\sqrt{1-\frac{(1-q)}{3q}\frac{r_\star}{8}}\,|C|\sqrt{\frac{3\Delta_{\zeta,\star}r_\star}{2}}\,\pi M_p^2} \\ \left[1-(\mathcal{C}_E+1-\Sigma)\frac{r_\star}{16}+\frac{\mathcal{C}_E}{2}\left(n_{\zeta,\star}-1+\frac{r_\star}{8}\right)\right] & \text{for } \underline{\text{Case II}}, \end{cases} \quad \text{for } \underline{\text{AV}}. \tag{5.430}$$

This implies that for BD and AV we get roughly the following result from this analysis:

$$\left|\frac{\Delta T}{M_p}\right|_{\text{Assisted}} = \frac{1}{\sqrt{M}} \times \left|\frac{\Delta T}{M_p}\right|_{\text{Single}}, \tag{5.431}$$

which means that if the number of tachyonic fields participating in the assisted inflation gradually increases, then the tachyonic field excursion for assisted inflation becomes more and more sub-Planckian compared to the single field result.

5.2.8 Semi-analytical study and cosmological parameter estimation

In this subsection our prime objective are:

- To compute various inflationary observables from variants of tachyonic potentials in the presence of M identical degrees of freedom.
- To estimate the relevant cosmological parameters from the proposed models.
- To compare the effectiveness of all of these models in the light of recent Planck 2015 data along with other combined constraints.
- Finally to check the compatibility of all of these models with the CMB TT, TE and EE angular power spectra as observed by Planck 2015.

However, instead of computing everything in detail we will not do any further computation in the context of assisted inflation using all the individual five potentials for that we have already done the analysis in the context of single tachyonic field earlier in this paper. In this context the results are exactly the same for all potentials that have already done for a single field, provided for all the models the stringy parameter g, appearing almost everywhere, is rescaled by the number of identical scalar fields in the present context, i.e., for the sake of simplicity here we define a new stringy parameter $\tilde{g}$, which is given by

$$\tilde{g} = gM = \underbrace{\frac{\alpha'\lambda T_0^2}{M_p^2}} \times M = \underbrace{\frac{M_s^4}{(2\pi)^3 g_s}\frac{\alpha' T_0^2}{M_p^2}} \times M, \tag{5.432}$$

where the terms pointed by the $\underbrace{\quad}$ symbol signify the exact contribution from the single tachyonic field. Now from the observational constraints instead of constraining the parameter g here we need to constrain the value of $\tilde{g}$ for all five tachyonic potentials mentioned earlier. Let us mention all the constraints on the stringy parameter $\tilde{g}$ for the assisted inflationary framework:

- *Model I: inverse cosh potential*
  For $q = 1/2$, $q = 1$, $q = 3/2$ and $q = 2$ we fix $N_\star/\tilde{g} \sim 0.8$, which further implies that for $50 < N_\star < 70$, the prescribed window for $\tilde{g}$ from the $\Delta_\zeta + n_\zeta$ plot is given by $63 < \tilde{g} < 88$. If we additionally impose the constraint from the upper bound on the tensor-to-scalar ratio then also the allowed parameter range is lying within a similar window, i.e., $88 < \tilde{g} < 100$.

  Model II: logarithmic potential

  For $q = 1/2$, and $q = 1$ we fix $N_\star/\tilde{g} \sim 0.7$, which further implies that for $50 < N_\star < 70$, the prescribed window for $\tilde{g}$ from the $\Delta_\zeta + n_\zeta$ plot is given by $71.4 < g < 100$. If we additionally impose the constraint from the upper bound on the tensor-to-scalar ratio then also the allowed parameter range is lying within a similar window, i.e., $71.4 < \tilde{g} < 90$.

  Model III: exponential potential-type I

  For $q = 1/2$, $q = 1$, $q = 3/2$ and $q = 2$ case $\tilde{g}$ is not explicitly appearing in the various inflationary observables except the amplitude of scalar power spectrum in this case. To produce the correct value of the ampli-

Table 1 Comparison between the field excursion obtained from all the tachyonic potentials from the single field and assisted inflationary frameworks. Here we define $y_0 = T_0/M_p$, where $M_p = 2.43 \times 10^{18}$ GeV. The numerics clearly implies that the assisted tachyonic inflationary framework pushes the field excursion value to a sub-Planckian value for large M by a large amount, compared to the value obtained from single inflationary set-up. Technically this implies the doing effective field theory (EFT) with assisted framework is safer compared to single field case, as it involves an additional parameter M

Model	Parameters (2σ bound)	Single field $X_S := (\|\Delta T\|/M_p)_{\text{Single}}$	Assisted $X_A := (\|\Delta T\|/M_p)_{\text{Assisted}}$
Inverse cosh potential	$80 < g, \tilde{g} < 100$	$0.34 y_0 < X_S < 1.00 y_0$	$\frac{0.34 y_0}{\sqrt{M}} < X_A < \frac{1.00 y_0}{\sqrt{M}}$
	$1/2 < q < 2$	*EFT* For $y_0 < 1.00$	*EFT* For I. $y_0 < 1.00$
			II. $M \geq 2$
Logarithmic potential	$71.4 < g, \tilde{g} < 100$	$0.93 y_0 < X_S < 1.12 y_0$	$\frac{0.93 y_0}{\sqrt{M}} < X_A < \frac{1.12 y_0}{\sqrt{M}}$
	$1/2 < q < 1$	*EFT* For $y_0 < 0.892$	*EFT* For I. $y_0 < 0.892$
	$c = 0.07$		II. $M \geq 2$
Exponential potential Type-I	$360 < g, \tilde{g} < 400$	$4.26 y_0 < X_S < 4.27 y_0$	$\frac{4.26 y_0}{\sqrt{M}} < X_A < \frac{4.27 y_0}{\sqrt{M}}$
	$1 < q < 2$	*EFT* For $y_0 < 0.234$	*EFT* For I. $y_0 < 0.234$
			II. $M \geq 2$
Exponential potential Type-II	$73 < g, \tilde{g} < 82.3$	$3.18 y_0 < X_S < 6.27 y_0$	$\frac{3.18 y_0}{\sqrt{M}} < X_A < \frac{6.27 y_0}{\sqrt{M}}$
	$1/2 < q < 2$	*EFT* For $y_0 < 0.160$	*EFT* For I. $y_0 < 0.160$
	$6 < p = \sqrt{\frac{g}{2}} < 6.4$		II. $M \geq 2$
Inverse power-law potential	$600 < g, \tilde{g} < 700$	$7.2 y_0 < X_S < 7.9 y_0$	$\frac{7.2 y_0}{\sqrt{M}} < X_A < \frac{7.9 y_0}{\sqrt{M}}$
	$1 < q < 3/2$	*EFT* For $y_0 < 0.127$	*EFT* For I. $y_0 < 0.127$
			II. $M \geq 2$

tude of the scalar power spectra we fix the parameter $360 < \tilde{g} < 400$.

Model IV: exponential potential-type II

For $q = 1/2, q = 1, q = 3/2$ and $q = 2$ we fix $N_\star/g \sim 0.85$, which further implies that for $50 < N_\star < 70$, the prescribed window for g from $\Delta_\zeta + n_\zeta$ constraints is given by $59 < \tilde{g} < 82.3$. If we additionally impose the constraint from the upper bound on the tensor-to-scalar ratio then also the allowed parameter range is lying within the window, i.e., $73 < \tilde{g} < 82.3$.

Model V: inverse power-law potential

For the $q = 1/2$, $q = 1$, $q = 3/2$ and $q = 2$ cases $\tilde{g}$ is not explicitly appearing in the various inflationary observables except the amplitude of scalar power spectrum in this case. To produce the correct value of the amplitude of the scalar power spectra we fix the parameter $600 < \tilde{g} < 700$.

In Table 1 we have shown the comparison between the field excursion obtained from all the tachyonic potentials from single field and assisted inflationary framework. Here we define $y_0 = T_0/M_p$, where $M_p = 2.43 \times 10^{18}$ GeV. The numerics clearly implies that the assisted tachyonic inflationary framework pushes the field excursion value to a sub-Planckian value for large M with large amount, compared to the value obtained from the single inflationary set-up. Technically this implies that effective field theory (EFT) with assisted framework is safer compared to the single field case, as it involves an additional parameter M.

Additionally it is important to mention here that the other conclusions and the rest of the constraints are exactly the same as analyzed in the single field case. Similarly the CMB TT, TE, EE spectra for the scalar modes are exactly the same as obtained in the context of single tachyonic inflation and compatible with the observed Planck 2015 data.

5.3 Computation for the multi-field inflation

In case of multi-tachyonic inflation all the tachyons are not identical. In more technical language for the most generalized prescription one can state that

$$T_1 \neq T_2 \neq \cdots \neq T_M. \tag{5.433}$$

In the next subsections we will explore the detailed features of multi-tachyonic inflation by computing the curvature, isocurvature and tensor perturbations and then we discuss the observational constraints and cosmological consequences from the set-up. We will give all the analytical results for M non-identical tachyonic fields and for completeness also give the results for M number of non-identical inverse cosh separable potential.

5.3.1 Condition for inflation

For assisted tachyonic inflation, the prime condition for inflation is given by

$$\dot{H}+H^2=\left(\frac{\ddot{a}}{a}\right)=-\sum_{i=1}^{M}\frac{(\rho_i+3p_i)}{6M_p^2}>0 \tag{5.434}$$

which can be re-expressed in terms of the following constraint condition in the context of assisted tachyonic inflation:

$$\sum_{i=1}^{M}\frac{V(T_i)}{3M_p^2\sqrt{1-\alpha'\dot{T}_i^2}}\left(1-\frac{3}{2}\alpha'\dot{T}_i^2\right)>0. \tag{5.435}$$

Here Eq. (5.316) implies that to satisfy inflationary constraints in the slow-roll regime the following constraint always holds good:

$$\dot{T}_i<\sqrt{\frac{2}{3\alpha'}}\quad\forall\, i=1,2,\ldots,M, \tag{5.436}$$

$$\ddot{T}_i<3H\dot{T}_i<\sqrt{\frac{6}{\alpha'}}H\quad\forall\, i=1,2,\ldots,M. \tag{5.437}$$

Consequently the field equations are approximated by

$$3H\alpha'\dot{T}_i+\left(\sum_{j=1}^{M}V(T_j)\right)^{-1}\frac{\partial}{\partial T_i}\left(\sum_{j=1}^{M}V(T_j)\right)\approx 0, \tag{5.438}$$

Similarly, in the most generalized case,

$$\sum_{i=1}^{M}\frac{V(T_i)}{3M_p^2\left(1-\alpha'\dot{T}_i^2\right)^{1-q}}\left(1-(1+q)\alpha'\dot{T}_i^2\right)>0. \tag{5.439}$$

Here Eq. (5.439) implies that to satisfy inflationary constraints in the slow-roll regime the following constraint always holds good:

$$\dot{T}_i<\sqrt{\frac{1}{\alpha'(1+q)}}\quad\forall\, i=1,2,\ldots,M, \tag{5.440}$$

$$\ddot{T}_i<3H\dot{T}_i<\sqrt{\frac{9}{\alpha'(1+q)}}H\quad\forall\, i=1,2,\ldots,M. \tag{5.441}$$

Consequently the field equations are approximated by

$$6q\alpha'H\dot{T}_i+\left(\sum_{j=1}^{M}V(T_j)\right)^{-1}\frac{\partial}{\partial T_i}\left(\sum_{j=1}^{M}V(T_j)\right)\approx 0 \tag{5.442}$$

Also for both cases in the slow-roll regime the Friedmann equation is modified as

$$H^2\approx\sum_{i=1}^{M}\frac{V(T_i)}{3M_p^2}. \tag{5.443}$$

Further substituting Eq. (5.443) in Eqs. (5.438) and (5.442) we get

$$\sqrt{\sum_{j=1}^{M}V(T_j)}\frac{\sqrt{3}\alpha'}{M_p}\dot{T}_i+\left(\sum_{j=1}^{M}V(T_j)\right)^{-1}\frac{\partial}{\partial T_i}\left(\sum_{j=1}^{M}V(T_j)\right)\approx 0\quad\forall i=1,2,\ldots,M, \tag{5.444}$$

$$\frac{6q}{\sqrt{3}M_p}\sqrt{\sum_{j=1}^{M}V(T_j)}\alpha'\dot{T}_i+\left(\sum_{j=1}^{M}V(T_j)\right)^{-1}\frac{\partial}{\partial T_i}\left(\sum_{j=1}^{M}V(T_j)\right)\approx 0\quad\forall i=1,2,\ldots,M. \tag{5.445}$$

Finally the general solution for both cases can be expressed in terms of the single field tachyonic potential $V(T)$ as

$$t-t_{in,i}\approx-\frac{\sqrt{3}\alpha'}{M_p}\int_{T_{in,i}}^{T_i}dT_i\sqrt{\sum_{j=1}^{M}V(T_j)}\left[\left(\sum_{j=1}^{M}V(T_j)\right)^{-1}\frac{\partial}{\partial T_i}\left(\sum_{j=1}^{M}V(T_j)\right)\right]^{-1}, \tag{5.446}$$

$$t-t_{in,i}\approx-\frac{6q\alpha'}{\sqrt{3}M_p}\int_{T_{in,i}}^{T_i}dT_i\sqrt{\sum_{j=1}^{M}V(T_j)}\left[\left(\sum_{j=1}^{M}V(T_j)\right)^{-1}\frac{\partial}{\partial T_i}\left(\sum_{j=1}^{M}V(T_j)\right)\right]^{-1}. \tag{5.447}$$

Further using Eqs. (5.446), (5.447) and (5.443) we get the following solution for the scale factor in terms of the tachyonic field for the usual $q=1/2$ and for a generalized value of q:

$$a = a_{in,i} \times \begin{cases} \exp\left[-\frac{\alpha' M}{M_p^2}\int_{T_{in}}^{T_i} \mathrm{d}T_i \sum_{j=1}^{M} V(T_j)\left[\left(\sum_{j=1}^{M} V(T_j)\right)^{-1}\frac{\partial}{\partial T_i}\left(\sum_{j=1}^{M} V(T_j)\right)\right]^{-1}\right], & \text{for} \quad q = 1/2, \\ \exp\left[-\frac{2q\alpha' M}{M_p^2}\int_{T_{in}}^{T_i} \mathrm{d}T_i \sum_{j=1}^{M} V(T_j)\left[\left(\sum_{j=1}^{M} V(T_j)\right)^{-1}\frac{\partial}{\partial T_i}\left(\sum_{j=1}^{M} V(T_j)\right)\right]^{-1}\right]. & \text{for any} \quad q. \end{cases} \tag{5.448}$$

Sometimes it is convenient to identify the inflaton field direction as the direction in field space corresponding to the evolution of the background spatially homogeneous tachyonic fields during inflation. To serve this purpose one can write

$$\sigma = \int \sum_{i=1}^{M} \hat{\sigma}_i \dot{T}_i \, \mathrm{d}t, \tag{5.449}$$

where the inflaton direction is defined as

$$\hat{\sigma}_i \equiv \dot{T} \times \left[\sum_{j=1}^{M} \dot{T}_j^2\right]^{-1/2}. \tag{5.450}$$

The M evolution equations for the homogeneous scalar fields can be written as the evolution of single scalar field in the slow-roll regime as

$$\begin{aligned} 3H\dot{\sigma} &+ \left(\sum_{j=1}^{M} V(T_j)\right)^{-1}\frac{\partial}{\partial\sigma}\left(\sum_{j=1}^{M} V(T_j)\right) \\ &= 3H\dot{\sigma} + \sum_{i=1}^{M}\hat{\sigma}_i\left(\sum_{j=1}^{M} V(T_j)\right)^{-1}\frac{\partial}{\partial T_i}\left(\sum_{j=1}^{M} V(T_j)\right) = 0. \end{aligned} \tag{5.451}$$

5.3.2 Analysis using slow-roll formalism

Here our prime objective is to define slow-roll parameters for tachyon inflation in terms of the Hubble parameter and the multi-tachyonic inflationary potential, where the M tachyon fields are not identical. Using the slow-roll approximation one can expand various cosmological observables in terms of small dynamical quantities derived from the appropriate derivatives of the Hubble parameter and of the inflationary potential. To start with, in the present context the potential dependent slow-roll parameters are defined as

$$\epsilon_{V;T_jT_j}(T_i) = \frac{M_p^2}{2}\left(\frac{\partial_{T_j} V(T_i)}{V(T_i)}\right)^2, \tag{5.452}$$

$$\eta_{V;T_jT_j}(T_i) = M_p^2\left(\frac{\partial_{T_j}\partial_{T_j} V(T_i)}{V(T_i)}\right), \tag{5.453}$$

$$\Theta_{V;T_jT_k}(T_i) = M_p^2\left(\frac{\partial_{T_j}\partial_{T_k} V(T_i)}{V(T_i)}\right), \tag{5.454}$$

$$\Delta_{V;T_jT_k}(T_i) = \frac{M_p^2}{2}\left(\frac{\partial_{T_j} V(T_i)\partial_{T_k} V(T_i)}{V^2(T_i)}\right), \tag{5.455}$$

$$\xi^2_{V;T_jT_jT_jT_j}(T_i) = M_p^4\left(\frac{\partial_{T_j} V(T_i)\partial_{T_j}\partial_{T_j}\partial_{T_j} V(T_i)}{V^2(T_i)}\right), \tag{5.456}$$

$$\vartheta^2_{V;T_jT_jT_kT_k}(T_i) = M_p^4\left(\frac{\partial_{T_j} V(T_i)\partial_{T_j}\partial_{T_k}\partial_{T_k} V(T_i)}{V^2(T_i)}\right), \tag{5.457}$$

$$\vartheta^2_{V;T_kT_jT_kT_k}(T_i) = M_p^4\left(\frac{\partial_{T_k} V(T_i)\partial_{T_j}\partial_{T_k}\partial_{T_k} V(T_i)}{V^2(T_i)}\right), \tag{5.458}$$

$$\vartheta^2_{V;T_jT_kT_kT_k}(T_i) = M_p^4\left(\frac{\partial_{T_j} V(T_i)\partial_{T_k}\partial_{T_k}\partial_{T_k} V(T_i)}{V^2(T_i)}\right), \tag{5.459}$$

$$\begin{aligned}&\sigma^3_{V;T_jT_jT_jT_jT_jT_j}(T_i) \\ &= M_p^6\left(\frac{\partial_{T_j} V(T_i)\partial_{T_j} V(T_i)\partial_{T_j}\partial_{T_j}\partial_{T_j}\partial_{T_j} V(T_i)}{V^3(T_i)}\right),\end{aligned} \tag{5.460}$$

$$\begin{aligned}&\Upsilon^3_{V;T_jT_jT_kT_kT_kT_k}(T_i) \\ &= M_p^6\left(\frac{\partial_{T_j} V(T_i)\partial_{T_j} V(T_i)\partial_{T_k}\partial_{T_k}\partial_{T_k}\partial_{T_k} V(T_i)}{V^3(T_i)}\right),\end{aligned} \tag{5.461}$$

$$\begin{aligned}&\Upsilon^3_{V;T_jT_kT_kT_kT_kT_k}(T_i) \\ &= M_p^6\left(\frac{\partial_{T_j} V(T_i)\partial_{T_k} V(T_i)\partial_{T_k}\partial_{T_k}\partial_{T_k}\partial_{T_k} V(T_i)}{V^3(T_i)}\right),\end{aligned} \tag{5.462}$$

$$\begin{aligned}&\Upsilon^3_{V;T_jT_jT_jT_kT_jT_k}(T_i) \\ &= M_p^6\left(\frac{\partial_{T_j} V(T_i)\partial_{T_j} V(T_i)\partial_{T_j}\partial_{T_k}\partial_{T_k}\partial_{T_k} V(T_i)}{V^3(T_i)}\right),\end{aligned} \tag{5.463}$$

$$\begin{aligned}&\Upsilon^3_{V;T_jT_jT_jT_jT_kT_k}(T_i) \\ &= M_p^6\left(\frac{\partial_{T_j} V(T_i)\partial_{T_j} V(T_i)\partial_{T_j}\partial_{T_j}\partial_{T_k}\partial_{T_k} V(T_i)}{V^3(T_i)}\right),\end{aligned} \tag{5.464}$$

$$\begin{aligned}&\Upsilon^3_{V;T_jT_jT_jT_jT_jT_k}(T_i) \\ &= M_p^6\left(\frac{\partial_{T_j} V(T_i)\partial_{T_j} V(T_i)\partial_{T_j}\partial_{T_j}\partial_{T_j}\partial_{T_k} V(T_i)}{V^3(T_i)}\right),\end{aligned} \tag{5.465}$$

$$\begin{aligned}&\Upsilon^3_{V;T_jT_kT_jT_jT_jT_j}(T_i) \\ &= M_p^6\left(\frac{\partial_{T_j} V(T_i)\partial_{T_k} V(T_i)\partial_{T_j}\partial_{T_j}\partial_{T_j}\partial_{T_j} V(T_i)}{V^3(T_i)}\right),\end{aligned} \tag{5.466}$$

$$\Upsilon^3_{V;T_jT_kT_jT_jT_jT_k}(T_i) = M_p^6\left(\frac{\partial_{T_j}V(T_i)\partial_{T_k}V(T_i)\partial_{T_j}\partial_{T_j}\partial_{T_j}\partial_{T_k}V(T_i)}{V^3(T_i)}\right), \tag{5.467}$$

$$\Upsilon^3_{V;T_jT_kT_jT_jT_kT_k}(T_i) = M_p^6\left(\frac{\partial_{T_j}V(T_i)\partial_{T_k}V(T_i)\partial_{T_j}\partial_{T_j}\partial_{T_k}\partial_{T_k}V(T_i)}{V^3(T_i)}\right), \tag{5.468}$$

$$\Upsilon^3_{V;T_jT_kT_jT_kT_kT_k}(T_i) = M_p^6\left(\frac{\partial_{T_j}V(T_i)\partial_{T_k}V(T_i)\partial_{T_j}\partial_{T_k}\partial_{T_k}\partial_{T_k}V(T_i)}{V^3(T_i)}\right). \tag{5.469}$$

However, for the sake of clarity here we introduce new sets of potential dependent slow-roll parameters for multi-tachyonic inflation by rescaling with the appropriate powers of $\alpha'\left(\sum_{k=1}^M V(T_k)\right)$:

$$\begin{aligned}
\bar{\epsilon}_{V;T_jT_j}(T_i) &= \frac{\epsilon_{V;T_jT_j}(T_i)}{\alpha'\left(\sum_{k=1}^M V(T_k)\right)},\\
\bar{\Delta}_{V;T_jT_k}(T_i) &= \frac{\Delta_{V;T_jT_k}(T_i)}{\alpha'\left(\sum_{j=1}^M V(T_j)\right)},\\
\bar{\eta}_{V;T_jT_j}(T_i) &= \frac{\eta_{V;T_jT_j}(T_i)}{\alpha'\left(\sum_{j=1}^M V(T_j)\right)},\\
\bar{\Theta}_{V;T_jT_k}(T_i) &= \frac{\Theta_{V;T_jT_k}(T_i)}{\alpha'\left(\sum_{j=1}^M V(T_j)\right)},\\
\bar{\xi}^2_{V;T_jT_jT_jT_j}(T_i) &= \frac{\xi^2_{V;T_jT_jT_jT_j}(T_i)}{\alpha'^2\left(\sum_{j=1}^M V(T_j)\right)^2},\\
\bar{\vartheta}^2_{V;T_jT_jT_kT_k}(T_i) &= \frac{\vartheta^2_{V;T_jT_jT_kT_k}(T_i)}{\alpha'^2\left(\sum_{j=1}^M V(T_j)\right)^2},\\
\bar{\vartheta}^2_{V;T_kT_jT_kT_k}(T_i) &= \frac{\vartheta^2_{V;T_kT_jT_kT_k}(T_i)}{\alpha'^2\left(\sum_{j=1}^M V(T_j)\right)^2},\\
\bar{\vartheta}^2_{V;T_jT_kT_kT_k}(T_i) &= \frac{\vartheta^2_{V;T_kT_kT_jT_k}(T_i)}{\alpha'^2\left(\sum_{j=1}^M V(T_j)\right)^2},
\end{aligned}\tag{5.470}$$

$$\begin{aligned}
\bar{\sigma}^3_{V;T_jT_jT_jT_jT_jT_j}(T_i) &= \frac{\sigma^3_{V;T_jT_jT_jT_jT_jT_j}(T_i)}{\alpha'^3\left(\sum_{j=1}^M V(T_j)\right)^3},\\
\Upsilon^3_{V;T_jT_jT_kT_kT_kT_k}(T_i) &= \frac{\Upsilon^3_{V;T_jT_jT_kT_kT_kT_k}(T_i)}{\alpha'^3\left(\sum_{j=1}^M V(T_j)\right)^3},
\end{aligned}\tag{5.471}$$

$$\begin{aligned}
\bar{\Upsilon}^3_{V;T_jT_kT_kT_kT_kT_k}(T_i) &= \frac{\Upsilon^3_{V;T_jT_kT_kT_kT_kT_k}(T_i)}{\alpha'^3\left(\sum_{j=1}^M V(T_j)\right)^3},\\
\bar{\Upsilon}^3_{V;T_jT_jT_jT_kT_jT_k}(T_i) &= \frac{\Upsilon^3_{V;T_jT_jT_jT_kT_jT_k}(T_i)}{\alpha'^3\left(\sum_{j=1}^M V(T_j)\right)^3},
\end{aligned}\tag{5.472}$$

$$\begin{aligned}
\bar{\Upsilon}^3_{V;T_jT_jT_jT_jT_kT_k}(T_i) &= \frac{\Upsilon^3_{V;T_jT_jT_jT_jT_kT_k}(T_i)}{\alpha'^3\left(\sum_{j=1}^M V(T_j)\right)^3},\\
\bar{\Upsilon}^3_{V;T_jT_jT_jT_jT_jT_k}(T_i) &= \frac{\Upsilon^3_{V;T_jT_jT_jT_jT_jT_k}(T_i)}{\alpha'^3\left(\sum_{j=1}^M V(T_j)\right)^3},
\end{aligned}\tag{5.473}$$

$$\begin{aligned}
\bar{\Upsilon}^3_{V;T_jT_kT_jT_jT_jT_j}(T_i) &= \frac{\Upsilon^3_{V;T_jT_kT_jT_jT_jT_j}(T_i)}{\alpha'^3\left(\sum_{j=1}^M V(T_j)\right)^3},\\
\bar{\Upsilon}^3_{V;T_jT_kT_jT_jT_jT_k}(T_i) &= \frac{\Upsilon^3_{V;T_jT_kT_jT_jT_jT_k}(T_i)}{\alpha'^3\left(\sum_{j=1}^M V(T_j)\right)^3},
\end{aligned}\tag{5.474}$$

$$\begin{aligned}
\bar{\Upsilon}^3_{V;T_jT_kT_jT_jT_kT_k}(T_i) &= \frac{\Upsilon^3_{V;T_jT_kT_jT_jT_kT_k}(T_i)}{\alpha'^3\left(\sum_{j=1}^M V(T_j)\right)^3},\\
\bar{\Upsilon}^3_{V;T_jT_kT_jT_kT_kT_k}(T_i) &= \frac{\Upsilon^3_{V;T_jT_kT_jT_kT_kT_k}(T_i)}{\alpha'^3\left(\sum_{j=1}^M V(T_j)\right)^3}.
\end{aligned}\tag{5.475}$$

where in all cases $i, j, k = 1, 2, \ldots, M$ and $j \neq k$. For the sake of simplicity let us parametrize the flow-functions in the slow-roll regime via two angular parameters, by making use of the following transformation equations:

$$\cos\alpha_{V;T_jT_j} := \sqrt{\frac{\bar{\epsilon}_{V;T_jT_j}(T_i)}{\bar{\epsilon}_V}}, \tag{5.476}$$

$$\sin\alpha_{V;T_kT_k} := \sqrt{\frac{\bar{\epsilon}_{V;T_kT_k}(T_i)}{\bar{\epsilon}_V}}, \tag{5.477}$$

$$\cos\beta_{V;T_k} := M_p\,\bar{\epsilon}_{V;T_k}, \tag{5.478}$$

$$\sin\beta_{V;T_j} := M_p\,\bar{\epsilon}_{V;T_k}. \tag{5.479}$$

For the two-field set-up this can be visualized in a better way. In that case we need to fix $j = 1, k = 2$ or $j = 2, k = 1$. and i is the free index which can take values $i = 1, 2$ depending on the field derivative, ∂_{T_1} or ∂_{T_2} acting on it. In the present context these two sets of angular parameters physically represent the angle between the adiabatic perturbation, the tangent of the first slow-roll parameter and the field contents. Here also we define the following reduced parameters for multi-tachyonic inflation:

$$\bar{\epsilon}_V = \sum_{i=1}^M\sum_{j=1}^M \bar{\epsilon}_{V;T_jT_j}(T_i) + \sum_{i=1}^M\sum_{j=1}^M\sum_{k=1}^M\left(\bar{\Delta}_{V;T_jT_k}(T_i) + \bar{\Delta}_{V;T_kT_j}(T_i)\right), \tag{5.480}$$

$$\begin{aligned}\bar{\eta}_V &= \sum_{i=1}^{M}\sum_{j=1}^{M}\bar{\eta}_{V;T_jT_j}(T_i)\\&\quad+\sum_{i=1}^{M}\sum_{j=1}^{M}\sum_{k=1}^{M}\left(\bar{\Theta}_{V;T_jT_k}(T_i)+\bar{\Theta}_{V;T_kT_j}(T_i)\right),\end{aligned}\tag{5.481}$$

$$\begin{aligned}\bar{\xi}^2_V &= \sum_{i=1}^{M}\sum_{j=1}^{M}\bar{\xi}^2_{V;T_jT_jT_jT_j}(T_i)\\&\quad+\sum_{i=1}^{M}\sum_{j=1}^{M}\sum_{k=1}^{M}\Big(\bar{\vartheta}^2_{V;T_jT_jT_kT_k}(T_i)+\bar{\vartheta}^2_{V;T_kT_jT_kT_k}(T_i)\\&\quad+\bar{\vartheta}^2_{V;T_jT_kT_kT_k}(T_i)+\bar{\vartheta}^2_{V;T_jT_kT_jT_k}(T_i)\\&\quad+\bar{\vartheta}^2_{V;T_jT_kT_kT_j}(T_i)+\bar{\vartheta}^2_{V;T_kT_kT_jT_k}(T_i)\\&\quad+\bar{\vartheta}^2_{V;T_kT_kT_kT_j}(T_i)\Big),\end{aligned}\tag{5.482}$$

$$\begin{aligned}\bar{\sigma}^3_V &= \sum_{i=1}^{M}\sum_{j=1}^{M}\bar{\sigma}^3_{V;T_jT_jT_jT_jT_jT_j}(T_i)\\&\quad+\sum_{i=1}^{M}\sum_{j=1}^{M}\sum_{k=1}^{M}\Big(\Upsilon^3_{V;T_jT_jT_kT_kT_kT_k}(T_i)\\&\quad+\bar{\Upsilon}^3_{V;T_jT_kT_kT_kT_kT_k}(T_i)+\bar{\Upsilon}^3_{V;T_jT_jT_jT_jT_kT_k}(T_i)\\&\quad+\bar{\Upsilon}^3_{V;T_jT_jT_jT_jT_jT_k}(T_i)+\bar{\Upsilon}^3_{V;T_jT_kT_jT_jT_jT_j}(T_i)\\&\quad+\bar{\Upsilon}^3_{V;T_jT_kT_jT_jT_jT_k}(T_i)+\bar{\Upsilon}^3_{V;T_jT_kT_jT_jT_kT_k}(T_i)\\&\quad+\bar{\Upsilon}^3_{V;T_jT_kT_jT_kT_kT_k}(T_i)+\bar{\Upsilon}^3_{V;T_jT_jT_kT_jT_kT_k}(T_i)\\&\quad+\bar{\Upsilon}^3_{V;T_jT_jT_kT_kT_jT_k}(T_i)+\bar{\Upsilon}^3_{V;T_jT_jT_kT_kT_kT_j}(T_i)\\&\quad+\bar{\Upsilon}^3_{V;T_jT_jT_jT_kT_jT_k}(T_i)+\bar{\Upsilon}^3_{V;T_jT_jT_jT_kT_kT_j}(T_i)\\&\quad+\bar{\Upsilon}^3_{V;T_jT_jT_kT_jT_kT_j}(T_i)+\bar{\Upsilon}^3_{V;T_jT_jT_kT_jT_jT_k}(T_i)\\&\quad+\bar{\Upsilon}^3_{V;T_jT_jT_jT_jT_kT_j}(T_i)+\bar{\Upsilon}^3_{V;T_jT_jT_jT_kT_jT_j}(T_i)\\&\quad+\bar{\Upsilon}^3_{V;T_jT_jT_kT_jT_jT_j}(T_i)+\bar{\Upsilon}^3_{V;T_kT_jT_jT_jT_jT_j}(T_i)\\&\quad+\bar{\Upsilon}^3_{V;T_jT_kT_jT_jT_kT_j}(T_i)+\bar{\Upsilon}^3_{V;T_jT_kT_jT_kT_jT_j}(T_i)\\&\quad+\bar{\Upsilon}^3_{V;T_jT_kT_kT_jT_jT_j}(T_i)+\bar{\Upsilon}^3_{V;T_kT_jT_jT_jT_jT_k}(T_i)\\&\quad+\bar{\Upsilon}^3_{V;T_kT_jT_jT_jT_kT_j}(T_i)+\bar{\Upsilon}^3_{V;T_kT_jT_jT_kT_jT_j}(T_i)\\&\quad+\bar{\Upsilon}^3_{V;T_kT_jT_kT_jT_jT_j}(T_i)+\bar{\Upsilon}^3_{V;T_jT_kT_jT_kT_jT_k}(T_i)\\&\quad+\bar{\Upsilon}^3_{V;T_jT_kT_kT_jT_jT_k}(T_i)+\bar{\Upsilon}^3_{V;T_jT_kT_jT_kT_kT_j}(T_i)\\&\quad+\bar{\Upsilon}^3_{V;T_jT_kT_kT_jT_kT_j}(T_i)+\bar{\Upsilon}^3_{V;T_kT_jT_jT_jT_kT_k}(T_i)\\&\quad+\bar{\Upsilon}^3_{V;T_kT_jT_jT_kT_jT_k}(T_i)+\bar{\Upsilon}^3_{V;T_kT_jT_kT_jT_jT_k}(T_i)\\&\quad+\bar{\Upsilon}^3_{V;T_kT_jT_jT_kT_kT_j}(T_i)+\bar{\Upsilon}^3_{V;T_kT_jT_kT_jT_kT_j}(T_i)\\&\quad+\bar{\Upsilon}^3_{V;T_jT_kT_kT_jT_kT_k}(T_i)+\bar{\Upsilon}^3_{V;T_jT_kT_kT_kT_jT_k}(T_i)\\&\quad+\bar{\Upsilon}^3_{V;T_jT_kT_kT_kT_kT_j}(T_i)+\bar{\Upsilon}^3_{V;T_kT_jT_jT_kT_kT_k}(T_i)\\&\quad+\bar{\Upsilon}^3_{V;T_kT_jT_kT_jT_kT_k}(T_i)+\bar{\Upsilon}^3_{V;T_kT_jT_kT_kT_jT_k}(T_i)\\&\quad+\bar{\Upsilon}^3_{V;T_kT_jT_kT_kT_kT_j}(T_i)+\bar{\Upsilon}^3_{V;T_jT_jT_jT_kT_kT_k}(T_i)\Big).\end{aligned}\tag{5.483}$$

Now simplify the results let us mention the symmetries appearing due to various permutation of the indices:

$$\bar{\Delta}_{V;T_jT_k}(T_i)=\bar{\Delta}_{V;T_kT_j}(T_i),\tag{5.484}$$

$$\bar{\Theta}_{V;T_jT_k}(T_i)=\bar{\Theta}_{V;T_kT_j}(T_i),\tag{5.485}$$

$$\bar{\vartheta}^2_{V;T_jT_jT_kT_k}(T_i)=\bar{\vartheta}^2_{V;T_jT_kT_jT_k}(T_i)=\bar{\vartheta}^2_{V;T_jT_kT_kT_j}(T_i),\tag{5.486}$$

$$\bar{\vartheta}^2_{V;T_kT_jT_kT_k}(T_i)=\bar{\vartheta}^2_{V;T_kT_kT_jT_k}(T_i)=\bar{\vartheta}^2_{V;T_kT_kT_kT_j}(T_i),\tag{5.487}$$

$$\begin{aligned}\bar{\Upsilon}^3_{V;T_jT_jT_jT_kT_kT_k}(T_i)&=\bar{\Upsilon}^3_{V;T_jT_jT_kT_jT_kT_k}(T_i)\\&=\bar{\Upsilon}^3_{V;T_jT_jT_kT_kT_jT_k}(T_i)=\bar{\Upsilon}^3_{V;T_jT_jT_kT_kT_kT_j}(T_i),\end{aligned}\tag{5.488}$$

$$\begin{aligned}\bar{\Upsilon}^3_{V;T_jT_jT_jT_jT_kT_k}(T_i)&=\bar{\Upsilon}^3_{V;T_jT_jT_jT_kT_jT_k}(T_i)\\&=\bar{\Upsilon}^3_{V;T_jT_jT_jT_kT_kT_j}(T_i)=\bar{\Upsilon}^3_{V;T_jT_jT_kT_jT_kT_j}(T_i)\\&=\bar{\Upsilon}^3_{V;T_jT_jT_kT_jT_jT_k}(T_i),\end{aligned}\tag{5.489}$$

$$\begin{aligned}\bar{\Upsilon}^3_{V;T_jT_jT_jT_jT_jT_k}(T_i)&=\bar{\Upsilon}^3_{V;T_jT_jT_jT_jT_kT_j}(T_i)\\&=\bar{\Upsilon}^3_{V;T_jT_jT_jT_kT_jT_j}(T_i)=\bar{\Upsilon}^3_{V;T_jT_jT_kT_jT_jT_j}(T_i),\end{aligned}\tag{5.490}$$

$$\bar{\Upsilon}^3_{V;T_jT_kT_jT_jT_jT_j}(T_i)=\bar{\Upsilon}^3_{V;T_kT_jT_jT_jT_jT_j}(T_i),\tag{5.491}$$

$$\begin{aligned}\bar{\Upsilon}^3_{V;T_jT_kT_jT_jT_jT_k}(T_i)&=\bar{\Upsilon}^3_{V;T_jT_kT_jT_jT_kT_j}(T_i)\\&=\bar{\Upsilon}^3_{V;T_jT_kT_jT_kT_jT_j}(T_i)=\bar{\Upsilon}^3_{V;T_jT_kT_kT_jT_jT_j}(T_i),\end{aligned}\tag{5.492}$$

$$\begin{aligned}\bar{\Upsilon}^3_{V;T_kT_jT_jT_jT_jT_k}(T_i)&=\bar{\Upsilon}^3_{V;T_kT_jT_jT_jT_kT_j}(T_i)\\&=\bar{\Upsilon}^3_{V;T_kT_jT_jT_kT_jT_j}(T_i)=\bar{\Upsilon}^3_{V;T_kT_jT_kT_jT_jT_j}(T_i),\end{aligned}\tag{5.493}$$

$$\begin{aligned}\bar{\Upsilon}^3_{V;T_jT_kT_jT_jT_kT_k}(T_i)&=\bar{\Upsilon}^3_{V;T_jT_kT_jT_kT_jT_k}(T_i)\\&=\bar{\Upsilon}^3_{V;T_jT_kT_kT_jT_jT_k}(T_i)=\bar{\Upsilon}^3_{V;T_jT_kT_jT_kT_kT_j}(T_i)\\&=\bar{\Upsilon}^3_{V;T_jT_kT_kT_jT_kT_j}(T_i),\end{aligned}\tag{5.494}$$

$$\begin{aligned}\bar{\Upsilon}^3_{V;T_kT_jT_jT_jT_kT_k}(T_i)&=\bar{\Upsilon}^3_{V;T_kT_jT_jT_kT_jT_k}(T_i)\\&=\bar{\Upsilon}^3_{V;T_kT_jT_kT_jT_jT_k}(T_i)=\bar{\Upsilon}^3_{V;T_kT_jT_jT_kT_kT_j}(T_i)\\&=\bar{\Upsilon}^3_{V;T_kT_jT_kT_jT_kT_j}(T_i),\end{aligned}\tag{5.495}$$

$$\bar{\Upsilon}^3_{V;T_kT_jT_jT_kT_kT_k}(T_i) = \bar{\Upsilon}^3_{V;T_kT_jT_kT_jT_kT_k}(T_i) = \bar{\Upsilon}^3_{V;T_kT_jT_kT_kT_jT_k}(T_i) = \bar{\Upsilon}^3_{V;T_kT_jT_kT_kT_kT_j}(T_i), \tag{5.496}$$

$$\bar{\Upsilon}^3_{V;T_jT_kT_jT_kT_kT_k}(T_i) = \bar{\Upsilon}^3_{V;T_jT_kT_kT_jT_kT_k}(T_i) = \bar{\Upsilon}^3_{V;T_jT_kT_kT_kT_jT_k}(T_i) = \bar{\Upsilon}^3_{V;T_jT_kT_kT_kT_kT_j}(T_i). \tag{5.497}$$

Using these results one can finally re-express the reduced slow-roll parameters as

$$\bar{\epsilon}_V = \sum_{i=1}^{M}\sum_{j=1}^{M}\bar{\epsilon}_{V;T_jT_j}(T_i) + 2\sum_{i=1}^{M}\sum_{j=1}^{M}\sum_{k=1}^{M}\bar{\Delta}_{V;T_jT_k}(T_i), \tag{5.498}$$

$$\bar{\eta}_V = \sum_{i=1}^{M}\sum_{j=1}^{M}\bar{\eta}_{V;T_jT_j}(T_i) + 2\sum_{i=1}^{M}\sum_{j=1}^{M}\sum_{k=1}^{M}\bar{\Theta}_{V;T_jT_k}(T_i), \tag{5.499}$$

$$\bar{\xi}^2_V = \sum_{i=1}^{M}\sum_{j=1}^{M}\bar{\xi}^2_{V;T_jT_jT_jT_j}(T_i) + \sum_{i=1}^{M}\sum_{j=1}^{M}\sum_{k=1}^{M}\left(3\bar{\vartheta}^2_{V;T_jT_jT_kT_k}(T_i) + 3\bar{\vartheta}^2_{V;T_kT_jT_kT_k}(T_i) + \bar{\vartheta}^2_{V;T_jT_kT_kT_k}(T_i)\right), \tag{5.500}$$

$$\bar{\sigma}^3_V = \sum_{i=1}^{M}\sum_{j=1}^{M}\bar{\sigma}^3_{V;T_jT_jT_jT_jT_jT_j}(T_i) + \bar{\Upsilon}^3_{V;T_jT_kT_kT_kT_kT_k}(T_i) + \sum_{i=1}^{M}\sum_{j=1}^{M}\sum_{k=1}^{M}\left(\Upsilon^3_{V;T_jT_jT_kT_kT_kT_k}(T_i) + 5\bar{\Upsilon}^3_{V;T_jT_jT_jT_jT_kT_k}(T_i) + 4\bar{\Upsilon}^3_{V;T_jT_jT_jT_jT_jT_k}(T_i) + 2\bar{\Upsilon}^3_{V;T_jT_kT_jT_jT_jT_j}(T_i) + 8\bar{\Upsilon}^3_{V;T_jT_kT_jT_jT_jT_k}(T_i) + 10\bar{\Upsilon}^3_{V;T_jT_kT_jT_jT_kT_k}(T_i) + 8\bar{\Upsilon}^3_{V;T_jT_kT_jT_kT_kT_k}(T_i) + 4\bar{\Upsilon}^3_{V;T_jT_jT_jT_kT_kT_k}(T_i)\right). \tag{5.501}$$

Now in our computation we take separable potentials having same structural form for all M number of non-identical tachyons. In such case, for an example if take:

$$V(T_1) = A_1\exp(-T_1/T_{01}), \tag{5.502}$$

$$V(T_2) = A_2\exp(-T_2/T_{02}), \tag{5.503}$$

$$\cdots\cdots\cdots \quad \cdots\cdots\cdots\cdots\cdots\cdots \tag{5.504}$$

$$V(T_M) = A_M\exp(-T_M/T_{0M}), \tag{5.505}$$

which implies the structural form, we get the following simplified expression:

$$\bar{\epsilon}_V = \sum_{i=1}^{M}\sum_{j=1}^{M}\bar{\epsilon}_{V;T_jT_j}(T_i), \tag{5.506}$$

$$\bar{\eta}_V = \sum_{i=1}^{M}\sum_{j=1}^{M}\bar{\eta}_{V;T_jT_j}(T_i), \tag{5.507}$$

$$\bar{\xi}^2_V = \sum_{i=1}^{M}\sum_{j=1}^{M}\bar{\xi}^2_{V;T_jT_jT_jT_j}(T_i), \tag{5.508}$$

$$\bar{\sigma}^3_V = \sum_{i=1}^{M}\sum_{j=1}^{M}\bar{\sigma}^3_{V;T_jT_jT_jT_jT_jT_j}(T_i). \tag{5.509}$$

The cross terms only appear when the structural form of the M number of tachyons are different. For example, if we choose

$$V(T_1) = A_1\exp(-T_1/T_{01}), \tag{5.510}$$

$$V(T_2) = B_2\cosh(T_2/T_{02}), \tag{5.511}$$

$$\cdots\cdots\cdots \quad \cdots\cdots\cdots\cdots\cdots\cdots \tag{5.512}$$

then all the cross terms in slow-roll vanish. Also for non-separable potentials this explanation works.

5.3.3 The δN formalism for Multi tachyons

In this section we have used the δN formalism to compute the inflationary observables, for the multi-tachyonic field set-up. Here N signifies the number of e-foldings, which can be expressed in the multi-tachyonic set-up as

$$N = \int_t^{t_{\rm end}} Hdt = \begin{cases} \dfrac{\alpha'}{M_p^2}\displaystyle\sum_{i=1}^{M}\int_{T_{i,end}}^{T_i}\frac{V^2(T_i)}{V'(T_i)}\,dT_i, & \text{for} \quad q = 1/2, \\ \dfrac{\sqrt{2q}\alpha'}{M_p^2}\displaystyle\sum_{i=1}^{M}\int_{T_{i,end}}^{T_i}\frac{V^2(T_i)}{V'(T_i)}\,dT_i, & \text{for any arbitrary } q. \end{cases} \tag{5.513}$$

In the non-attractor regime, the δN formalism shows various non-trivial features which have to be taken into account during explicit calculations. Once the solution reaches the attractor behavior, the dominant contribution comes from only on the perturbations of the scalar-field trajectories with respect to the tachyon field value at the initial hypersurface, T_i, as the velocity, $\dot{T}_i$, is uniquely determined by T_i where $i = 1, 2, \ldots, M$. However, in the non-attractor regime of solution, both the information from the field value T_i and also $\dot{T}_i$ are required to determine the trajectory. This can be understood by providing two initial conditions on T_i and $\dot{T}_i$ on the initial hypersurface. During the computation of the trajectories let us assume here that the universe has already arrived at the adiabatic limit via attractor phase by this epoch, or equivalently it can be stated that a typical phase transition phenomenon appears to an attractor phase at the time $t = t_*$. More specifically, in the present context, we have assumed that the evolution of the universe is unique after the value of the scalar field arrives at $T = T_*$ where it is mimicking the role of a standard clock, irrespective of the value of its

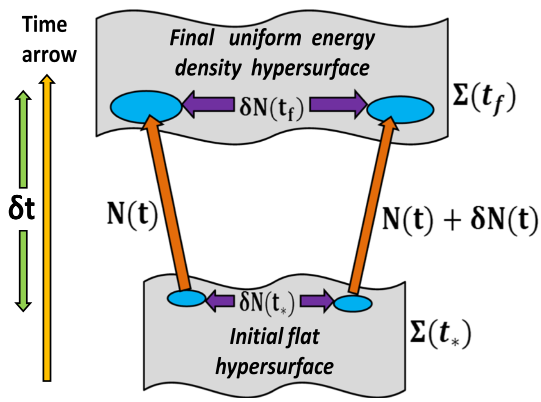

Fig. 25 Diagrammatic representation of δN formalism. In this schematic picture $\Sigma(t_i)$ and $\Sigma(t_f)$ represent the initial and final hypersurface where *time arrow* flows from $t_i \to t_f$

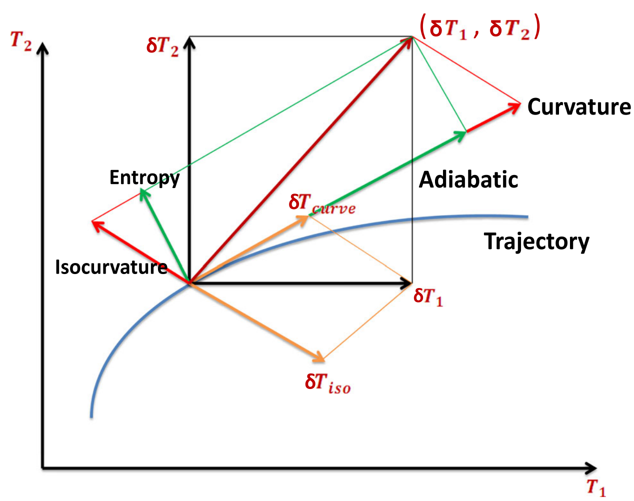

Fig. 26 Diagrammatic representation of trajectories and perturbation decompositions in the field space. Here it is explicitly shown that any perturbation including field perturbations can be decomposed into a curvature component "curve" and an isocurvature component "iso"

velocity $\dot{T}_*$. Let us mention that only in this case δN is equal to the final value of the comoving curvature perturbation ζ which is conserved at $t \geq t_*$. In Figs. 25 and 26, we have shown the schematic picture of the δN formalism and the trajectories and perturbation decompositions in the field space for the multi-field tachyon inflation.

On sufficiently large scales for given suitable assumptions as regards the dynamical behavior which permit us to ignore time derivatives of the perturbations, we expect that each horizon volume will evolve in such a manner that it behaves as a self contained universe, and consequently the curvature perturbation can be written beyond linear order in cosmological perturbation theory as [18,139]

$$\zeta = \delta N$$
$$= \sum_{i=1}^{M} N_{,i}\delta T^i + \frac{1}{2!}\sum_{i=1}^{M}\sum_{j=1}^{M} N_{,ij}\delta T^i \delta T^j + \frac{1}{3!}\sum_{i=1}^{M}\sum_{j=1}^{M}\sum_{k=1}^{M} N_{,ijk}\delta T^i \delta T^j \delta T^k + \cdots, \tag{5.514}$$

where we use the following short hand notations:

$$N_{,i} = \partial_{T_i} N, \tag{5.515}$$
$$N_{,ij} = \partial_{T_i}\partial_{T_j} N, \tag{5.516}$$
$$N_{,ijk} = \partial_{T_i}\partial_{T_j}\partial_{T_k} N. \tag{5.517}$$

More precisely here $\delta T_i \;\; \forall i = 1, 2, \ldots, M$ represent the deviations of the fields from their unperturbed values in some specified region of the universe.

When the potential is sum-separable, the derivatives of N can be simplified to the following expressions:

$$N_{,i} = \frac{1}{\sqrt{2\bar{\epsilon}_V(T_i^\star)}} \frac{V(T_i^\star) + Z_i^c}{\left(\sum_{j=1}^{M} V(T_j^\star)\right)}, \tag{5.518}$$

$$N_{,ij} = \delta_{ij}\left[1 - \frac{\bar{\eta}_V(T_i^\star)}{2\bar{\epsilon}_V(T_i^\star)} \frac{V(T_i^\star) + Z_i^c}{\left(\sum_{j=1}^{M} V(T_j^\star)\right)}\right] + \frac{1}{\sqrt{2\bar{\epsilon}_V(T_j^\star)}\left(\sum_{m=1}^{M} V(T_m^\star)\right)} Z_{j,i}^c, \tag{5.519}$$

where Z_i^c and $Z_{i,j}^c$ is defined as

$$Z_i^c = \left(\sum_{m=1}^{M} V(T_m^c)\right)\frac{\bar{\epsilon}_V(T_i^c)}{\bar{\epsilon}_V^c} - V(T_i^c), \tag{5.520}$$

$$Z_{i,j}^c = -\frac{\left(\sum_{m=1}^{M} V(T_m^c)\right)^2}{\sum_{p=1}^{M} V(T_p^\star)}\sqrt{\frac{2}{\bar{\epsilon}_V(T_j)}} \times \left[\sum_{k=1}^{M} \bar{\epsilon}_V(T_k)\left(\frac{\bar{\epsilon}_V(T_i)}{\bar{\epsilon}_V} - \delta_{ik}\right)\left(\frac{\bar{\epsilon}_V(T_j)}{\bar{\epsilon}_V} - \delta_{jk}\right) \times \left(1 - \frac{\bar{\eta}_V(T_k)}{\bar{\epsilon}_V}\right)\right]_c$$
$$= \sqrt{\frac{2}{\bar{\epsilon}_V(T_j)}}\left(\sum_{m=1}^{M} V(T_m^\star)\right)\mathcal{K}_{ij}, \tag{5.521}$$

where $\star$ indicates the horizon crossing and c denotes the constant density surface. In this context additionally we get

$$dN = \sum_{j=1}^{M}\left[\left(\frac{V(T_j)}{\partial_j V(T_i)}\right) - \sum_{i=1}^{M}\frac{\partial T_i^c}{\partial T_j^\star}\left(\frac{V(T_i)}{\partial_i V(T_k)}\right)\right] dT_j^\star, \tag{5.522}$$

where

$$\frac{\partial T_i^c}{\partial T_j^\star} = -\frac{\sum_{k=1}^{M} V(T_k^c)}{\sum_{m=1}^{M} V(T_m^\star)}\sqrt{\frac{\bar{\epsilon}_V(T_i^c)}{\bar{\epsilon}_V(T_j^\star)}}\left(\frac{\bar{\epsilon}_V(T_i^c)}{\sum_{p=1}^{M}\bar{\epsilon}_V(T_p)} - \delta_{ij}\right). \tag{5.523}$$

Further using this, one can write the following differential operator identity which is very useful to compute various inflationary observables mentioned in the next section:

$$\frac{\mathrm{d}}{\mathrm{d}N} = \sum_{j=1}^{M}\left[\left(\frac{V(T_j)}{\partial_j V(T_i)}\right) - \sum_{i=1}^{M}\frac{\partial T_i^c}{\partial T_j^\star}\left(\frac{V(T_i)}{\partial_i V(T_k)}\right)\right]^{-1}\frac{\mathrm{d}}{\mathrm{d}T_j^\star}. \tag{5.524}$$

In the next section we will write all the inflationary observables in terms of the components of δN by including all the effects of non-linearities in cosmological perturbations for multi-tachyons.

5.3.4 Computation of scalar power spectrum

In this subsection we start with two point function for multi-tachyonic scalar modes. Implementing the δN procedure we get:

$$\langle\zeta_{\mathbf{k}}\zeta_{\mathbf{k}'}\rangle = \sum_{i=1}^{M}\sum_{j=1}^{M}\langle\zeta^i_{\mathbf{k}}\zeta^j_{\mathbf{k}'}\rangle = (2\pi)^3\delta^3(\mathbf{k}+\mathbf{k}')\frac{2\pi^2}{k^3}\Delta_\zeta(k), \tag{5.525}$$

where the primordial power spectrum for the scalar modes at any arbitrary momentum scale k can be expressed as

$$\Delta_\zeta(k) = \sum_{i=1}^{M}\sum_{j=1}^{M} N_{,i}N_{,j}G^{ij}\frac{k^3 P_\zeta(k)}{2\pi^2}. \tag{5.526}$$

Sometimes it is convenient to express everything in terms of the normalized adiabatic curvature power spectrum in the following way:

$$\langle\bar{\zeta}_{\mathbf{k}}\bar{\zeta}_{\mathbf{k}'}\rangle = (2\pi)^3\delta^3(\mathbf{k}+\mathbf{k}')\frac{2\pi^2}{k^3}\bar{\Delta}_\zeta(k), \tag{5.527}$$

where

$$\bar{\zeta} = -\frac{H}{\dot{T}_0}\sum_{i=1}^{M}\sum_{j=1}^{M}\Theta_i\delta T_j G^{ij}, \tag{5.528}$$

$$\bar{\Delta}_\zeta(k) = \frac{1}{2\bar{\epsilon}_V}\sum_{i=1}^{M}\sum_{j=1}^{M}\Theta_i\Theta_j G^{ij}\frac{k^3 P_\zeta(k)}{2\pi^2}. \tag{5.529}$$

Here $\Theta_i = \frac{\dot{T}_i}{\dot{T}_0}$ is a basis vector that projects δT_i along the direction of classical background trajectory. The vector Θ and a complementary set of $(M-1)$ mutually orthonormal basis vectors $\mathbf{s_p}$ form the kinematic basis. Applying the Gram–Schmidt orthogonalization technique one can determine $\mathbf{s_p}$.

On the other hand for the multi-tachyonic scenario the isocurvature perturbations $\mathcal{S}_p$ is the orthogonal projection along the $\mathbf{s_K}$ directions:

$$\mathcal{S}_p = -\frac{H}{\dot{T}_0}\sum_{j=1}^{M}\sum_{m=1}^{M} s_{pj}G^{jm}\delta T_m. \tag{5.530}$$

Using this one can write down the expression for the normalized isocurvature perturbation:

$$\begin{aligned}\langle\mathcal{S}_{\mathbf{k}}\mathcal{S}_{\mathbf{k}'}\rangle &= \sum_{p=1}^{M-1}\sum_{q=1}^{M-1}\langle\mathcal{S}_{p\mathbf{k}}\mathcal{S}_{q\mathbf{k}'}\rangle \\ &= (2\pi)^3\delta^3(\mathbf{k}+\mathbf{k}')\frac{2\pi^2}{k^3}\bar{\Delta}_{\mathcal{S}}(k),\end{aligned} \tag{5.531}$$

where

$$\bar{\Delta}_{\mathcal{S}}(k) = \frac{1}{2\bar{\epsilon}_V}\sum_{p=1}^{M-1}\sum_{q=1}^{M-1}\sum_{j=1}^{M}\sum_{m=1}^{M} s^p_j s^q_m G^{jm}\frac{k^3 P_\zeta(k)}{2\pi^2}, \tag{5.532}$$

where we have explicitly shown all the summations to indicate that the isocurvature basis vectors are $(M-1)$-dimensional. For the sake of simplicity applying the Gram–Schmidt orthogonalization technique one can choose a basis where G^{ij} is diagonal and given by $G^{ij} = \delta^{ij}$.

Similarly, for completeness one can define the adiabatic-isocurvature cross spectra in the following fashion:

$$\begin{aligned}\langle\bar{\zeta}_{\mathbf{k}}\mathcal{S}_{\mathbf{k}'}\rangle &= \sum_{p=1}^{M-1}\langle\bar{\zeta}_{\mathbf{k}}\mathcal{S}_{p\mathbf{k}'}\rangle \\ &= (2\pi)^3\delta^3(\mathbf{k}+\mathbf{k}')\frac{2\pi^2}{k^3}\bar{\Delta}_{\zeta\mathcal{S}}(k),\end{aligned} \tag{5.533}$$

where

$$\bar{\Delta}_{\zeta\mathcal{S}}(k) = \frac{1}{2\bar{\epsilon}_V}\sum_{p=1}^{M-1}\sum_{j=1}^{M}\sum_{m=1}^{M}\Theta_j s^p_m\left(G^{jm}+G^{mj}\right)\frac{k^3 P_\zeta(k)}{2\pi^2}. \tag{5.534}$$

Cross correlations are generically expected if the background trajectory is curved as the modes of interest leave the horizon.

Now we write down the expressions for all the inflationary observables computed from the multi-tachyonic set-up at a horizon crossing:

- In the present context the amplitude of scalar power spectrum can be computed as

$$\Delta_{\zeta,\star}=\begin{cases}\sum_{i=1}^{M}\sum_{j=1}^{M}N_{,i}N_{,j}G^{ij}\left\{[1-(\mathcal{C}_E+1)\bar{\epsilon}_V-\mathcal{C}_E\,(3\bar{\epsilon}_V-\bar{\eta}_V)]^2\,\frac{H^2}{4\pi^2 c_S}\right\}_{\star}, & \text{for } q=1/2,\\ \sum_{i=1}^{M}\sum_{j=1}^{M}N_{,i}N_{,j}G^{ij}\left\{\left[1-(\mathcal{C}_E+1)\frac{\bar{\epsilon}_V}{2q}-\frac{\mathcal{C}_E}{\sqrt{2q}}\,(3\bar{\epsilon}_V-\bar{\eta}_V)\right]^2\frac{qH^2}{2\pi^2 c_S}\right\}_{\star}, & \text{for any } q,\end{cases}\tag{5.535}$$

where $H^2=V/3M_p^2=\sum_{k=1}^{M}V(T_k)/3M_p^2$ and $\mathcal{C}_E=-2+\ln 2+\gamma\approx-0.72$. Using the slow-roll approximations one can further approximate the expression for the sound speed as

$$c_S^2=\begin{cases}1-\frac{2}{3}\bar{\epsilon}_V+\mathcal{O}\left(\bar{\epsilon}_V^2\right)+\cdots, & \text{for } q=1/2,\\ 1-\frac{(1-q)}{3q^2}\bar{\epsilon}_V+\mathcal{O}\left(\bar{\epsilon}_V^2\right)+\cdots, & \text{for any } q,\end{cases}\tag{5.536}$$

where $\bar{\epsilon}_V$ and $\bar{\eta}_V$ are the cumulative or total contribution to the slow-roll parameter as defined earlier. Hence using the result in Eq. (5.535) we get the following simplified expression for the primordial scalar power spectrum:

$$\Delta_{\zeta,\star}=\begin{cases}\sum_{i=1}^{M}\sum_{j=1}^{M}N_{,i}N_{,j}G^{ij}\left\{\left[1-\left(\mathcal{C}_E+\frac{5}{6}\right)\bar{\epsilon}_V-\mathcal{C}_E\,(3\bar{\epsilon}_V-\bar{\eta}_V)\right]^2\frac{H^2}{4\pi^2}\right\}_{\star}, & \text{for } q=1/2\\ \sum_{i=1}^{M}\sum_{j=1}^{M}N_{,i}N_{,j}G^{ij}\left\{\left[1-(\mathcal{C}_E+1-\Sigma)\frac{\bar{\epsilon}_V}{2q}-\frac{\mathcal{C}_E}{\sqrt{2q}}\,(3\bar{\epsilon}_V-\bar{\eta}_V)\right]^2\frac{qH^2}{2\pi^2}\right\}_{\star}, & \text{for any } q.\end{cases}\tag{5.537}$$

Similarly, using the normalized adiabatic curvature power spectrum, we get

$$\bar{\Delta}_{\zeta,\star}=\begin{cases}\sum_{i=1}^{M}\sum_{j=1}^{M}\Theta_i\Theta_jG^{ij}\left\{\left[1-\left(\mathcal{C}_E+\frac{5}{6}\right)\bar{\epsilon}_V-\mathcal{C}_E\,(3\bar{\epsilon}_V-\bar{\eta}_V)\right]^2\frac{H^2}{8\pi^2\bar{\epsilon}_V}\right\}_{\star}, & \text{for } q=1/2,\\ \sum_{i=1}^{M}\sum_{j=1}^{M}\Theta_i\Theta_jG^{ij}\left\{\left[1-(\mathcal{C}_E+1-\Sigma)\frac{\bar{\epsilon}_V}{2q}-\frac{\mathcal{C}_E}{\sqrt{2q}}\,(3\bar{\epsilon}_V-\bar{\eta}_V)\right]^2\frac{qH^2}{4\pi^2\bar{\epsilon}_V}\right\}_{\star}, & \text{for any } q.\end{cases}\tag{5.538}$$

- In the present context the normalized amplitude of isocurvature power spectrum can be computed as

$$\bar{\Delta}_{\mathcal{S},\star}=\begin{cases}\sum_{p,q=1}^{M-1}\sum_{j,m=1}^{M}s_j^p s_m^q G^{jm}\left\{[1-(\mathcal{C}_E+1)\bar{\epsilon}_V-\mathcal{C}_E\,(3\bar{\epsilon}_V-\bar{\eta}_V)]^2\,\frac{H^2}{8\pi^2 c_S\bar{\epsilon}_V}\right\}_{\star}, & \text{for } q=1/2,\\ \sum_{p,q=1}^{M-1}\sum_{j,m=1}^{M}s_j^p s_m^q G^{jm}\left\{\left[1-(\mathcal{C}_E+1)\frac{\bar{\epsilon}_V}{2q}-\frac{\mathcal{C}_E}{\sqrt{2q}}\,(3\bar{\epsilon}_V-\bar{\eta}_V)\right]^2\frac{qH^2}{4\pi^2 c_S\bar{\epsilon}_V}\right\}_{\star}, & \text{for any } q,\end{cases}\tag{5.539}$$

where $H^2=V/3M_p^2=\sum_{k=1}^{M}V(T_k)/3M_p^2$ and $\mathcal{C}_E=-2+\ln 2+\gamma\approx-0.72$. Further using an approximated expression for c_S in the slow-roll regime and also using the result in Eq. (5.539) we get the following simplified expression for the power spectrum:

$$\bar{\Delta}_{\mathcal{S},\star}=\begin{cases}\sum_{p,q=1}^{M-1}\sum_{j,m=1}^{M}s_j^p s_m^q G^{jm}\left\{\left[1-\left(\mathcal{C}_E+\frac{5}{6}\right)\bar{\epsilon}_V-\mathcal{C}_E\,(3\bar{\epsilon}_V-\bar{\eta}_V)\right]^2\frac{H^2}{8\pi^2\bar{\epsilon}_V}\right\}_{\star}, & \text{for } q=\frac{1}{2}\\ \sum_{p,q=1}^{M-1}\sum_{j,m=1}^{M}s_j^p s_m^q G^{jm}\left\{\left[1-(\mathcal{C}_E+1-\Sigma)\frac{\bar{\epsilon}_V}{2q}-\frac{\mathcal{C}_E}{\sqrt{2q}}\,(3\bar{\epsilon}_V-\bar{\eta}_V)\right]^2\frac{qH^2}{4\pi^2\bar{\epsilon}_V}\right\}_{\star}, & \text{for any } q.\end{cases}\tag{5.540}$$

- Similarly the normalized amplitude of the adiabatic-isocurvature cross power spectrum can be computed as

$$\bar{\Delta}_{\zeta\mathcal{S},\star} = \begin{cases} \sum_{p=1}^{M-1}\sum_{j,m=1}^{M} \Theta_j s^p_m \left(G^{jm}+G^{mj}\right)\left\{[1-(\mathcal{C}_E+1)\bar{\epsilon}_V-\mathcal{C}_E\,(3\bar{\epsilon}_V-\bar{\eta}_V)]^2\,\frac{H^2}{8\pi^2 c_S\bar{\epsilon}_V}\right\}_\star, & \text{for } q=1/2,\\ \sum_{p=1}^{M-1}\sum_{j,m=1}^{M} \Theta_j s^p_m \left(G^{jm}+G^{mj}\right)\left\{\left[1-(\mathcal{C}_E+1)\frac{\bar{\epsilon}_V}{2q}-\frac{\mathcal{C}_E}{\sqrt{2q}}\,(3\bar{\epsilon}_V-\bar{\eta}_V)\right]^2\frac{qH^2}{4\pi^2 c_S\bar{\epsilon}_V}\right\}_\star, & \text{for any } q, \end{cases} \tag{5.541}$$

where $H^2 = V/3M_p^2 = \sum_{k=1}^{M} V(T_k)/3M_p^2$ and $\mathcal{C}_E = -2+\ln 2+\gamma \approx -0.72$. Further using an approximated expression for c_S in the slow-roll regime and also using the result in Eq. (5.541) we get the following simplified expression for the power spectrum:

$$\bar{\Delta}_{\zeta\mathcal{S},\star} = \begin{cases} \sum_{p=1}^{M-1}\sum_{j,m=1}^{M} \Theta_j s^p_m \left(G^{jm}+G^{mj}\right)\left\{\left[1-\left(\mathcal{C}_E+\frac{5}{6}\right)\bar{\epsilon}_V-\mathcal{C}_E\,(3\bar{\epsilon}_V-\bar{\eta}_V)\right]^2\frac{H^2}{8\pi^2\bar{\epsilon}_V}\right\}_\star, & \text{for } q=\frac{1}{2}\\ \sum_{p=1}^{M-1}\sum_{j,m=1}^{M} \Theta_j s^p_m \left(G^{jm}+G^{mj}\right)\left\{\left[1-(\mathcal{C}_E+1-\Sigma)\frac{\bar{\epsilon}_V}{2q}-\frac{\mathcal{C}_E}{\sqrt{2q}}\,(3\bar{\epsilon}_V-\bar{\eta}_V)\right]^2\frac{qH^2}{4\pi^2\bar{\epsilon}_V}\right\}_\star & \text{for any } q. \end{cases} \tag{5.542}$$

- Next one can compute the scalar spectral tilt $(n_\zeta, n_\mathcal{S}, n_{\zeta\mathcal{S}})$ of the primordial adiabatic, isocurvature and cross power spectrum as

$$n_{\zeta,\star}-1 \approx \begin{cases} (2\bar{\eta}_V-8\bar{\epsilon}_V)-\frac{2}{\sum_{i=1}^{M}\sum_{j=1}^{M}N_{,i}N_{,j}G^{ij}} \\ +\frac{2}{\sum_{m=1}^{M}V(T_m)}\frac{\sum_{n=1}^{M}\sum_{i=1}^{M}\sum_{j=1}^{M}\sum_{l=1}^{M}\sum_{k=1}^{M}V_{,ij}(T_n)N_{,l}N_{,k}G^{il}G^{jk}}{\sum_{i'=1}^{M}\sum_{j'=1}^{M}N_{,i'}N_{,j'}G^{i'j'}}+\cdots, & \text{for } q=1/2,\\ \sqrt{\frac{2}{q}}\bar{\eta}_V-\left(\frac{1}{q}+3\sqrt{\frac{2}{q}}\right)\bar{\epsilon}_V-\frac{1}{q\sum_{i=1}^{M}\sum_{j=1}^{M}N_{,i}N_{,j}G^{ij}} \\ +\frac{1}{q\sum_{m=1}^{M}V(T_m)}\frac{\sum_{n=1}^{M}\sum_{i=1}^{M}\sum_{j=1}^{M}\sum_{l=1}^{M}\sum_{k=1}^{M}V_{,ij}(T_n)N_{,l}N_{,k}G^{il}G^{jk}}{\sum_{i'=1}^{M}\sum_{j'=1}^{M}N_{,i'}N_{,j'}G^{i'j'}}+\cdots, & \text{for any } q, \end{cases} \tag{5.543}$$

and additionally we have

$$n_{\mathcal{S},\star}-1 \approx n_{\zeta,\star}-1 \approx n_{\zeta\mathcal{S},\star}-1. \tag{5.544}$$

- One can also compute the expression for the running and running of the running by following the same procedure as mentioned above.

For completeness let us mention the behavior of the cosmological perturbation at later times for multi Gtachyonic inflation. To start with it is important to mention here that in a more generalized physical prescription the time dependence of adiabatic and entropy perturbations in the large cosmological scale limit can always be written in the following simplified form for multi Gtachyonic inflationary paradigm as

$$\frac{d\zeta}{dt} = \dot{\zeta} = \Upsilon H\mathcal{S}, \tag{5.545}$$

$$\frac{d\mathcal{S}}{dt} = \dot{\mathcal{S}} = \Sigma H\mathcal{S}, \tag{5.546}$$

where Υ and Σ physically represent the generalized time-dependent dimensionless functions in cosmological perturbation theory of multi Gtachyonic fields. Now to extract more informations form Eqs. (5.545) and (5.546), we further integrate both equations over the specified cosmological time scale and finally following this prescription one can easily compute the expression for the generalized form of the transfer matrix which relates the curvature and entropic perturbations generated during the situation where the fluctuating mode is stretched outside the expansion (Hubble) scale during the epoch of inflation to the curvature and entropic perturbations at later time via the following simplified form of the matrix equation:

$$\begin{pmatrix} \zeta(t) \\ \mathcal{S}(t) \end{pmatrix} = \begin{pmatrix} 1 & \hat{T}_{\zeta\mathcal{S}} \\ 0 & \hat{T}_{\mathcal{S}\mathcal{S}} \end{pmatrix} \begin{pmatrix} \zeta(t_\star) \\ \mathcal{S}(t_\star) \end{pmatrix}, \tag{5.547}$$

where the transfer functions are represented by the following equations in the context of multi-tachyonic inflation from the effective GTachyon set-up:

$$\hat{T}_{\zeta\mathcal{S}}(t_\star, t) = \int_{t_\star}^{t} \Upsilon(t'')\hat{T}_{\mathcal{S}\mathcal{S}}(t_\star, t'')H(t'')\mathrm{d}t'', \tag{5.548}$$

$$\hat{T}_{\mathcal{S}\mathcal{S}}(t_\star, t) = \exp\left(\int_{t_\star}^{t} \Sigma(t')H(t'')\mathrm{d}t''\right). \tag{5.549}$$

It is also important to note that the evolution in the large-scale limit is independent of the cosmological scale under consideration in the present context and consequently the derived generalized form of the transfer functions $\hat{T}_{\zeta\mathcal{S}}$ and $\hat{T}_{\mathcal{S}\mathcal{S}}$ are implicit functions of the cosmological scale due to their dependence upon the cosmic time scale $t_\star(k)$ as appearing in the argument of the transfer functions. The scale dependence of the transfer functions are governed by the following sets of evolution equations:

$$\left(H_\star^{-1}\partial_{t_\star} + \Sigma_\star\right)\hat{T}_{\zeta\mathcal{S}} + \Upsilon_\star = 0, \tag{5.550}$$

$$\left(H_\star^{-1}\partial_{t_\star} + \Sigma_\star\right)\hat{T}_{\mathcal{S}\mathcal{S}} = 0. \tag{5.551}$$

where we introduce the notation $\partial_{t_\star} = \partial/\partial t_\star$ to define the partial differentiation in a simplified way. In the present context, the cosmological (momentum) scale dependence of the generalized transfer functions for the multi-tachyonic inflationary paradigm is explicitly determined by the two factors, $\Upsilon_\star$ and $\Sigma_\star$, which physically represent the cosmic time scale evolution of the curvature and entropic fluctuations at the horizon crossing during the epoch of multi GTachyonic inflation.

Now one can apply the above mentioned generalized transfer matrix as stated in Eq. (5.547) to the primordial scalar power spectra explicitly computed in the previous subsection. After doing the detailed analysis one can finally compute the resulting curvature and entropic primordial power spectra at the beginning point of the radiation dominated epoch:

$$\bar{\Delta}_{\zeta} = \left(1 + \hat{T}^2_{\zeta\mathcal{S}}\right)\bar{\Delta}_{\zeta,\star}, \tag{5.552}$$

$$\bar{\Delta}_{\mathcal{S}} = \hat{T}^2_{\mathcal{S}\mathcal{S}}\bar{\Delta}_{\zeta,\star}, \tag{5.553}$$

$$\bar{\Delta}_{\zeta\mathcal{S}} = \hat{T}_{\zeta\mathcal{S}}\hat{T}_{\mathcal{S}\mathcal{S}}\bar{\Delta}_{\zeta,\star}. \tag{5.554}$$

For the sake of simplicity let us define a dimensionless cosmological measure of the correlation function in terms of a correlation angle θ in the following simplified way:

$$\cos\theta \equiv \frac{\bar{\Delta}_{\zeta\mathcal{S}}}{\sqrt{\bar{\Delta}_{\zeta}\bar{\Delta}_{\mathcal{S}}}} = \frac{\hat{T}_{\zeta\mathcal{S}}}{\sqrt{1 + \hat{T}^2_{\zeta\mathcal{S}}}}, \tag{5.555}$$

$$\sin\theta \equiv \sqrt{1 - \left(\frac{\bar{\Delta}_{\zeta\mathcal{S}}}{\sqrt{\bar{\Delta}_{\zeta}\bar{\Delta}_{\mathcal{S}}}}\right)^2} = \frac{1}{\sqrt{1 + \hat{T}^2_{\zeta\mathcal{S}}}}, \tag{5.556}$$

$$\theta = \cot^{-1}(\hat{T}_{\zeta\mathcal{S}}), \tag{5.557}$$

which are surely very useful for further computation in the present context. Further using Eq. (5.552) in Eq. (5.555), finally we get the following expression for the scalar metric perturbation at the horizon crossing which is expressed in terms of the observed curvature perturbation at later times in the cosmic time scale and also in terms of the cross-correlation angle:

$$\bar{\Delta}_{\zeta,\star} \simeq \bar{\Delta}_{\zeta}\sin^2\theta. \tag{5.558}$$

Next using Eqs. (5.552–5.554), the spectral indices of the primordial power spectrum at later stage of times in cosmological time scale can be expressed by the following simplified expressions:

$$n_{\zeta} - 1 = n_{\zeta,\star} - 1 + H_\star^{-1}\left(\partial_{t_\star}\hat{T}_{\zeta\mathcal{S}}\right)\sin 2\theta, \tag{5.559}$$

$$n_{\mathcal{S}} - 1 = n_{\zeta,\star} - 1 + 2H_\star^{-1}\left(\partial_{t_\star}\hat{T}_{\mathcal{S}\mathcal{S}}\right), \tag{5.560}$$

$$n_{\mathcal{C}} - 1 = n_{\zeta,\star} - 1 + H_\star^{-1}\left\{\left(\partial_{t_\star}\hat{T}_{\zeta\mathcal{S}}\right)\tan\theta + \left(\partial_{t_\star}\hat{T}_{\mathcal{S}\mathcal{S}}\right)\right\}, \tag{5.561}$$

which are very useful to study the scale dependent behavior of the primordial power spectra in the present context. Following the same procedure one can also compute the expressions for the running and running of the running of the spectral indices. Additionally, it is important to mention here that the overall amplitude of the generalized transfer functions $\hat{T}_{\zeta\mathcal{S}}$ and $\hat{T}_{\mathcal{S}\mathcal{S}}$ are dependent on the time scale evolution after horizon crossing via the reheating phenomenon and into the radiation dominated epoch. But in spite of this important fact, the spectral tilts of the resulting primordial perturbation spectra can be finally expressed in terms of the slow-roll parameters at the horizon crossing during the epoch of inflation and also in terms of the cross-correlation angle θ, which we have already introduced earlier in Eq. (5.557).

5.3.5 Computation of tensor power spectrum

In this subsection we will not derive the crucial results for multi-Gtachyonic inflation. But we will state the results for BD vacuum where the changes will appear due to the presence of M number of different tachyon field. One can similarly write down the detailed expressions for AV (including α vacuum) as well.

$$\langle h_{\mathbf{k}} h_{\mathbf{k}'}\rangle = \sum_{i=1}^{M}\sum_{j=1}^{M}\langle h^i_{\mathbf{k}} h^j_{\mathbf{k}'}\rangle = (2\pi)^3\delta^3(\mathbf{k}+\mathbf{k}')\frac{2\pi^2}{k^3}\Delta_h(k), \tag{5.562}$$

where the primordial power spectrum for the scalar modes at any arbitrary momentum scale k can be expressed as

$$\Delta_h(k) = 8\frac{\sum_{m=1}^{M}\sum_{n=1}^{M} N_{,m}N_{,n}G^{mn}}{\sum_{i=1}^{M}\sum_{j=1}^{M} N_{,i}N_{,j}G^{ij}}\frac{k^3 P_\zeta(k)}{2\pi^2} = \frac{4k^3 P_\zeta(k)}{\pi^2}. \tag{5.563}$$

The changes will appear in the expressions for the following inflationary observables at the horizon crossing:

- In the present context amplitude of tensor power spectrum can be computed as

$$\Delta_{h,\star} = \begin{cases} \left\{[1-(\mathcal{C}_E+1)\bar{\epsilon}_V]^2\,\dfrac{2H^2}{\pi^2 M_p^2}\right\}_\star, & \text{for } q=1/2,\\[2ex] \left\{\left[1-(\mathcal{C}_E+1)\dfrac{\bar{\epsilon}_V}{2q}\right]^2\dfrac{2H^2}{\pi^2 M_p^2}\right\}_\star, & \text{for any } q,\end{cases} \tag{5.564}$$

  where $\mathcal{C}_E = -2+\ln 2+\gamma \approx -0.72$.
- Next one can compute the tensor spectral tilt (n_h) of the primordial scalar power spectrum as

$$n_{h,\star} \approx \begin{cases} -2\bar{\epsilon}_V\left[1+\bar{\epsilon}_V+2\left(\mathcal{C}_E+1\right)\left(3\bar{\epsilon}_V-\bar{\eta}_V\right)\right]+\cdots, & \text{for } q=1/2,\\[2ex] -\dfrac{\bar{\epsilon}_V}{q}\left[1+\dfrac{\bar{\epsilon}_V}{2q}+\sqrt{\dfrac{2}{q}}\left(\mathcal{C}_E+1\right)\left(3\bar{\epsilon}_V-\bar{\eta}_V\right)\right]+\cdots, & \text{for any } q.\end{cases} \tag{5.565}$$

- Finally the tensor-to-scalar ratio for the multi-tachyonic set-up can be expressed as

$$r_\star \approx \begin{cases} \dfrac{8}{\sum_i^M\sum_{j=1}^M N_{,i}N_{,j}G^{ij}}+\cdots, & \text{for } q=1/2,\\[2ex] \dfrac{4}{q\sum_i^M\sum_{j=1}^M N_{,i}N_{,j}G^{ij}}+\cdots, & \text{for any } q.\end{cases} \tag{5.566}$$

On the contrary, compared to the scalar (curvature and entropic) part of the cosmological perturbations, the tensor perturbations remain frozen in on the large cosmological scales and finally decoupled from the scalar (curvature and entropic) part of the cosmological perturbations at the linear order of the cosmological perturbation theory. Consequently, in the present context, the primordial cosmological perturbation spectrum for gravitational waves is given by the following simplified expression:

$$\Delta_h = \Delta_{h,\star}, \tag{5.567}$$

$$n_h = n_{h,\star}. \tag{5.568}$$

Finally, it also important to note that the consistency condition for the tensor-to-scalar amplitudes of the primordial power spectrum at the Hubble-crossing can be rewritten, using Eqs. (5.558) and (5.567), as a model independent consistency relation between the tensor-to-scalar amplitudes of the primordial power spectrum at late times in cosmological scale for GTachyon as

$$\begin{aligned} r &= \frac{\Delta_h}{\Delta_\zeta} \simeq -8n_h\sin^2\theta+\cdots\\ &= -8n_{h,\star}\sin^2\theta+\cdots = r_\star\sin^2\theta+\cdots. \end{aligned} \tag{5.569}$$

In the present context, the scale dependence of the final scalar (curvature and entropic) power spectra depends on both on the cosmological scale dependence of the initial spectral index ($n_{\zeta,\star}$) and on the explicit form of the generalized transfer functions $T_{\zeta\mathcal{S}}$ and $T_{\mathcal{S}\mathcal{S}}$. Here we have not explicitly discussed the cosmological parameter estimation and numerical estimations from a specific class of multi-tachyonic potentials. But to understand this more clearly, one can carry forward the results obtained in this section to test various models of the multi-tachyonic potential.

5.3.6 Analytical study for the multi-field model

Here we compute the expression for the inverse cosh potential. One can repeat the computation for the other proposed models of multi-field inflation as well. For the multi-field case the inverse cosh potential is given by

$$V(T_j) = \frac{\lambda_j}{\cosh\left(\frac{T_j}{T_{0j}}\right)} \quad \forall\ j = 1, 2, \ldots, M, \tag{5.570}$$

and the total effective potential is given by

$$V = \sum_{j=1}^{M} V(T_j) = \sum_{j=1}^{M} \frac{\lambda_j}{\cosh\left(\frac{T_j}{T_{0j}}\right)}, \tag{5.571}$$

where λ_j characterize the scale of inflation in each branch and T_{0j} are j number of different parameter of the model. Next using specified form of the potential the potential dependent slow-roll parameters for i th species are computed as

$$\bar{\epsilon}_V(T_i) = \frac{1}{\sum_{m=1}^{M} \lambda_m \mathrm{sech}\left(\frac{T_m}{T_{0m}}\right)} \left[\frac{\lambda_i}{2g_i} \frac{\sinh^2\left(\frac{T_i}{T_{0i}}\right)}{\cosh\left(\frac{T_i}{T_{0i}}\right)}\right], \tag{5.572}$$

$$\bar{\eta}_V(T_i) = \frac{1}{\sum_{m=1}^{M} \lambda_m \mathrm{sech}\left(\frac{T_m}{T_{0m}}\right)} \times \left\{\frac{\lambda_i}{g_i}\left[\tanh^2\left(\frac{T_i}{T_{0i}}\right) - \mathrm{sech}^2\left(\frac{T_i}{T_{0i}}\right)\right]\right\}. \tag{5.573}$$

Also the total contribution in the slow-roll is expressed through the reduced slow-roll parameters:

$$\bar{\epsilon}_V = \frac{1}{\sum_{m=1}^{M} \lambda_m \mathrm{sech}\left(\frac{T_m}{T_{0m}}\right)} \left[\sum_{i=1}^{M} \frac{\lambda_i}{2g_i} \frac{\sinh^2\left(\frac{T_i}{T_{0i}}\right)}{\cosh\left(\frac{T_i}{T_{0i}}\right)}\right], \tag{5.574}$$

$$\bar{\eta}_V = \frac{1}{\sum_{m=1}^{M} \lambda_m \mathrm{sech}\left(\frac{T_m}{T_{0m}}\right)} \times \left\{\sum_{i=1}^{M} \frac{\lambda_i}{g_i}\left[\tanh^2\left(\frac{T_i}{T_{0i}}\right) - \mathrm{sech}^2\left(\frac{T_i}{T_{0i}}\right)\right]\right\}. \tag{5.575}$$

Additionally here we introduce a new factor g_j for each non-identical j number of multi-tachyonic fields, defined as

$$g_j = \frac{\alpha' \lambda_j T_{0j}^2}{M_p^2} = \frac{M_{sj}^4}{(2\pi)^3 g_{sj}} \frac{\alpha' T_{0j}^2}{M_p^2}. \tag{5.576}$$

Next we compute the number of e-foldings from this model:

$$N = \begin{cases} \sum_{j=1}^{M} g_j \ \ln\left[\frac{\tanh\left(\frac{T_{end,j}}{2T_{0j}}\right)}{\tanh\left(\frac{T_j}{2T_{0j}}\right)}\right], & \text{for} \quad q = 1/2, \\ \sum_{j=1}^{M} \sqrt{2q}\ g_j \ \ln\left[\frac{\tanh\left(\frac{T_{end,j}}{2T_{0j}}\right)}{\tanh\left(\frac{T_j}{2T_{0j}}\right)}\right], & \text{for any arbitrary } q. \end{cases} \tag{5.577}$$

Further using the condition to end inflation:

$$\bar{\epsilon}_V(T_{end,i}) = 1, \tag{5.578}$$

$$|\bar{\eta}_V(T_{end,i})| = 1, \tag{5.579}$$

we get the following field value at the end of inflation:

$$T_{end,i} = T_{0i}\ \mathrm{sech}^{-1}(g_i). \tag{5.580}$$

Next using $N_i = N_{\mathrm{cmb},i} = N_{\star,i}$ and $T_i = T_{\mathrm{cmb},i} = T_i^\star$ at the horizon crossing we get

$$T_i^\star \approx 2T_{0,i} \times \begin{cases} \tanh^{-1}\left[\exp\left(-\frac{N_{\star,i}}{g_i}\right)\right], & \text{for} \quad q = 1/2, \\ \tanh^{-1}\left[\exp\left(-\frac{N_{\star,i}}{\sqrt{2q}\, g_i}\right)\right]. & \text{for any arbitrary } q. \end{cases} \tag{5.581}$$

Using these results one can compute

$$\begin{aligned} N_{,i} &= \frac{1}{\sqrt{2\bar{\epsilon}_V(T_i^\star)}} \frac{V(T_i^\star) - V(T_i^c) + \left(\sum_{m=1}^{M} V(T_m^c)\right) \frac{\bar{\epsilon}_V(T_i^c)}{\bar{\epsilon}_V^c}}{\left(\sum_{j=1}^{M} V(T_j^\star)\right)} \\ &= \frac{\lambda_i \mathrm{sech}\left(\frac{T_i^\star}{T_{0i}}\right) - \lambda_i \mathrm{sech}\left(\frac{T_i^c}{T_{0i}}\right) + \left(\sum_{m=1}^{M} \lambda_m \mathrm{sech}\left(\frac{T_m^c}{T_{0m}}\right)\right) \frac{\bar{\epsilon}_V(T_i^c)}{\bar{\epsilon}_V^c}}{\sqrt{\left[\frac{\lambda_i}{g_i} \frac{\sinh^2\left(\frac{T_i}{T_{0i}}\right)}{\cosh\left(\frac{T_i}{T_{0i}}\right)}\right] \left(\sum_{j=1}^{M} \lambda_j \mathrm{sech}\left(\frac{T_j^\star}{T_{0j}}\right)\right)}} \end{aligned} \tag{5.582}$$

which is very useful to further compute the inflationary observables from the multi-tachyonic set-up. Here $\star$ indicates the horizon crossing and c denotes the constant density surface.

Using these results finally we compute the following inflationary observables:

$$\Delta_{\zeta,\star}=\sum_{i=1}^{M}\left(\frac{\lambda_i\,\mathrm{sech}\left(\frac{T_i^\star}{T_{0i}}\right)-\lambda_i\,\mathrm{sech}\left(\frac{T_i^c}{T_{0i}}\right)+\left(\sum_{m=1}^{M}\lambda_m\,\mathrm{sech}\left(\frac{T_m^c}{T_{0m}}\right)\right)\frac{\bar{\epsilon}_V(T_i^c)}{\bar{\epsilon}_V^c}}{\sqrt{\left[\frac{\lambda_i}{g_i}\frac{\sinh^2\left(\frac{T_i}{T_{0i}}\right)}{\cosh\left(\frac{T_i}{T_{0i}}\right)}\right]\left(\sum_{j=1}^{M}\lambda_j\,\mathrm{sech}\left(\frac{T_j^\star}{T_{0j}}\right)\right)}}\right)^2$$

$$\times\begin{cases}\left\{\frac{\left(\sum_{j=1}^{M}\lambda_j\,\mathrm{sech}\left(\frac{T_j^\star}{T_{0j}}\right)\right)}{12\pi^2M_p^2}\right\}_\star, & \text{for } q=1/2,\\[2ex] \left\{\frac{q\left(\sum_{j=1}^{M}\lambda_j\,\mathrm{sech}\left(\frac{T_j^\star}{T_{0j}}\right)\right)}{6\pi^2M_p^2}\right\}_\star, & \text{for any } q,\end{cases} \tag{5.583}$$

$$\Delta_{\zeta,c}=\left[\sum_{i=1}^{M}\frac{\lambda_i}{2g_i}\frac{\sinh^2\left(\frac{T_i}{T_{0i}}\right)}{\cosh\left(\frac{T_i}{T_{0i}}\right)}\right]_c^{-1}\times\begin{cases}\left\{\frac{\left(\sum_{j=1}^{M}\lambda_j\,\mathrm{sech}\left(\frac{T_j^\star}{T_{0j}}\right)\right)^2}{12\pi^2M_p^2}\right\}_c, & \text{for } q=1/2,\\[2ex] \left\{\frac{q\left(\sum_{j=1}^{M}\lambda_j\,\mathrm{sech}\left(\frac{T_j^\star}{T_{0j}}\right)\right)^2}{6\pi^2M_p^2}\right\}_c, & \text{for any } q,\end{cases} \tag{5.584}$$

$$n_{\zeta,\star}-1\approx\begin{cases}(2\bar{\eta}_V-8\bar{\epsilon}_V)-\frac{2}{\sum_{i=1}^{M}\left(\frac{\lambda_i\,\mathrm{sech}\left(\frac{T_i^\star}{T_{0i}}\right)-\lambda_i\,\mathrm{sech}\left(\frac{T_i^c}{T_{0i}}\right)+\left(\sum_{m=1}^{M}\lambda_m\,\mathrm{sech}\left(\frac{T_m^c}{T_{0m}}\right)\right)\frac{\bar{\epsilon}_V(T_i^c)}{\bar{\epsilon}_V^c}}{\sqrt{\left[\frac{\lambda_i}{g_i}\frac{\sinh^2\left(\frac{T_i}{T_{0i}}\right)}{\cosh\left(\frac{T_i}{T_{0i}}\right)}\right]\left(\sum_{j=1}^{M}\lambda_j\,\mathrm{sech}\left(\frac{T_j^\star}{T_{0j}}\right)\right)}}\right)^2}+\cdots, & \text{for } q=1/2,\\[2ex] \sqrt{\frac{2}{q}}\bar{\eta}_V-\left(\frac{1}{q}+3\sqrt{\frac{2}{q}}\right)\bar{\epsilon}_V \\ -\frac{1}{q\sum_{i=1}^{M}\left(\frac{\lambda_i\,\mathrm{sech}\left(\frac{T_i^\star}{T_{0i}}\right)-\lambda_i\,\mathrm{sech}\left(\frac{T_i^c}{T_{0i}}\right)+\left(\sum_{m=1}^{M}\lambda_m\,\mathrm{sech}\left(\frac{T_m^c}{T_{0m}}\right)\right)\frac{\bar{\epsilon}_V(T_i^c)}{\bar{\epsilon}_V^c}}{\sqrt{\left[\frac{\lambda_i}{g_i}\frac{\sinh^2\left(\frac{T_i}{T_{0i}}\right)}{\cosh\left(\frac{T_i}{T_{0i}}\right)}\right]\left(\sum_{j=1}^{M}\lambda_j\,\mathrm{sech}\left(\frac{T_j^\star}{T_{0j}}\right)\right)}}\right)^2}+\cdots, & \text{for any } q,\end{cases} \tag{5.585}$$

$$n_{\zeta,c}-1\approx\begin{cases}-6\bar{\epsilon}_V+2\frac{\sum_{i=1}^{M}\bar{\epsilon}_V(T_i)\bar{\eta}_V(T_i)}{\bar{\epsilon}_V}+\cdots, & \text{for } q=1/2,\\[2ex] -3\sqrt{\frac{2}{q}}\bar{\epsilon}_V+\frac{\sum_{i=1}^{M}\bar{\epsilon}_V(T_i)\bar{\eta}_V(T_i)}{q\bar{\epsilon}_V}\cdots, & \text{for any } q,\end{cases} \tag{5.586}$$

$$r_\star \approx \begin{cases} \dfrac{8}{\sum_{i=1}^{M}\left(\dfrac{\lambda_i \,\text{sech}\left(\frac{T_i^\star}{T_{0i}}\right)-\lambda_i \,\text{sech}\left(\frac{T_i^c}{T_{0i}}\right)+\left(\sum_{m=1}^{M}\lambda_m \,\text{sech}\left(\frac{T_m^c}{T_{0m}}\right)\right)\frac{\bar{\epsilon}_V(T_i^c)}{\bar{\epsilon}_V^c}}{\sqrt{\left[\frac{\lambda_i}{g_i}\frac{\sinh^2\left(\frac{T_i}{T_{0i}}\right)}{\cosh\left(\frac{T_i}{T_{0i}}\right)}\right]\left(\sum_{j=1}^{M}\lambda_j \,\text{sech}\left(\frac{T_j^\star}{T_{0j}}\right)\right)}}\right)^2}+\cdots, & \text{for } q=1/2, \\ \dfrac{4}{q\sum_{i=1}^{M}\left(\dfrac{\lambda_i \,\text{sech}\left(\frac{T_i^\star}{T_{0i}}\right)-\lambda_i \,\text{sech}\left(\frac{T_i^c}{T_{0i}}\right)+\left(\sum_{m=1}^{M}\lambda_m \,\text{sech}\left(\frac{T_m^c}{T_{0m}}\right)\right)\frac{\bar{\epsilon}_V(T_i^c)}{\bar{\epsilon}_V^c}}{\sqrt{\left[\frac{\lambda_i}{g_i}\frac{\sinh^2\left(\frac{T_i}{T_{0i}}\right)}{\cosh\left(\frac{T_i}{T_{0i}}\right)}\right]\left(\sum_{j=1}^{M}\lambda_j \,\text{sech}\left(\frac{T_j^\star}{T_{0j}}\right)\right)}}\right)^2}+\cdots, & \text{for any } q. \end{cases} \tag{5.587}$$

For the inverse cosh potential we get the following consistency relations:

$$n_{\zeta,\star}-1+\frac{r_\star}{4} \approx \begin{cases} (2\bar{\eta}_V-8\bar{\epsilon}_V)+\cdots, & \text{for } q=1/2, \\ \sqrt{\dfrac{2}{q}}\bar{\eta}_V-\left(\dfrac{1}{q}+3\sqrt{\dfrac{2}{q}}\right)\bar{\epsilon}_V+\cdots, & \text{for any } q. \end{cases} \tag{5.588}$$

6 Conclusion

In this paper, we have explored various cosmological consequences from the GTachyonic field. We start with the basic introduction of tachyons in the context of non-BPS string theory, where we also introduce the GTachyon field, in the presence of which the tachyon action is modified, and one can quantify the amount of the modification via a superscript q instead of 1/2. This modification exactly mimics the role of effective field theory operators and, studying the various cosmological features from this theory, one of the final objectives is to constrain the index q and a specific combination ($\propto \alpha' M_s^4/g_s$) of the Regge slope parameter α', the string coupling constant g_s and the mass scale of tachyon M_s, from the recent Planck 2015 and Planck+BICEP2/Keck Array joint data. To serve this purpose, we introduce various types of tachyonic potentials: the inverse cosh, logarithmic, exponential and inverse polynomials, using which we constrain the index q. To explore this issue in detail, we start with the detailed characteristic features of each of the potentials. Next we discuss the dynamics of GTachyon as well as usual tachyon for single, assisted and multi-field scenario. We also derive the dynamical solutions for various phases of the universe, including two situations, $T << T_0$ and $T >> T_0$, where T_0 is interpreted as the minimum or the mass scale of the tachyon. Next we have explicitly studied the inflationary paradigm from single field, assisted field and multi-field tachyon set-ups. Specifically for the single field and assisted field cases we have derived the results in the quasi-de Sitter background in which we have utilized the details of: (1) cosmological perturbations and quantum fluctuations for scalar and tensor modes, (2) slow-roll prescription up to all orders. In this context we have derived the expressions for all inflationary observables using any arbitrary vacuum and also for the Bunch–Davies vacuum by exactly solving the Mukhanov–Sasaki equation as obtained from the fluctuation of scalar and tensor modes. For the single field and assisted field cases in the presence of a GTachyon we have derived the inflationary Hubble flow and potential dependent flow equations, new sets of consistency relations, which are valid in the slow-roll regime and also derived the expression for the field excursion formula for the tachyon in terms of inflationary observables from both of the solutions obtained from arbitrary and the Bunch–Davies initial conditions for inflation. Particularly the derived formula for the field excursion for the GTachyon can be treated as one of the probes through which one can: (1) test the validity and the applicability of the effective field theory prescription within the present set-up, (2) distinguish between various classes of models from an effective field theory point of view. Also we have shown that in the case of assisted tachyon inflation the validity of the effective field theory prescription is much better compared to the single field case. This is because of the fact that the field excursion for assisted inflation is expressed in terms of the field excursion for the single field, provided the multiplicative scaling factor is $1/\sqrt{M}$, where M is the number of identical tachyons participating in assisted inflation. This derived formula also suggests that if M is a very large number then it is very easy to validate effective theory techniques, as in that case $|\Delta T|_{\rm Assisted} << M_p$. Next using the explicit form of the tachyonic potentials we have studied the inflationary constraints and quantified the allowed range of the generalized index q for each of the potentials. Hence using each of the specific forms of the tachyonic potentials in the context of the single field scenario, we have studied the features of CMB angular power spectrum from TT, TE and EE correlations from scalar fluctuations within the allowed range of q for each of the potentials. We also put in the constraints from the Planck temperature anisotropy and polarization data, which shows that our analysis matches well with the data. We have additionally studied the features of the tensor contribution in the CMB angular power spectrum from TT, BB, TE and EE correlations, which will give more interesting information in the near future once one can detect the signature of primordial B-modes. Further, using the δN formalism we have derived the expressions for the inflationary observables in the context of multi-field tachyons. We have also demonstrated the results for the two-field tachyonic case to understand the cosmological implications of the results in a better way.

The future prospects of our work are appended below:

- Throughout this analysis one finds each an every detail, but one can further study the features of primordial non-Gaussianity from the single field, assisted field and multi-field cases [96,97,140–144]. Due to the presence of a generalized index q one would expect that the consistency relations, which connect non-Gaussian parameters with the inflationary observables, are getting modified in the slow-roll regime of inflation and consequently one can generate large amount of primordial non-Gaussianity from the GTachyonic set-up. Also our aim is generalize the results as well as the consistency relations in all order of cosmological perturbations by incorporating the effect of sound speed c_S and the generalized parameter q. Using this set-up one can also compute the cosmological Ward identities for inflation [143–145], through which one can write down the recursion relation between correlation functions. This will help to derive the modified consistency relations in the present context. Additionally, one can also explore the possibility of devising cosmological observables which violate Bell's inequalities recently pointed out in Ref. [146]. Such observables could be used to argue that cosmic scale features were produced by quantum mechanical effects in the very early universe, specifically in the context of inflation. We are planning to report on these issues explicitly very soon.
- One would also like to ask what happened when we add additional higher derivatives in the gravity sector within tachyonic set-up, which are important around the string scale M_s. How the higher derivative gravity sector will change the cosmological dynamics and details of the primordial non-Gaussianity in the presence of a non-canonical GTachyonic sector is completely unknown. We have also plans to extend this project in that direction.
- The generation of the seed (primordial) magnetic field from the inflationary sector [129,147] is a long standing issue in primordial cosmology. To address this well-known issue one can also study the cosmological consequences from the effective field theory of inflationary magnetogenesis from the GTachyon within the framework of Type-IIA/IIB string theory.
- Also, our present analysis has been performed for five different potentials motivated from tachyonic string theory, specifically in the context of single field and assisted field inflation. For the multi-field we have quoted the results only for a specific kind of separable potential. It would be really very interesting to check whether we can study the behavior of non-separable potentials in the present context [148,149]. Also it is interesting to reconstruct any general form of a tachyonic inflationary potential, using which one can study the applicability of the effective field theory framework within this present set-up.
- One can also carry forward our analysis in the context of non-minimal set-up where the usual Einstein–Hilbert term in the gravity sector is coupled with the GTachyonic field. By applying the conformal transformation in the metric one can construct an equivalent representation of the gravity sector[11] in which the gravity sector is decoupled from the tachyonic sector and the usual tachyonic matter sector modified in the presence of an extra conformal factor. This clearly implies that the tachyonic potentials that we have studied in this paper all get modified via the additional conformal factor. Consequently it is expected that the cosmological dynamics will be modified in this context. Also one can check the applicability of the slow-roll prescription, which helps further to understand the exact behavior of cosmological perturbations in the presence of conformally rescaled modified tachyonic potentials.
- The detailed study of the generation of the dark matter using effective field theory framework,[12] other crucial particle physics issues i.e., the reheating phenomenon, leptogenesis and baryogenesis from the GTachyonic set-up is also an unexplored issue till date.

[11] In the cosmological literature this frame is known as the Einstein frame.

[12] For completeness, it is important to note that, very recently in Ref. [150], we have explicitly studied the effective field theory framework from membrane inflationary paradigm with Randall Sundrum single brane set-up. We also suggest the reader to study Refs. [151,152], in which the effective theory of dark matter has already been studied very well.

Acknowledgments SC would like to thank Department of Theoretical Physics, Tata Institute of Fundamental Research, Mumbai for providing me Visiting (Post-Doctoral) Research Fellowship. SC takes this opportunity to thank sincerely to Sandip P. Trivedi, Shiraz Minwalla, Soumitra SenGupta, Varun Sahni, Sayan Kar and Supratik Pal for their constant support and inspiration. SC takes this opportunity to thank all the active members and the regular participants of weekly student discussion meet "COSMOMEET" from Department of Theoretical Physics and Department of Astronomy and Astrophysics, Tata Institute of Fundamental Research for their strong support. SC also thanks Sandip Trivedi and Shiraz Minwalla for giving the opportunity to be part of the String Theory and Mathematical Physics Group. SC also thanks the other post-docs and doctoral students from String Theory and Mathematical Physics Group for providing an excellent academic ambiance during the research work. SC also thanks Institute of Physics (IOP), Bhubaneswar and specially Prof. Sudhakar Panda, for arranging the official visit where the problems have been formulated and the initial part have been done. SC also thanks the organizers of COSMOASTRO, 2015, Institute of Physics (IOP), Bhubaneswar, for giving the opportunity to give an invited talk on related issues of effective field theory and primordial non-Gaussianity. SC additionally thanks Inter University Centre for Astronomy and Astrophysics (IUCAA), Pune and specially Varun Sahni for extending hospitality during the work. Additionally SC takes this opportunity to thank the organizers of STRINGS, 2015, International Centre for Theoretical Science, Tata Institute of Fundamental Research (ICTS,TIFR) and Indian Institute of Science (IISC) for providing the local hospitality during the work and give a chance to discuss with Prof. Nima Arkani-Hamed related issues, which finally helped us to improve the qualitative and quantitative discussion in the paper. Last but not the least, we would like to acknowledge our debt to the people of India for their generous and steady support for research in the natural sciences, especially as regards string theory and cosmology.

Funded by SCOAP^3.

References

1. J. Martin, C. Ringeval, First CMB constraints on the inflationary reheating temperature. Phys. Rev. D **82**, 023511 (2010). arXiv:1004.5525 [astro-ph.CO]
2. J. Martin, C. Ringeval, V. Vennin, EncyclopÃ ędia inflationaris. Phys. Dark Univ. (2014) arXiv:1303.3787 [astro-ph.CO]
3. J. Martin, C. Ringeval, V. Vennin, How well can future CMB missions constrain cosmic inflation?. JCAP **1410**(10), 038 (2014). arXiv:1407.4034 [astro-ph.CO]
4. J. Martin, C. Ringeval, R. Trotta, V. Vennin, Compatibility of Planck and BICEP2 in the light of inflation. Phys. Rev. D **90**(6), 063501 (2014). arXiv:1405.7272 [astro-ph.CO]
5. J. Martin, C. Ringeval, R. Trotta, V. Vennin, The best inflationary models after Planck. JCAP **1403**, 039 (2014). arXiv:1312.3529 [astro-ph.CO]
6. A. Linde, Inflationary cosmology after Planck (2013). arXiv:1402.0526 [hep-th]
7. D.H. Lyth, A. Riotto, Particle physics models of inflation and the cosmological density perturbation. Phys. Rept. **314**, 1 (1999). arXiv:hep-ph/9807278
8. D.H. Lyth, Particle physics models of inflation. Lect. Notes Phys. **738**, 81 (2008). arXiv:hep-th/0702128
9. D. Baumann, L. McAllister, Inflation and string theory. arXiv:1404.2601 [hep-th]
10. D. Baumann, TASI lectures in inflation (2009). arXiv:0907.5424 [hep-th]
11. R. Durrer, The theory of CMB anisotropies. J. Phys. Stud. **5**, 177 (2001). arXiv:astro-ph/0109522
12. W. Hu, S. Dodelson, Cosmic microwave background anisotropies. Ann. Rev. Astron. Astrophys. **40**, 171 (2002). arXiv:astro-ph/0110414
13. M. Kamionkowski, A. Kosowsky, The cosmic microwave background and particle physics. Ann. Rev. Nucl. Part. Sci. **49**, 77 (1999). arXiv:astro-ph/9904108
14. C. Cheung, P. Creminelli, A.L. Fitzpatrick, J. Kaplan, L. Senatore, The effective field theory of inflation. JHEP **0803**, 014 (2008). arXiv:0709.0293 [hep-th]
15. S. Weinberg, Effective field theory for inflation. Phys. Rev. D **77**, 123541 (2008). arXiv:0804.4291 [hep-th]
16. D. Lopez Nacir, R. A. Porto, L. Senatore, M. Zaldarriaga, Dissipative effects in the effective field theory of inflation. JHEP **1201**, 075 (2012). arXiv:1109.4192 [hep-th]
17. S. Choudhury, A. Mazumdar, E. Pukartas, Constraining $\mathcal{N} = 1$ supergravity inflationary framework with non-minimal Kähler operators. JHEP **1404**, 077 (2014). arXiv:1402.1227 [hep-th]
18. S. Choudhury, Constraining $\mathcal{N} = 1$ supergravity inflation with non-minimal Kähler operators using δN formalism. JHEP **1404**, 105 (2014). arXiv:1402.1251 [hep-th]
19. S. Choudhury, S. Pal, DBI Galileon inflation in background SUGRA. Nucl. Phys. B **874**, 85 (2013). arXiv:1208.4433 [hep-th]
20. S. Choudhury, S. Pal, Primordial non-Gaussian features from DBI Galileon inflation. Eur. Phys. J. C **75**(6), 241 (2015). arXiv:1210.4478 [hep-th]
21. S. Unnikrishnan, V. Sahni, A. Toporensky, Refining inflation using non-canonical scalars. JCAP **1208**, 018 (2012). arXiv:1205.0786 [astro-ph.CO]
22. S. Unnikrishnan, V. Sahni, Resurrecting power law inflation in the light of Planck results. JCAP **1310**, 063 (2013). arXiv:1305.5260 [astro-ph.CO]
23. V. Assassi, D. Baumann, D. Green, L. McAllister, Planck-suppressed Operators. JCAP **1401**(01), 033 (2014). arXiv:1304.5226 [hep-th]
24. F.L. Bezrukov, M. Shaposhnikov, The standard model Higgs boson as the inflaton. Phys. Lett. B **659**, 703 (2008). arXiv:0710.3755 [hep-th]
25. S. Choudhury, T. Chakraborty, S. Pal, Higgs inflation from new Kähler potential. Nucl. Phys. B **880**, 155 (2014). arXiv:1305.0981 [hep-th]
26. A.A. Starobinsky, A new type of isotropic cosmological models without singularity. Phys. Lett. B **91**, 99 (1980)
27. L. Randall, R. Sundrum, A Large mass hierarchy from a small extra dimension. Phys. Rev. Lett. **83**, 3370 (1999). arXiv:hep-ph/9905221
28. L. Randall, R. Sundrum, An alternative to compactification. Phys. Rev. Lett. **83**, 4690 (1999). arXiv:hep-th/9906064
29. G.R. Dvali, G. Gabadadze, M. Porrati, 4-D gravity on a brane in 5-D Minkowski space. Phys. Lett. B **485**, 208 (2000). arXiv:hep-th/0005016
30. H. Maeda, V. Sahni, Y. Shtanov, Braneworld dynamics in Einstein–Gauss–Bonnet gravity. Phys. Rev. D **76**, 104028 (2007)
31. H. Maeda, V. Sahni, Y. Shtanov, Phys. Rev. D **80**, 089902 (2009). arXiv:0708.3237 [gr-qc]
32. Y. Shtanov, V. Sahni, Bouncing brane worlds. Phys. Lett. B **557**, 1 (2003). arXiv:gr-qc/0208047
33. V. Sahni, Y. Shtanov, Brane world models of dark energy. JCAP **0311**, 014 (2003). arXiv:astro-ph/0202346
34. V. Sahni, Y. Shtanov, New vistas in brane world cosmology. Int. J. Mod. Phys. D **11**, 1515 (2000). arXiv:gr-qc/0205111

35. Y. Shtanov, V. Sahni, Unusual cosmological singularities in brane world models. Class. Quant. Grav. **19**, L101 (2002). arXiv:gr-qc/0204040
36. S. Kar, Bulk-brane models: an overview and some queries. J. Phys. Conf. Ser. **405**, 012002 (2012)
37. S. Choudhury, S. Sengupta, Features of warped geometry in presence of Gauss–Bonnet coupling. JHEP **1302**, 136 (2013). arXiv:1301.0918 [hep-th]
38. S. Choudhury, S. SenGupta, Thermodynamics of charged Kalb Ramond AdS black hole in presence of Gauss-Bonnet coupling. arXiv:1306.0492 [hep-th]
39. S. Choudhury, J. Mitra, S. SenGupta, Modulus stabilization in higher curvature dilaton gravity. JHEP **1408**, 004 (2014). arXiv:1405.6826 [hep-th]
40. S. Choudhury, S. Pal, Brane inflation in background supergravity. Phys. Rev. D **85**, 043529 (2012). arXiv:1102.4206 [hep-th]
41. S. Choudhury, S. Pal, Reheating and leptogenesis in a SUGRA inspired brane inflation. Nucl. Phys. B **857**, 85 (2012). arXiv:1108.5676 [hep-ph]
42. S. Choudhury, S. Pal, Brane inflation: a field theory approach in background supergravity. J. Phys. Conf. Ser. **405**, 012009 (2012). arXiv:1209.5883 [hep-th]
43. S. Choudhury, A. Dasgupta, Galileogenesis: a new cosmophenomenological zip code for reheating through R-parity violating coupling. Nucl. Phys. B **882**, 195 (2014). arXiv:1309.1934 [hep-ph]
44. S. Choudhury, Can effective field theory of inflation generate large tensor-to-scalar ratio within RandallâĂŞ Sundrum single braneworld? Nucl. Phys. B **894**, 29 (2015). arXiv:1406.7618 [hep-th]
45. S. Choudhury, J. Mitra, S. SenGupta, Fermion localization and flavour hierarchy in higher curvature spacetime. arXiv:1503.07287 [hep-th]
46. S. Choudhury, S. SenGupta, A step toward exploring the features of Gravidilaton sector in Randall–Sundrum scenario via lightest Kaluza–Klein graviton mass. Eur. Phys. J. C **74** (2014) 11, 3159 arXiv:1311.0730 [hep-ph]
47. S. Choudhury, S. Sadhukhan, S. SenGupta, Collider constraints on Gauss–Bonnet coupling in warped geometry model. arXiv:1308.1477 [hep-ph]
48. A. Sen, Tachyon condensation on the brane anti-brane system. JHEP **9808**, 012 (1998). arXiv:hep-th/9805170
49. E.A. Bergshoeff, M. de Roo, T.C. de Wit, E. Eyras, S. Panda, T duality and actions for nonBPS D-branes. JHEP **0005**, 009 (2000). arXiv:hep-th/0003221
50. A. Sen, Dirac–Born–Infeld action on the tachyon kink and vortex. Phys. Rev. D **68**, 066008 (2003). arXiv:hep-th/0303057
51. M. Cederwall, A. von Gussich, A.R. Mikovic, B.E.W. Nilsson, A. Westerberg, On the Dirac-Born-Infeld action for d-branes. Phys. Lett. B **390**, 148 (1997). arXiv:hep-th/9606173
52. J.M. Maldacena, The Large N limit of superconformal field theories and supergravity. Int. J. Theor. Phys. **38**, 1113 (1999)
53. J.M. Maldacena, Adv. Theor. Math. Phys. **2**, 231 (1998). arXiv:hep-th/9711200
54. A. Sen, Rolling tachyon. JHEP **0204**, 048 (2002). arXiv:hep-th/0203211
55. F. Leblond, A.W. Peet, SD brane gravity fields and rolling tachyons. JHEP **0304**, 048 (2003). arXiv:hep-th/0303035
56. C.J. Kim, H.B. Kim, Y.B. Kim, O.K. Kwon, Electromagnetic string fluid in rolling tachyon. JHEP **0303**, 008 (2003). arXiv:hep-th/0301076
57. A. Sen, Universality of the tachyon potential. JHEP **9912**, 027 (1999). arXiv:hep-th/9911116
58. A. Sen, Field theory of tachyon matter. Mod. Phys. Lett. A **17**, 1797 (2002). arXiv:hep-th/0204143
59. A. Sen, Tachyon matter. JHEP **0207**, 065 (2002). arXiv:hep-th/0203265
60. A. Sen, Time and tachyon. Int. J. Mod. Phys. A **18**, 4869 (2003). arXiv:hep-th/0209122
61. R. Gopakumar, S. Minwalla, A. Strominger, Symmetry restoration and tachyon condensation in open string theory. JHEP **0104**, 018 (2001). arXiv:hep-th/0007226
62. S. Minwalla, T. Takayanagi, Evolution of D branes under closed string tachyon condensation. JHEP **0309**, 011 (2003). arXiv:hep-th/0307248
63. P. Basu, J. Bhattacharya, S. Bhattacharyya, R. Loganayagam, S. Minwalla, V. Umesh, Small hairy black holes in global AdS spacetime. JHEP **1010**, 045 (2010). arXiv:1003.3232 [hep-th]
64. J.R. David, M. Gutperle, M. Headrick, S. Minwalla, Closed string tachyon condensation on twisted circles. JHEP **0202**, 041 (2002). arXiv:hep-th/0111212
65. M. Aganagic, R. Gopakumar, S. Minwalla, A. Strominger, Unstable solitons in noncommutative gauge theory. JHEP **0104**, 001 (2001). arXiv:hep-th/0009142
66. R. Gopakumar, J.M. Maldacena, S. Minwalla, A. Strominger, S duality and noncommutative gauge theory. JHEP **0006**, 036 (2000). arXiv:hep-th/0005048
67. L. Rastelli, A. Sen, B. Zwiebach, String field theory around the tachyon vacuum. Adv. Theor. Math. Phys. **5**, 353 (2002). arXiv:hep-th/0012251
68. A. Sen, Fundamental strings in open string theory at the tachyonic vacuum. J. Math. Phys. **42**, 2844 (2001). arXiv:hep-th/0010240
69. K. Ohmori, A review on tachyon condensation in open string field theories. arXiv:hep-th/0102085
70. W. Taylor, Lectures on D-branes, tachyon condensation, and string field theory. arXiv:hep-th/0301094
71. M. Headrick, S. Minwalla, T. Takayanagi, Closed string tachyon condensation: an overview. Class. Quant. Grav. **21**, S1539 (2004). arXiv:hep-th/0405064
72. M. Berasaluce-GonzÃąlez, M. Montero, A. Retolaza, ÃĄ. M. Uranga, Discrete gauge symmetries from (closed string) tachyon condensation. JHEP **1311**, 144 (2013). arXiv:1305.6788 [hep-th]
73. A. Das, S. Panda, S. Roy, Origin of the geometric tachyon. Phys. Rev. D **78**, 061901 (2008). arXiv:0804.2863 [hep-th]
74. A. Sen, Remarks on tachyon driven cosmology. Phys. Scripta T **117**, 70 (2005). arXiv:hep-th/0312153
75. A. Deshamukhya, S. Panda, Warm tachyonic inflation in warped background. Int. J. Mod. Phys. D **18**, 2093 (2009). arXiv:0901.0471 [hep-th]
76. S. Panda, M. Sami, S. Tsujikawa, Inflation and dark energy arising from geometrical tachyons. Phys. Rev. D **73**, 023515 (2006). arXiv:hep-th/0510112
77. P. Chingangbam, S. Panda, A. Deshamukhya, Non-minimally coupled tachyonic inflation in warped string background. JHEP **0502**, 052 (2005). arXiv:hep-th/0411210
78. D. Choudhury, D. Ghoshal, D.P. Jatkar, S. Panda, On the cosmological relevance of the tachyon. Phys. Lett. B **544**, 231 (2002). arXiv:hep-th/0204204
79. A. Mazumdar, S. Panda, A. Perez-Lorenzana, Assisted inflation via tachyon condensation. Nucl. Phys. B **614**, 101 (2001). arXiv:hep-ph/0107058
80. G.W. Gibbons, Thoughts on tachyon cosmology. Class. Quant. Grav. **20**, S321 (2003). arXiv:hep-th/0301117
81. N. Barbosa-Cendejas, J. De-Santiago, G. German, J. C. Hidalgo, R. R. Mora-Luna, Tachyon inflation in the N-formalism. arXiv:1506.09172 [astro-ph.CO]
82. I.E.G. Sánchez, O.P. Santillan, Perturbations in some models of tachyonic inflation. arXiv:1508.03376 [gr-qc]
83. M. Sami, P. Chingangbam, T. Qureshi, Aspects of tachyonic inflation with exponential potential. Phys. Rev. D **66**, 043530 (2002). arXiv:hep-th/0205179

84. D. Cremades, F. Quevedo, A. Sinha, Warped tachyonic inflation in type IIB flux compactifications and the open-string completeness conjecture. JHEP **0510**, 106 (2005). arXiv:hep-th/0505252
85. L. Kofman, A.D. Linde, Problems with tachyon inflation. JHEP **0207**, 004 (2002). arXiv:hep-th/0205121
86. D.A. Steer, F. Vernizzi, Tachyon inflation: tests and comparison with single scalar field inflation. Phys. Rev. D **70**, 043527 (2004). arXiv:hep-th/0310139
87. K. Nozari, N. Rashidi, Some aspects of Tachyon field cosmology. Phys. Rev. D **88** (2013) 2, 023519 arXiv:1306.5853 [gr-qc]
88. S. Li, A.R. Liddle, Observational constraints on tachyon and DBI inflation. JCAP **1403**, 044 (2014). arXiv:1311.4664 [astro-ph.CO]
89. K. Nozari, N. Rashidi, Tachyon field inflation in light of BICEP2. Phys. Rev. D **90** (2014) 4, 043522 arXiv:1408.3192 [astro-ph.CO]
90. G.W. Gibbons, Cosmological evolution of the rolling tachyon. Phys. Lett. B **537**, 1 (2002). arXiv:hep-th/0204008
91. A.V. Frolov, L. Kofman, A.A. Starobinsky, Prospects and problems of tachyon matter cosmology. Phys. Lett. B **545**, 8 (2002). arXiv:hep-th/0204187
92. M. Fairbairn, M.H.G. Tytgat, Inflation from a tachyon fluid? Phys. Lett. B **546**, 1 (2002). arXiv:hep-th/0204070
93. G. Shiu, I. Wasserman, Cosmological constraints on tachyon matter. Phys. Lett. B **541**, 6 (2002). arXiv:hep-th/0205003
94. T. Padmanabhan, T.R. Choudhury, Can the clustered dark matter and the smooth dark energy arise from the same scalar field? Phys. Rev. D **66**, 081301 (2002). arXiv:hep-th/0205055
95. S. Mukohyama, Brane cosmology driven by the rolling tachyon. Phys. Rev. D **66**, 024009 (2002). arXiv:hep-th/0204084
96. J.M. Maldacena, Non-Gaussian features of primordial fluctuations in single field inflationary models. JHEP **0305**, 013 (2003). arXiv:astro-ph/0210603
97. J.M. Maldacena, G.L. Pimentel, On graviton non-Gaussianities during inflation. JHEP **1109**, 045 (2011). arXiv:1104.2846 [hep-th]
98. G. Calcagni, Non-Gaussianity in braneworld and tachyon inflation. JCAP **0510**, 009 (2005). arXiv:astro-ph/0411773
99. K. Enqvist, A. Jokinen, A. Mazumdar, T. Multamaki, A. Vaihkonen, Non-Gaussianity from instant and tachyonic preheating. JCAP **0503**, 010 (2005). arXiv:hep-ph/0501076
100. N. Barnaby, J.M. Cline, Nongaussianity from Tachyonic Preheating in Hybrid Inflation. Phys. Rev. D **75**, 086004 (2007). arXiv:astro-ph/0611750
101. N. Barnaby, J.M. Cline, Large Nongaussianity from Nonlocal Inflation. JCAP **0707**, 017 (2007). arXiv:0704.3426 [hep-th]
102. B. Dutta, L. Leblond, J. Kumar, Tachyon mediated non-Gaussianity. Phys. Rev. D **78**, 083522 (2008). arXiv:0805.1229 [hep-th]
103. M.V. Libanov, V.A. Rubakov, O.S. Sazhina, M.V. Sazhin, CMB anisotropy induced by tachyonic perturbations of dark energy. J. Exp. Theor. Phys. **108**, 226 (2009)
104. M.V. Libanov, V.A. Rubakov, O.S. Sazhina, M.V. Sazhin, Phys. Rev. D **79**, 083521 (2009). arXiv:0812.1459 [astro-ph]
105. J.M. Cline, H. Firouzjahi, P. Martineau, Reheating from tachyon condensation. JHEP **0211**, 041 (2002). arXiv:hep-th/0207156
106. R.K. Jain, P. Chingangbam, L. Sriramkumar, Reheating in tachyonic inflationary models: Effects on the large scale curvature perturbations. Nucl. Phys. B **852**, 366 (2011). arXiv:0902.1067 [astro-ph.CO]
107. J.S. Bagla, H.K. Jassal, T. Padmanabhan, Cosmology with tachyon field as dark energy. Phys. Rev. D **67**, 063504 (2003). arXiv:astro-ph/0212198
108. Z. Keresztes, L. Gergely, Combined cosmological tests of a bivalent tachyonic dark energy scalar field model. JCAP **1411**(11), 026 (2014). arXiv:1408.3736 [astro-ph.CO]
109. E.J. Copeland, M.R. Garousi, M. Sami, S. Tsujikawa, What is needed of a tachyon if it is to be the dark energy? Phys. Rev. D **71**, 043003 (2005). arXiv:hep-th/0411192
110. K. Bamba, S. Capozziello, S. Nojiri, S.D. Odintsov, Dark energy cosmology: the equivalent description via different theoretical models and cosmography tests. Astrophys. Space Sci. **342**, 155 (2012). arXiv:1205.3421 [gr-qc]
111. N.D. Birrell, P.C.W. Davies, Quantum fields in curved space. Cambridge monographs on mathematical physics
112. U.H. Danielsson, On the consistency of de Sitter vacua. JHEP **0212**, 025 (2002). arXiv:hep-th/0210058
113. J. de Boer, V. Jejjala, D. Minic, Alpha-states in de Sitter space. Phys. Rev. D **71**, 044013 (2005). arXiv:hep-th/0406217
114. K. Goldstein, D.A. Lowe, A Note on alpha vacua and interacting field theory in de Sitter space. Nucl. Phys. B **669**, 325 (2003). arXiv:hep-th/0302050
115. H. Collins, R. Holman, M.R. Martin, The fate of the alpha vacuum. Phys. Rev. D **68**, 124012 (2003). arXiv:hep-th/0306028
116. H. Collins, M.R. Martin, The Enhancement of inflaton loops in an alpha vacuum. Phys. Rev. D **70**, 084021 (2004). arXiv:hep-ph/0309265
117. R. Brunetti, K. Fredenhagen, S. Hollands, A Remark on alpha vacua for quantum field theories on de Sitter space. JHEP **0505**, 063 (2005). arXiv:hep-th/0503022
118. S. Naidu, R. Holman, Inflaton decay in an alpha vacuum. Phys. Rev. D **71**, 064026 (2005). arXiv:hep-th/0409013
119. S. Choudhury, B. K. Pal, B. Basu, P. Bandyopadhyay, Measuring CP violation within Effective Field Theory of inflation from CMB. arXiv:1409.6036 [hep-th]
120. P. A. R. Ade et al. [Planck Collaboration], Planck 2015 results. XX. Constraints on inflation. arXiv:1502.02114 [astro-ph.CO]
121. P.A.R. Ade et al. [BICEP2 and Planck Collaborations], Joint analysis of BICEP2/*KeckArray* and *Planck* data. Phys. Rev. Lett. **114**, 101301 (2015). arXiv:1502.00612 [astro-ph.CO]
122. A. Sen, Tachyon dynamics in open string theory. Int. J. Mod. Phys. A **20**, 5513 (2005). arXiv:hep-th/0410103
123. A. Sen, Tachyon dynamics in string theory. Prog. Theor. Phys. Suppl. **152**, 80 (2004)
124. A. Sen, Tachyon dynamics in string theory. Prog. Theor. Phys. Suppl. [Pramana **62** (2004) 403]
125. A. Sen, NonBPS states and branes in string theory. arXiv:hep-th/9904207
126. N.D. Lambert, H. Liu, J.M. Maldacena, Closed strings from decaying D-branes. JHEP **0703**, 014 (2007). arXiv:hep-th/0303139
127. J. Raeymaekers, Tachyonic inflation in a warped string background. JHEP **0410**, 057 (2004). arXiv:hep-th/0406195
128. L.R.W. Abramo, F. Finelli, Cosmological dynamics of the tachyon with an inverse power-law potential. Phys. Lett. B **575**, 165 (2003). arXiv:astro-ph/0307208
129. S. Choudhury, Reconstructing inflationary paradigm within effective field theory framework. arXiv:1508.00269 [astro-ph.CO]
130. S. Choudhury, A. Mazumdar, Sub-Planckian inflation & large tensor to scalar ratio with $r \geq 0.1$. arXiv:1404.3398 [hep-th]
131. S. Choudhury, A. Mazumdar, Reconstructing inflationary potential from BICEP2 and running of tensor modes. arXiv:1403.5549 [hep-th]
132. S. Choudhury, A. Mazumdar, An accurate bound on tensor-to-scalar ratio and the scale of inflation. Nucl. Phys. B **882**, 386 (2014). arXiv:1306.4496 [hep-ph]
133. D. Hanson et al. [SPTpol Collaboration], Detection of B-mode polarization in the cosmic microwave background with data from the south pole telescope. Phys. Rev. Lett. **111**(14), 141301 (2013). arXiv:1307.5830 [astro-ph.CO]

134. A.R. Liddle, A. Mazumdar, F.E. Schunck, Assisted inflation. Phys. Rev. D **58**, 061301 (1998). arXiv:astro-ph/9804177
135. E.J. Copeland, A. Mazumdar, N.J. Nunes, Generalized assisted inflation. Phys. Rev. D **60**, 083506 (1999). arXiv:astro-ph/9904309
136. K.A. Malik, D. Wands, Dynamics of assisted inflation. Phys. Rev. D **59**, 123501 (1999). arXiv:astro-ph/9812204
137. Y.S. Piao, R.G. Cai, X.M. Zhang, Y.Z. Zhang, Assisted tachyonic inflation. Phys. Rev. D **66**, 121301 (2002). arXiv:hep-ph/0207143
138. S. Dimopoulos, S. Kachru, J. McGreevy, J.G. Wacker, N-flation. JCAP **0808**, 003 (2008). arXiv:hep-th/0507205
139. N.S. Sugiyama, E. Komatsu, T. Futamase, δ N formalism. Phys. Rev. D **87**(2), 023530 (2013). arXiv:1208.1073 [gr-qc]
140. N. Arkani-Hamed, J. Maldacena, Cosmological collider physics. arXiv:1503.08043 [hep-th]
141. I. Mata, S. Raju, S. Trivedi, CMB from CFT. JHEP **1307**, 015 (2013). arXiv:1211.5482 [hep-th]
142. A. Ghosh, N. Kundu, S. Raju, S.P. Trivedi, Conformal invariance and the four point scalar correlator in slow-roll inflation. JHEP **1407**, 011 (2014). arXiv:1401.1426 [hep-th]
143. N. Kundu, A. Shukla, S.P. Trivedi, Constraints from conformal symmetry on the three point scalar correlator in inflation. JHEP **1504**, 061 (2015). arXiv:1410.2606 [hep-th]
144. N. Kundu, A. Shukla, S.P. Trivedi, Ward identities for scale and special conformal transformations in inflation. arXiv:1507.06017 [hep-th]
145. K. Hinterbichler, L. Hui, J. Khoury, An infinite set of ward identities for adiabatic modes in cosmology. JCAP **1401**, 039 (2014). arXiv:1304.5527 [hep-th]
146. J. Maldacena, A model with cosmological Bell inequalities. arXiv:1508.01082 [hep-th]
147. S. Choudhury, Inflamagnetogenesis redux: unzipping sub-Planckian inflation via various cosmoparticle probes. Phys. Lett. B **735**, 138 (2014). arXiv:1403.0676 [hep-th]
148. F. Vernizzi, D. Wands, Non-gaussianities in two-field inflation. JCAP **0605**, 019 (2006). arXiv:astro-ph/0603799
149. L. Senatore, M. Zaldarriaga, The effective field theory of multifield inflation. JHEP **1204**, 024 (2012). arXiv:1009.2093 [hep-th]
150. S. Choudhury, A. Dasgupta, Effective field theory of dark matter from membrane inflationary paradigm. arXiv:1510.08195 [hep-th]
151. G. Busoni, A. De Simone, E. Morgante, A. Riotto, On the validity of the effective field theory for dark matter searches at the LHC. Phys. Lett. B **728**, 412 (2014). arXiv:1307.2253 [hep-ph]
152. G. Busoni, A. De Simone, J. Gramling, E. Morgante, A. Riotto, On the validity of the effective field theory for dark matter searches at the LHC, Part II: complete analysis for the s-channel. JCAP **1406**, 060 (2014). arXiv:1402.1275 [hep-ph]
153. G. Busoni, A. De Simone, T. Jacques, E. Morgante, A. Riotto, On the validity of the effective field theory for dark matter searches at the LHC Part III: analysis for the t-channel. JCAP **1409**, 022 (2014). arXiv:1405.3101 [hep-ph]